Oceans and Coasts

Annual Science Report 2023

Report No. 23

forestry, fisheries & the environment
Department:
Forestry, Fisheries and the Environment
REPUBLIC OF SOUTH AFRICA

Oceans and Coasts

Annual Science Report

2023

Department of Forestry, Fisheries and the Environment

CONTENTS

SCIENCE TO POLICY

PLATFORMS, TECHNOLOGY & INNOVATION

TRAINING & OUTREACH

OUTPUTS FOR 2023

ACKNOWLEDGEMENTS

Most staff members of the Chief Directorate: Oceans & Coastal Research contributed in one way or another to the contents and production of the Oceans and Coasts Annual Science Report, 2023. The Department wishes to express its appreciation to the many other agencies that have contributed to the work presented in this report. The at-sea, ship-based work and many coastal field trips for data collection and community engagements undertaken by the Branch: Oceans and Coasts are facilitated by the Chief Directorate's science managers and made possible by the various units within the Branch's Corporate Management Services and Financial Management Services.

EDITORS

JA Huggett, T Lamont, T, Haupt, I Halo, SP Kirkman

AUTHORS, CONTRIBUTORS AND AFFILIATIONS

DFFE, Oceans and Coasts, Oceans and Coastal Research (OC Research)
Baliwe N, Basson R, Bebe L, Britz K, Crawford R, Dakwa F, Filander Z, Gebe Z, Goldman T, Halo I, Haupt T, Hlati K, Huggett JA, Jacobs LM, Janson L, Kirkman SP, Kiviets G, Krug M, Kupczyk A, Lamla S, Lamont T, Louw GS, Maduray S, Makhado AB, Mahanjana A, Masotla MJ, Mdazuka Y, Mdokwana BW, Mooi G, Mtshali T, Mushanganyisi K, Nemanshe E, Nhleko J, Pillay K, Rasehlomi T, Rasmeni B, Russo CS, Samaai T, Samuels K, Seakamela M, Setati S, Siswana K, Soares B, Soeker MS, Swart L, Tsanwani M, Tutt G, Upfold L, van den Berg MA, Vena K, Williams LL, Worship MM

DFFE, Fisheries Management, Fisheries Research and Development (Fisheries R&D)
Auerswald L, Erasmus C, Lamberth S, Shabangu FW, Snyders L, Somhlabe S, van der Lingen C, Williamson C, Yemane D

Aarhus University, Denmark (AU)
Carstensen J

Benguela Current Marine Spatial Management and Governance Project (MARISMA)

Blue Tide Solutions
Kowalski P

CapeNature
Hufke A

Cape Peninsula University of Technology (CPUT)
Evertson M, Findlay K, Meyer S, Puckree-Padua C, Sejeng C, Sparks C, Walker DR

City of Cape Town (CoCT)
Amos K, Hahndiek V, Slier M

Cornell University, USA
Klinck H, Tessaglia-Hymes CT

Council for Scientific and Industrial Research (CSIR)
Hamnca S, Pretorius S, van Niekerk L

Leibniz Centre for Tropical Marine Research, Germany (ZMT)
Rixen T

Nelson Mandela University (NMU)
Holness SD, Noyon M

Parthenope University of Naples, Italy
Controneo Y, Fortunato L

South African Environmental Observation Network (SAEON)
Morris T, Rautenbach G

South African National Parks (SANParks)
Kock A, van Wilgen N

Southern African Foundation for the Conservation of Coastal Birds (SANCCOB)
Ludynia K, Ngathu N, Petersen G

South African Weather Service (SAWS)

Two Oceans Aquarium
Lewis K

University of Cape Town (UCT)
Ansorge I, Branch G, Daniel M, Daniels R, du Preez SA, Kajee M, Petzer K, Pfaff M, Ramsarup N, Rouault M†

University of Exeter, UK
Sherley RB

Universität Hamburg, Germany (UHH)
Lahajnar N

University of KwaZulu-Natal (UKZN)
Carrasco NK, Mdluli NM

University of Pretoria (UP)
de Bruyn PJN, Jordaan RK

University of the Western Cape (UWC)
Ras V

University of Zululand (UNIZULU)
Harris SA†

World Wildlife Fund South Africa (WWF-SA)
Adams R, Smith C

Unaffiliated
Hart C, Walker S

CONTACT INFORMATION

Branch: Oceans and Coasts
Physical Address:
2 East Pier Shed, East Pier Road,
Victoria & Alfred Waterfront, Cape Town,
Western Cape, South Africa
Tel: 021 819 2410

Website: https://www.dffe.gov.za

Chief Director, Oceans and Coastal Research – Ashley S Johnson (Acting)
Director, Oceans Research – Ashley S Johnson (ajohnson@dffe.gov.za)
Director, Biodiversity and Coastal Research – Gerhard J Cilliers (gcilliers@dffe.gov.za)
Editors – Jenny A Huggett (jhuggett@dffe.gov.za), Tarron Lamont (tlamont@dffe.gov.za),
Tanya Haupt (thaupt@dffe.gov.za), Issufo Halo (ihalo@dffe.gov.za), Stephen P Kirkman (skirkman@dffe.gov.za)

COVER IMAGE:

Photo by Janik Alheit
The glowing bioluminescent plankton in Kogel Bay on Cape Town's False Bay. https://www.janikalheit.com
Limpet images courtesy of George Branch

Design and layout:
Catherine Boucher, DFFE, Corporate Management Services

RP75/2024
ISBN: 978-0-621-51919-8
doi:10/5281/zenodo.12600890

SUMMARY AND PERSPECTIVES

Introduction

The oceans constitute the largest body of water on earth, covering 71% of the Earth's surface. They are critical for the regulation of Earth's climate and weather patterns, while serving as habitat for billions of organisms and providing people with food, raw materials and a medium for transportation. In order to realise the full potential of the oceans to contribute to economic development and provide for growing human populations, countries with developing economies and extensive coastlines are striving to develop their ocean economies. The ocean economy encompasses a wide range of economic activities related to oceans and coasts, including fisheries, aquaculture, offshore oil and gas exploration, renewable energy, maritime transport, tourism and marine biotechnology. In South Africa, Operation Phakisa and more recently, the developing Oceans Economy Master Plan, aim to advance growth of several sectors within the ocean economy to ensure increased contribution to job creation, GDP and economic recovery.

However, the health of the oceans is deteriorating globally, leading to loss of biodiversity and ecosystem services. This is due to a range of threats associated with human population growth, such as overfishing, coastal development and pollution, as well as accelerating climate change and ocean acidification. The fundamental tension between the drive to develop ocean economies and deteriorating ocean health and productivity, has led to the emergence of the blue economy concept. This is a more holistic concept, which places stronger emphasis on sustainability and achieving balanced integration of economic growth, environmental health and social well-being, while supporting economic development and improving livelihoods. Practices that are integral to the blue economy, in addition to sustainable economic practices, include biodiversity conservation, climate change adaptation and mitigation, inclusiveness towards local communities and traditional ocean economy sectors, equitable distribution of benefits from ocean-related economic activities, enhancing ocean governance and policy, and capacity building initiatives. As such, the blue economy concept is intrinsically linked to several of the United Nations' Sustainable Development Goals (SDGs) for the 2030 Agenda for Sustainable Development. It is also intrinsically linked to goals and targets of multilateral environmental agreements that were established to address the global issues of climate change and biodiversity loss, namely the United Nations' Framework Convention on Climate Change (UNFCCC) and the Convention on Biological Diversity (CBD), both of which South Africa is a party to. Many maritime countries around the world are committing to strengthening their blue economies and promoting resilience to climate change. These include the countries belonging to regional conventions of which South Africa is a member, such as the Benguela Current Convention and the Nairobi Convention.

Science is critically important for the blue economy – scientific research and technological innovation underpin the sustainable development and management of ocean resources. In South Africa, management and strategic leadership of our ocean space are the purpose of DFFE Branch Oceans and Coasts, underscoring the importance of its Chief Directorate OC Research in supporting this role. Science and science-related activities of OC Research are relevant to various aspects of the blue economy, including conserving biodiversity and maintaining ecosystem services, studying the impacts of climate change and ocean acidification on marine environments, assessing impacts of human activities such as tourism, monitoring ocean health, identifying and quantifying pollutants in the ocean, promoting innovation, developing capacity, and generally providing an evidence base for agreements, regulations, and policies aimed at sustainable ocean management. For example, monitoring and assessment by OC Research are key for South Africa's reporting against the SDGs, particularly for SDG 14: Life below water. The OC Research activities are also increasingly relevant to the UNFCCC and CBD, given that the global ocean agenda has been advanced in climate and biodiversity discussions in recent years, and ocean matters now receive much greater prominence in these agreements than in the past. This is well aligned with the contemporary Decade of Ocean Science for Sustainable Development (2021–2030), which was proclaimed by the United Nations to support efforts to reverse the cycle of decline in ocean health and create improved conditions for the sustainable development of ocean economies whilst conserving the ecosystem.

The increasing call for science to understand the ocean and inform ocean policy and management decisions for sustainable development, biodiversity conservation and climate resilience, is reflected in this "bumper edition" of the Oceans and Coasts Annual Science Report, for 2023. The report contains 45 individual report cards on science and science-related activities of OC Research. These activities are carried out in partnership with marine research nodes of other departments and universities in South Africa, and from other countries and organisations, and are guided by a science plan. The science plan was developed to support the Branch Oceans and Coasts in fulfilling their mandate of managing and conserving South Africa's coastal and marine environment, as well as addressing the country's international and regional commitments to the conservation and sustainable use of the ocean and its biodiversity. It promotes the development and maintenance of programmes that provide continuous or sustained monitoring and descriptions of key aspects of the marine environment, with a very specific emphasis on the establishment of long-term datasets. Shorter-term research projects are also conducted, in search of a deeper, more fundamental understanding of specific areas or ecosystem processes, or to support evidence-based recommendations for ocean policy and management. The science plan also emphasises the need to continually develop new and innovative platforms and technologies in order to sustain and enhance ocean monitoring, prediction and management. The development of human capacity in marine research is integral to the science plan, and the training and development of staff, interns, students and outside researchers is embedded into all programmes and projects.

These different aspects represent the different sections of this report, which are dedicated to Monitoring Programmes; Research Highlights; Science to Policy; Platforms, Tech-

nology and innovation; and Training and Outreach. As in previous reports, a list of scientific outputs for the calendar year is provided at the end, including peer-reviewed publications and other products that reflect both the volume and quality of work accomplished by OC Research in 2023.

Monitoring Programmes

One of the core functions of OC Research is to establish and maintain long-term measurements in South Africa's coastal and offshore marine environment, to assess ecosystem status and ocean health. Recent warming, acidification and declining oxygen levels associated with climate change have greatly affected physical and chemical conditions in oceans. Consequent changes in marine habitats have led to shifts in the distribution and phenology (biological life cycles) of many organisms, with major implications for the biological productivity of marine ecosystems. Observations of key ocean indicators are thus critical to inform policy and support ocean governance and management.

That warming of the oceans around South Africa is taking place is supported by numerical models of sea surface temperature that were applied to the southern Benguela Upwelling Ecosystem (sBUS). These indicate long-term warming since the 1950s, especially over the past two decades (Report Card 1). In parallel, satellite-derived measurements of chlorophyll *a*, an index of ocean productivity, indicate small but significant long-term declines off both the south and west coasts since the late 1990s (Report Cards 2 and 3). Warmer and less productive oceans will yield less food for fish and other organisms like squid, seabirds and whales, and will also negatively impact fisheries.

A symptom of climate change is an increasing frequency of extreme temperature or weather events, which can have devastating impacts on biodiversity. Several extreme rainfall events during 2023 resulted in the flooding of nests of the Endangered African penguin at several important breeding sites (Report Card 4). This led to eggs and chicks being abandoned by the adults, as well as the deaths of many chicks, although SANCCOB was able to rescue and rehabilitate a substantial number. Extreme conditions can also result in harmful algal blooms (HABs). Several areas off the west coast are prone to HABs, which can lead to reduced oxygen in the water. Such low oxygen events, as well as marine heatwaves, can lead to rock lobster "walkouts" and mortalities (Report Cards 5 and 6). Off Hondeklip Bay, considerably higher oxygen levels were recorded in 2023 compared to the previous few years, and no "hypoxia" (very low oxygen) conditions were observed.

Time series of measurements increase in value as they become longer. Ten-year datasets are now available for several parameters measured seasonally along four lines of stations off the west coast, as part of the Integrated Ecosystem Programme (IEP; Report Cards 7–9). *In situ* (seawater) measurements indicate increasing trends in dissolved oxygen along all four lines, in both summer and winter. This is an interesting finding given the global trend of declining ocean oxygen concentrations. It may reflect the decadal-scale variability that is typical for upwelling ecosystems, but it also underscores the importance of sustained observations in our marine ecosystems. While too little oxygen can be harmful to organisms, so can too much oxygen.

The IEP is also yielding new information on the abundance, distribution and composition of the planktonic communities, which can be useful indicators or "sentinels" of change in marine ecosystems, given their fast growth rates and response to environmental changes. This includes the tiny microplankton (<0.2 mm in size) that are an important food resource for young pelagic fish (e.g. anchovies and sardines) that recruit off the west coast (Report Card 10). Off the south coast, copepods dominate the mesozooplankton (2–200 mm in size) and are an important food source for the pelagic fish that spawn there. A long-term decline in biomass of both large and small key copepod taxa over a 24-year period was strongly associated with a concurrent increase in fish biomass, but there are also signs of an overall decline in copepod size (and hence ecosystem production), which is likely linked to warming in this region (Report Card 11).

Off the east coast, variability in the size and composition of the phytoplankton (tiny marine plants that contribute to oxygen production) in the Agulhas Current are being monitored to assess possible changes in the ecosystem (Report Card 12). Models indicate that there has been an increase in the frequency of "early retroflections" in recent years, whereby the Agulhas Current changes direction further east than normal (Report Card 13). This could result in less production overall off the south coast and could also influence global climate through reduced "leakage" of heat and salt into the Atlantic Ocean.

At the Prince Edwards Islands in the Southern Ocean, bottom currents and temperature on the shelf continue to be monitored, to detect possible changes in ocean circulation and production that may influence the many seabirds and marine mammals that breed in this marine protected area (Report Cards 14–16).

Research Highlights

Studies of the impacts of environmental changes and their impacts, including those related to climate change, ocean acidification and pollution, are a clear theme for much of the research undertaken by OC Research. This is reflected in report cards on the frequency of marine heatwaves and warm events off the Cape Peninsula (Report Card 17), effects of flooding on the abundance of fish and macrofauna (animals >0.5 mm in size in the Great Kei Estuary in the Eastern Cape (Report Card 18), and effects of long-term cooling (due to increased upwelling) of the westernmost coastal area on the south coast (Report Card 19). The latter seems to have caused both anchovy and sardine (but not redeye) to shift their distribution eastwards towards warmer water, with potentially negative consequences for some of their predators (e.g. the Endangered African penguin) as well as the pelagic fishery. Report Card 20 describes ocean acidity measurements off the west coast during summer, and Report Card 21 provides the first assessment of trace and heavy metal concentrations along the west coast. Measurements showed elevated concentrations of Cadmium

in some areas, which exceeded the recommended coastal toxicity threshold value for this heavy metal. Further investigation is required to determine its source, which could be linked to river run-off or mining operations.

Species invasions have been highlighted as another serious threat to South Africa's marine environment and the blue economy, with introductions of non-native species potentially being caused by shipping or aquarium releases, and invasion potential exacerbated by climate change. Report Card 22 describes the first record of the invasive moon jellyfish *Aurelia coerulea* (size: ca. 20–40 cm across) in South Africa's waters. This is an example of an invasive species that can have serious consequences for our blue economy – for example, blooms of this species have reportedly clogged nuclear power plant water intakes in Korea – and it is important to try and mitigate the potential threat of this species and prevent its spread in South African waters.

Much lower down the plankton size spectrum, baseline measurements of picophytoplankton, the smallest marine primary producers (< 0.002 mm in size), are reported for the southern Benguela in Report Card 23. Phytoplankton are critically important in the ocean for several key reasons, including because they contribute significantly to oxygen production, carbon sequestration and nutrient cycling, but especially because they are the basis for marine food webs, providing food for zooplankton. On the Agulhas Bank, phytoplankton and zooplankton communities spanning several size classes were compared over two summers with contrasting environmental patterns, providing insights into "who eats who" and ecosystem functioning (Report Card 24). Another study compared the diversity and abundance of zooplankton communities between productive submarine (underwater) canyons and nearby non-canyon sites in KwaZulu-Natal (KZN; Report Card 25).

All of the above research was based on *in situ* sampling, but OC Research also makes use of less direct approaches to address questions about marine biodiversity and the environment. This includes the use of models, in this case a hydrodynamic model that was able to simulate current patterns near the Diepgat Canyon off the KZN coast, indicating its potential use as a tool for exploring upwelling processes and biological connectivity in canyon environments (Report Card 26). Also, the use of museum specimens, such as plankton-eating stony corals in the case of Report Card 27. These corals are shown to provide a valuable resource to explore genetic diversity patterns in relation to sea bottom depth for the entire South African coastline.

Marine protected areas (MPAs) are seen by many as a cornerstone of marine biodiversity conservation in South Africa, especially "no-take" MPAs or MPA zones that exclude pressures such as harvesting. ReportCards 28 and 29 highlight the effectiveness of no-take areas within the Table Mountain National Park MPA for conserving commonly harvested limpets and Galjoen, respectively. Marine Protected Areas are intended to provide other benefits besides conservation. These include socio-economic benefits (e.g. through ecotourism ventures), while they can provide "natural laboratories" for scientific research and monitoring. Report Card 30 details a study conducted at the Robberg MPA in Plettenberg Bay, to assess disturbance effects of "swim-with-seal" ecotourism on the resident seal colony and inform adaquate management of the industry in line with a sustainable blue economy.

South Africa's Southern Ocean territory, namely the PEIs and the adjacent waters including the PEI MPA, provide one of country's best known natural laboratories for scientific study. Research on the marine processes of this region is key for understanding potential climate change effects on the system and its multitudinous marine life, including the vast breeding colonies of seabirds and seals on the islands, their prey and their predators. Report Card 31 showed that the proximity of ocean fronts and eddies to the islands has a major influence on the zooplankton communities there, while a separate modelling study indicated that enhanced production at the PEIs may be partly explained by persistent anti-clockwise circulation over the shelf, which induces upwelling (Report Card 32). Report Card 33 demonstrates the influence of various environmental or oceanographic features on the nature of seabird assemblages between South Africa and Antarctica, including the PEI region.

Underwater acoustics is an emerging field of marine research with considerable possibilities. Report Card 34 shows how an acoustic recorder located between the two islands of the PEIs detected killer whale sounds throughout the year, corresponding with both the number of whales sighted visually by observers on Marion Island and the abundance of southern elephant seals, one of their favoured prey species. The final report card of this section describes how an acoustic recorder positioned further south near the edge of the Antarctic sea ice during summer was able to detect the distinctive sounds of six different whale species, including the first local record of sperm whales (Report Card 35).

Science to Policy

Closure of purse-seine fishing around six of the largest remaining breeding colonies of the Endangered African penguin, for at least 10 years, is an outcome of many years of research and debate involving OC Research and partner institutions (Report Card 36). The closures, which are aimed at increasing the species' chances of survival by safeguarding its food supply, are an example of the type of measure required to address ambitious targets of the recently adopted Kunming-Montreal Global Biodiversity Framework (GBF) of the CBD to halt biodiversity loss. The most well-known of the GBF targets is the so-called "30 x 30" target, which calls for the conservation of 30% of land, waters and seas by 2030. In addition to conventional protected areas, this target makes provision for "other effective area-based conservation measures" (OECMs) to achieve the target objectives – a novel concept in South Africa especially in our marine space. Report Card 37 presents a process aimed to establish a coherent understanding of this concept in South Africa's unique marine context.

The GBF has strong synergies with the United Nations' SDGs, including with regard to assessing and combatting

pollution and its impacts on biodiversity and the environment, in line with clean oceans and a blue economy. Report Card 38 reflects on South Africa's role in testing standardised collection and analysis protocols for sampling microplastics (<5 mm) in beach sand and water, that member states have agreed upon. The protocols have been developed to address a global SDG indicator to monitor the densities of plastic debris.

Platforms, Technology and Innovation

Ocean models are potentially powerful tools for understanding and predicting ocean systems. The following two report cards describe the evaluation of different ocean models to accurately reproduce seawater temperature and salinity measurements off the west coast of South Africa (Report Card 39) and at the Prince Edward Islands (PEIs) in the Southern Ocean (Report Card 40). This is done by comparing modelled values to *in situ* measurements. Despite some seasonal biases, the models performed reasonably well, demonstrating they can help to improve understanding of oceanographic variability, particularly in remote areas such as the PEIs.

Contemporary interest in the impacts of underwater noise such as ship engine noise and seismic survey airgun emissions on marine biodiversity, has incentivised the creation of an underwater acoustics science programme in OC Research. Report Card 41 describes the testing and deployment of acoustic instruments being used to provide baseline data on marine "soundscapes" (the acoustic environment) and to assess the impacts of underwater noise on marine biodiversity and ecosystem functioning, for example during seismic surveys.

The large volumes of data collected by underwater acoustic instruments, once retrieved, will be safeguarded in South Africa's Marine Information Management System (MIMS). This is an open data repository that archives and publishes validated marine-related datasets for the DFFE and its regional partners. It has recently received formal, global accreditation by the International Oceanographic Data and Information Exchange (IODE) of the Intergovernmental Oceanographic Commission of UNESCO and has been fully integrated into the IODE Ocean Infohub (Report Card 42). The MIMS team has also embarked on a climate data "rescue" initiative, to digitise and preserve invaluable paper-based data related to South Africa's coastal and marine environments, including records such as hourly weather data from lighthouses dating back to 1970 (Report Card 43).

Training and Outreach

Datasets archived in MIMS are accessible to the Oceans and Coastal Information Management System (OCIMS), a national decision support system for the effective governance of South Africa's oceans and coasts. Stakeholders have benefitted from its decision support tools, such as for water quality or harmful algal blooms, as demonstrated at a national stakeholder engagement workshop in 2023 (Report Card 44). The workshop encouraged further collaboration and identified new requirements for OCIMS.

Collaborative initiatives of the Department, including with local and international research institutions and universities, have been a catalyst for the growth of early career scientists and students, from South Africa and abroad. In the final Report Card (45), a group of university students who were privileged to join research cruises on the SA *Agulhas* II to Antarctica, and on the RS *Algoa* off the west coast of South Africa, provide their perspective of their experiences and skills development on these expeditions.

MONITORING PROGRAMMES

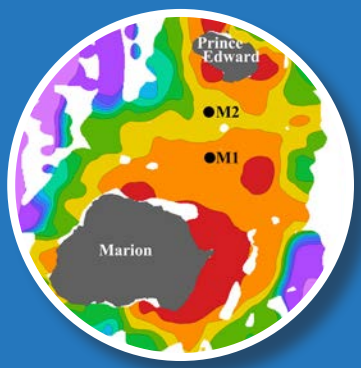

1. CLIMATE MODEL SIMULATIONS OF THE LONG-TERM VARIABILITY OF SEA SURFACE TEMPERATURE IN THE SOUTHERN BENGUELA

Sea temperature is classified as one of the Global Ocean Observing System (GOOS) Essential Ocean Variables (EOVs). Many global and regional ocean observing system programmes monitor the temporal and spatial evolution of EOVs to derive trends and infer environmental changes across multiple scales, e.g. from intra-seasonal to decadal time scales, and from local to global spatial scales.

The DFFE, through scientific programmes within OC Research, regularly conduct oceanographic surveys within and around its jurisdictional waters to generate relevant information about the state of the coastal and marine environment. One such programme is the Integrated Ecosystem Program (IEP) which monitors the southern Benguela along the west coast of South Africa (Fig. 1).

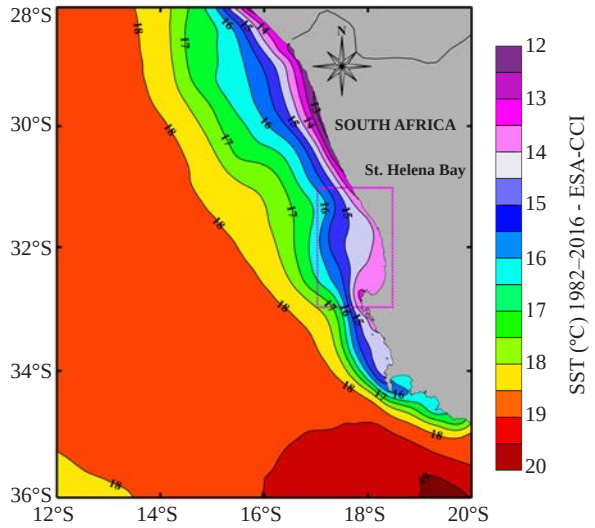

Figure 1. The southern Benguela region, showing long-term (1982–2016) mean sea surface temperature from the ESA CCI reanalysis dataset. The inserted box highlights the area used to generate Fig. 3. Contour spacing is 0.5°C.

However, to generate long-term *in situ* data at suitable scales to assess the variability of EOVs and derive climate indicators is challenging. Therefore climate studies by the international Inter-governmental Panel for Climate Change (IPCC) rely on numerical model simulations, despite their inherent limitations. This quite often prompts the question: How realistic are such model simulations? Data-to-model comparison exercises have become an ongoing practice in attempt to answer this question.

Satellite-derived sea surface temperature (SST) for the period 1982 to 2016 (Fig. 1), from the European Space Agency (ESA) Climate Change Initiative (CCI) Programme, has been used to evaluate the performance of four IPCC models in reproducing the mean state of SST in the southern Benguela. The evaluated models included the Norwegian Earth System Model (NorESM; Fig. 2a), the Canadian Earth System Model (CanESM; Fig. 2b), the French Centre National de Recherches Météorologiques (CNRM; Fig. 2c) and the American Geophysical Fluid Dynamics Laboratory (GFDL; Fig. 2d).

All models (Fig. 2) struggled to reproduce the SST spatial pattern as observed from satellite (Fig. 1), possibly due to their coarse grid resolution. The closest matches to satellite SST distribution were simulated by the CanESM (Fig. 2b) and the GFDL (Fig. 2d), while the worst, characterised by excessive warmer SST, was simulated by the CNRM (Fig. 2c).

Regardless of their performance, moving averages of the long-term SST variability from all models (Fig. 3) reveal an increase of warmer-than-normal SSTs, especially in the past two decades. This suggests that long-term warming is occurring in the region, which is expected to reduce the productivity of the ecosystem, with likely adverse impacts on the South African economy. *In situ* monitoring programmes in the region need to be reinforced to generate sustained long-term data to verify these conclusions drawn from IPCC numerical models.

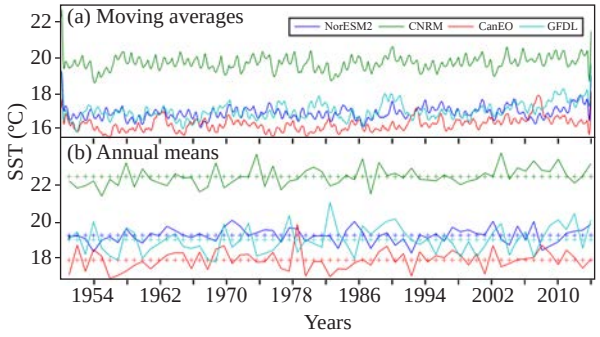

Figure 3. (a) Long-term moving averages of model-derived SST. (b) Annual averages (lines) and long-term mean (crosses) SST simulated by the models.

Authors: Halo I, Lamont T, Tutt G (OC Research)

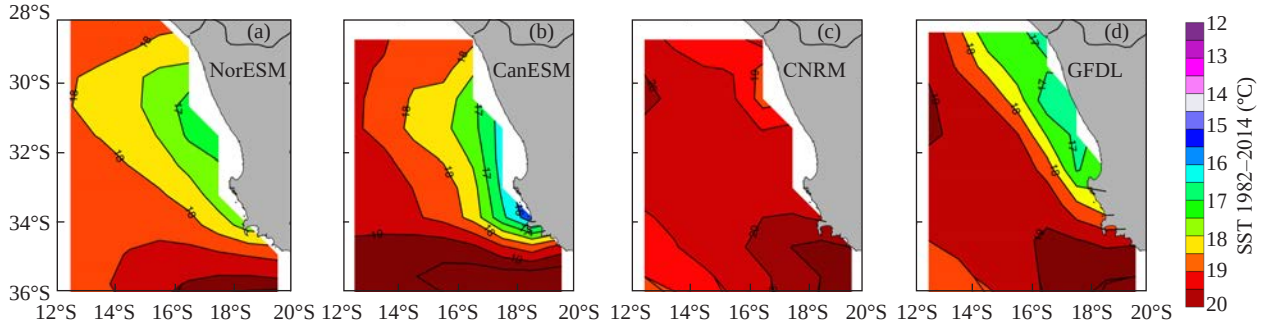

Figure 2. Mean state (1950–2014) of SST simulated by the four climate models.

2. CHLOROPHYLL VARIABILITY ON THE WEST AND SOUTH COASTS

Phytoplankton are crucial for a number of key marine processes, such as food web modulation, CO_2 exchanges, and the cycling of carbon and other nutrients. On the west and south coasts of southern Africa, the Benguela upwelling system and the Agulhas Bank are ecologically and economically significant as they host productive ecosystems with complex trophic structures that support numerous commercially harvested resources. To monitor productivity levels, an index of chlorophyll *a* is computed by integrating satellite-derived surface values between the coast and the 1 mg m^{-3} contour of chlorophyll *a* concentration further offshore (Fig. 1).

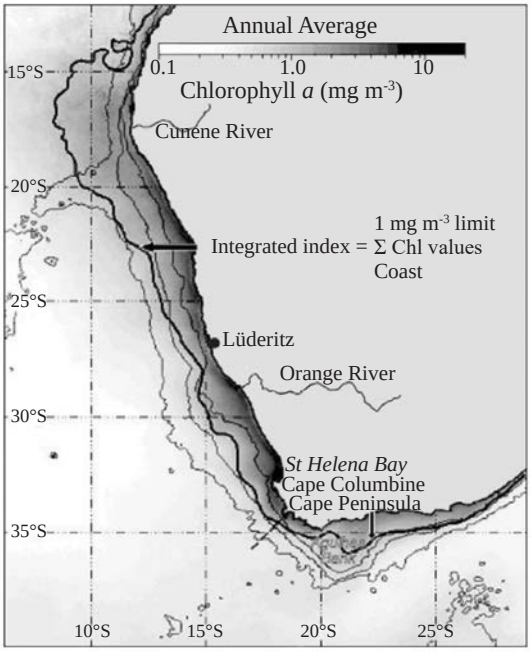

Figure 1. Annual average chlorophyll *a* concentration and location of the 1 mg m^{-3} contour (black line).

Higher values are associated with greater phytoplankton biomass and a more productive ecosystem, while lower values indicate lower biomass and a less productive ecosystem. The highest index values were usually found off Namibia (16–26°S; Fig. 2). Biomass here in 2018 was the lowest since 2013. While biomass was elevated in 2019 and 2020, values since 2021 have been somewhat lower and more variable. In June–July 2023, the highest index values occurred at 16°S. Persistent upwelling and offshore transport at Lüderitz (ca. 27°S) are typically associated with very low index values. Elevated values here during the summers of 2020 and 2021 suggested decreased upwelling, while lower values in 2022 and 2023 implied stronger upwelling. Along South Africa's west coast (SAWC, 28–34°S), index values were elevated around the Namaqualand, Cape Columbine and Cape Peninsula upwelling cells. Off Namaqualand (28.5–30°S), values in 2018 were the highest since 2013. Elevated values in 2022 suggested high productivity, but lower values during 2021 and 2023 reflected less productivity. Along South Africa's south coast (SASC, 18.5–29°E), index values were generally lower than on the WC. During 2013–2023, the highest values occurred at 22°E in January–February 2014, with declining peak biomass levels in subsequent years. Low values in 2016 suggested this was the least productive year for the SASC during 2013–2023. Slightly higher values throughout 2023 suggested improved productivity compared to 2022. The varying trends in productivity across the region, i.e. a small but significant long-term increase in chlorophyll *a* off Namibia, and a decrease off the SAWC and SASC, appear to have continued over the past year.

Author: Lamont T (OC Research)

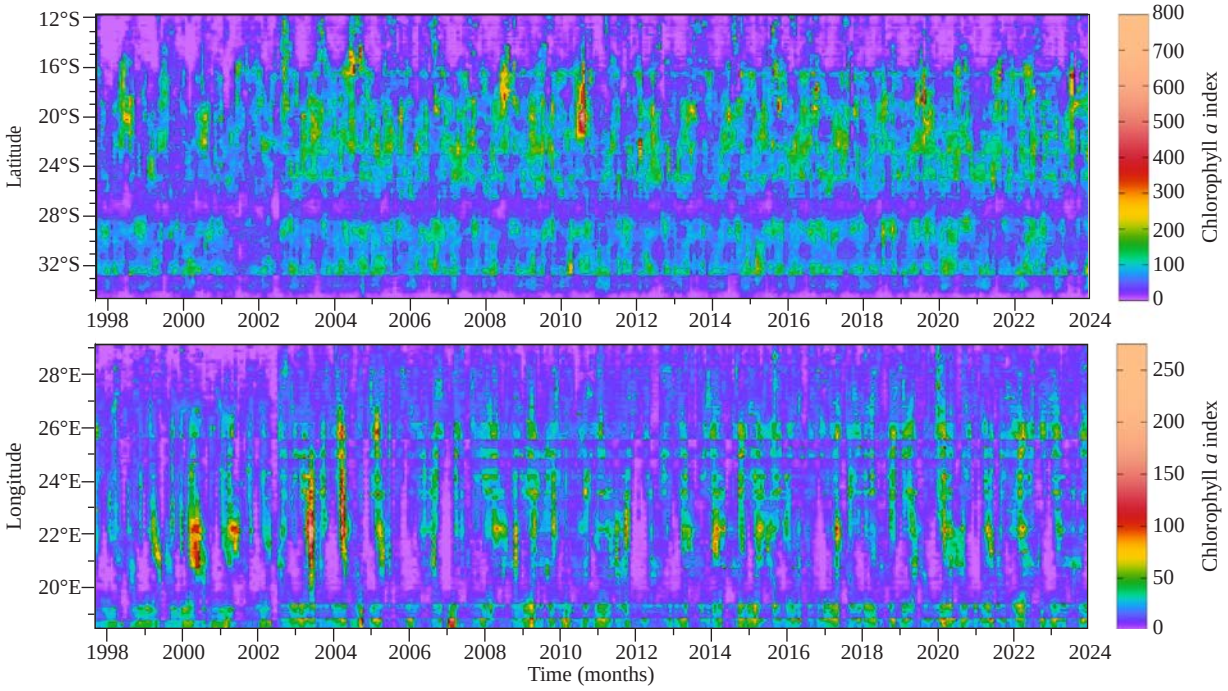

Figure 2. Monthly chlorophyll *a* indices (1997–2023) for the west coasts of Namibia and South Africa (top panel) and for South ica's south coast (bottom panel).

3. SURFACE CHLOROPHYLL *A* CONCENTRATIONS ALONG THE ST HELENA BAY MONITORING LINE

St Helena Bay on the west coast of South Africa (Fig. 1) is one of the most productive areas of the Benguela ecosystem and has been the focus of environmental research and monitoring for several decades. It is a retention area, with significantly elevated plankton biomass compared to other areas off South Africa, and is an important region for many species such as small pelagic fish, hake, whales, and rock lobster.

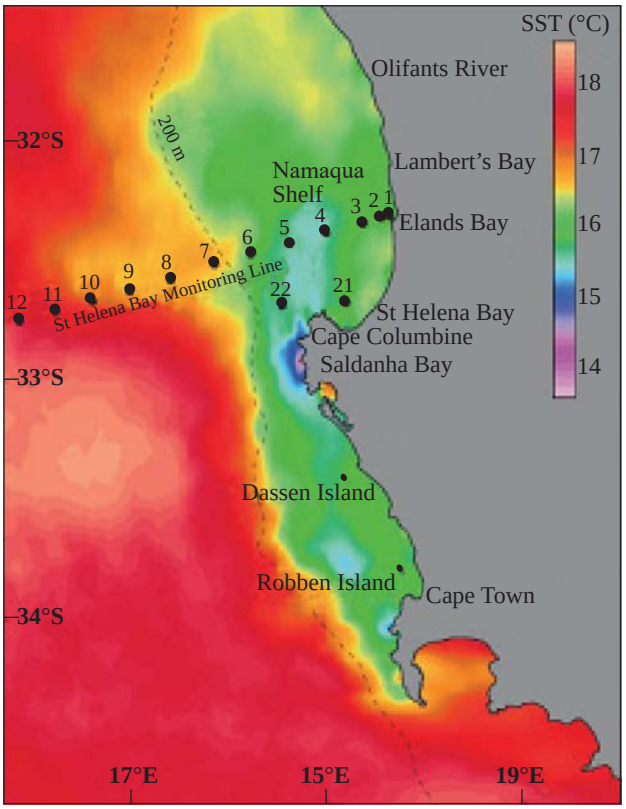

Figure 1. Map of the west coast of South Africa, showing the location of St Helena Bay and the St Helena Bay Monitoring Line. Colours represent satellite-derived sea surface temperatures, which indicate cooler waters typically found inshore and warmer waters offshore.

Along the west coast, southeasterly winds transfer surface waters offshore, resulting in cool, nutrient-rich waters being uplifted to the surface from deeper depths (i.e. upwelling). On a seasonal scale, higher chlorophyll *a* coincides with larger amounts of upwelling that occur during October–March each year (the upwelling season). Satellite-derived surface chlorophyll *a* illustrates this seasonality, with maxima in spring/early summer (usually October) and during the late summer/autumn months of February and March (Fig. 2).

Higher chlorophyll *a* is usually associated with greater phytoplankton biomass and a more productive ecosystem, which largely results from the higher nutrient availability in the upper ocean during upwelling. In contrast, lower chlorophyll *a* indicates lower phytoplankton biomass and a less productive ecosystem, usually associated with less upwelling and nutrient availability in the upper ocean during late autumn to early spring (April–September) each year. Generally, higher chlorophyll *a* occurs close to the coast and decreases with distance offshore (Fig. 2). During 2015, high values (>20 mg m^{-3}) extended ca. 20 km offshore in autumn (March) and late spring/early summer (September–November). Values >20 mg m^{-3} were observed much closer to the coast during 2016–2019 and in 2021. Such high values extended ca. 10 km offshore in February–March 2020 and October 2022, but in December 2023 they extended >30 km offshore. Elevated chlorophyll *a* (>5 mg m^{-3}) extended ca. 110 km offshore in March 2015 – the farthest offshore extent for such elevated values since March 2010. Since then, the farthest offshore extent (ca. 80 km) of values above 5 mg m^{-3} was observed in February and March 2016 and in April 2022. Such values did not extend beyond 70 km offshore during 2017–2021 and in 2023. Chlorophyll *a* in 2017 was lower overall than in 2016 but remained elevated throughout the year. Generally lower values in 2018 and 2021 suggested a less productive ecosystem during these years. In contrast, higher values during 2019, 2020 and 2022 suggested increased productivity. While chlorophyll *a* was higher in January–February and in December 2023, values during March–November were much lower, suggesting a much less productive autumn-to-spring period compared to the previous decade.

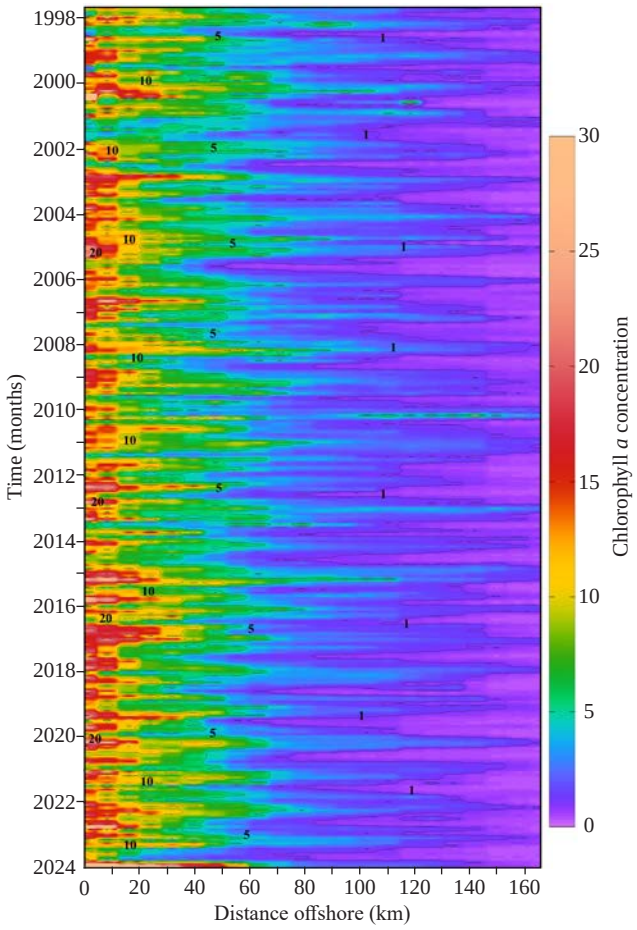

Figure 2. Time series of satellite-derived monthly chlorophyll *a* (mg m^{-3}) along the St Helena Bay Monitoring Line between September 1997 and December 2023.

Author: Lamont T (OC Research)

4. EXTREME RAINFALL EVENTS ORPHAN AFRICAN PENGUIN CHICKS

African penguins (AP) *Spheniscus demersus* are endemic to the coasts of South Africa and Namibia. Significant declines in their population size led the International Union for Conservation of Nature to classify the species as Endangered in 2010. Several factors threaten their well-being, including, but not limited to, environmental factors such as storms and extreme rainfall events. Resultant storm surges, wave run-up, as well as intense rainfall run-off from areas adjacent to the colonies, can flood AP nests resulting in parents abandoning their offspring or chicks drowning (Fig. 1). Such extreme rainfall events took place during May, June, and September 2023 in South Africa. Some of the affected AP colonies included Robben Island (RI), Stony Point (SP), and Boulders Beach (BB) in the Western Cape, and Bird Island (BI) in Algoa Bay (Fig. 2). Here, we have evaluated the total precipitation from the near real-time daily ERA5 reanalysis product, produced by the European Centre for Medium-Range Weather Forecasts to monitor the occurrence of such events, and we document six events that occurred during 2023.

Figure 1. African penguin chicks from the (a) Stony Point and (b) Robben Island colonies affected by heavy rains on 25 May 2023, illustrating severe damage to their nests (photo credit: SANCCOB).

Extreme rainfall (up to 60 mm more than the expected average) on 16 May at BI (Fig. 2) resulted in the abandonment of 37 AP chicks. Later that month, on 25 May, the Western Cape sites were impacted by a strong frontal system that produced rainfall >100 mm above the average for that time of year (Fig. 2). This resulted in flooding of many nests and consequent abandonment of 19 chicks by the adults at SP and BB. Five days later (30 May) another frontal system yielded between 55–105 mm more than the typically expected rainfall (Fig. 2), resulting in the abandonment of 91 chicks and the death of 44 chicks at SP and BB, while RI penguins appeared unaffected. A further 62 chicks and 30 eggs were abandoned between 3–8 June due to elevated rainfall at SP and BB. The biggest storm of 2023 hit the Western Cape on 24 September with >150 mm above-average rainfall (Fig. 2), resulting in the abandonment of 24 chicks at SP.

While these events had a considerable impact on nesting penguins, SANCCOB was able to rescue and rehabilitate a total of 226 chicks and 47 eggs during these events, reflecting the critical role that SANCCOB plays in the conservation of seabirds. This study has shown that the ERA5 product was useful for identifying the 2023 rainfall events which impacted the penguins, despite its coarse spatial resolution of 0.25°. A newly expanded Memorandum of Understanding between the DFFE and SAWS aims to further improve this kind of monitoring by expanding the existing network of *in situ* weather stations to better reflect local environmental conditions at AP nesting sites. Together with strengthened collaborations with SANCCOB, SANParks, CapeNature, and the City of Cape Town municipality, we anticipate that this will improve monitoring, enhance understanding of environmental impacts, and allow for more impactful conservation interventions for the AP population.

Authors: Russo CS, Kupczyk A, Soares BK, Lamont T (OC Research); Ludynia K (SANCCOB); van Wilgen N, Kock A (SANParks); Morris T (SAEON); SAWS
Contributors: Petersen G, Ngathu N (SANCCOB); Hahndiek V, Amos K, Slier M (CoCT, SANCCOB); Hufke A (CapeNature)

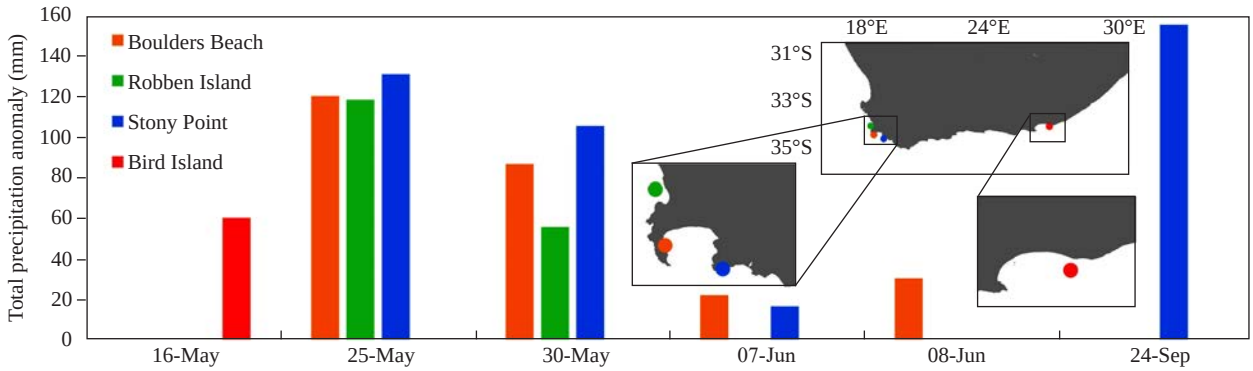

Figure 2. Selected daily ERA5 total precipitation anomalies calculated against a 30-year (1993–2023) mean, highlighting extreme rainfall events at the AP nesting sites of Robben Island, Boulders Beach, Stony Point and Bird Island. Locations of these colonies are depicted on the map insets.

5. DISSOLVED OXYGEN AND TEMPERATURE VARIABILITY OFF HONDEKLIP BAY

On the west coast of South Africa, the southern Benguela Upwelling System (sBUS) experiences seasonal wind-driven upwelling that introduces nutrients to the surface layers, promoting enhanced phytoplankton production and sustaining a diverse ecosystem (Fig. 1). One of the consequences of such enhanced productivity is the development of an oxygen minimum zone (OMZ), where dissolved oxygen (DO) is consumed as organic matter decays. In the sBUS, the OMZ is most pronounced in the bottom waters of St Helena Bay, but also develops elsewhere in nearshore regions towards the end of the upwelling season (January–April).

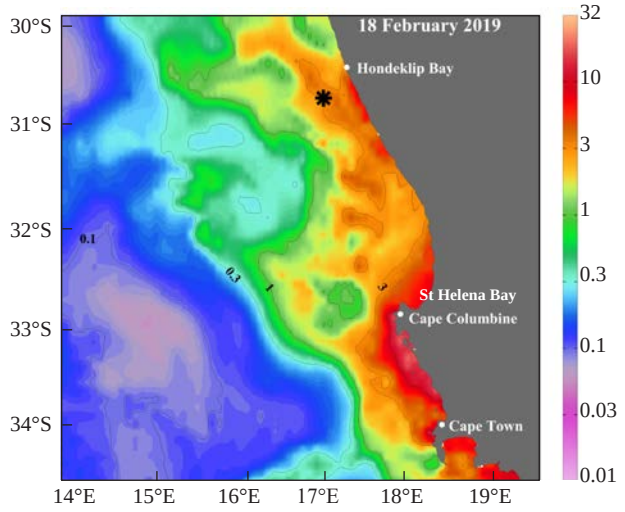

Figure 1. The west coast of South Africa, showing the site of the mooring used in this study (black star). Colours depict satellite-derived chlorophyll *a* concentrations (mg m^{-3}) for 18 February 2019.

In February 2019, a mooring equipped with a miniDOT sensor (MDO) was deployed at 30.64°S and 17.02°E, southwest of Hondeklip Bay (Fig. 1). It measured temperature and DO at 96 m depth (ca. 74 m above the sea floor) over 10-minute intervals, from February 2019 to September 2021. Subsequently, the MDO was deployed at 75 m depth (ca. 95 m above the sea floor) following inclusion of additional sensors on the mooring. This depth change has not impacted the observed temporal patterns since there was no change in the water mass sampled. Rapid event-scale fluctuations over periods of a few days at a time are evident for both temperature and DO (Fig. 2). During 2019–2021, there were seven hypoxic days, when DO levels decreased below 2 ml L^{-1} (Fig. 2b). In contrast, no hypoxia was observed in 2022–2023. Seasonal temperature changes were minimal, but April–July 2023 was ca. 0.5°C warmer than previous years (Fig. 3a). DO seasonality near Hondeklip Bay was marked by minima during winter and maxima in summer (Fig. 3b). This contrasted with DO seasonality further south in St Helena Bay, where minima usually occur at the end of the upwelling season, with maxima in winter. In 2023, the DO was ca. 1 ml L^{-1} higher than in previous years, indicating a much better oxygenated water column, possibly due to the overall lower phytoplankton biomass observed in the Hondeklip Bay region for most of the year (see Report Card 2). Continuous, long-term, high temporal resolution observations along the entire sBUS coast are required to determine where the change in DO seasonality occurs, and to better understand the impact of phytoplankton variability on DO changes.

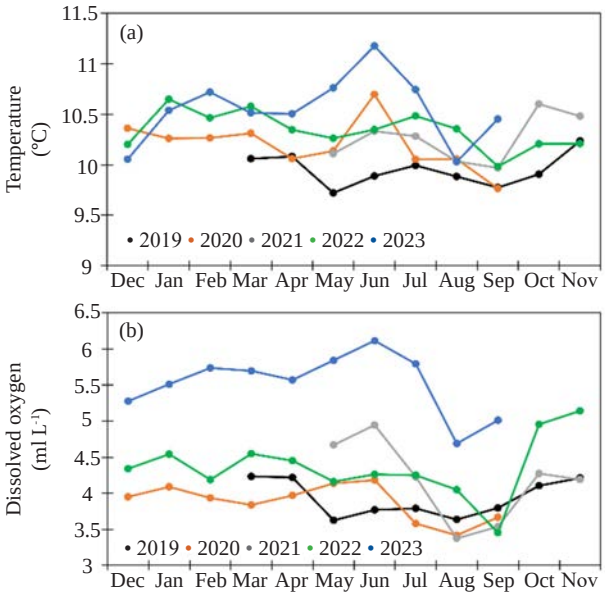

Figure 3. Monthly-averaged (a) temperature and (b) DO at the mooring near Hondeklip Bay.

Authors: Lamont T, van den Berg MA (OC Research); Lahajnar N (UHH); Rixen T (ZMT)

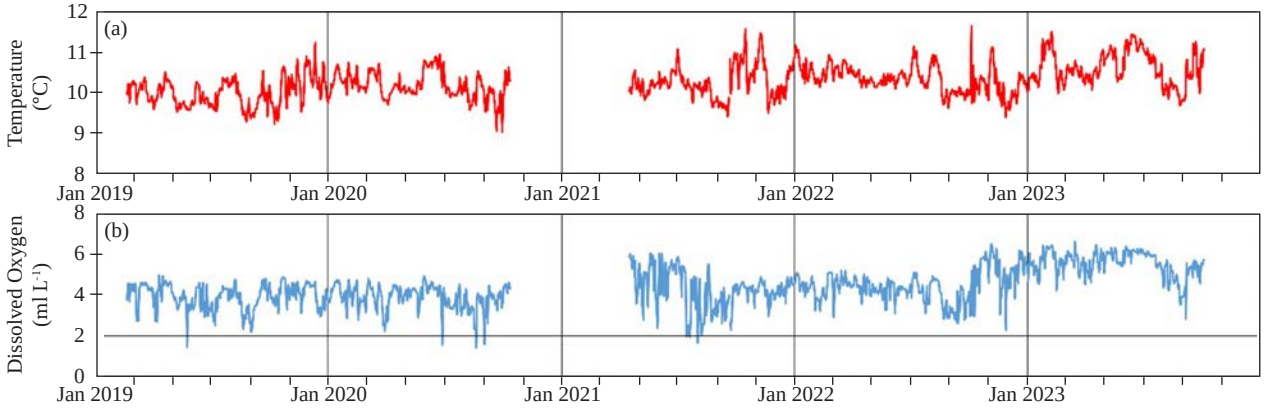

Figure 2. Daily-averaged (a) temperature and (b) DO at the mooring near Hondeklip Bay.

6. MONITORING OF INSHORE TEMPERATURES TO SUPPORT PHYSIOLOGICAL RESEARCH

To better understand the physiological effects of climate change and ocean acidification on marine organisms, information on the environmental conditions experienced in their natural habitats is required. Data from long term monitoring studies capture *in situ* variability of environmental parameters that are used to relate experimental findings with field conditions. Elands Bay on the west coast of South Africa is a key location for such research and monitoring. It is a popular location for west coast rock lobster fishing and therefore an important sentinel site for a commercial fishery species and the benthic communities upon which they depend. Low pH conditions exist along the west coast due to effects of upwelling, while cold-bottom waters in Elands Bay often result in low oxygen events responsible for mass walkouts of rock lobster. Additional exposure to extreme stressors associated with climate change can exacerbate impacts on their physiological processes. For example, acute thermal stress experienced during a marine heatwave may cause a rapid deterioration of cellular processes and performances beyond tolerance limits, affecting survival, growth and development. In South Africa, occurrences of marine heatwaves are increasing all along the coastline, and occur on average at least once a year. Data on temperature extremes are therefore important to design experiments and calculate thermal windows.

We initiated long-term monitoring of inshore environmental parameters in Elands Bay by deploying temperature loggers in representative habitat types: intertidal rock pools varying in surface area, volume and position along the shore, sun-exposed habitats, and subtidal habitats. In rock pools (Fig. 1a), temperature loggers attached to ibolts (Fig. 1b), recorded significantly higher temperatures compared to those housed in moorings (Fig. 1c and d), but were more often subject to theft, with loss of data.

During routine visits between November 2022 and June 2023, the subtidal mooring was found detached in nearby rock pools – representative subtidal temperatures are therefore only available from June 2023 onwards. Temperature measurements from November 2022 to October 2023 (Fig. 2), revealed autumn-winter minima of 5°C and 11°C in sun-exposed and subtidal habitats respectively, and a mean of 9°C in rock pools. Spring-summer maxima in sun-exposed and subtidal habitats were 40°C and 18°C, respectively, with a mean of 27°C in rock pools.

A series of floods due to heavy rainfall affected the west coast in September 2023. Consequently, rock pool 4 (Fig. 3a), the shallowest rock pool and situated furthest inshore, is now directly in the path of a steady flow of freshwater (Fig. 3b) that broke through from the nearby Verlorenvlei estuary. Warmer estuarine waters may therefore explain higher temperatures in rock pool 4 compared to those in 1–3 and 5 during September–October 2023 (Fig. 2). Storms with exceedingly high rainfall and flooding dilute seawater, and inshore, sessile or semi-motile invertebrates become physiologically stressed. Such organisms are particularly vulnerable to extreme weather events such as storms, floods, and marine heatwaves, since they cannot escape them. The flooding event emphasises the need for monitoring of other environmental parameters besides temperature in the Elands Bay area that may vary with extreme conditions, such as salinity, pH and dissolved oxygen levels.

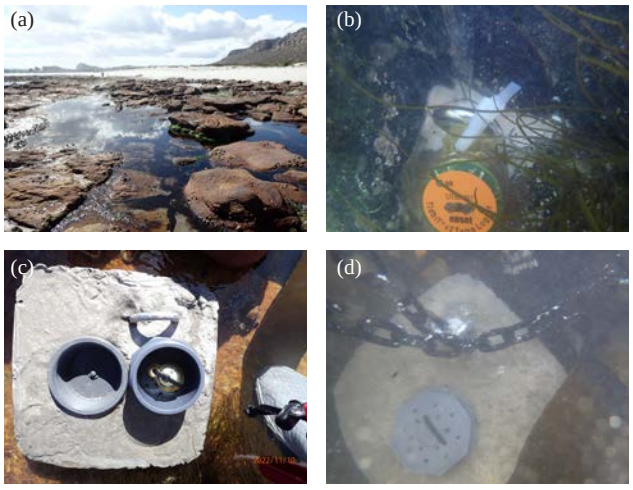

Figure 1. In intertidal rock pools (a), temperature loggers are attached via a cable tie to either an ibolt drilled into the rock (b), or housed inside a mooring block (c-d).

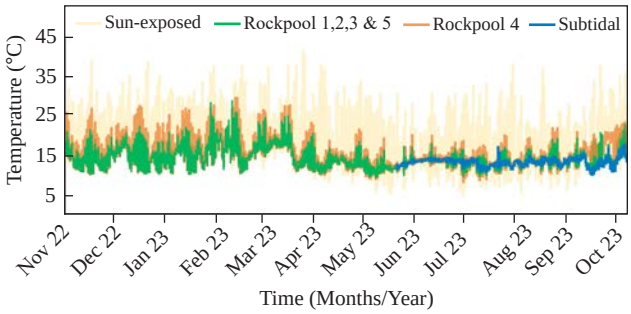

Figure 2. Temperatures of intertidal rock pools, including sun-exposed and subtidal habitats, from November 2022 to October 2023. Data are from the temperature loggers housed inside mooring blocks, which provided the most consistent dataset. Rock pool 4 (ibolt) was the exception and is therefore plotted separately from other rock pools.

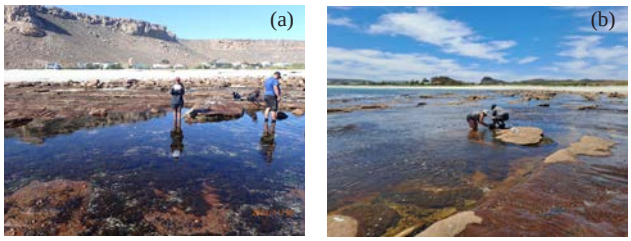

Figure 3. Rock pool 4 before (a) and after (b) the storm.

Authors: Haupt T, Janson L (OC Research); Auerswald L (Fisheries R&D)
Contributors: Snyders L (Fisheries R&D); Samaai T, Samuels K (OC Research)

7. SPATIO-TEMPORAL VARIABILITY OF SEA SURFACE CHLOROPHYLL *A* CONCENTRATIONS OFF THE WEST COAST OF SOUTH AFRICA

Phytoplankton has a major influence on marine ecosystem functioning through the production of oxygen and absorption of atmospheric CO_2. It therefore plays a critical role in maintaining marine life and mitigating climate change. Phytoplankton biomass depends on the rate of primary production (PP) in the ocean and is generally estimated by measuring chlorophyll *a* (chl *a*) concentrations. Understanding the distribution of PP in marine systems both in space and over time is important for ecosystem management, fisheries sustainability and monitoring the health of our oceans. Here we report on a 10-year dataset of sea surface chl *a* concentrations along the west coast of South Africa in summer (February) and winter (August), with a comparison of inshore and offshore regions (Fig. 1).

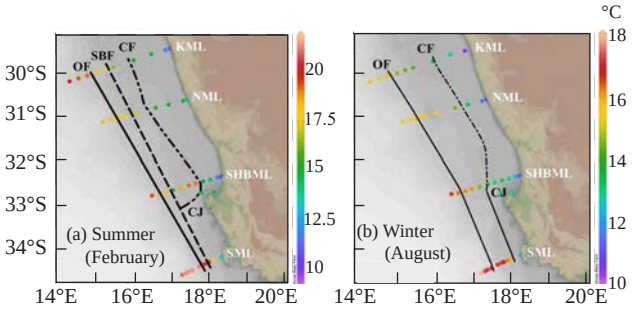

Figure 1. Map showing the west coast of South Africa and the locations of four monitoring lines (KML - Kleinsee, NML - Namaqua, SHBML - St Helena Bay, SML - Scarborough) in relation to important fronts (OF - Oceanic Front, SBF - Shelf Break Front, CF - Columbine Front, CJ - Cape Jet), in (a) summer (February) and (b) winter (August). Colours indicate sea surface temperatures (°C).

Seawater samples for chl *a* analysis were collected during the Integrated Ecosystem Programme: Southern Benguela (IEP: SB) cruises from 2013 to 2023, onboard the RS *Algoa*, using a Conductivity, Temperature, Depth (CTD) rosette. Sampling was conducted along four monitoring lines, namely Kleinsee (KML), Namaqua (NML), St Helena Bay (SHBML) and Scarborough (SML), with 10–14 stations each (Fig. 1). Inshore stations were defined as those within the Columbine Front (CF, at 15°C in summer and 14°C in winter), and offshore stations as those beyond the CF (Fig. 1). As the CF is absent from the southernmost monitoring line (SML) in summer, data for this line are not presented here. Chlorophyll *a* concentration was measured using a Turner Fluorometer.

In general, higher mean chl *a* concentrations were recorded for SHBML, for both the inshore and offshore regions, compared to KML and NML (Fig. 2). Whereas the interannual patterns for KML and NML corresponded closely with each other (especially inshore in summer and offshore in both seasons), SHBML showed greater variability with large fluctuations in some years. The higher values and distinct temporal patterns of SHBML compared to the other lines are not suprising, as this region is known to be highly productive due to pulsed enrichment from the Cape Columbine upwelling cell, and retention of nutrients due to circulation in the bay and isolation from strong alongshore currents. Inshore values were higher than offshore values along all the monitoring lines in both winter and summer. This highlights higher nutrient inputs in the inshore region, from terrestrial dust input, upwelling of nutrient-rich waters, river run-off, and other sources.

Seasonally, mean chl *a* concentration was significantly higher in summer (both inshore and offshore) than in winter. This indicates higher biological activity during summer resulting from greater light availability and greater stratification due to heating, leading to a shallower, more productive mixed layer. As more nutrients are supplied to the coastal waters, elevated chl *a* concentrations could lead to the development of harmful algal blooms, which are detrimental to marine life. Therefore monitoring chl *a* is key for informing coastal water management and needs to be maintained.

Authors: Mtshali T, Tsanwani M (OC Research)
Contributors: Kiviets G, Britz K, Vena K, Mdokwana B, Siswana K (OC Research)

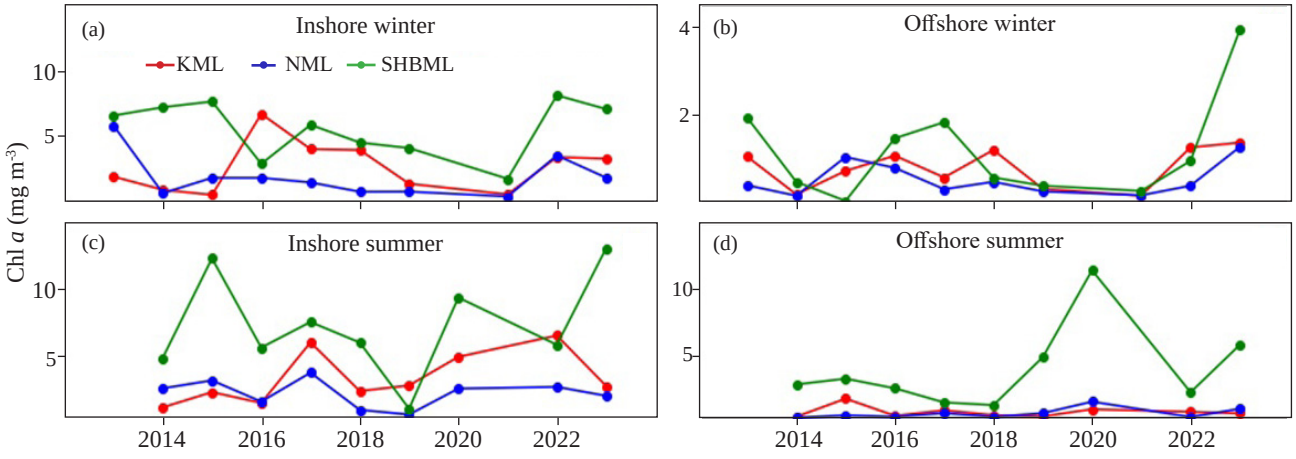

Figure 2. Time series of sea surface mean chl *a* concentration (mg m^{-3}) for (a) inshore and (b) offshore during winter, and (c) inshore and (d) offshore during summer, along the Kleinsee (KML), Namaqua (NML) and St Helena Bay (SHBML) monitoring lines.

8. SPATIO-TEMPORAL VARIABILITY OF SEA SURFACE DISSOLVED OXYGEN IN THE SOUTHERN BENGUELA

Dissolved oxygen (DO), the amount of oxygen present in seawater, is essential for marine life. Its concentration affects marine biogeochemical processes as well as the survival and distribution of marine organisms. However, DO concentrations in the ocean have been declining globally, especially in coastal waters, due to the impacts of climate change and warming ocean temperatures. Marine organisms that are vulnerable to low oxygen or 'hypoxia' conditions (such as some fish and lobsters) may be severely impacted by declining DO levels. Low oxygen events are characteristic of the southern Benguela Upwelling System (sBUS), thus it is important to monitor and understand DO bio-physico-chemical dynamics and hypoxia risk in this highly variable environment. Here we report on a 10-year dataset of the near-surface (1–5 m depth) DO concentrations obtained in the sBUS during winter (August) and summer (February), from both inshore and offshore waters.

Seawater samples for DO analysis were collected during the Integrated Ecosystem Programme: Southern Benguela (IEP: SB) cruises from 2013 to 2023 onboard the RS *Algoa*, using a CTD (Conductivity, Temperature, Depth) rosette. The DO concentrations were measured using a Winkler titration method. We used the Columbine Front (CF, at 15°C in summer and 14°C in winter, see Fig. 1 in Report 7,) as a cut-off between inshore and offshore waters. Samples from three monitoring lines are reported here, namely Kleinsee (KML), Namaqua (NML) and St Helena Bay (SHBML) Monitoring Lines.

In general, there was high variability in mean DO concentration between years for all lines, for both seasons, and for both inshore and offshore regions (Fig. 1). For offshore waters, the interannual patterns of the different lines tended to resemble one another quite closely (i.e. there was synchrony in fluctuations from year to year). This was not the case for inshore waters, however, where there was little correspondence in the temporal patterns between lines. Despite the variability, increasing trends in DO were apparent for all lines, for both seasons, and for both inshore and offshore regions. The most pronounced increase was observed offshore during summer along the SHBML (Fig. 1d), along with elevated chlorophyll *a* concentrations (see Fig. 2 in Report Card 7) and depletion of dissolved inorganic nitrogen (DIN) concentrations (see Fig. 1 in Report Card 9). This likely reflects the complex interplay between physical (upwelling) and biological (phytoplankton blooms) processes that are known to occur in this region. Upwelling brings cold and nutrient-rich deep waters to the surface waters, where it drives sunlit ocean productivity that facilitates the air-sea carbon dioxide exchange through photosynthesis, with the release of oxygen.

Overall, the lowest mean DO concentration of 3.7 ml L^{-1} was recorded in 2017 along KML (summer, inshore region), which was lower than the minimum value of 4 ml L^{-1} required for survival of pelagic fish populations. A DO concentration of 7.8 ml L^{-1} was recorded in 2022 along the SHBML, indicating supersaturation, which can be detrimental to marine organisms. Despite the global ocean decline in DO concentrations, our results exhibited increasing trends in surface DO concentration in the sBUS, indicating that this region is becoming supersaturated. This can have harmful effects on marine life, with potentially negative consequences for pelagic fisheries. Hence, the spatio-temporal distributions of DO concentrations need to be monitored.

Authors: Mtshali T, Tsanwani M (OC Research)
Contributors: Kiviets G, Britz K, Vena K, Mdokwana B, Siswana K (OC Research)

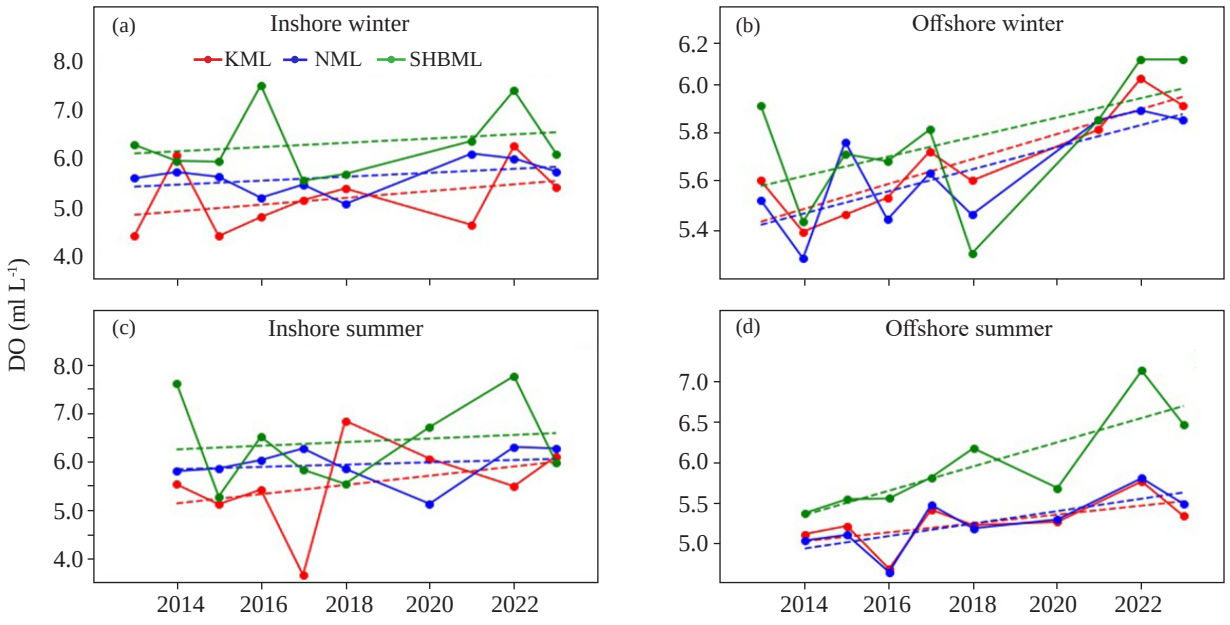

Figure 1. Trends of mean DO concentrations (ml L^{-1}) for (a) inshore and (b) offshore time series of measurements during winter, and (c) inshore and (d) offshore time series of measurements during summer, along three monitoring lines (Kleinsee - KML, Namaqua - NML, St Helena Bay - SHBML). Dashed lines are lines of best fit included to show the trends. Note the scale differences in the y-axis.

9. SPATIO-TEMPORAL VARIABILITY OF SEA SURFACE MACRONUTRIENT CONCENTRATIONS IN THE SOUTHERN BENGUELA

Phytoplankton succession and community composition reflect the environmental conditions of the ecosystem, with the availability of macronutrients, [DIN = Nitrate (NO_3^-) + Nitrite (NO_2^-), Phosphate (PO_4^{3-}) and Silicate (SiO_4^{4-})], playing a significant role in their growth. However, an increased supply of macronutrients to coastal waters can lead to increased phytoplankton biomass production that can disturb the natural ecological balance of marine ecosystems. Here, we report on a 10-year dataset of interannual variation in surface (1–10 m depth) macronutrient concentrations within the southern Benguela Upwelling System (sBUS) during summer (February) and winter (August).

Seawater samples for macronutrient analysis were collected during the Integrated Ecosystem Programme: Southern Benguela (IEP: SB) cruises onboard the RS *Algoa* using a CTD (Conductivity, Temperature and Depth) rosette along three monitoring lines from 2013 to 2023, namely the Kleinsee (KML), Namaqua (NML) and St Helena Bay (SHBML) monitoring lines (see Fig. 1 in Report Card 7). To characterise our dataset, we used the Columbine Front (CF, at 15°C in summer and 14°C in winter) as a cut-off between inshore and offshore regions.

Sea surface distributions of the mean macronutrient concentrations were highly variable, with both increasing and decreasing trends observed, but were generally higher in winter than in summer (Fig. 1). This reflects enhanced mixing and entrainment of nutrient-rich deep waters into the surface layers as well as increased nutrient inputs from river outflows in winter, and greater biological uptake in summer due to increased light availability. Concentrations inshore were higher than those offshore during both summer and winter. Coastal waters are characterised by complex and variable dynamics, as they are subject to both internal and external inputs. These include upwelling of deep nutrient-rich waters, recycling, deposition of dust inputs from land, and human activities (e.g. wastewater and sewage discharge and agriculture). In contrast, the offshore region is almost unaffected by human factors and natural influences such as dust deposition. Here, the macronutrient concentrations are usually lower with reduced variability.

Seasonally, high macronutrient concentrations were observed along the KML in winter for both inshore and offshore regions (Figs. 1a, b), while in summer, elevated concentrations of SiO_4^{-4} and PO_4^{3-} were recorded along the SHBML (Figs. 1c, d). A pronounced drawdown of DIN (both offshore and inshore) and PO_4^{3-} (offshore region only) concentrations was observed along the SHBML during summer, indicating high biological uptake. This is in line with the SHBML being one of the most productive areas in the sBUS and is further reflected in the elevated chorophyll *a* concentrations observed along this monitoring line (see Fig. 2 in Report Card 7). During summer, DIN concentrations were depleted to zero in some years (both inshore and offshore), likely reflecting the occurrence of early and intense phytoplankton blooms, which would have reduced the nutrient concentrations.

Interannual macronutrient variability in coastal waters can have far-reaching implications for marine ecosystems, for example by triggering harmful algal blooms or shifts in phytoplankton species composition. These, in turn, can affect the entire marine food web, with consequences for pelagic fish species.

Authors: Mtshali T, Tsanwani M (OC Research)
Contributors: Kiviets G, Britz K, Vena K, Mdokwana B, Siswana K (OC Research)

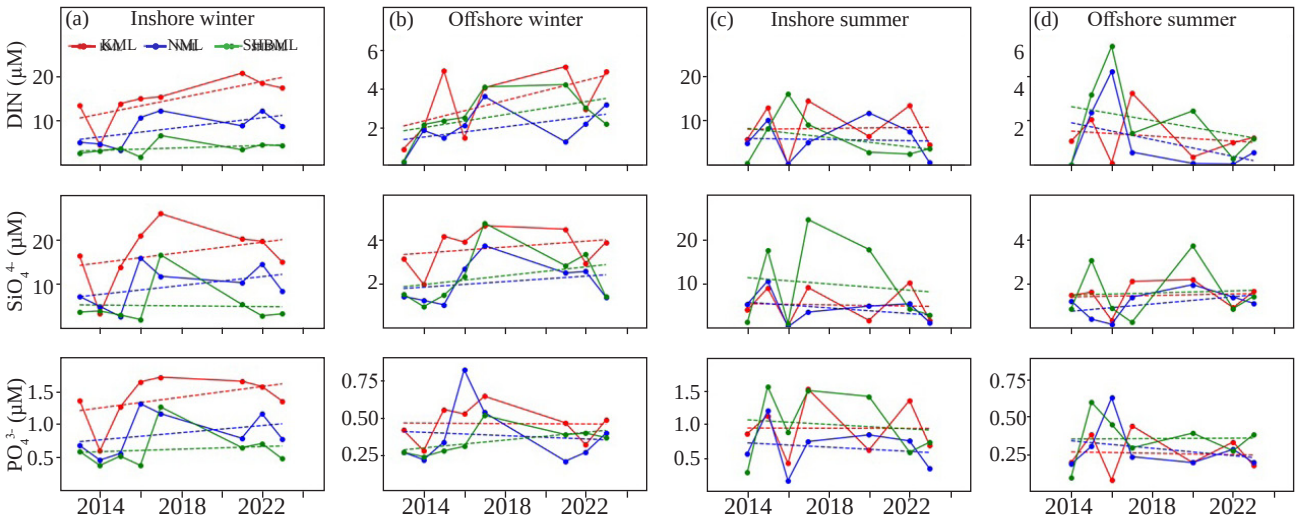

Figure 1. Interannual variability of the mean DIN (upper panel), SiO_4^{4-} (middle panel) and PO_4^{3-} (lower panel) concentrations (µM) along three monitoring lines - Kleinsee (KML), Namaqua (NML) and St Helena Bay (SHBML). Columns (a) and (b), and (c) and (d), show data for the inshore and offshore regions, in winter and summer respectively, with dotted lines representing linear fits. Note different scales for Y-axes. Standard deviations are excluded for clarity.

10. MICROZOOPLANKTON ABUNDANCE OFF THE WEST COAST OF SOUTH AFRICA

Microzooplankton are a group of planktonic organisms that range from 20–200 µM. They include heterotrophic (obtain energy and nutrients from other organisms) and mixotrophic organisms (can obtain energy and nutrients from other organisms, or produce their own). The group comprises flagellates, radiolarians, foraminiferans, ciliates including tintinnids, copepod nauplii, among others, and plays a key role in many ecosystem processes. They are primary grazers of marine phytoplankton, major secondary producers (the intermediary between primary producers and copepods), and are instrumental in nutrient and carbon cycling. Their relatively short life cycles (ranging from one week to a year) and rapid responses to environmental changes allow them to be used as robust indicators in marine ecosystems. Little is known about their abundance and impacts on the ecosystem off the west coast (Fig. 1).

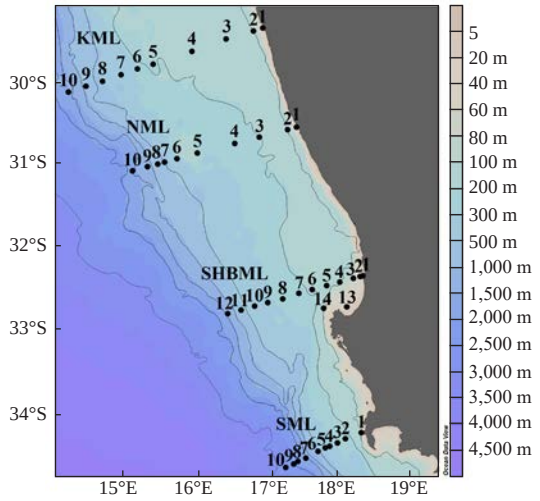

Figure 1. Map of the west coast indicating sampling stations along four Integrated Ecosystem Programme (IEP:SB) monitoring lines, namely Kleinsee (KML), Namaqua (NML), St. Helena Bay (SHBML), and Scarborough (SML) Monitoring Lines.

The Integrated Ecosystem Program (IEP: SB) samples four monitoring lines biannually (Fig. 1). Here, we present data from August (winter) and February (summer) of 2018–2020, for surface microplankton abundance, which was assessed for each station using FlowCam© and VisualSpreadsheet software. Abundance of the most prevalent microzooplankton groups, including naked ciliates (without a shell), tintinnids (with a shell) and copepod nauplii (Fig. 2), was calculated for each station (Fig. 3).

In general, higher microzooplankton abundance was observed inshore of Station 4 for Kleinsee (KML) and St Helena Bay (SHBML) Monitoring Lines, and Station 3 for Namaqua Monitoring Line (NML) (Fig. 3a-c). In contrast, higher abundance occurred offshore of Station 4 for Scarborough (SML) (Fig. 3d). With a few exceptions, where copepod nauplii were more abundant, tintinnids and ciliates were the largest contributors to the high microzooplankton abundances in the coastal region. These findings

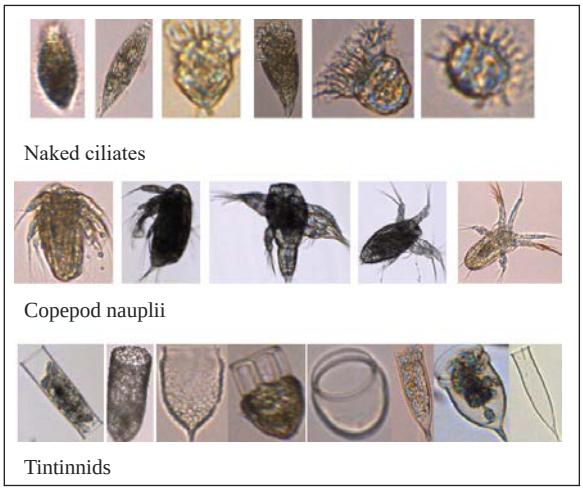

Figure 2. Selected images of some of the observed microzooplankton groups.

were not surprising for the three monitoring lines, given that phytoplankton biomass, which is the main food source for tintinnids, is usually elevated in these regions, thus allowing tintinnids to thrive in the coastal region. Copepod nauplii, which are an important food source for larval pelagic fish, were more prevalent during winter (peak pelagic fish recruitment season off the west coast) than in summer, along all monitoring lines (Fig. 3). In contrast, such large seasonal differences were not observed for tintinnids and ciliates.

Historically, there have not been any similar detailed investigations of tintinnids, copepod nauplii, and naked ciliates for the west coast. Thus, this study describes previously undocumented variations in the cross-shelf distributions and seasonal changes for these microzooplankton. Further research is required to better understand the spatial and temporal variability of these groups and their impact on primary and secondary producers.

Authors: Maduray S, Soeker MS, Worship M (OC Research)
Contributor: Mdazuka Y (OC Research)

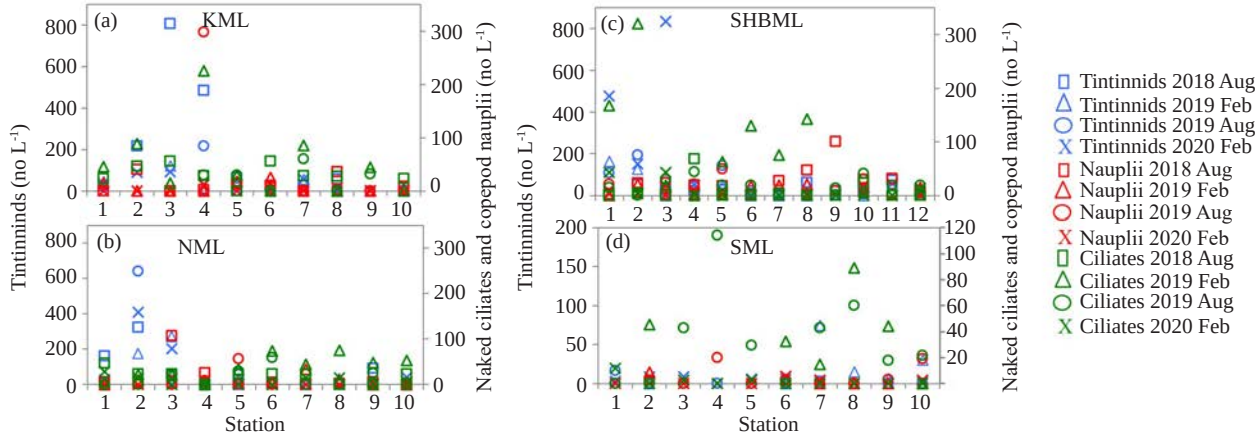

Figure 3. Abundance of microzooplankton groups along the four monitoring lines (a) KML (b) NML (c) SHBML (d) SML, from inshore (Station 1) to offshore (Station 10 for KML, NML, SML, and Station 12 for SHBML). Note the different y-axis scales.

11. LONG-TERM VARIABILITY OF DOMINANT COPEPOD TAXA ON THE AGULHAS BANK

Copepods dominate the zooplankton community on the Agulhas Bank (AB) off South Africa (Fig. 1), providing an important food resource for pelagic fish and other biota. Studies have shown a long-term decline in biomass of *Calanus agulhensis*, a key species strongly associated with the productive cold ridge of upwelled water on the central and eastern AB. However, it was unknown whether the biomass of other common copepod taxa had also changed over time. To address this question, zooplankton samples were collected annually in late spring during hydro-acoustic stock-assessment surveys of pelagic fish on the AB. Samples were then analysed to explore variability in biomass of the copepod community over 24 years (1988–2011).

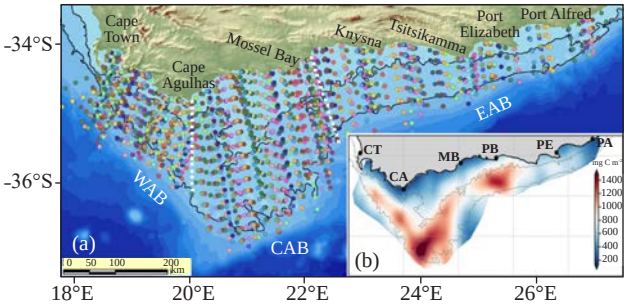

Figure 1. (a) Map of the Agulhas Bank, showing stations where samples were collected. Dashed white lines separate the western (WAB), central (CAB) and eastern Agulhas Bank (EAB); (b) distribution of mean total copepod biomass (mg C m^{-2}).

Eight taxa collectively comprised 94% of total copepod biomass on the AB (Fig. 2). Mean total copepod biomass declined significantly over the 24-year time series (Fig. 2a), but patterns of interannual variability in biomass varied between the dominant copepod taxa (Fig. 2). The long-term pattern for *C. agulhensis* (Fig. 2b) was similar to that for total copepod biomass, with very high levels in 1988 on the central (CAB) and eastern (EAB) AB, and a significant long-term decline thereafter. There was also a significant decline for the small calanoid taxa, despite marked fluctuations (Fig. 2c). There were no significant trends in biomass for the other dominant copepod taxa over the study period, with most showing considerable interannual variability in all areas of the AB. Biomass of *Metridia lucens*, abundant in the Benguela upwelling system, was greatest but most variable on the western AB (WAB). Biomass of the upwelling-associated *Calanoides natalis* was also very high on the CAB and EAB in 1988 compared to subsequent years (Fig. 2e), but the decline was not significant when 1988 data were excluded. *Centropages* spp. showed strong (3 to 4-fold) interannual variability in biomass for all areas (Fig. 2f). Biomass of the Oncaeidae was particularly high (>3 times above average) in 1995 (Fig. 2g), with moderate interannual variability in other years. Similarly, biomass of the tiny but abundant Oithonidae was >3 times above average in both 1995 and 1996 (Fig. 2i). The significant decline in total copepod biomass over the 24-year time series was driven by declines in both the large calanoid *C. agulhensis* and small calanoids, which together comprised 73% of total copepod biomass. This decline is thought to be strongly linked to predation by planktivorous fish which increased in biomass during the latter part of the time series. The role of environmental forcing during the study period was not clear, but long-term ocean warming could result in smaller copepods, lower copepod biomass and reduced fisheries production.

Authors: Huggett JA (OC Research); Noyon M (NMU); Carstensen J (Aarhus University, Denmark); Walker DR (CPUT)

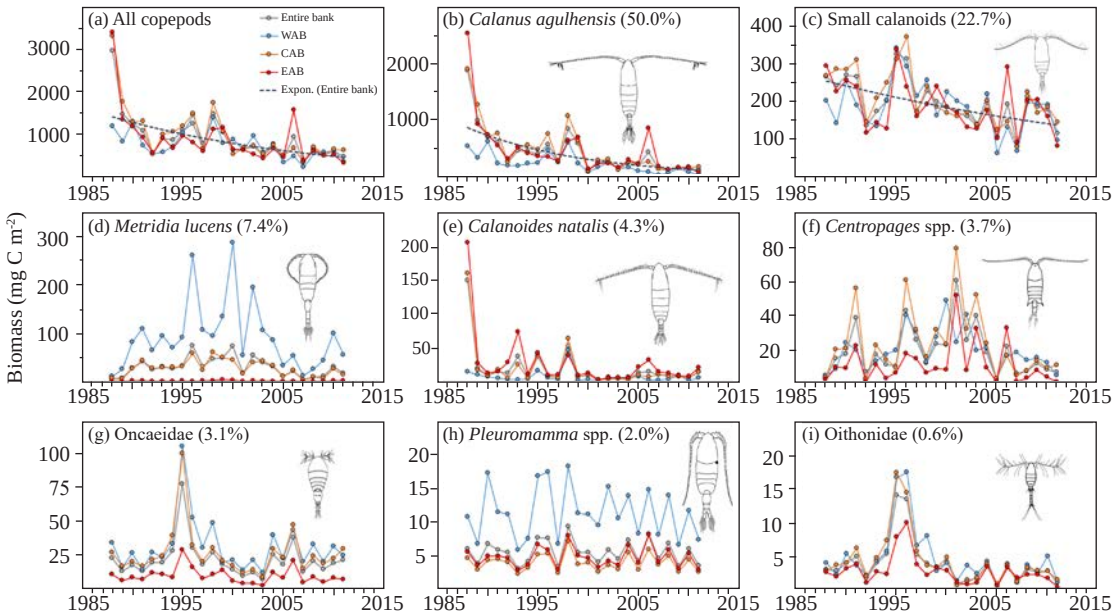

Figure 2. Time series of mean biomass (mg C m^{-2}) for (a) all copepods, (b) *Calanus agulhensis*, (c) small calanoids (Paracalanidae and Clausocalanidae), (d) *Metridia lucens*, (e) *Calanoides natalis*, (f) *Centropages* spp., (g) *Oncaeidae*, (h) *Pleuromamma* spp., (i) *Oithonidae* over the entire Agulhas Bank (grey lines), and for the western (WAB; blue lines), central (CAB; orange lines) and eastern (EAB; red lines) sectors, during late spring from 1988–2011. Exponential (best) fits are shown for the entire bank, where significant trends were found. Note the different y-axis scales. Numbers in brackets indicate percentage (%) of total copepod biomass comprised per taxon. Line drawings of female copepods are not to scale. Mean total lengths range from 0.79 mm (Oithonidae) to 3.22 mm (*Pleuromamma* spp.).

12. CHLOROPHYLL *A* VARIABILITY ACROSS THE AGULHAS CURRENT

The Agulhas Current is a strong, narrow and warm ocean current that flows southwestward along the east coast of South Africa (Fig. 1). It plays an important role in the transport of heat and salt from the Indian to the Atlantic Ocean. The Agulhas System Climate Array (ASCA) transect is a line of stations extending 300 km offshore across the width of the Agulhas Current (AC), aligned perpendicular to the coast near East London (Fig. 1). Monitoring of environmental conditions along the ASCA transect was initiated to improve understanding of the role that the AC plays in the climate system. One of the essential ocean variables that is measured is phytoplankton variability, which can provide valuable insights into ecosystem functioning and nutrient cycling.

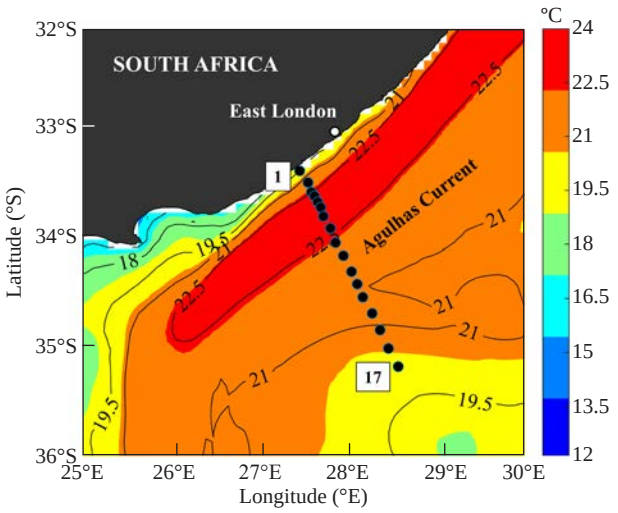

Figure 1. The southeast coast of South Africa, showing sea surface temperature (°C) and the locations of 17 ASCA transect stations from inshore (Station 1) to offshore (Station 17).

During June 2023, water samples were collected from 17 stations (six depths per station) along the ASCA transect (Fig. 1) during a cruise on the SA *Agulhas* II. We measured chlorophyll *a* (chl *a*) concentration, a proxy for phytoplankton biomass, including the contribution of three size classes to total chl *a*. Glass-fibre filters with various pore sizes were used for filtration, namely 10 µm to retain microphytoplankton, 2.7 µm for nanophytoplankton, and 0.3 µm for picophytoplankton. Fluorescence values were converted to chl *a*, allowing the contribution of each size class to be determined for each station.

Figure 2 shows the mean total chl *a* (average of six depths; 0–130 m) at each station. Mean chl *a* biomass was highest inshore (Stns 1–2; 0.98 mg m^{-3}), lower across the AC core (Stns 3–8; 0.55 mg m^{-3}) and higher again at the current edge (Stns 9–11; 0.7 mg m^{-3}; Fig. 2). Nanophytoplankton was the dominant size class with a chl *a* contribution of >50% across all stations, and the largest contribution inshore (0.7 mg m^{-3}; 73%). Of the three groups, microphytoplankton generally showed the lowest contribution (<0.1 mg m^{-3}; 10%) with decreased biomass at the offshore stations (Fig. 2). Picophytoplankton showed an increase in chl *a* contribution at the station farthest offshore (Stn 17; 0.4 mg m^{-3}; 55%; Fig. 2).

The Agulhas Current System is considered a low-nutrient environment. The observed high contribution of nano- and picophytoplankton aligns with the notion that cells exhibiting a small surface area-to-volume ratio dominate nutrient-poor ecosystems. Mechanisms such as turbulence and unfavourable light conditions from possible turbidity could explain the low biomass observed for microphytoplankton, but further research is required to confirm this. Our study contributes toward improved understanding of phytoplankton biomass and size distributions in the region, and their role in ecosystem functioning across the Agulhas Current. While a similar distribution could be expected during June each year, more frequent sampling is recommended to assess not only interannual variability, but also seasonal and event-scale variability in phytoplankton biomass.

Authors: Kupczyk A (OC Research, CPUT); Walker D (CPUT)
Contributor: Meyer S (CPUT)

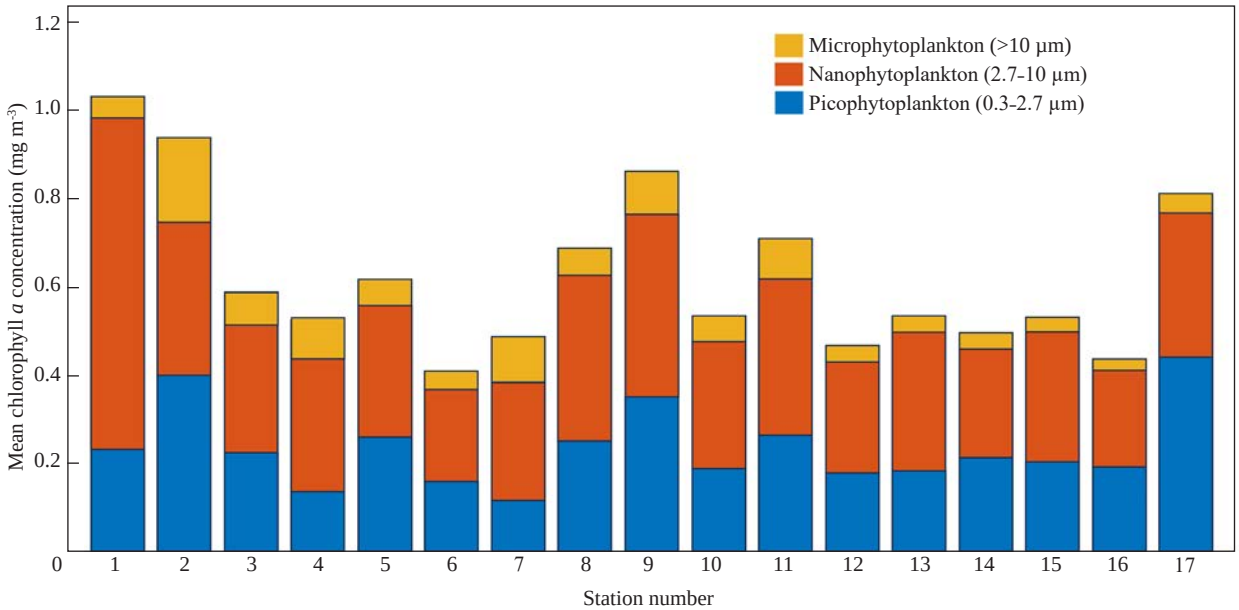

Figure 2. Distribution of mean total chlorophyll *a* concentration (mg m^3) and phytoplankton size classes across the ASCA transect. Station 1 represents the inshore station, and station 17 represents the offshore station.

13. IS THE AGULHAS CURRENT INCREASING ITS TENDENCY TO EARLY RETROFLECT?

The Agulhas Current (AC) is the warm and energetic Western Boundary Current (WBC) located along South Africa's east and south coasts (Fig. 1). It is one of the five major subtropical WBCs in the world, responsible for the poleward distribution of equatorial waters. The AC's westernmost location, known as the Agulhas Retroflection region (AR), typically occurs south of Cape Town, between 16°E and 22°E. Here, warm and saline Indian Ocean water is transported into the Atlantic Ocean. This process is known as Agulhas leakage, which has strong regulatory effects on the global thermohaline circulation, as well as on global climate. On occasion, the AC retroflects considerably further east than usual, with such events known as early retroflections (ERs). While ERs can substantially impact the regional shelf ecosystems, they can also alter Agulhas leakage, which could have considerable global implications.

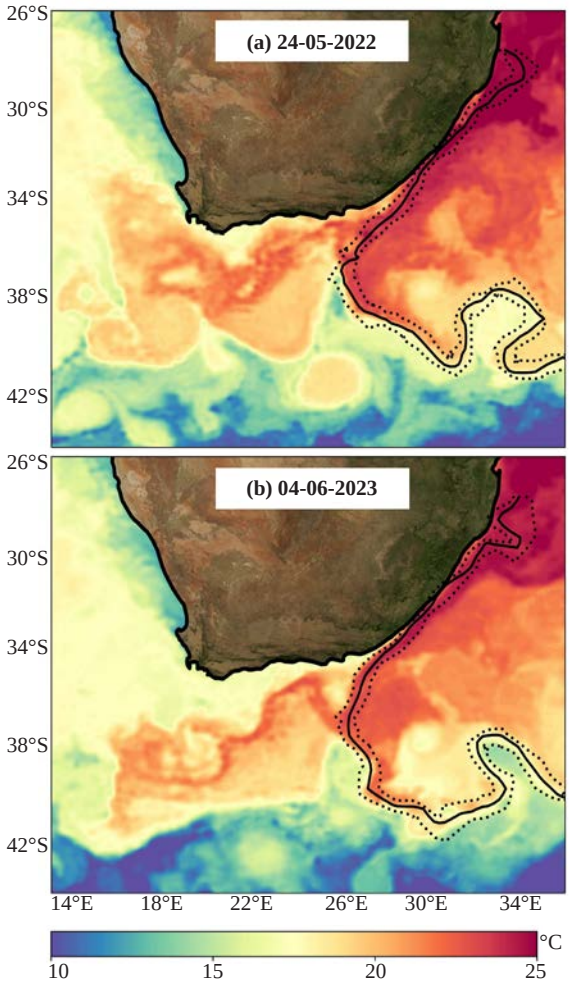

Figure 1. The location of the Agulhas Current (AC) core (solid black line) and edges (dotted black lines), indicating the start day of the (a) 2022 and (b) 2023 early retroflection events. Colour shading indicates daily near-real time sea surface temperature (°C).

The location of the AR is monitored through the application of the LACCE (Location of the Agulhas Current's Core and Edges) tool to daily satellite altimetry data. Figure 2 shows the longitudinal position (°E) of the AR from 1993 to 2023, and the considerable movement of the AR illustrates its dynamic nature. ERs are indicated by the retreat of the AR east of 22.54°E. Over the last 31 years, there were seven ERs, with the majority occurring in the latter half of the time series (Fig. 2).

The largest and longest lasting ER (142 days) occurred from October 2000 to March 2001, when the AR retreated as far east as 27.95°E. The second longest ER event (42 days) occurred in 2008, after several years with no ERs (Fig. 2). While most previous ERs occurred during austral summer and spring, it is noteworthy that there have been two ERs in the last two years that occurred during winter and autumn. In 2022, a 22-day (fourth longest) ER began on 24 May 2022 (Fig. 1a). In 2023, a 27-day (third longest) ER began on 4 June 2023 (Fig. 1b).

Figure 2 suggests an increased frequency of ERs in recent years, in agreement with studies that have shown an increase in the number of Agulhas meanders (cyclonic eddies embedded in the AC), which are known to trigger ERs. An increase in the frequency of ERs could result in reduced production on the south coast shelf through more frequent offshore advection of biological communities. It could also influence global climate through reduced amounts of Agulhas leakage into the Atlantic Ocean. Longer time series and continued monitoring are required to determine if this pattern indeed indicates a long-term trend, or whether it is simply reflecting previously unobserved interannual variability of the AR.

Authors: Russo CS, Lamont T (OC Research)

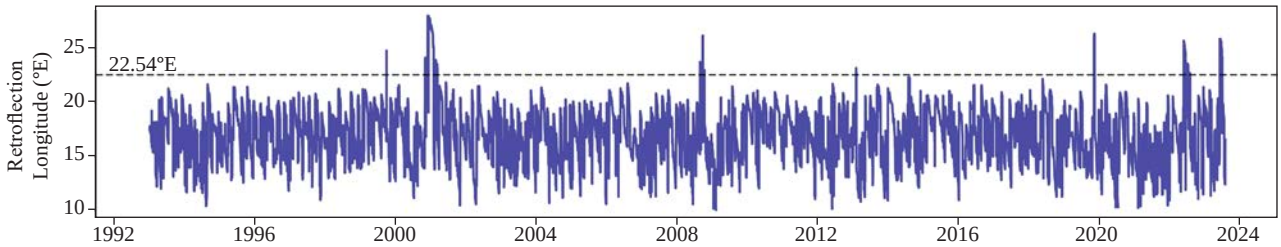

Figure 2. Time series of the longitude (°E) of the Agulhas Retroflection as identified by the LACCE monitoring tool. The black dashed line illustrates the cut-off longitude of 22.54°E used to identify early retroflections.

14. LONG-TERM OBSERVATIONS OF CURRENTS ON THE PRINCE EDWARD ISLANDS SHELF

The Prince Edward Islands (PEIs) are a remote island archipelago in the sub-Antarctic zone of the Southern Ocean. They provide crucial breeding habitat for vast populations of seabirds and marine mammals. It is well-known that there are strong links between the oceanography and biological communities at the PEIs, but observations have been largely limited to periods coinciding with annual island relief voyages in April–May. To contribute to long-term oceanographic observations, two moorings deployed on the inter-island shelf (Fig. 1) have been providing continuous measurements of water column current speed and direction since April 2014.

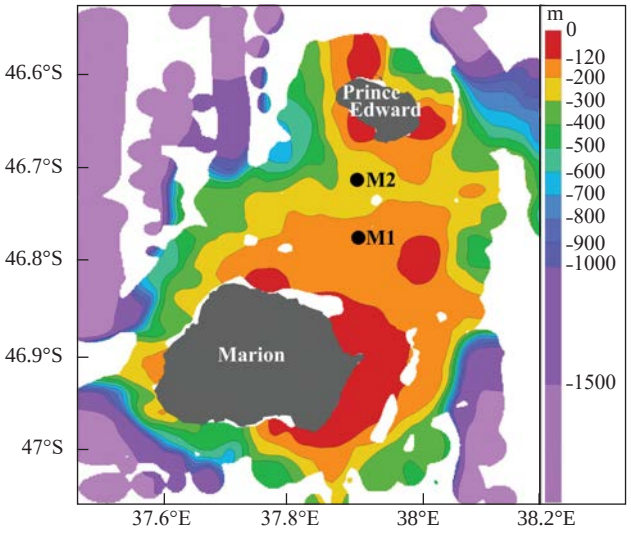

Figure 1. The Prince Edward Islands (PEIs) showing the bathymetry of the PEI shelf. Mooring positions M1 and M2 are shown as black dots.

The eastward-flowing Antarctic Circumpolar Current results in much stronger zonal (east/west) than meridional (north/south) flow at the PEIs. During 2014–2023, daily mean current speeds at mooring M1 ranged between 0.01 and 50.90 cm s^{-1}, while those at M2 varied from 0.03 to 67.32 cm s^{-1}. A Taylor column (stationary anticyclonic circulation over the shelf) is indicated by westerly flow in the bottom waters at M2 (Fig. 2). This westerly flow is persistent but can be enhanced or interrupted for short periods when fronts or mesoscale eddies interact with the PEI shelf. Retention of nutrients and biota by the Taylor column maintains enhanced productivity on the shelf, accounting for the high concentrations of marine biota at the PEIs.

Two periods of notably increased eastward flow (>34.00 cm s^{-1}), with rapid switching to strong westward flow, occurred during June–August 2022, and March–April 2023 (Fig. 2). Increased eastward flow resulted from northward migration of the southern branch of the sub-Antarctic Front (S-SAF), while the subsequent westward flow was due to cyclonic eddies which formed northeast of the PEIs, as the S-SAF migrated south again

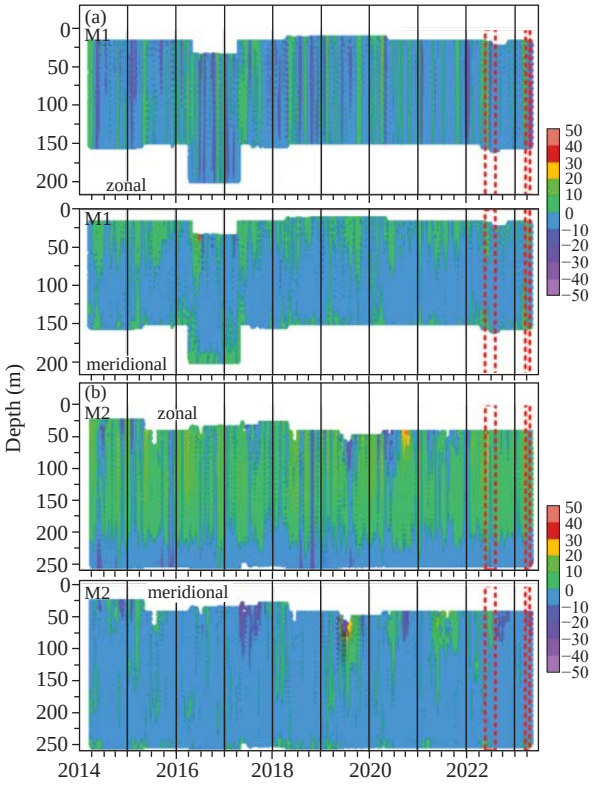

Figure 2. Daily mean zonal and meridional current components (cm s^{-1}) at M1 (a), and M2 (b), from 2014–2023. Positive values denote eastward (zonal) and northward (meridional) flow; negative values denote westward (zonal) and southward (meridional) flow. Dashed red boxes highlight cooling events during 5 June–7 August 2022 and 23 March–23 April 2023.

(Fig. 3). Both events resulted in cooling on the shelf (see Report Card 15). Changes in the direction of current flow may influence the distribution of preferred prey, and hence the feeding patterns of seabirds and marine mammals breeding at the PEIs. Detailed comparisons between current patterns and the feeding behaviour, diet, and reproductive performance of selected predators are required to evaluate the impact of these changing flow dynamics on top predators.

Authors: van den Berg MA, Lamont T (OC Research)
Contributors: Jacobs L, Louw GS (OC Research)

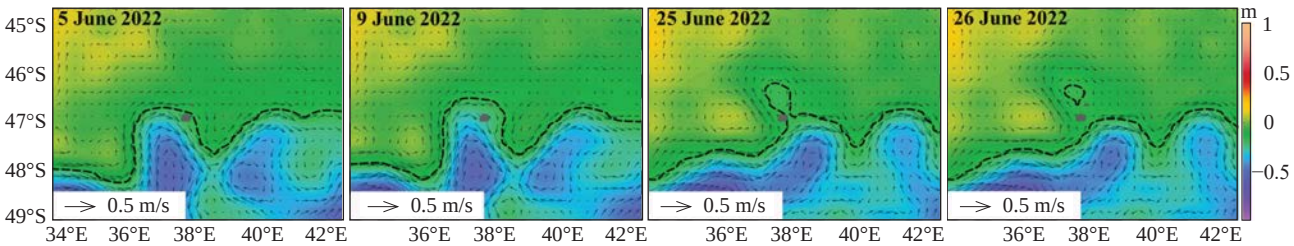

Figure 3. Selected maps of sea surface height (m), with the southern branch of the sub-Antarctic Front (S-SAF), indicated by the dashed black contour line.

15. LONG-TERM VARIABILITY IN BOTTOM TEMPERATURE ON THE PRINCE EDWARD ISLANDS SHELF

Despite their small size, the Prince Edward Islands (PEIs) provide crucial breeding habitat for vast populations of marine mammals and birds that depend strongly on the ambient oceanographic conditions at and around the islands. While annual relief voyages to re-supply the research base only allow hydrographic data collection during April–May each year, two moorings on the inter-island shelf (Fig. 1) have been providing continuous measurements of bottom temperature since 2014.

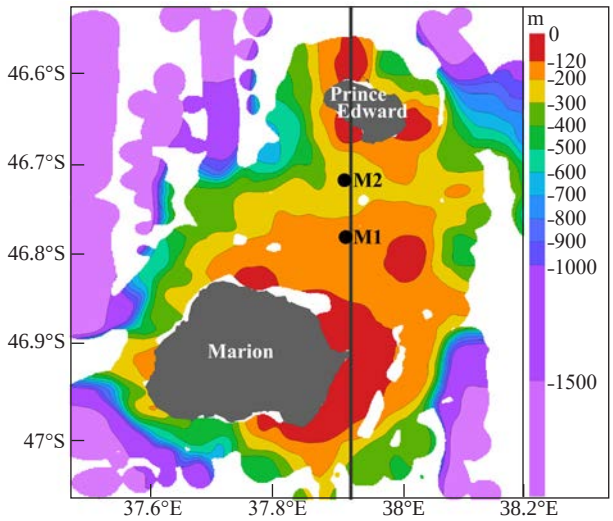

Figure 1. The Prince Edward Islands (PEIs) showing the bathymetry of the PEI shelf. Mooring positions M1 and M2 are shown as black dots. The vertical solid black line indicates 37.875°E longitude, along which the sea surface height data in Figure 3 was extracted.

Bottom temperatures exceed the long-term (2014–2023) mean for extended periods when the southern branch of the sub-Antarctic Front (S-SAF) is located south of the PEIs. In contrast, when the S-SAF is north of the PEIs, temperatures are below the long-term mean. During 2014–2017, overall lower temperatures reflected more frequent northward excursions of the S-SAF (Fig. 2). Since 2018, generally elevated temperatures indicate a more southerly location of the S-SAF. This pattern of S-SAF variability was also observed in satellite altimetry data (Fig. 3). While five notable cooling events occurred during 2021, there were only two such events in 2022–2023. The first occurred from 5 June–7 August 2022, and the second lasted from

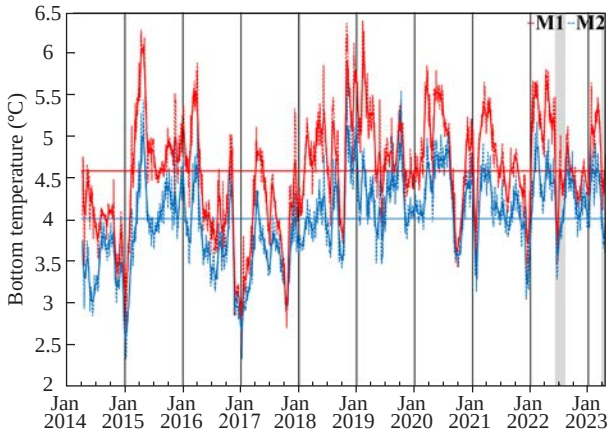

Figure 2. Daily mean bottom temperature (°C) at moorings M1 (red) and M2 (blue). Dashed lines indicate measurements while solid lines show low-pass filtered values. Horizontal lines show mean temperatures for each mooring across the time series (2014–2023). Grey shading highlights cooling events during 2022 and 2023.

23 March–23 April 2023 (Fig. 2). Both events resulted from northward movements of the S-SAF, combined with subsequent cooling from cyclonic eddies after the S-SAF had migrated south again (see Report Card 14). Temperature variations could affect the distances that seabirds and marine mammals have to travel from the islands to find food. This has consequences for time and energy spent foraging, for the survival of dependent young, and ultimately for the reproductive success and abundance trends of these populations. The reduced cooling likely means less food availability at the PEIs, and hence longer travel times for seabirds and marine mammals.

Authors: van den Berg MA, Lamont T (OC Research)
Contributors: Jacobs L, Louw GS (OC Research)

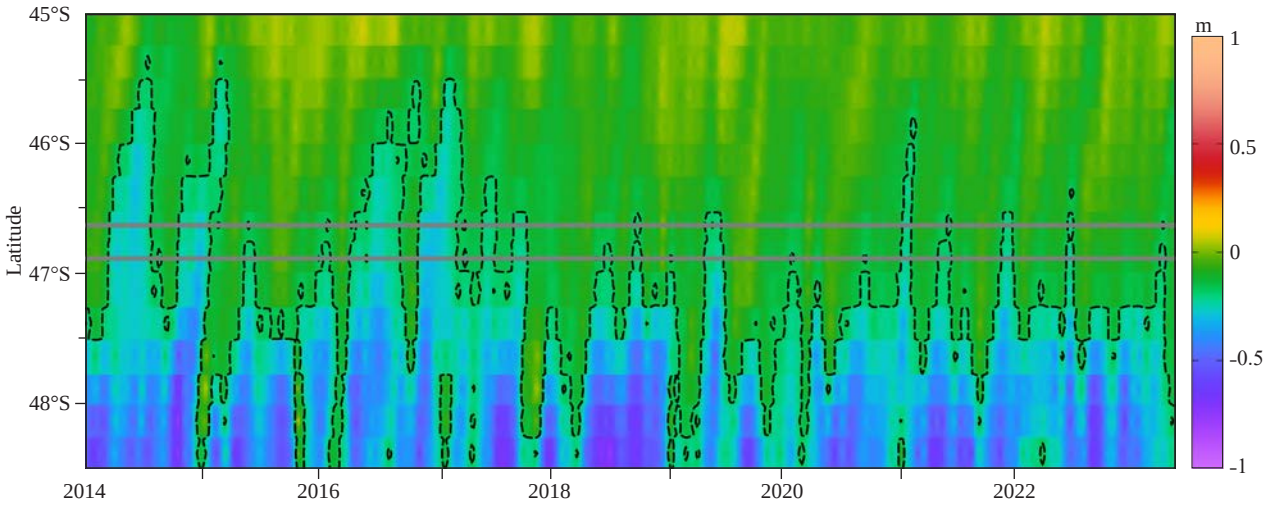

Figure 3. Time series of sea surface height extracted along 37.875°E longitude. The southern branch of the sub-Antarctic Front (S-SAF) is shown as a dashed black contour line. The solid horizontal grey lines indicate the locations of Prince Edward Island and Marion Island, respectively.

16. DECADAL VARIATION IN TEMPERATURE AND CURRENT SPEED AT THE PRINCE EDWARD ISLANDS

The oceanic region surrounding the sub-Antarctic Prince Edward Islands (PEIs) in the Southern Ocean (Fig. 1) provides necessary feeding habitat for the large populations of marine mammals and seabirds that seasonally breed on the islands. To better understand the influence of oceanographic conditions on long-term population trends for these species, it is necessary to determine the long-term oceanographic changes that have occurred. We investigated decadal variations in reanalysis (blended observations and model output) sea surface temperature (SST) and satellite surface geostrophic current speed at the PEIs, and examined how well the GLORYS (Global Ocean Reanalysis and Simulations) reanalysis model simulated these variations.

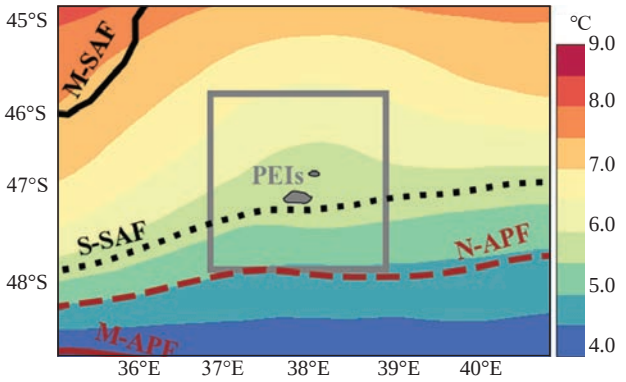

Figure 1. Long-term (1993–2022) mean sea surface temperature around the PEIs. Long-term mean positions of the middle (M-SAF) and southern (S-SAF) branches of the sub-Antarctic Front, and the northern (N-APF) and middle (M-APF) branches of the Antarctic Polar Front are indicated. The box indicates the 2° x 2° area over which the data in Figures 2 and 3 were averaged.

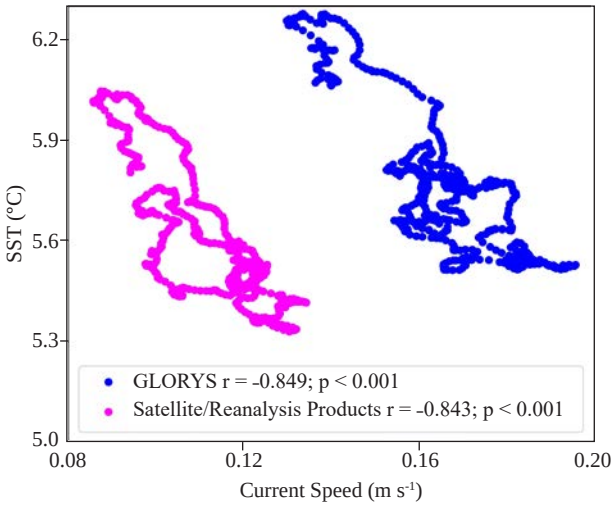

Figure 2. Scatterplots showing the relationship between the 5-year running means of SST (°C) and geostrophic current speed (m s^{-1}) for satellite/reanalysis products (pink), and the GLORYS model (blue).

The GLORYS model generally overestimated the SST and current speed (Fig. 2). Despite this, similar strong, statistically significant, inverse relationships were observed between SST and current speed from GLORYS and the satellite and reanalysis products (Fig. 2). Decadal variability was also remarkably similar (Fig. 3). Elevated SST was associated with lower current speeds prior to 2001 and during 2008–2014. The reverse relationship (lower SST and stronger currents) occurred during 2001–2007 and since 2015. During the 2001–2007 cool period, minimum GLORYS SST (Fig. 3b) was reached earlier and maintained for longer (2003–2007) than minimum reanalysis SST (2005–2007) (Fig. 3a). Although cooler conditions are expected to promote a more productive ecosystem, the overall stronger currents observed during cooler periods could likely result in stronger advection of water and prey away from the islands. Mammals and seabirds at the PEIs may thus need to travel further from the islands to feed. Further research is required to determine the relationships between decadal environmental variations and the foraging patterns of mammals and seabirds breeding at the PEIs. The conformity of GLORYS to satellite and reanalysis data gives confidence in the simulated GLORYS output. This suggests GLORYS could be used to determine if similar decadal variability occurs throughout the water column, which is particularly important for the PEI region where existing *in situ* water column observations are insufficient for such investigations.

Authors: Lamont T, Russo CS (OC Research)

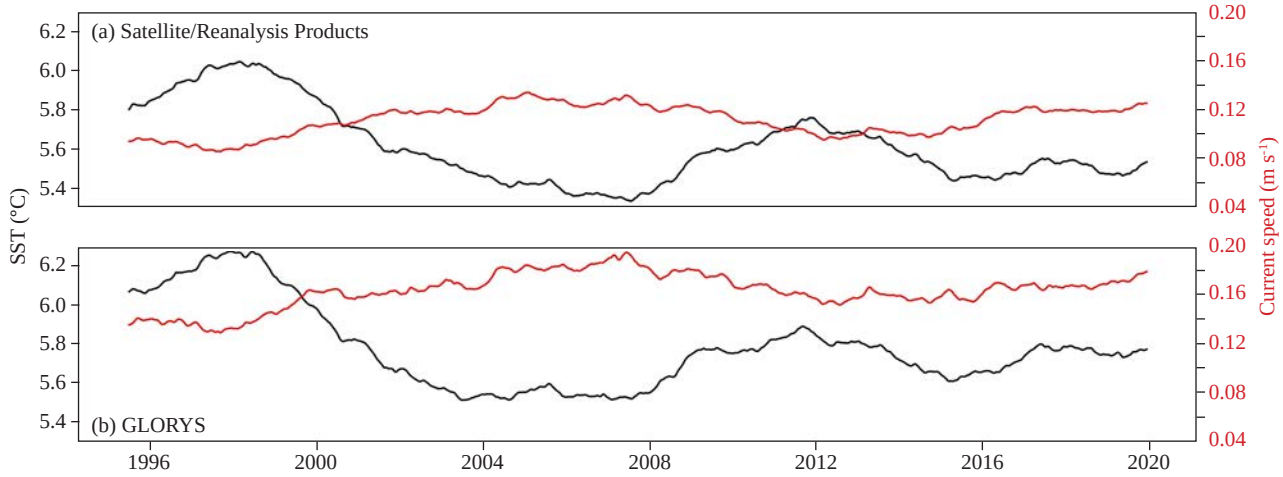

Figure 3. Time series of the 5-year running means of (a) reanalysis SST (°C; black) and satellite geostrophic current speed (m s^{-1}; red), and (b) GLORYS SST (°C; black) and geostrophic current speed (m s^{-1}; red).

RESEARCH HIGHLIGHTS

17. MARINE HEATWAVES OFF CAPE POINT

As a result of climate change, one of the emerging risks for coastal countries is the storage of large amounts of heat in the ocean. The continued accumulation of heat can result in the occurrence of marine heatwaves (MHWs), which have been associated with widespread coral bleaching and mass mortalities of marine life. MHWs are extreme events that last for at least five consecutive days with sea surface temperatures (SSTs) that are higher than 90% of the historical SSTs for those days.

This study used *in situ* SST measurements from a moored buoy located at 34.204°S; 18.287°E, along the 70 m isobath, about 5.4 km off the Cape Peninsula (Fig. 1). These observations have been maintained by the Council for Scientific and Industrial Research (CSIR) since 2003. Reanalysis wind data, produced by a combination of model and observational data, were used to investigate the characteristics and drivers of MHWs off the Cape Peninsula. Due to the high SST variability in the Benguela Upwelling System (apart from MHWs), our study also investigated the occurrence of "warm events" (WEs), defined as consecutive 3-day periods when the SST exceeded 90% of the historical SSTs for those days.

During the 2003 to March 2020 period, MHWs and WEs persisted for an average of 6–7 days during the upwelling (October–March) and non-upwelling (April–September) seasons. During the upwelling season, these events reached overall higher SSTs, with averages of 20°C and maximum values between 23 and 24°C (Fig. 2). A total of 35 events (14 MHWs and 21 WEs) were identified between 2003 and 2020 (Fig. 3). Of these, a total of 27 events began with northwesterly winds, and 30 ended with southeasterly winds. Figure 4 illustrates an example of such an event.

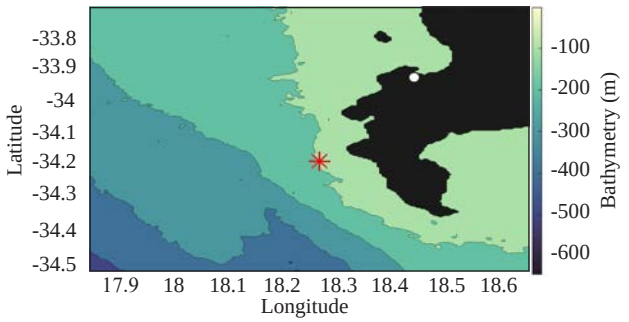

Figure 1. The position of the mooring (red asterisk) to the west of Cape Point. Colours represent different depth zones, and the city centre of Cape Town is indicated by the white circle.

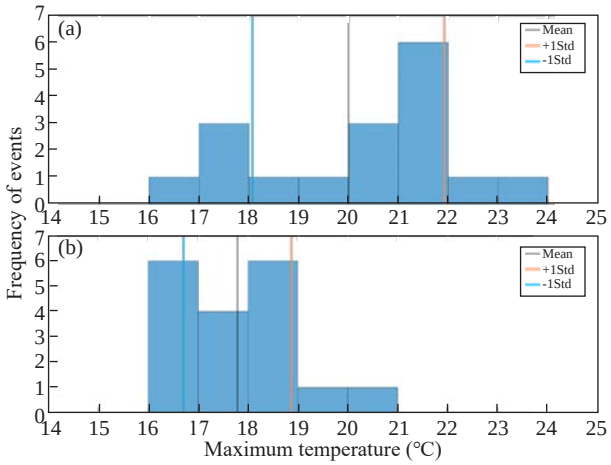

Figure 2. Frequency of MHWs and WEs of different SST (°C) maxima of the events during the (a) upwelling and (b) non-upwelling seasons, from 2003 to March 2020.

These results suggest that a large majority of the events began with transport of warm water from offshore toward the mooring location, and that upwelling was a key mitigator of the duration of MHWs and WEs off the Cape Peninsula. Some events could not be associated with wind as a driver and thus further research is required to identify other drivers of these events. More research should also focus on determining and monitoring the impacts of MHWs and WEs on marine life in the vicinity of Cape Peninsula.

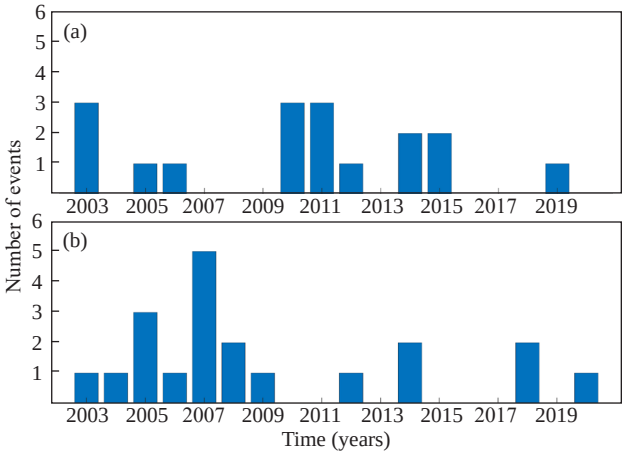

Figure 3. The annual total number of MHWs and WEs during the (a) upwelling and (b) non-upwelling season, from 2003 to March 2020.

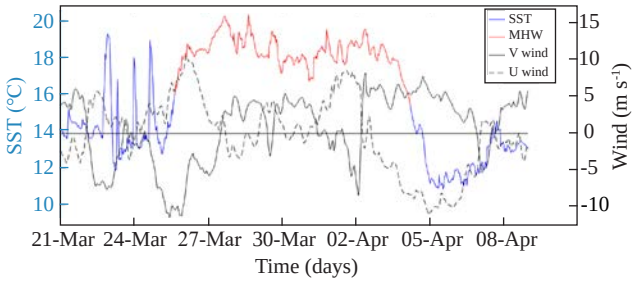

Figure 4. Sea surface temperature (°C) and wind speed components (m s^{-1}) from 21 March to 8 April 2014. SST during the MHW is highlighted in red, while SST before and after the MHW is indicated in blue. The V (meridional) component indicates northward (positive) and southward (negative) wind speeds, while the U (zonal) component indicates eastward (positive) and westward (negative) wind speeds.

Authors: Petzer K (UCT); Lamont T (OC Research); Rouault M† (UCT)

18. FISH AND MACROFAUNA RESPONSE TO A FLOOD EVENT IN A FLUVIALLY DOMINATED ESTUARY

Estuaries are prone to droughts and floods, which are expected to increase in intensity and duration with ongoing climate change. Both droughts and floods can disrupt the ecological functioning of estuaries. For example, reduced flows due to drought can reduce productivity, while floods decrease salinity and increase turbidity, affecting primary and secondary production, recruitment and food availability. The objective of this study was to investigate the effects of a flood on the biota of a fluvially (river) dominated estuary.

The Great Kei Estuary is situated next to the Amathole Marine Protected Area in the Eastern Cape (Fig. 1). The Kei River catchment receives its rainfall mainly in summer and the estuary drains into the Indian Ocean. Sampling was conducted biannually during 2017–2018: in February/March to represent the high flow period, and in September/October for the low flow period. Water parameters such as salinity and turbidity were measured *in situ*, while flow measurements were obtained from the Department of Water and Sanitation. Fish and macrofaunal invertebrates were also sampled.

Flows reached 132 million m^3 during the flood and were <30 million m^3 during non-flooding periods. This greatly affected salinity and turbidity levels (Table 1). The fish community was dominated (>40%) by the solely estuarine (SE) group of fish for most of the sampling period, except during the flood when they were entirely absent (Fig. 2a). The SE group is dominated by *Gilchristella aestuaria*, a species that spawns throughout the year and is most abundant between September–April. The maximum length of this species as recorded in estuaries is 9 cm, and since swimming abilities of fish are largely dependent on body length, it can be washed away easily. The catch per unit effort (CPUE) of the marine estuarine-dependent (MED) group was similar (40–43%), but these were absent during the high flow period before the flood occurred (where the SE group was most abundant) and present during the flood (Fig. 2a). The MED group consists of species that are tolerant of a wide salinity range and have stronger swimming abilities, enabling them to swim against the current. The CPUE of the freshwater estuarine-opportunist (FEO) group increased during the flood due to the influx of fresh water (Fig. 2b). The macrofauna community was dominated by the classes Malacostraca and Polychaeta during the low flow periods before and after the flood (Fig. 2b). Both classes were almost completely absent during the flood – this is because the top layers of sediment erode and macrofauna residing in them are usually washed away unless they can burrow deeper. Macrofaunal species density was highest during the post-flood low flow season, possibly due to the flood resetting the estuary and allowing for re-colonisation by macrofauna. The results of this study have shown that a flood caused a temporary decline in the abundance of fish and macrofauna. Anticipated increases in flooding due to climate change can therefore be expected to have detrimental effects on biota, especially if it occurs during a recruitment period.

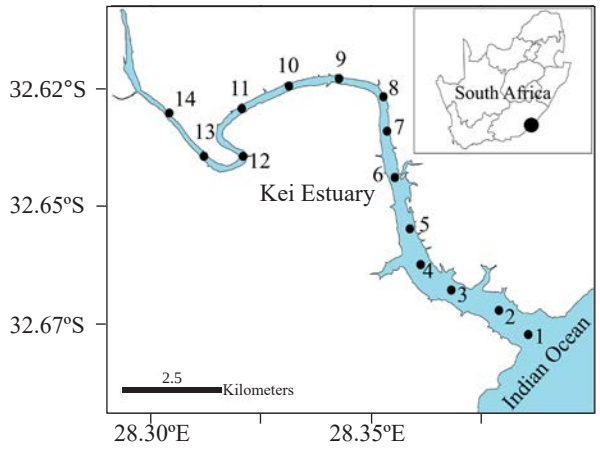

Figure 1. Map showing the locations of the 14 sampling sites.

Table 1. Physico-chemical variables recorded in the estuary (HF - high flow, LF - low flow).

Variable	HF (before)	LF (before)	HF (flood)	LF (after)
Flow volume (million m^3)	24.2	1.09	132	4.69
Mean salinity (ppt)	21.6	26.8	4	23.7
Mean turbidity (NTU)	329	73.6	1013	34.6

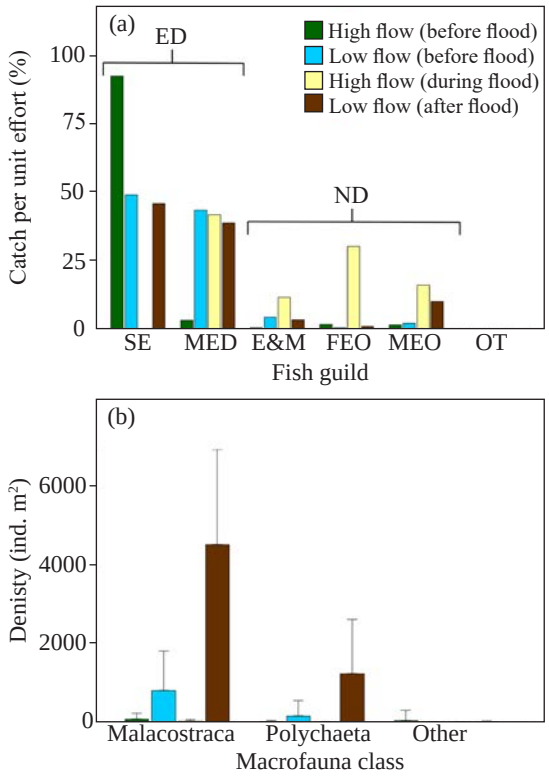

Figure 2. (a) Percentage CPUE of fish guild categories recorded in the estuary in different flow periods. Estuarine-dependent (ED) species include solely estuarine (SE) and marine estuarine-dependent (MED) species; non-dependent (ND) species include estuarine and marine (E&M), freshwater estuarine-opportunist (FEO), marine estuarine-opportunist (MEO) and other (OT). (b) Mean densities of the macrofauna recorded in the estuary.

Author: Nhleko J (OC Research)
Contibutors: Lamberth S, Erasmus C, Williamson C (Fisheries R&D); Bebe L, Mushanganyisi K (OC Research); Van Niekerk L (CSIR)

19. TEMPERATURE CHANGES ON THE SOUTH COAST INFLUENCE ANCHOVY AND SARDINE DISTRIBUTIONS

Anchovy *Engraulis encrasicolus*, sardine *Sardinops sagax* and round herring or "redeye" (*Etrumeus whiteheadi*) are three small epipelagic fish species that reside predominantly on the continental shelf off the west and south coasts of South Africa. These fish play a vital ecological role as an energy link between plankton and higher trophic level species such as predatory fish, marine mammals and seabirds. They are also commercially important for South Africa's fishing industry. Most of their spawning takes place on the south coast shelf (Fig. 1), with newly spawned eggs and larvae (mostly from the west of Cape Agulhas) transported to nursery areas on the west coast. Previous studies showed that an abrupt environmental change on the south coast was associated with a shift in the relative biomass of anchovy from west to east of Cape Agulhas. Here, we investigate whether this still holds true, and expand the study to include sardine and redeye.

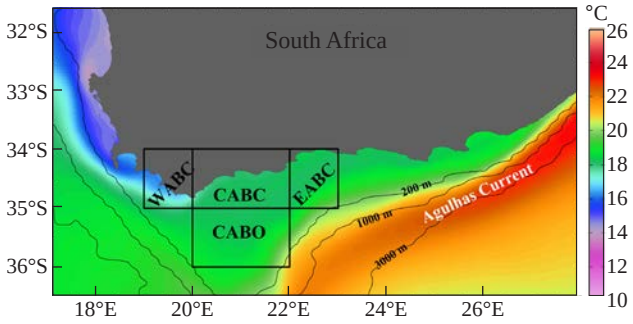

Figure 1. Long-term (1981-2022) mean sea surface temperature (SST, °C) for the west and south coasts of South Africa. Black boxes indicate coastal (Western Agulhas Bank Coastal – WABC; Central Agulhas Bank Coastal – CABC; and Eastern Agulhas Bank Coastal – EABC) and offshore (Central Agulhas Bank Offshore – CABO) regions used to compute SST differences.

Long-term satellite observations of mean sea surface temperature (SST) reveal that the Western Agulhas Bank Coastal (WABC) area is ca. 2°C cooler than the Central Agulhas Bank Coastal (CABC) and Eastern Agulhas Bank Coastal (EABC) areas (Fig. 1). The Central Agulhas Bank Offshore (CABO) region is comparatively warmer because it is influenced by the Agulhas Current. The difference in SST between the CABO and WABC regions has increased since 1984 (Fig. 2). This difference is driven by long-term cooling in the WABC region, resulting from increased wind-driven upwelling, coupled with long-term warming in the CABO region, arising from warming of the Agulhas Current. Differences in SST between CABO and the other coastal regions (CABC and EABC) also appeared to increase moderately over time due to the offshore warming (Fig. 2).

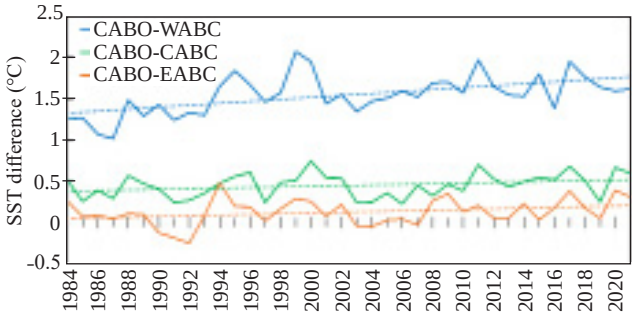

Figure 2. Annual mean SST difference (solid lines) between the offshore area (CABO) and each of the coastal areas (WABC, CABC, and EABC) from 1984 to 2022. Dashed lines illustrate linear relationships between SST differences and year – only the CABO-WABC SST difference showed a statistically significant increase over time ($p < 0.001$).

The biomass of anchovy occurring east of Cape Agulhas increased dramatically from 20% in 1995 to 80% in 1996. At the same time, sardine also began shifting eastward, and by 1999 >50% of their biomass was distributed to the east of Cape Agulhas (Fig. 3). These shifts were significantly correlated with the CABO-WABC SST difference (Fig. 4). We postulate that water temperatures in the WABC region cooled to below the preferred levels for these species, which then responded by moving eastwards. The proportion of redeye occurring eastward of Cape Agulhas has been fairly constant over time (Fig. 3) and was not correlated with SST differences (Fig. 4), suggesting that there was no marked distributional shift of this species.

Fluctuations in population size and distribution of these fish are expected to have substantial impacts on the health of higher trophic level species, as well as the economic sustainability of the small pelagic fishing industry. Continued monitoring is thus required to better understand environmental drivers of their distributions.

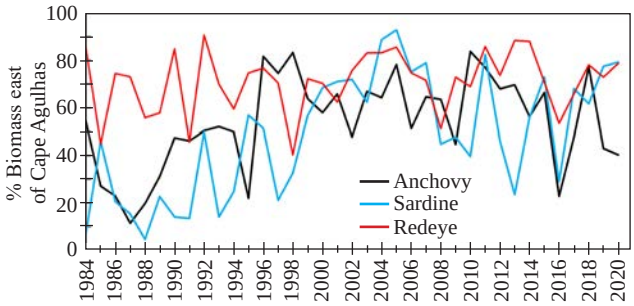

Figure 3. Annual percentage (%) of total biomass east of Cape Agulhas for anchovy, sardine and redeye.

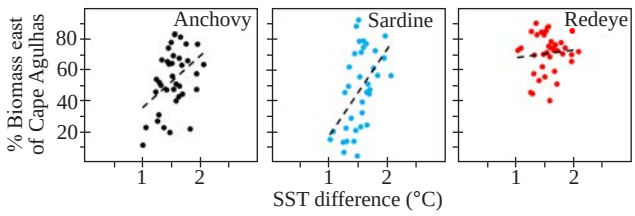

Figure 4. Scatterplots of the annual CABO-WABC SST difference against percentage (%) biomass for the three species. Dashed lines illustrate linear relationships – only redeye did not show a statistically significant relationship ($p > 0.05$).

Authors: Lamont T (OC Research); Torr M (UCT); van der Lingen CD (Fisheries R&D)

20. SURFACE pH DISTRIBUTIONS OFF THE WEST COAST OF SOUTH AFRICA

Since the Industrial Revolution began, the concentration of carbon dioxide (CO_2) in the atmosphere has increased. The ocean plays a vital role in regulating atmospheric CO_2. However, the pH (a measure of how acidic or alkaline a liquid is) of global surface ocean waters has decreased by about 0.1 units due to the uptake of atmospheric CO_2, making it more acidic. In the southern Benguela, little is known about the distribution of the surface pH. Based on measurements obtained during August 2022, we present a snapshot of the distribution of pH in the southern Benguela. Also presented are the distributions of three related parameters, namely sea surface partial pressure of CO_2 (pCO_2), dissolved oxygen (O_2) and sea surface temperature (SST).

The surface pCO_2 was measured continuously with a non-dispersive infrared spectrometer integrated into a General Oceanics underway pCO_2 system on board the RS *Algoa* during August 2022. The underway seawater supply, which has an intake at ca. 5 m depth, continuously pumped seawater through the pCO_2 system, and the Thermosalinograph (TSG), which provided temperature measurements. The atmospheric air intake was installed ca. 10 m above the sea surface. Surface seawater pH was measured continuously with a pH sensor connected to the underway seawater supply system. Surface seawater O_2 was measured continuously with a dissolved oxygen Optode sensor connected to the underway seawater supply system.

The outer shelf was warmer, with surface temperatures above 15°C, pCO_2 below 417 µatm, pH above 8.0, and O_2 below 6.0 ml L^{-1} (Fig. 1). Since these pCO_2 values were below the atmospheric CO_2 level, the offshore region acted as a sink of the atmospheric CO_2.

Figures 1a and 2a show that the surface waters in the nearshore area between 29–31°S latitude were colder, with sea surface temperatures below 12.5°C, high pCO_2 above the atmospheric value of 417 µatm, low pH below 7.8, and

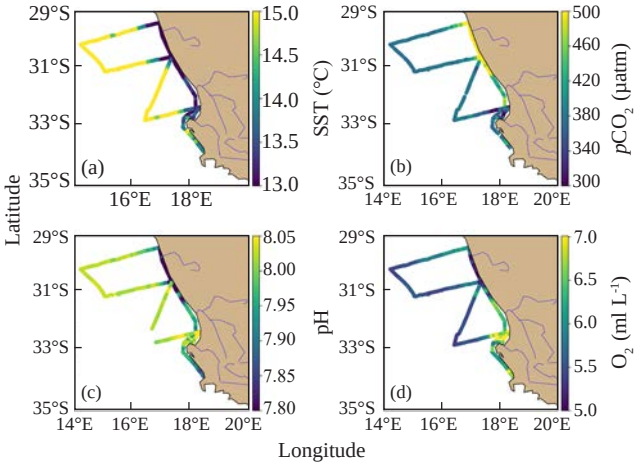

Figure 1. Map showing the distribution of (a) sea surface temperature (SST), (b) partial pressure of carbon dioxide (pCO_2), (c) pH, and (d) dissolved oxygen (O_2), off the west coast of South Africa in August 2022.

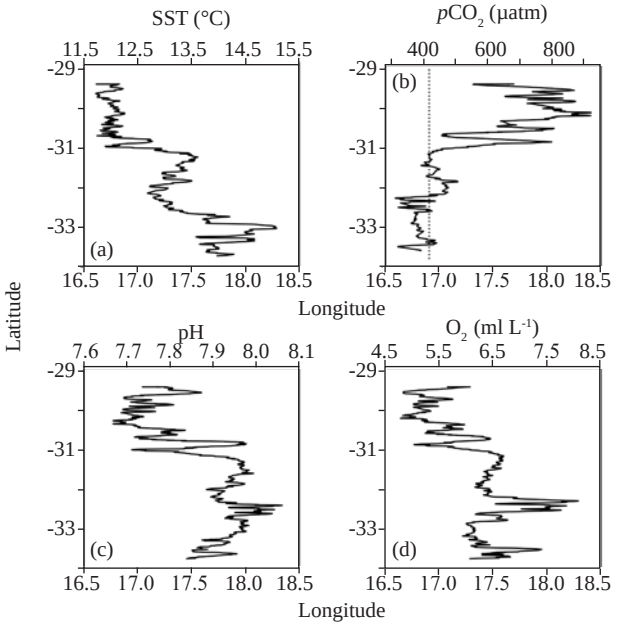

Figure 2. Nearshore distributions of the (a) sea surface temperature (SST), pH, (b) partial pressure of carbon dioxide (pCO_2), (c) pH, and (d) dissolved oxygen (O_2), off the west coast of South Africa in August 2022. The black dotted line in panel B indicates the annual atmospheric CO_2 value of 417 µatm.

O_2 below 6.0 ml L^{-1}. Surface pCO_2 values exceeding the atmospheric CO_2 (Fig. 2b) indicated that the area was releasing CO_2 into the atmosphere. Therefore, the nearshore region between 29–31°S latitude acted as a strong source of CO_2 to the atmosphere during the winter of 2022. The pH values below 7.8 in the nearshore area between 29–31°S latitude can have harmful effects on marine life, impacting reproduction and growth. The likelihood of concurrent low pH and low O_2 conditions may leave marine life vulnerable to multiple stressors. Hence, low pH and low O_2 conditions need to be monitored.

Authors: Tsanwani M, Mtshali T, Mdokwana B (OC Research), Hamnca S (CSIR)
Contributors: Kiviets G, Britz K, Vena K, Siswana K (OC Research)

21. TRACE AND HEAVY METAL DISTRIBUTIONS ALONG THE WEST COAST OF SOUTH AFRICA

The pollution of the marine environment by trace and heavy metals is ongoing and has received much attention because of the accumulative toxic properties. Most trace and heavy metals, such as Cobalt (Co), Lead (Pb), and Cadmium (Cd), are non-essential in the physiological systems of marine organisms and toxic at high concentrations. In contrast, Iron (Fe), Manganese (Mn), and Zinc (Zn) are essential elements that are required by marine organisms in small concentrations. This study is the first to report the coastal distribution of trace and heavy metal concentrations along the west coast of South Africa (Fig. 1).

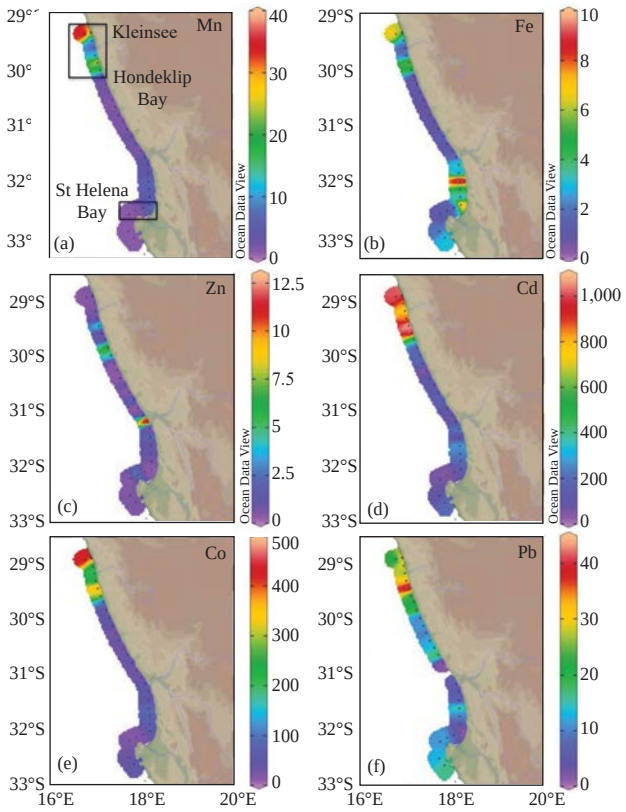

Figure 1. Surface distribution of essential elements (nmol kg^{-1}) (a) Mn, (b) Fe and (c) Zn, and non-essential elements (pmol kg^{-1}) (d) Cd, (e) Co and (f) Pb, during November 2022. Areas of high metal concentrations are shown in black squares.

A trace clean towed torpedo fish system deployed 5 m away from the ship's wake, at depths of ca. 2–5 m, was used to collect seawater samples along the coast during the Integrated Ecosystem Program: Southern Benguela (IEP: SB) cruise onboard the RS *Algoa* in November 2022 (Fig. 1). Samples were analysed and quantified using certified reference material to ensure accuracy and precision.

Along the coastline, Mn concentrations were higher than Fe and Zn (Fig. 2a). Elevated concentrations were observed in the vicinity of St Helena Bay (32.5–32.1°S latitude) with values reaching maxima of 7.3 nmol kg^{-1} for Mn and 7.1 nmol kg^{-1} for Fe, while Zn values remained low, varying from 0.3–3.0 nmol kg^{-1}. Between Hondeklip Bay and Kleinsee (30.5–29.9°S), maximum values of 24.3 nmol kg^{-1} for Mn, 5.6 nmol kg^{-1} for Fe, and 6.6 nmol kg^{-1} for Zn were recorded (Fig. 2a). Along the transect, Zn concentrations were lower than the coastal toxicity threshold value of 30 nmol kg^{-1}. Concentrations of Cd were higher than Co and Pb (Fig. 2b). Between St Helena Bay and Hondeklip Bay (33.1–30.3°S latitude), Cd concentrations were highly variable, with values ranging from 36.3–276.1 pmol kg^{-1}. In contrast, both Co and Pb remained relatively low in this region, ranging from 18.2–88.2 and 1.0–20.0 pmol kg^{-1}, respectively. Elevated concentrations of Cd and Co were observed near the Hondeklip Bay and Kleinsee areas, with Cd ranging from 167.2–1077,9 pmol kg^{-1}, exceeding the recommended coastal toxicity threshold value of 1042,6 pmol kg^{-1} (Fig. 2b). Cobolt concentrations varied from 47.5–498.8 pmol kg^{-1} (Fig. 2b).

The observed elevated trace and heavy metal concentrations could be due to input from internal sources (e.g. upwelling of deep metal-rich waters, or sediment resuspension due to mining operations) and/or external sources (e.g. dust deposition or river runoff). Further investigation is required to determine these sources. Coastal waters of South Africa support a rich diversity of marine life, and data on the distribution and/or contamination levels of trace and heavy metal concentrations are important for understanding ecosystem health.

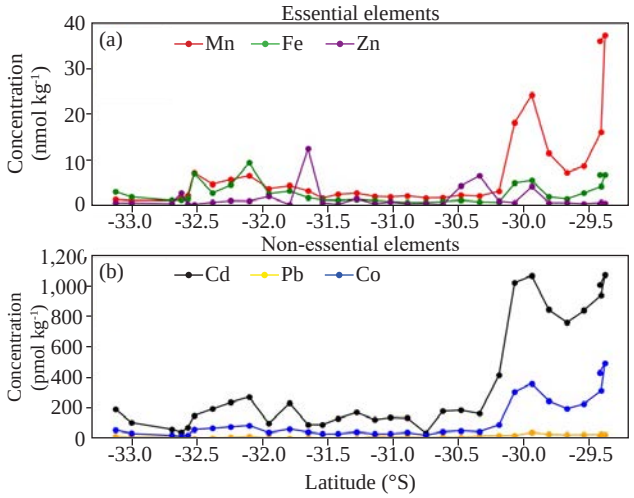

Figure 2. Surface distributions of trace and heavy metal concentrations for (a) essential elements (nmol kg^{-1}), and (b) non-essential elements (pmol kg^{-1}) along the west coast.

Authors: Mtshali T, Tsanwani M (OC Research)
Contributors: Kiviets G, Britz K, Vena K, Mdokwana B, Siswana K (OC Research)

22. MOLECULAR AND MORPHOLOGICAL IDENTIFICATION OF MOON JELLYFISH POLYPS IN THE V&A WATERFRONT MARINA

The "moon jelly" *Aurelia* (class Scyphozoa) is the most common jellyfish found in coastal waters around the world. In suitable conditions, newly introduced populations of this genus reproduce rapidly forming jellyfish blooms (mass populations of jellyfish; Fig. 1).

Figure 1. A moon jellyfish bloom in the UK (Source: C Hinton).

In Cape Town, blooms of moon jellyfish ephyrae (immature jellyfish) were observed on several occasions during 2022 and 2023 in the V&A Waterfront Marina. Jellyfish polyps, the sessile stage of most free-swimming jellyfish species, were subsequently observed by means of SCUBA (Fig. 2). At the time, the species of *Aurelia* that made the bloom was unknown.

An integrated approach combining genetics and morphometrics was used to identify the species of *Aurelia*. The morphological forms of twenty-five polyps were identified visually (Fig. 3), highlighting key characteristics to confirm species identity. Genetic data were also analysed and compared with sequences on GenBank, an open-access database (https://www.ncbi.nlm.nih.gov/genbank).

Morphological data indicated a mean tentacle number of 18, with 16 individuals possessing a cruciform (cross-like) shape, consistent with features of *Aurelia coerulea* polyps found in the Mediterranean Sea. Additionally, morphological features such as total body length, mouth-disk diameter, and length of calyx (cup-like part of body) and hypostome (oral opening), shared some similarities with *A. coerulea* polyps in literature, but were inconclusive. The fact that morphology may be influenced by factors such as diet, surrounding water parameters and locality, underscored the need for molecular analysis.

Figure 2. A colony of jellyfish polyps observed in the V&A Waterfront Marina.

Molecular analysis revealed an overall group mean percentage identity of 99% when compared with sequences of *A. coerulea* and *Aurelia* sp. 1 (redescribed as *A. coerulea*) extracted from GenBank, indicating a genetic difference of only 1% in our analysis. Furthermore, the analysis revealed a 99% identity when compared with specimens at the Two Oceans Aquarium. The range to differentiate between jellyfish species is a genetic difference greater than ca. 5–6%, therefore confirming the species in the study to be *A.coerulea.*

The occurrence of *A. coerulea* in waters worldwide has led to substantial economic losses. In Korea for example, blooms of *Aurelia* clog the intake water screens of nuclear power plants, and affect fishing operations by reducing the product value of commercial catches. This study is the first to document *A. coerulea* in South Africa's waters and it is important to act swiftly after early detection to mitigate the potential threat of this invasive species.

Figure 3. A polyp from the V&A Waterfront Marina at 20x magnification.

Authors: Evertson M, Puckree-Padua C, Sejeng C (CPUT); Huggett JA (OC Research)
Contributors: Lewis K (Two Oceans Aquarium), Ras V (UWC)

23. BASELINE *IN SITU* MEASUREMENTS OF PICOPHYTOPLANKTON IN THE SOUTHERN BENGUELA UPWELLING SYSTEM

To date, there have been many *in situ* plankton studies on and around the west coast of South Africa. However, these studies have tended to focus on assessing larger plankton communities, with investigations on smaller plankton using mainly satellite, chemical and wind data from moorings and weather stations, as well as outputs from ecosystem models. In comparison, this study is the first to provide *in situ* abundance measurements of smaller picophytoplankton groups. Picophytoplankton are autotrophic organisms that range in size between 0.2 to 2 µm, and knowledge on their ecological role in energy and carbon cycling transfer of food webs is still limited. The focus of this study is on the most abundant picocyanobacterial groups (*Prochlorococcus* and *Synechococcus*) and an integration of picoeukaryotic groups.

The study was conducted along monitoring lines off the west coast of South Africa over two seasonal cycles during eight cruises, from May 2015 to February 2017, as part of the quarterly Integrated Ecosystem Programme (IEP). Sample collection was achieved by collecting sea water samples from the surface and fluorescence maximum (Fmax; the depth at which light-absorbing organisms emit the most light), along with measurements of environmental variables (Fig. 1). These samples were then analysed using a flow cytometer to determine abundance of *Prochlorococcus* (0.5–0.7 µm), *Synechococcus* (0.8–2.0 µm) and picoeukaryotes (1.0–3.0 µm).

Abundances of all three groups varied across several orders of magnitude (Fig. 2). Very large abundances were sporadic in the data, with some indication that these high abundances co-occurred among the groups. Overall, *Prochlorococcus* tended to be most abundant (density of 10,385 cells ml^{-1} across a total of 324 samples), followed by picoeukaryotes (7,529 cells ml^{-1} across 492 samples), and *Synechococcus* was least abundant (1,838 cells ml^{-1} across 270 samples).

Variability in nutrient concentrations over the sampled cruise periods accounted for 72.3% and 69.3% of the variability in picophytoplankton abundance at the surface and Fmax, respectively (Fig. 3). Temperature and salinity were negatively related to macronutrients (nitrate, silicate, phosphate), as would be expected in an upwelling ecosystem. However, there was no significant association between picophytoplankton and these environmental variables. Oxygen concentrations influenced the distribution of some picophytoplankton groups during spring and summer.

As the first of its kind, this study provides a baseline, extending the knowledge on picophytoplankton groups and their interactions with other plankton groups in the highly productive and variable southern Benguela ecosystem. This knowledge is needed to better understand the plankton dynamics of the system.

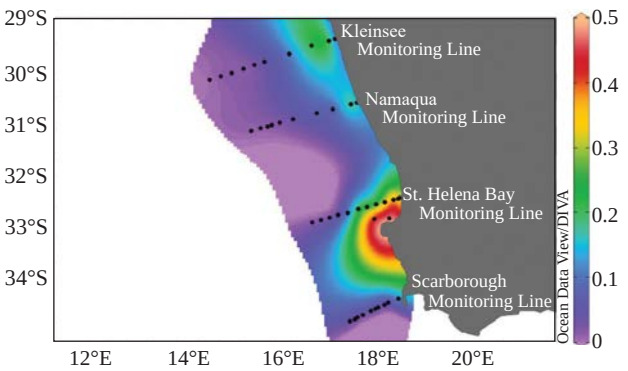

Figure 1. Surface fluorescence (mg m^{-3}) map of the southern Benguela off the west coast of South Africa in May 2016. Black dots indicate locations of the sampled stations.

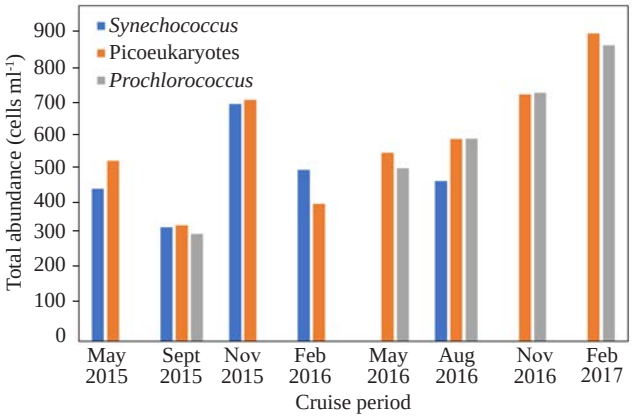

Figure 2. Total abundance (cells ml^{-1}) of the three picophytoplankton groups on the west coast of South Africa from May 2015 to February 2017 (values were transformed to allow easy comparison of the large range in abundance, which varied between $10^2 - 10^5$ cells ml^{-1}).

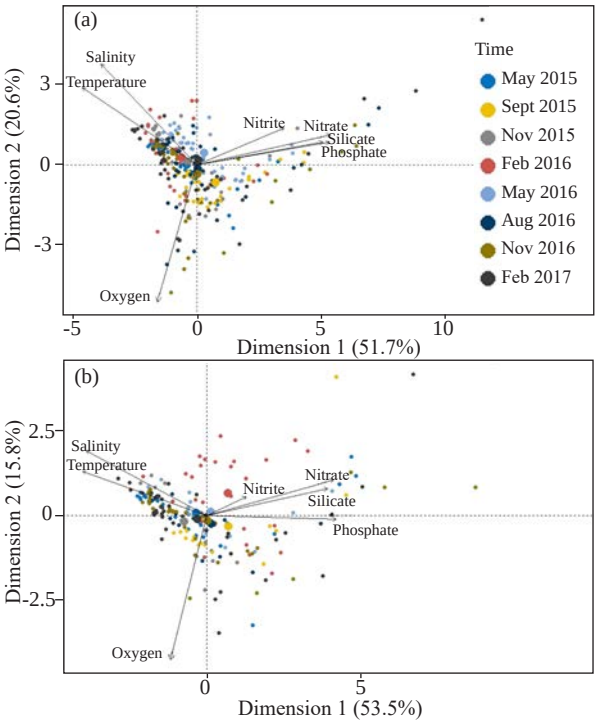

Figure 3. Plots showing the contribution of different environmental variables to the variability among samples, at the surface (a) and at Fmax (b). The direction and length of the arrows representing each variable, indicate the relative contribution of each variable, with arrows in opposite directions indicating that there are no relationships between variables.

Author: Gebe Z (OC Research)

24. CROSS-SHELF VARIABILITY IN PLANKTON COMMUNITIES ON THE AGULHAS BANK

The Agulhas Bank, the triangular-shaped continental shelf off the south coast of South Africa, is an area of high ecological and economic significance. It hosts a diverse and productive ecosystem with complex trophic interactions that are susceptible to a changing ocean environment. Plankton are the foundation of most marine food webs and are instrumental in marine processes. Microplankton (phyto- and zooplankton, from 20–200 µm in size) are preyed upon by mesozooplankton (>200 µm) which in turn feed large populations of economically important fish species, marine mammals and seabirds. Many plankton species have short lifespans (days to months), respond rapidly to changes in the environment, and are thus suitable for monitoring climate-related environmental variations.

The Mossel Bay Monitoring Line (MBML) extends across the broad expanse of the Agulhas Bank (Fig. 1) and provides a good platform to explore changes in the ecosystem. Plankton samples were collected at 10 stations along the MBML during pelagic surveys aboard the FRS *Africana* in November/December 2018 and 2019. Taxonomic composition was evaluated using image and microscopic analysis. Satellite-derived maps of sea surface temperature (SST) and chlorophyll *a* concentration (chl *a*) were used for spatial contextualisation of environmental variability.

During 2018, warm (>21°C) and low chl *a* (<1 mg m^{-3}) surface water was located beyond the eastern edge of the Agulhas Bank (Figs. 1a, b). This pattern reflected the typical location of the Agulhas Current (AC) core and edges along the continental slope (Fig. 1a). In contrast, shorewards of the 200 m isobath, surface waters were much cooler (<19°C) with elevated chl *a* (>3 mg m^{-3}) that appeared to be advected westwards across the MBML from the eastern Agulhas Bank (EAB). Phytoplankton (diatoms and dinoflagellates) abundance was highest along the continental slope between the 200–1000 m isobaths (Fig. 2a). This elevated abundance (especially of diatoms) was likely attributable to the advection of phytoplankton from the EAB (where high biomass was observed) along the inshore edge of the AC. Microplankton abundance (dominated by dinoflagellates and copepod nauplii) was higher inshore and offshore compared to the mid-shelf region (Fig. 2b), with tintinnids (ciliates with vase-shaped shells) occurring near the shelf-edge.

Mesozooplankton abundance in 2018 was greatest inshore (Fig. 2c) in cooler (<18°C) water compared to further offshore. Biomass of copepods (which usually dominate zooplankton biomass) was greatest over the mid-shelf region, with *Calanus agulhensis* the largest contributor to biomass (Fig. 2d). Copepod nauplii (juveniles) were more abundant inshore where adults were less abundant (Figs. 2b, d). Inverse (negative) relationships between phytoplankton and zooplankton abundance, and between microplankton abundance (especially dinoflagellates) and copepod biomass, suggest a strong feeding impact by zooplankton on the phytoplankton community.

During 2019, environmental conditions differed substantially. Eastwards of the MBML, warm (Fig. 1c) and low chl *a* (Fig. 1d) surface waters were located further offshore due to offshore movement of the AC. Between the AC and the 1,000 m isobath, cooler water (<20°C) with elevated chl *a* appears to have been advected from the shelf (Fig. 1d). As a result, surface chl *a* along the MBML was much lower than in 2018. *In situ* data reflected the same pattern, with lower phytoplankton and zooplankton abundance in 2019 than in 2018, and highest abundance for all biota occurring at the coast (Figs. 2e–g). Increased microplankton levels at the two offshore stations (Figs. 2e, f)

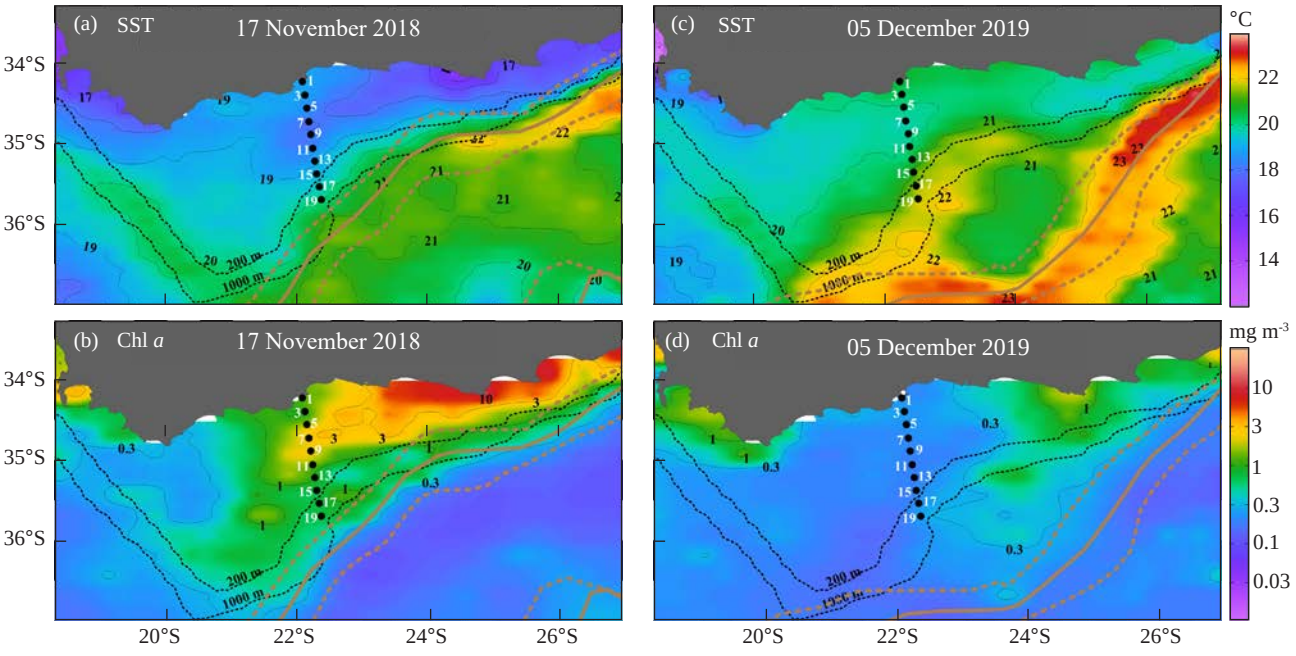

Figure 1. Satellite maps of daily sea surface temperature (SST, °C) and chlorophyll *a* (chl *a*, mg m^{-3}) concentration on 17 November 2018 (a, b) and 5 December 2019 (c, d) overlain with the location of the Agulhas Current's core (solid brown line) and edges (dashed brown line). Black dots indicate sampling stations 1-19 along the MBML, and the 200 and 1000 m isobaths (dotted black lines) are shown.

corresponded with elevated chl *a* observed there (Fig. 1d). Tintinnids and other ciliates were most abundant inshore and near the shelf-edge (Fig. 2f). Similar to 2018, *C. agulhensis* was the dominant copepod species in 2019 (Fig. 2h).

These results provide insight into top-down (zooplankton preying on phytoplankton) and bottom-up (environmental influence on plankton) processes of this ecosystem. However, to fully understand the ecosystem response, the role of the fish species that prey on plankton must also be considered. Long-term monitoring of all these variables is essential to understand the potential effects of climate related changes on the productivity of the south coast.

Authors: Maduray S, Lamont T, Russo CS, Huggett JA (OC Research)
Contributors: Soeker MS, Mdazuka Y (OC Research)

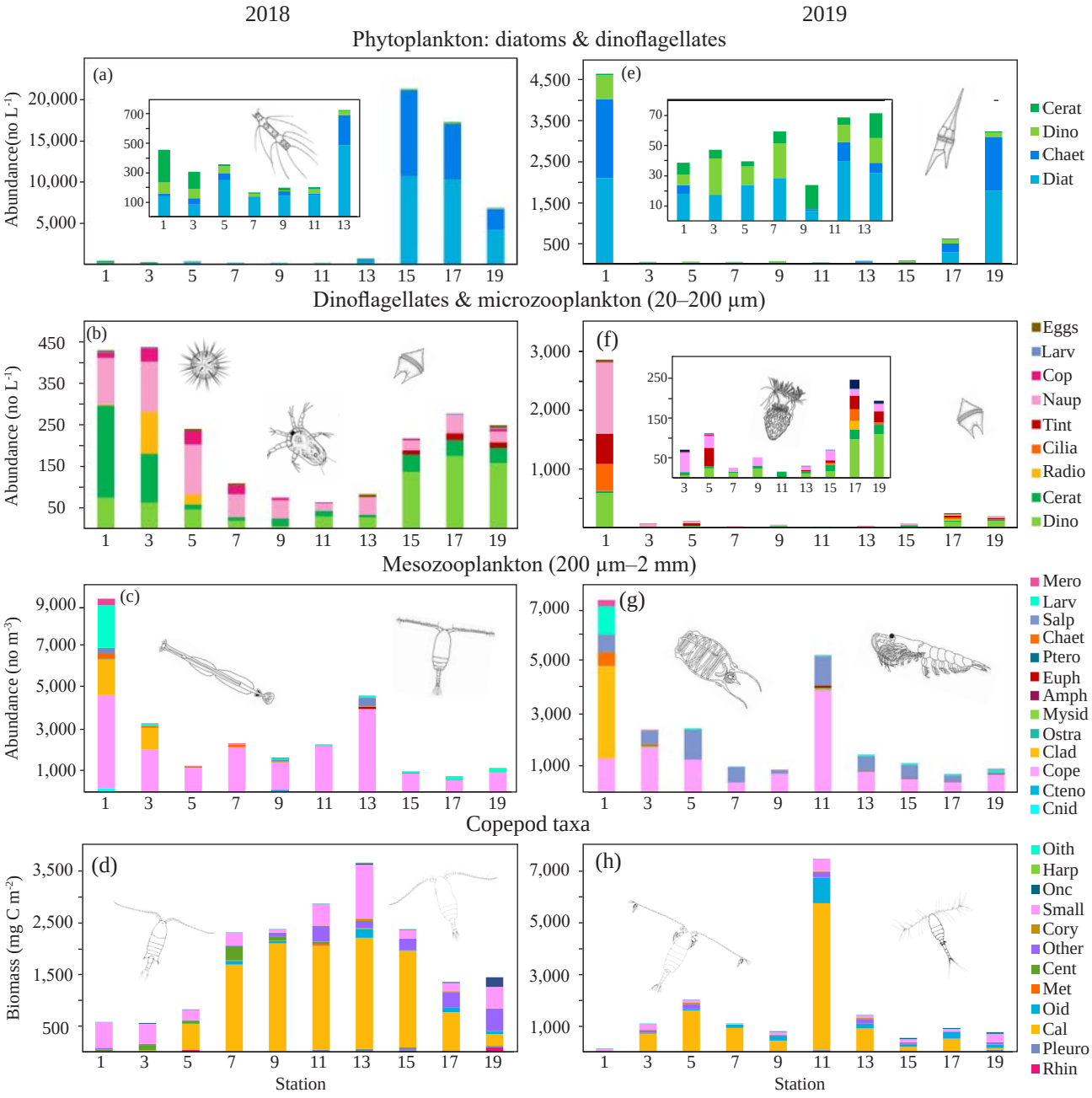

Figure 2. Phytoplankton and microzooplankton abundance (1000 L^{-1}) in 2018 (a, b) and 2019 (e, f), as well as mesozooplankton abundance (no m^{-3}) and copepod biomass (mg C m^{-3}) in 2018 (c, d) and 2019 (g, h). Inserts highlight patterns observed for stations with lower abundance. Abbreviations: Diat: Diatoms, Chaet: *Chaetoceros* spp. Dino: Dinoflagellates, Cerat: *Ceratium* spp., Radio: Radiolarians,Tin: Tintinnids, Cilia: Ciliates, Naup: copepod nauplii, Cop: copepodites, Larv: Larvaceans, Eggs: crustacean eggs, Cnid: cnidarians, Cteno: ctenophores, Cope: copepods, Clad: Cladocerans, Ostra: Ostracods, Amph: amphipods, Euph: euphausiids, Ptero: Pteropods, Chaet: chaetognaths, Mero: meroplankton, Rhin: *Rhincalanus* spp., Pleuro: *Pleuromamma* spp., Cal = *Calanus agulhensis,* Oid: *Calanoides natalis*, Met: *Metridia lucens*, Cent: *Centropages* spp., Other: other copepod species, Cory: *Corycaeus* spp., Small: small calanoids, Onc: oncaeids, Harp: harpacticoids, Oith: *Oithona* spp.

25. ZOOPLANKTON ASSEMBLAGES ASSOCIATED WITH SUBMARINE CANYONS OFF THE EAST COAST OF SOUTH AFRICA

Several submarine canyons incise the continental shelf off KwaZulu-Natal (KZN) on the northeast coast of South Africa. There is limited knowledge of their ecological significance and interaction with the pelagic zone. Research worldwide indicates that habitat complexity, abundance, and diversity of marine taxa are usually higher within submarine canyons compared to adjacent continental shelf areas. The complex interaction between canyons and the coastal currents can result in localised upwelling, downwelling and eddies that enhance primary productivity. The objective of this study was to compare mesozooplankton (200–2,000 µm) abundance, biomass, and diversity from Bongo net samples collected in the canyon and non-canyon environments (Fig. 1). Samples were collected aboard the RV *Angra Pequena* in June 2018 and July 2019 as part of the African Coelacanth Ecosystem Programme (ACEP) project on Canyon Connections.

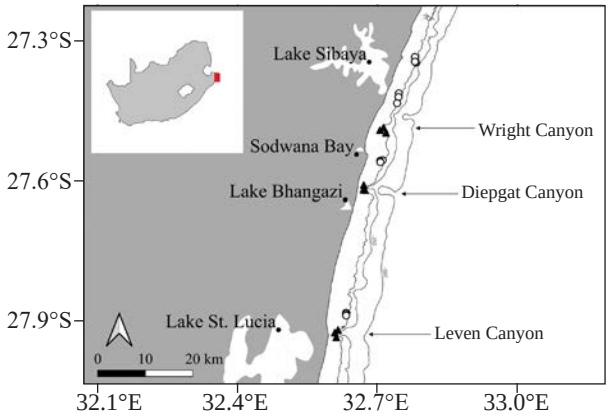

Figure 1. Sampling sites off the northern KZN coast. Solid triangles represent replicate samples from the submarine canyon sites. Open circles represent replicate samples from the non-canyon sites.

The canyons showed generally lower temperatures compared to non-canyon sites in both years, most noticeable at Diepgat, possibly suggesting some upwelling occurs over the canyons (Fig. 2). Zooplankton abundance and biomass did not differ significantly between canyon and non-canyon sites but differed between years and locations (Fig. 3). The zooplankton community was highly diverse, with 87 taxa identified in 2018 and 84 taxa in 2019, 70% of which were copepods. Small copepods such as *Paracalanus* and *Oncaea* spp. were dominant, which was not surprising for oligotrophic (nutrient-poor) systems. Given the high variability among sites and temporally limited sampling, there was insufficient evidence to support the hypothesis that the submarine canyons investigated are significant biomass or diversity nodes for zooplankton in the northern KZN. Future long-term sampling coupled with canyon flow models would enhance our understanding of these unique ecosystems.

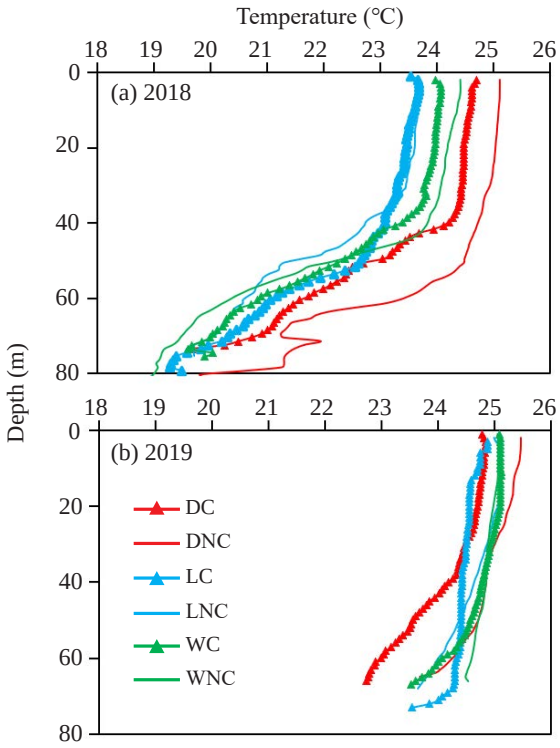

Figure 2. Temperature profiles from a Temperature, Depth, and Conductivity (CTD) sensor. C = Canyon, NC = Non-canyon, D = Diepgat, L = Leven, W = Wright.

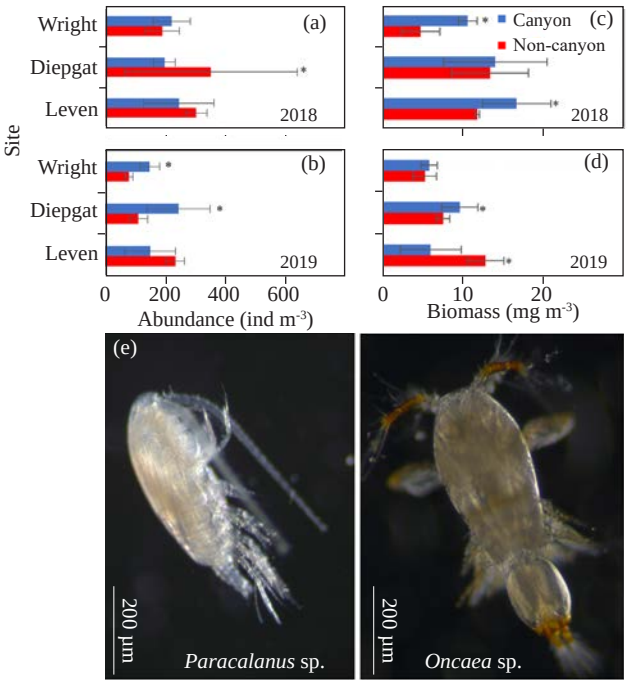

Figure 3. Zooplankton abundance (a) and (b), dry weight biomass (c) and (d), and (e) images of the most abundant copepod species. Error bars indicate standard deviation. Asterisks (*) indicate a significant difference between canyon and non-canyon sites.

Authors: Mdluli NM (UKZN); Carrasco C (UKZN); Huggett J (OC Research); Harris S† (UNIZULU)

26. MODELLING THE SHELF AND SLOPE CURRENTS IN SUBMARINE CANYONS

Northern Kwazulu-Natal (KZN) on the east coast of South Africa (Fig. 1) is an area with high ecological, economic, recreational and cultural value. The ocean environment is characterised by high spatio-temporal variability and rich biodiversity. A key feature of the seafloor is the narrow, closely-spaced submarine canyons that extend across the shelf-break (Fig. 1), intersecting marine protected areas (MPAs) such as iSimangaliso.

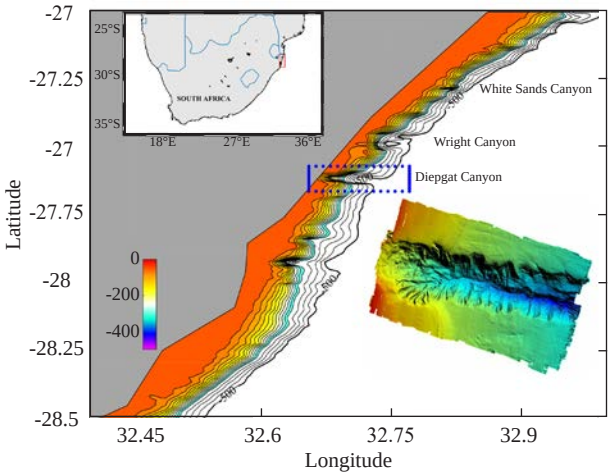

Figure 1. The continental shelf off northern KwaZulu-Natal, showing shelf-break submarine canyons. The dotted blue box highlights Diepgat canyon, illustrated in the inset on the right. The 500 m isobath is shown in black.

Adequately characterising the oceanography of these vulnerable ecosystems is required to inform their conservation and management, but this is difficult due to a lack of high-resolution *in situ* data, sampled consistently in time and space throughout the water column. One solution is to use model simulations, which can provide reliable approximations of the oceanographic conditions. Models complement the data deficiency problems and help to consolidate theories. Therefore, we used a hydrodynamic model to simulate bathymetry and coastal currents at scales that were able to capture the geomorphology of the submarine canyons. The model-derived version of Diepgat canyon (Fig. 2) shows much broader and smoother bathymetry than indicated by data retrieved from *in situ* single-beam echo sounders and satellites (Fig. 1), owing to the coarser spatial resolution of the model. Despite this difference, the simulation provided a reasonable annual pattern of the coastal current system that dominates the region (Figs. 2 and 3). The inner-shelf circulation was characterised by a year-round strong northward current (Fig. 2), which was most intense and better defined in July–December. This current was spatially confined between the coast and the shelf-break (50 m) isobath (Fig. 3). We hypothesise that it is part of the recently discovered Natal Bight Coastal Counter-Current. Similarly, the southward-flowing slope current, located between the 50–600 m isobaths, was present year-round and exhibited notable seasonal variations in strength (Fig. 3). We infer that this poleward flow is the inner limb of the Agulhas Current. Considering the lack of sufficient *in situ* data, results from this model simulation can facilitate research into key processes driving upwelling in the canyons, as well as biological connectivity between MPAs, benthic and pelagic fish migration, and larval dispersal in the region.

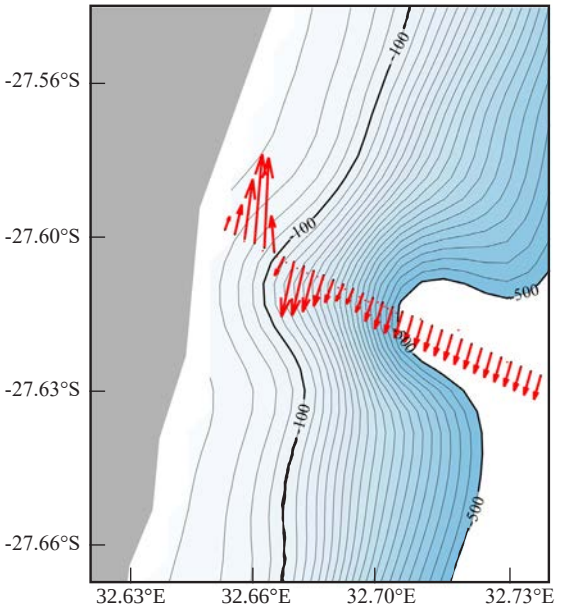

Figure 2. Modelled bathymetry (colour shading) zoomed over Diepgat canyon (see Fig. 1), with isobaths (black contours, at 20 m intervals). Annual averaged flow within the canyon is indicated by red arrows (longer arrows indicate greater flow).

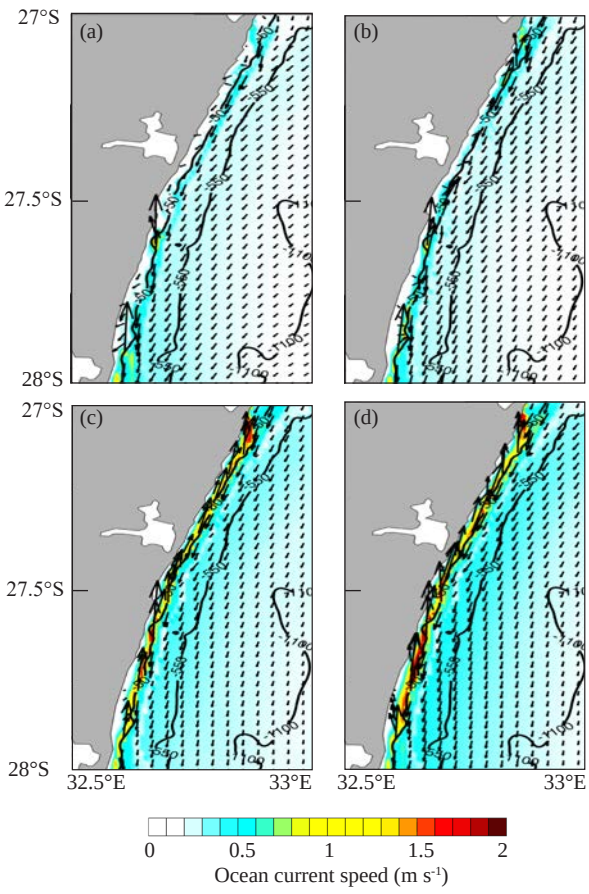

Figure 3. Averaged model-derived ocean currents (vectors) and current speed (colour shading) for (a) January–March, (b) April–June, (c) July–September, (d) October–December. Background contours show isobaths of 50, 550 and 1,100 m.

Authors: Halo I, Lamont T (OC Research); Rautenbach G (SAEON)

27. DIVERSITY PATTERNS OF SOUTH AFRICA'S AZOOXANTHELLATE SCERACTINIAN CORALS (CNIDARIA: ANTHOZOA)

With the increasing global commitment to sustainable ocean ecosystem management, there is a growing need to quantify biodiversity trends, especially for lesser-known taxa in poorly studied environments. Azooxanthellate scleractinian (stony) corals, which lack a symbiotic relationship with dinoflagellates, are one of these poorly understood taxonomic groups. Despite a recent taxonomic review of azooxanthellate scleractinians in South Africa, there is a lack of knowledge on their diversity gradients. This study aimed to address this gap by analysing sample-specific data from museum specimens of azooxanthellate coral fauna (Fig. 1).

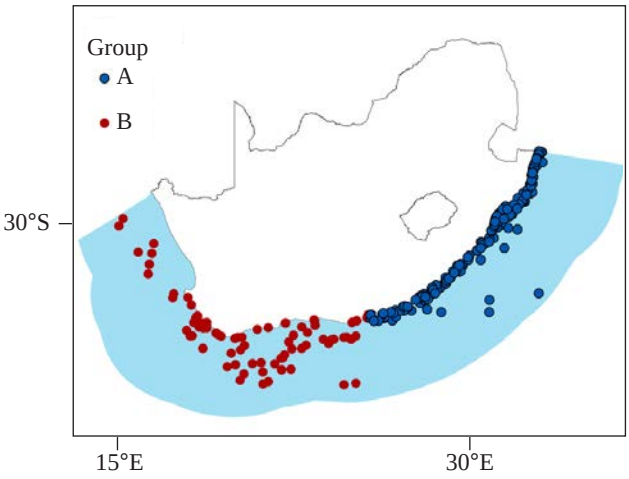

Figure 1. Sample locations within the South African maritime domain (illustrated by light blue shading). The symbol A reprsents the eastern margin group, and B represents the southern and western margin group.

The coral-associated coordinate data were georeferenced, with the bottom depth obtained from a national bathymetric dataset, prior to undertaking multivariate analysis. This analysis encompassed several steps, including linking the longitude and depth (environmental data) to a 50 x 50 km spatial grid, and incorporating genetic data to account for diversity at a phylogenetic level.

Results confirmed two longitudinal groups, an eastern margin group (A), and a southern and western margin group (B) (Fig. 1). The number of samples varied between groups, with over twice the number of samples in Group A than in Group B (Table 1). In contrast, the related area (number of grids) representing the samples was larger for Group B than for Group A. Both diversity measures (i.e., Shannon diversity index and Delta+) followed the same pattern of higher measures in Group A compared with Group B. Dendrophylliids were characteristic of Group A, whilst caryophylliids defined Group B.

Of eleven depth categories represented within two bathymetric zones, shallow (50–200 m) and deep (300–1,000 m), the highest number of samples and species richness was recorded at the shallowest depth category (50 m; Fig. 2). This was mirrored by the Shannon diversity index (highest at 50 m). In contrast, the average taxonomic distinctiveness measure Delta+, which takes into account species phylogeny (evolutionary relationships), showed coral diversity to be marginally highest at 1,000 m. Three

Table 1. Sampling effort in relation to longitudinal gradient.

Group	Number of samples (N)	Number of 50 x 50 km grids	Species richness (S)	Shannon diversity index (H')	Delta+
A	569	37	86	3.96	90.91
B	192	43	37	3.25	89.29

of the eleven families represented in the dataset accounted for the greatest differences between bathymetric zones (shallow vs deep). These were the caryophylliids, which were more abundant at the deeper stations, and the dendrophylliids and flabellids, which were most abundant at the shallow stations (Fig. 3, opposite page).

Whilst sampling biases were observed (e.g. distribution of sampling by longitude and depth category), the study demonstrates that museum samples provide a valuable data source that can help improve understanding of biodiversity patterns in under-sampled marine ecosystems. A key application for this existing coral data set will be its integration into multi–taxa biogeography analyses and other data-driven approaches to improve ecosystem description and mapping. These products are invaluable for ongoing spatial biodiversity prioritisation and marine spatial planning efforts.

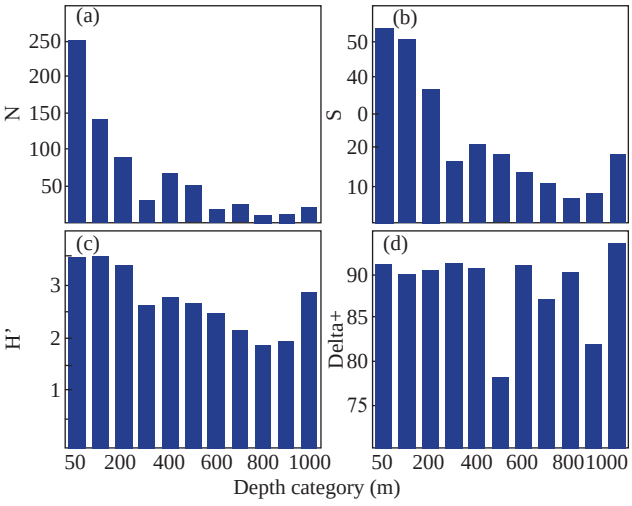

Figure 2. Values at depth for (a) number of coral samples (N), (b) species richness (S), (c) Shannon diversity index (H'), and (d) average taxonomic distinctiveness (Delta+).

Author: Filander Z (OC Research)

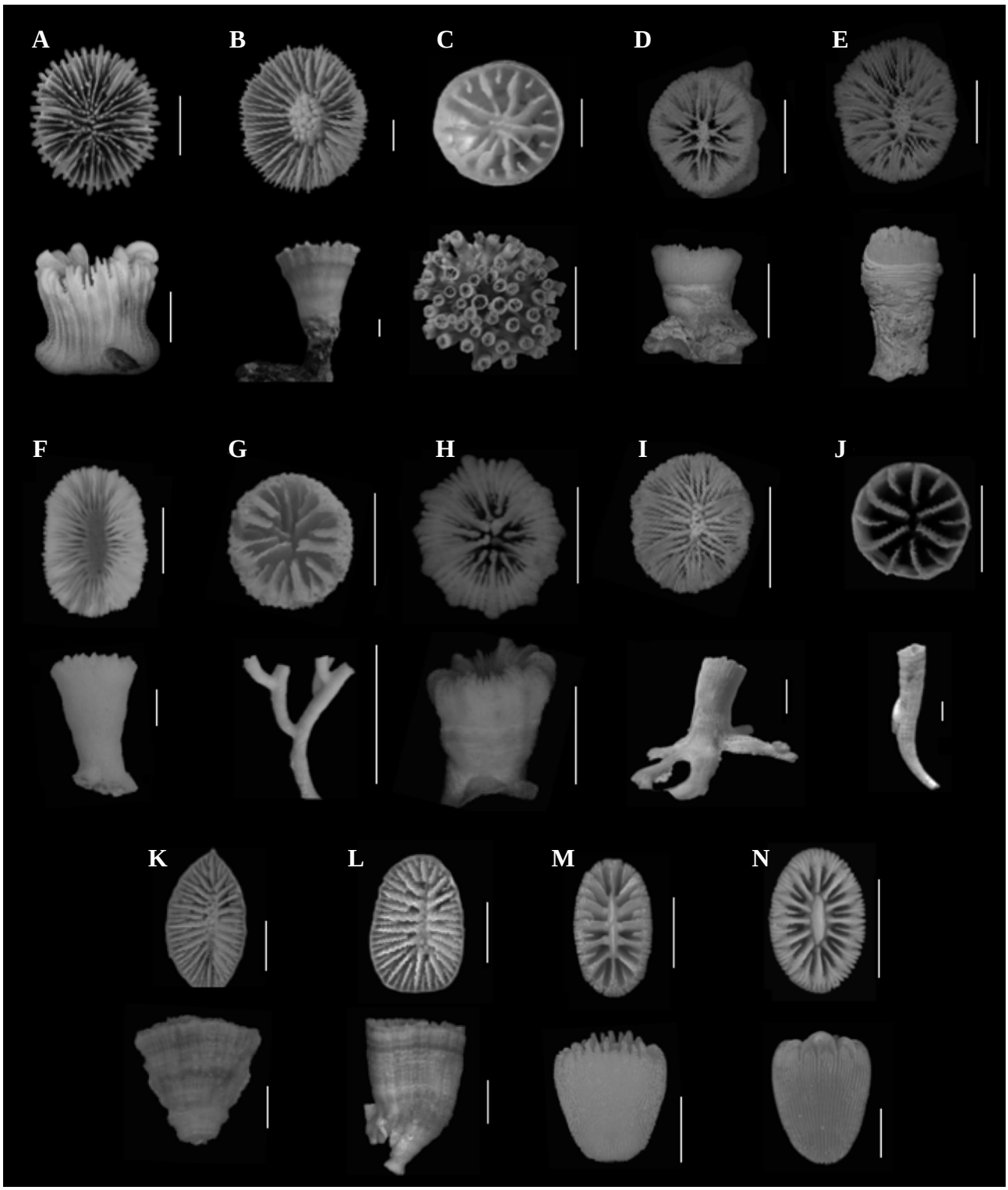

Figure 3. Calicular (from above, top) and lateral (bottom) views of caryophyllid species: (A) ***Heterocyathus monileseptatum*** (off Durban Harbour, 99 m), (B) *Monohedotrochus capensis* (off Kidds Beach, 247–147m) and (C) (off Scottburgh, 690 m, top) ***Atlantia denticulata*** (off Gouritsmond, 170 m, bottom): Close-up of corallites. Dendrophylliid species: (D) *Balanophyllia (Balanophyllia) bonaespei* (off the Agulhas, 32 m), (E) *Balanophyllia (Balanophyllia) capensis* (off Cape Point, depth unknown, top and locality unknown, bottom), (F**)** *Balanophyllia (Balanophyllia) diademata* (off Richards Bay, 500 m), (G) *Ednapsammia columnapriva* (off Mossel Bay, 212 m), (H) *Pourtalopsammia togata* (off Kei River mouth, 159 m), (I) *Rhizopsammia annae* (off the Agulhas, depth unknown); flabellid species: (J) *Flabellum (Flabellum) leptoconus* (locality unknown), (K) *Truncatoflabellum inconstans* (SAM_H1241, off Kei Mouth, 66 m), (L) *Truncatoflabellum zuluense* (off Cape Vidal, 85 m); and turbinolid species: (M) *Sphenotrochus (Eusthenotrochus) gilchristi* (off Cape Point, 24 m), (N) *Sphenotrochus (Sphenotrochus) aurantiacus* (off the Agulhas, 366 m). All scale bars = 10 mm, except (C) (bottom), (D) (bottom) and (F) (bottom) = 100 mm. Bold text indicates new species. All other species are only known from South African waters (endemic).

28. EFFECTS OF HARVESTING ON DENSITY AND SIZE OF LIMPETS

Intertidal rocky shores are the most accessible marine habitats and therefore heavily impacted by harvesting pressures, which have intensified in recent decades especially near growing urban areas. This includes subsistence, recreational and illegal harvesting of intertidal and shallow-water organisms. Harvesting can result in substantial changes in population structure and community composition by reducing the size and densities of target organisms. This study evaluated the effects of harvesting and the role of Table Mountain National Park Marine Protected Area (MPA) on the size and density of two limpet species, one that is commonly harvested and the other, rarely. This was done through comparison of populations inside and outside of no-take areas of the MPA. Four study sites were selected including two harvested areas and two areas that are protected inside the Cape of Good Hope no-take zones. Surveys were conducted in February 2017 by sampling quadrats to determine limpet density and also measuring shell length in four intertidal zones.

The density of commonly harvested *Scutellastra argenvillei* was significantly higher in Scarborough South (no-take area) compared with other sites, where few individuals of this species occurred (Fig.1). Their density at Scarborough North (no-take area) was relatively low, counter to expectations. Densities of rarely harvested *S. granularis* at Kommetjie, a harvested site, was similar to densities of this species inside the no-take areas. Again however, the result was not consistent, because its density was lowest at Wireless Point, the other harvested site. The pattern with size between no-take and harvested areas was clearer. The mean shell length of *S. argenvillei* was significantly larger inside the no-take areas than in the harvested areas, with smallest size at Kommetjie (harvested). The shell length of rarely harvested *S. granularis* was also smallest at Kommetjie, but was largest at the other harvested site, Wireless Point, with the no-take sites intermediate (Fig. 2).

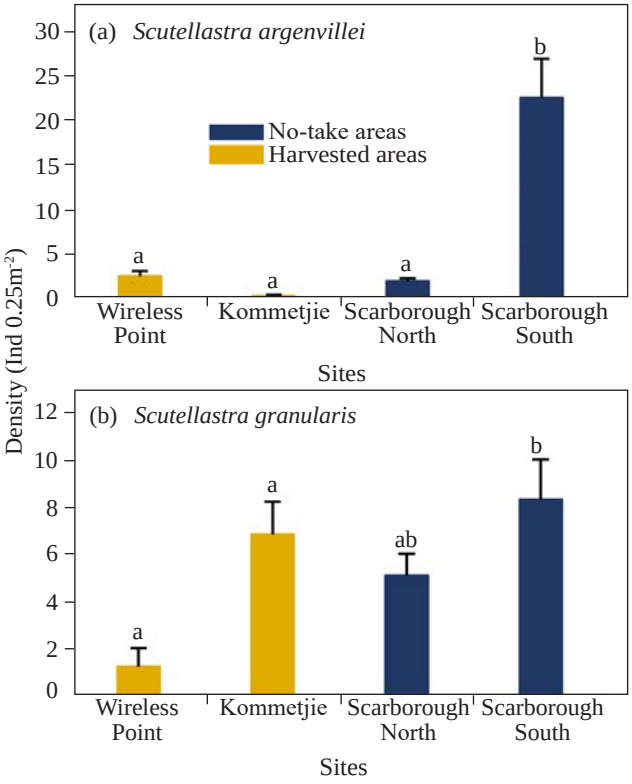

Figure 1. Mean (+1 SE) densities of the limpets *S. argenvillei* (a) and *S. granularis* (b) at the four study sites. Sites with common labels (a, b or c) are not significantly different from each other; sites without common labels are.

Through comparison of the densities and sizes of harvested and non-harvested species between no-take and harvested areas, the overall results of this study support that no-take areas of the Table Mountain National Park MPA are effective at protecting rocky shore invertebrates such as limpets. Results were not entirely equivocal, considering that densities of the harvested species at a no-take area (Scarborough North) were similar to the harvested areas, although their mean size was greater. This, and the low density of the non-harvested species at a harvested site (Wireless Point), despite their large mean size, confirm that other factors besides harvesting also influence the abundance and growth of these species.

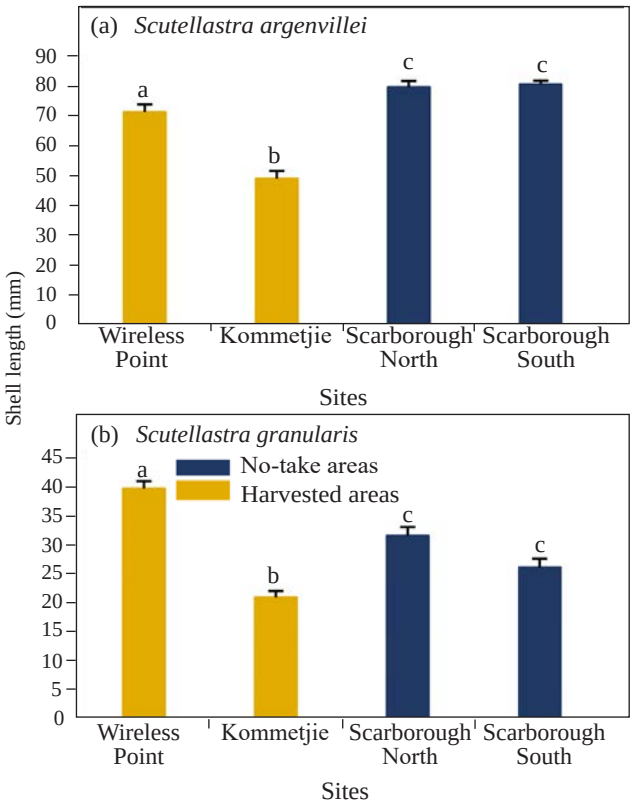

Figure 2. Mean (+1 SE) shell lengths of the limpets *S. argenvillei* (a) and *S. granularis* (b) at the four study sites. Sites with common labels (a, b or c) are not significantly different from each other; sites without common labels are.

Authors: Baliwe N (DFFE, UCT); Pfaff M, Branch G (UCT)

29. ASSESSING THE EFFECTIVENESS OF A NO-TAKE MARINE PROTECTED AREA USING GALJOEN AS A PROXY

The status of galjoen *Dichistius capensis* (Fig. 1), the national fish of South Africa, has previously been assessed as Collapsed (declined to a point where it is not economically viable to harvest them) in 2003, and as Near-Threatened (in terms of IUCN criteria) in 2016. Galjoen are mainly resident species, meaning that they complete all life cycle stages in a local area, although a small percentage of the population have been shown to be nomadic. As such, it can be expected that marine protected areas (MPAs), especially no-take areas, will be effective for the conservation and recovery of local populations of galjoen, and also allow for spill-over to adjacent unprotected areas. An ongoing tag-and-release monitoring study in the Table Mountain National Park (TMNP) MPA (Fig. 2) collects data that can be used to test the effectiveness of the no-take areas. These include catch per unit effort (CPUE) data, and data that can be used to assess survival rates and dispersal. In this study, we report on the comparison of CPUE data between restricted (no-take) and controlled zones (harvested; i.e. open to angling) of the TMNP MPA.

Figure 1. A tagged galjoen lying on a measuring stretcher to minimise handling effects.

Monitoring has been conducted through a controlled angling survey since 1999, allowing for long-term trends to be analysed. Two research anglers are responsible for capturing, measuring, tagging, and releasing galjoen within restricted (Olifantsbos) and controlled (Pegram's Point) zones (Fig. 2). Angling takes place during the recreational fishing season (April to late November), with fishing days distributed randomly throughout the season, and with equal effort in each zone type.

Significant interannual variability in CPUE for both zones was recorded over the years (Fig. 3). Conspicuous patterns in the time series include a spike in CPUE in 2001, especially in the restricted zone, and declining CPUE towards the end of the time series for both zone types. The mean CPUE in the restricted zone was higher than in the controlled zone in most years and was significantly higher overall (Fig. 3). This indicates that there is greater availability of galjoen in the no-take compared to fished areas. The difference in CPUE between restricted and controlled zones was greater in some years than in others, and in two years (2008 and 2016) CPUE was greater in the controlled zone.

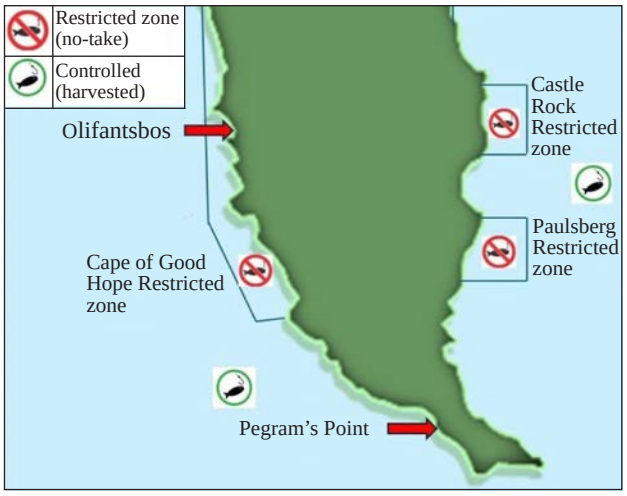

Figure 2. Map of restricted and controlled zones within TMNP MPA and the two study sites (Olifantsbos and Pegram's Point).

Environmental factors can be an important driver of variability in galjoen availability, which may account for the fluctuations in CPUE in both restricted and controlled zones throughout the study period. However, the timing of fluctuations in CPUE did not always correspond between the two zone types. This suggests that the relationship of environmental variability to CPUE patterns is not that clear-cut and may be affected by levels of fishing pressure. Although most galjoen (90%) are highly resident, some movement between zones is likely, and it would be expected that movement would be greater from areas of higher abundance (restricted zones) to those of lower abundance (controlled zones). Such movement could also affect the CPUE patterns found in this study. Data of tag-recaptures between zones, and size differences of fish between zones, may provide further insights to the effects of spatial management on the galjoen resource in the MPA.

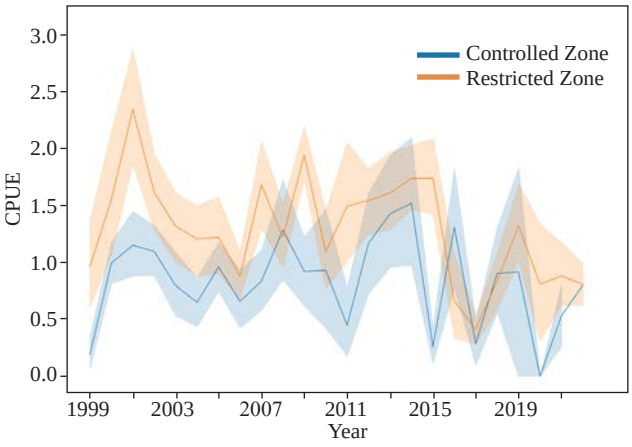

Figure 3. Catch per unit effort (CPUE) in restricted and controlled zones of the TMNP MPA. Shaded areas represent 95% confidence intervals (i.e. possible values of the estimates are expected to occur within the intervals 95% of the time).

Authors: Nemanashe E, Swart L (OC Research)
Contributors: Walker S, Hart C (research anglers)

30. HUMAN AND ENVIRONMENTAL FACTORS AFFECTING BEHAVIOURAL RESPONSES OF CAPE FUR SEALS TO SWIM-WITH-SEAL TOURISM

Swim-with-seal (SWS) ventures (Fig. 1) are an increasingly popular tourist activity. Research conducted at the Cape fur seal *Arctocephalus pusillus pusillus* colony at the Robberg Marine Protected Area, Plettenberg Bay, by the DFFE in collaboration with the Cape Peninsula University of Technology and Nature's Valley Trust, aimed to assess impacts of SWS activity on seal behaviour in the colony.

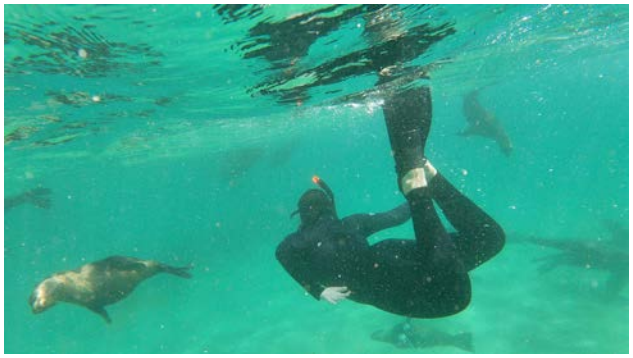

Figure 1. A tourist swimming with seals (Source: Offshore Adventures).

We used a modified before-after-control-impact behavioural study with simultaneous observations of an impact site (adjacent to SWS) and a control site (away from SWS), during three temporal phases – before, during and after SWS activities occurred at the impact site. Data collection was carried out from elevation, and consisted mostly of sequential photography of the colony at 10-minute intervals. This provided the basis for classifying and counting seals into different behavioural categories, and for statistical comparisons. Statistically significant changes in behaviour at the impact site versus the control site during SWS activity, relative to before, were taken as an indication of seal responses to SWS. Data on environmental variables and characteristics of SWS activity, were also collected.

Responses were by no means homogenous for different behavioural categories, and were sometimes difficult to interpret. For example, a decline in the proportion of the animals lying down and an increase in the proportion sitting, was interpreted as a decreased state of restfulness in response to tourist activity. However, the state of restfulness increased with decreasing distance of the boat (Fig. 2) or swimmers (not shown) to the impact site. This could suggest that the seals are most responsive to activity when they first become aware of the disturbance (i.e. from a distance), but become accustomed to it, so that responses decline as activity gets closer to the colony. While seal responses, when they occurred, were typically significantly greater at the impact site than at the control site (e.g. Fig. 3), responses were also observed at the control site (Figs. 2–3), indicating that it was not entirely free of disturbance (likely due to the visibility of the boat from the control site). Responses also appeared to be significantly affected by environmental factors such as air or sea temperature (Fig. 3).

Although results showed statistically significant differences in seal responses to SWS activities, between sites and between phases, with significant interactive effects, it was always only a small proportion of animals that were affected (< ca. 2% of seals at impact site). Importantly, seals at the experimental sites were mostly at rest throughout the study (>70% lying down), and no extreme reactions such as stampedes occurred throughout 54 observation sessions. Overall, the results support that the seals are likely habituated to SWS activities, while the code of conduct that the operator adhered to (setting limits on tourist numbers, distances, boat approaches, etc.) is apparently effective in preventing excessive disturbance to the seal colony.

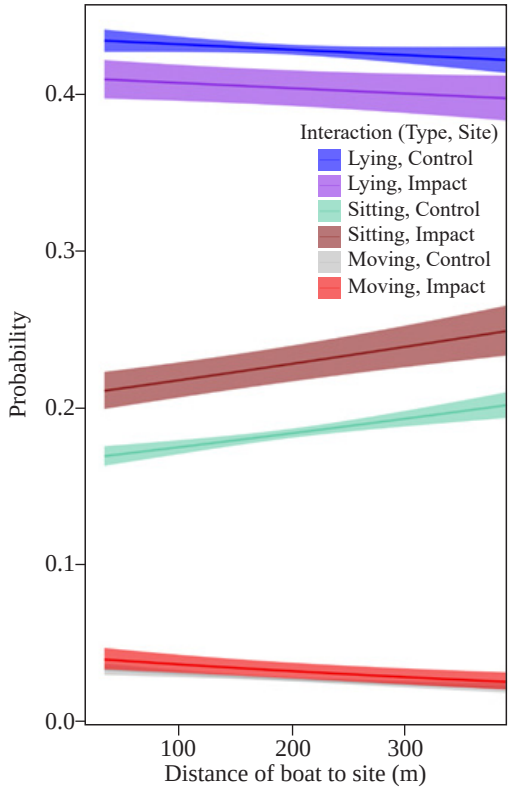

Figure 2. Changes in the probability of seals for the behavioural categories (lying, sitting or moving), in relation to distance of the boat from shore.

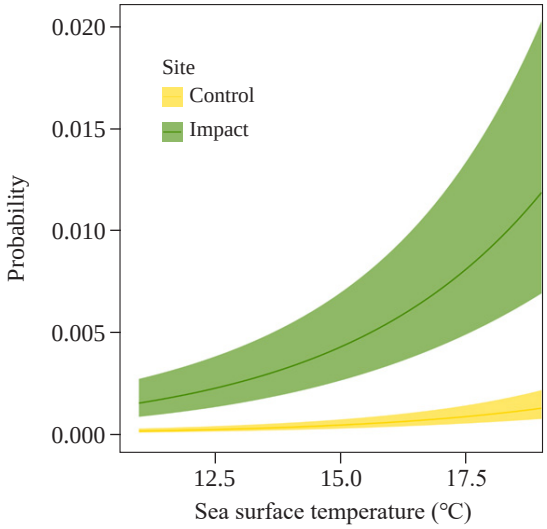

Figure 3. Changes in the probability of seals showing alert behaviour in relation to sea surface temperature.

Authors: Basson R (OC Research, CPUT); Yemane D (Fisheries R&D); Findlay K (CPUT); Kirkman SP (OC Research)

31. ZOOPLANKTON VARIABILITY AT THE PRINCE EDWARD ISLANDS

The Prince Edward Islands (PEIs) are a sub-Antarctic archipelago located between the sub-Antarctic Front (SAF) and the Antarctic Polar Front (APF). In this region of high frontal mixing and mesoscale (10–100 km) variability, zooplankton are an essential component of the food web, supporting an abundance of top predators. This study explores the oceanographic features influencing the abundance, biovolume and composition of the zooplankton community surrounding the PEIs.

Sampling of zooplankton abundance and biovolume (a proxy for biomass), was conducted during the annual Marion Island relief voyages of 2018 and 2019. In 2018, sampling was conducted along transect lines upstream and downstream of the PEIs and between the two islands of the archipelago, Marion and Prince Edward (Fig. 1a, b). In 2019, only the inter-island and upstream transect lines were sampled (Fig. 1c, d). Zooplankton were collected using a 200 µm Bongo net and enumerated using image analysis. In 2018, a CTD (Conductivity-Temperature-Depth instrument) was deployed to obtain temperature, salinity, and chlorophyll *a* (chl *a*) profiles. The positions of the various frontal branches and mesoscale features were identified using satellite Absolute Dynamic Topography data.

In 2018, the southern branch of the sub-Antarctic Front (S-SAF) was located south of the PEIs resulting in reduced current velocities in the inter-island region, and enhanced retention downstream (meaning that upwelled waters, nutrients, and biota were retained longer in this area). This likely contributed towards the elevated plankton levels observed downstream in 2018 (Fig. 1a, b). Peaks in zooplankton abundance and biovolume in 2018 corresponded with elevated *in situ* chl *a*, but only biovolume showed a strong, statistically significant correlation with chl *a* (Fig. 2), suggesting that their growth was more closely linked to an increase in food availability than their overall population abundance. Such a relationship reflects the importance of the Island Mass Effect (locally enhanced chl *a*) on the zooplankton communities of the region. In contrast, the S-SAF was closer to the PEI shelf in 2019 (Fig. 1c, d), resulting in higher current velocities promoting a flow-through system which likely inhibited retention and primary production.

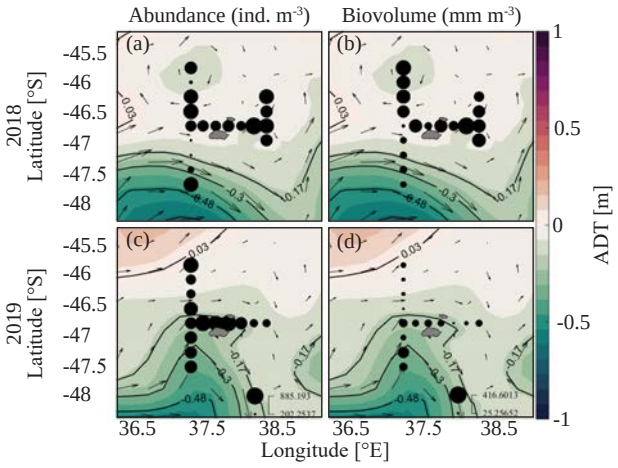

Figure 1. Mean daily Absolute Dynamic Topography (m) with overlaid geostrophic current vectors (arrows sizes depict strength of current in m s^{-1}) for 23–28 April 2018 (a, b) and 24–27April 2019 (c, d). Black dots indicate sampling station positions, and bubble size indicates total zooplankton abundance (a, c) and biovolume (b, d) sampled at each station. Black contours indicate the positions of various branches of the SAF and APF (Middle-SAF: 0.03 m; Southern-SAF: -0.17 m; Northern-APF: -0.3 m; Middle-APF: -0.48 m; Southern-APF: -0.63 m).

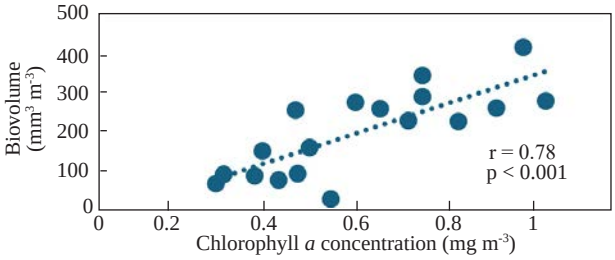

Figure 2. The correlation between chlorophyll *a* concentration (mg m^{-3}) in the upper 200 m of the water column and the corresponding zooplankton biovolume (mm^3 m^{-3}) in 2018. The correlation coefficient (r) and p-value indicate a strong, significant relationship.

Mean zooplankton abundance was similar in both years, however, the mean biovolume in 2018 (201 mm^3 m^{-3}; Fig. 1b) was significantly higher than in 2019 (75 mm^3 m^{-3}; Fig. 1d). Size composition metrics derived from image analysis show larger individuals in 2018 that may account for this. Copepods dominated zooplankton abundance (>90%) in both years, whereas the biovolume was largely accounted for by chaetognaths (2018: 44.9%; 2019: 39.2%), copepods (2018: 33.9%; 2019: 35.7%) and euphausiids (2018: 14.0%; 2019: 6.3%). We hypothesise that the differences in community composition between years may be due to variability in oceanographic conditions, such as the more retentive conditions in 2018 and high chl *a*, which we have shown to have a strong relationship with the zooplankton biovolume.

This study revealed the substantial influence that mesoscale features, fronts, and the Island Mass Effect have on the distribution and magnitude of zooplankton abundance and biovolume around the PEIs. Variations in zooplankton communities may exert a bottom-up effect on the food web structure, thereby affecting the ability of certain species to meet their energy requirements. It is therefore essential to understand the dynamics of such variability in the context of a changing ocean environment and climate.

Authors: du Preez SA (UCT); Lamont T, Huggett JA (OC Research)
Contributor: Mdluli NM (UKZN)

32. THE GLORYS MODEL SIMULATES A TAYLOR COLUMN AT THE PRINCE EDWARD ISLANDS

The Prince Edward Islands (PEIs; Fig. 1), consisting of Prince Edward Island and Marion Island are home to a multitude of species that are supported by a sensitive and complex oceanic environment. Understanding the mechanisms that sustain this rich ecosystem is therefore imperative for both the ecological management of the PEIs, and to discern future environmental changes in response to climate change and variability. The presence of a Taylor column (a persistent anticyclonic circulation) has been suggested as the main driver supporting and maintaining the PEI ecosystem. We used the GLORYS (Global Ocean Reanalysis and Simulations) reanalysis model output to examine whether a Taylor column exists at the PEIs by studying a cooling event that took place between 10 and 28 June 2021.

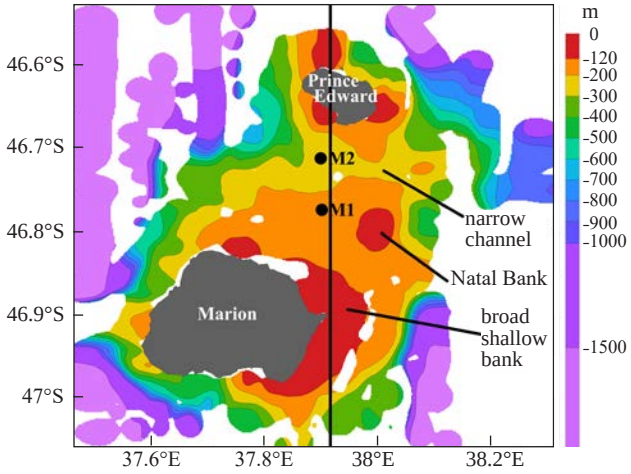

Figure 1. *In situ* bathymetry around the PEIs. Points denote the position of two moorings, and the vertical line denotes the transect presented in Fig. 2. White shading indicates areas of no bathymetry data.

In 2021, data from sensors moored on the shelf between the two islands (Fig. 1) indicated five cooling events. One of these events occurred in June and could not be linked to either mesoscale eddies or frontal interactions. This suggested the presence of a Taylor column at the PEIs. A scaling analysis was conducted to investigate this possibility during the strongest cooling period (13–17 June). This included the calculation of three parameters (Table 1), namely the Rossby number (Ro), which compares inertial and rotational circulation to describe instabilities of the flow; the Burger number (B), which describes how stratified the water column is; and the blocking parameter (Bl), which defines whether a Taylor column can be formed.

For a Taylor column to form, each parameter must meet set thresholds (Ro < 2, B < 1, and Bl > 2). During the June 2021 cooling event, the daily calculated parameters satisfied each of these thresholds (Table 1). The calculated

Table 1. Daily Rossby number (Ro), Burger number (B) and blocking parameter (Bl), from 13 to 17 June 2021, averaged for the upper 150 m on the PEI shelf, between 45.75°S and 48.00°S, at a mean longitudinal position of 37.92°E.

	13 Jun	14 Jun	15 Jun	16 Jun	17 Jun
Ro	0.02	0.02	0.02	0.02	0.02
B	0.26	0.26	0.26	0.51	0.46
Bl	2.24	2.20	2.51	2.21	2.11

values indicated Ro << 1, implying a strong influence of the Earth's rotation on the flow dynamics. Values of B < 1 implied a nearly unstratified water column due to increased mixing, and values of Bl > 2 suggested the formation and persistence of a Taylor column. This allows us to infer that a Taylor column can indeed form over the PEI shelf.

During June 2021, daily zonal (east-west) current speeds (Fig. 2) indicated westward flow (negative values), reflecting the anticyclonic circulation expected when a Taylor column is present, in agreement with *in situ* observations (see Report Card 14). This westward flow was concentrated over the PEI shelf but did not always extend to the surface. This provides the first evidence that, instead of a Taylor column, a "Taylor cap", may form predominantly over the PEI shelf. Compared to a Taylor column, a Taylor cap has a similar anticyclonic circulation but it does not present a surface expression. On occasion, this circulation may reach the surface, as on 15 June 2021 (Fig. 2), thus changing the Taylor cap into a Taylor column. This switching state may explain why researchers have thus far been unable to clearly prove the persistence of a Taylor column at the PEIs.

Authors: Soares BK (OC Research, UCT); Lamont T, Halo I, Russo CS (OC Research)

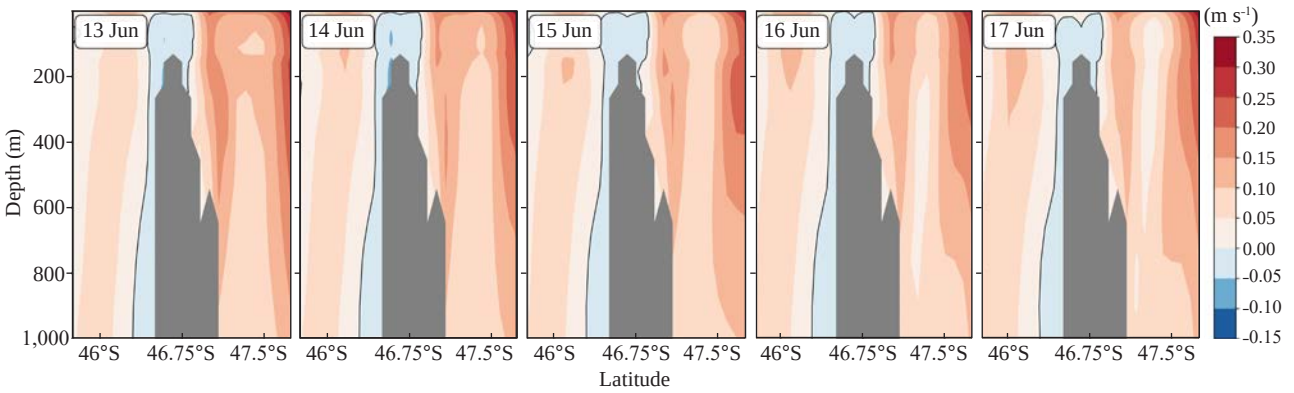

Figure 2. Daily GLORYS vertical sections, showing the zonal (east-west) current component (m s^{-1}) within the upper 1,000 m of the water column, along 37.92°E between 13 and 17 June 2021, the period of strongest cooling. Flow toward the east is positive, while westward flow is negative. Grey shading denotes the bathymetry of the PEI shelf between Prince Edward Island and Marion Island.

33. SEABIRD ASSEMBLAGES AND DISTRIBUTIONS IN THE AFRICAN SECTOR OF THE SOUTHERN INDIAN OCEAN

Seabird distributions in the Southern Ocean are influenced by the location and accessibility of suitable breeding sites, but also by the environmental factors that influence the distribution and availability of their prey. For example, oceanic fronts, which are boundaries between two water masses, may concentrate potential prey at their surface and therefore present important foraging areas for many seabird species. Oceanic fronts also define biogeographical boundaries for many species in the Southern Ocean and play a critical role in structuring seabird assemblages. We investigated the latitudinal distribution and abundance of seabirds in the African sector of the Southern Ocean (to the south of Africa up to Antarctica), which is one of the least studied regions of the world's oceans. In particular, we investigated the relationship of seabird assemblages and densities in this region to key physical and biological environmental parameters and to the main oceanic fronts of the region, namely the Subtropical Front Convergence (STC), the sub-Antarctic Front (SAF) and the Antarctic Polar Front (APF).

We used data from the Atlas of Seabirds at Sea (AS@SA-SAS), a collaborative citizen science programme between the DFFE, BirdLife South Africa, the Percy FitzPatrick Institute of African Ornithology, and the South African Environmental Observation Network. Densities of ten numerically dominant seabird species were binned at one-degree latitudinal intervals (Fig. 1).

There was a high density of seabirds between 30°S and the STC, which is situated at approximately 39°S, with declining densities further southwards (Fig. 1). There was spatial segregation between several species in terms of their latitudinal distribution, e.g. Cape gannets *Morus capensis* and white-chinned petrels *Procellaria aequinoctialis* occurred north of the STC, and Antarctic prions *Pachyptila desolata*, Antarctic petrels *Thalassoica antarctica*, and blue petrels *Halobaena caerulea* occurred to the south of it. The STC acts as a biogeographical boundary between the Southern Ocean and warmer subtropical waters north of 39°S, resulting in a significant barrier for seabirds. The SAF and the APF had less influence on seabird populations than the STC. The density of Antarctic prions peaked in the Sub-Antarctic Zone between the SAF and APF (Fig. 1).

Latitude was the greatest predictor of seabird assemblages and densities, reflecting environmental gradients in physical and biological parameters, within and between water masses, and their influences on prey distributions. Of the environmental parameters, SST and bathymetry had the strongest influence on seabird assemblages, consistent with earlier research in other parts of the Southern Ocean. In particular, the density of seabirds declined, in a non-linear manner, with increasing SST, and there was a non-linear, negative relationship between seabird density and bathymetry, with most seabirds occurring in shallower waters (Fig. 2).

In contrast, seabird density had a positive linear relationship with sea surface height (SSH), which may be explained by their proclivity for frontal areas. Relationships with other environmental parameters, namely wind, sea surface salinity and chlorophyll *a* (as a proxy for productivity), were less well defined. Strong relationships between the distributions and densities of seabirds and certain oceanic features or environmental parameters, suggest that the biogeography of seabird assemblages in the study region is likely to be considerably affected by climate change-related shifts in the ocean environment. This will have implications for spatial management measures in particular marine protected areas designed for seabird conservation.

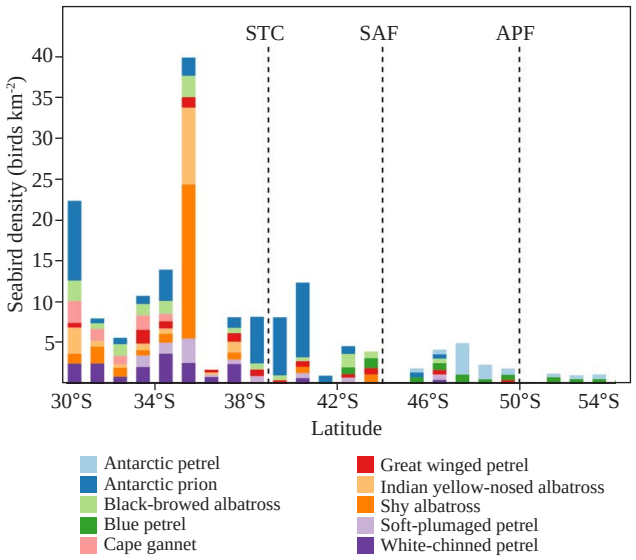

Figure 1. Mean densities of the ten most numerically abundant seabird species at intervals of one-degree latitude. Dashed lines show the mean annual latitudinal positions of the Subtropical Front Convergence (STC), Sub-Antarctic Front (SAF) and the Antarctic Polar Front (APF).

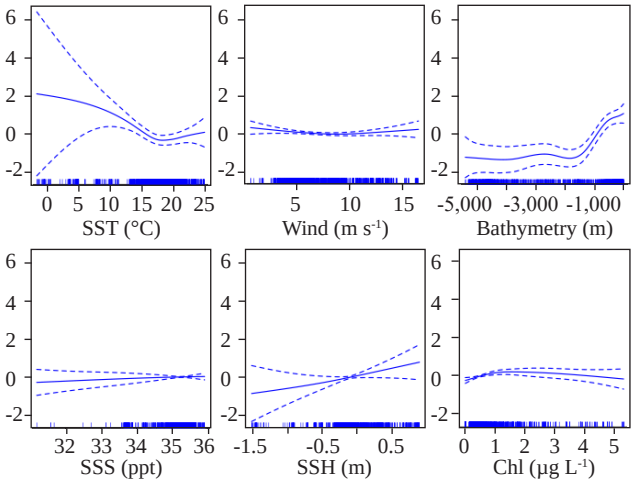

Figure 2. Relationships between environmental variables and the density of all seabirds from 2016–2019, determined from a Generalised Additive Model. The dashed lines indicate the 95% confidence intervals (SST = sea surface temperature; SSS = sea surface salinity; SSH = sea surface height; Chl = chlorophyll *a*).

Authors: Makhado AB, Masotla MM, Dakwa F (OC Research)
Contributors: Shabangu FW, Somhlabe S (Fisheries R&D); Seakamela M (OC Research)

34. KILLER WHALES, PREY ABUNDANCE, AND ENVIRONMENTAL VARIABILITY AT THE PRINCE EDWARD ISLANDS

Killer whales *Orcinus orca* are apex predators of the marine ecosystem that exert top-down control on their diverse prey populations. However, their ecology and behaviour are poorly understood in most regions due to limited research, often because of logistical challenges. Fortunately, killer whales produce sounds for socialising, called social calls. These differ from echolocation clicks that they produce for finding prey and for navigation. These various sounds can be used to study their ecology and behaviour over time. Here, we report on killer whale occurrence and behaviour recorded by an acoustic recorder, SoundTrap ST500 STD, which was deployed on an oceanographic mooring for 376 days (mid-2021 to mid-2022) between the two islands of South Africa's Prince Edward Islands in the Southern Ocean, namely Marion Island and Prince Edward Island (Fig. 1).

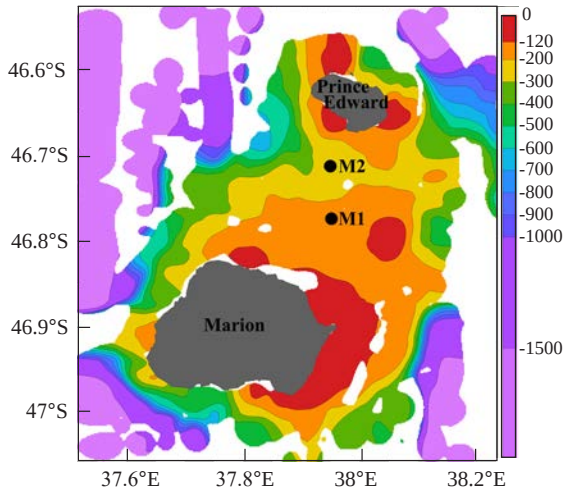

Figure 1. Bathymetry and locations of oceanographic moorings (M1 and M2) between Marion Island and Prince Edward Island. The acoustic recorder was deployed on M1.

Killer whale sounds were detected intermittently throughout the year (Fig. 2). The number of sounds detected corresponded to the number of whales sighted visually by observers on Marion Island, as well as the abundance of one of their favoured prey species, namely southern elephant seals *Mirounga leonina* (SES). Killer whales vocalised more during the day in most seasons. Wind speed was the main predictor of the occurrence of both echolocation clicks and social calls, while sea surface height, chlorophyll *a*, and sea surface temperature were moderately important (Fig. 3). Hour of the day, number of SES, month, and number of killer whales sighted were the least important predictors (Fig. 3). These results show that killer whales respond adaptively to changes in environmental conditions and prey abundance. Long-term simultaneous collection of acoustic and environmental data is recommended to allow researchers to establish temporal trends and variations in acoustic presence of killer whales in this region. Acoustic propagation modelling of killer whale calls linked to biologging data is desired in the future to determine the precise location of animals relative to the mooring location.

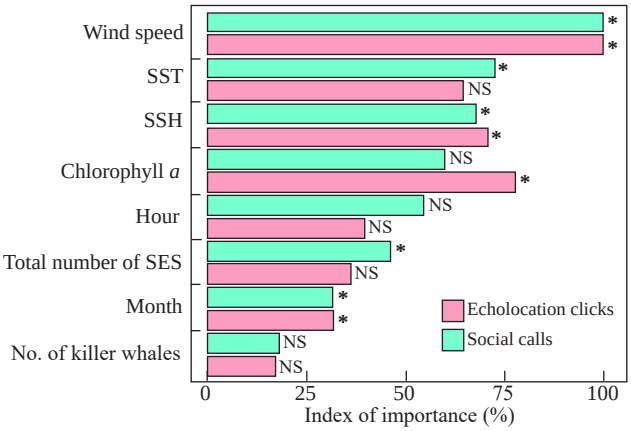

Figure 3. Relative importance (%) of different predictor variables on the occurrence of killer whale echolocation clicks and social calls based on random forest model output. * indicates statistically significant ($p < 0.05$) importance; NS = not significant.

Authors: Shabangu FW (Fisheries R&D); Daniels R (UCT); Jordaan RK, de Bruyn PJN (UP); van den Berg MA, Lamont T (OC Research)

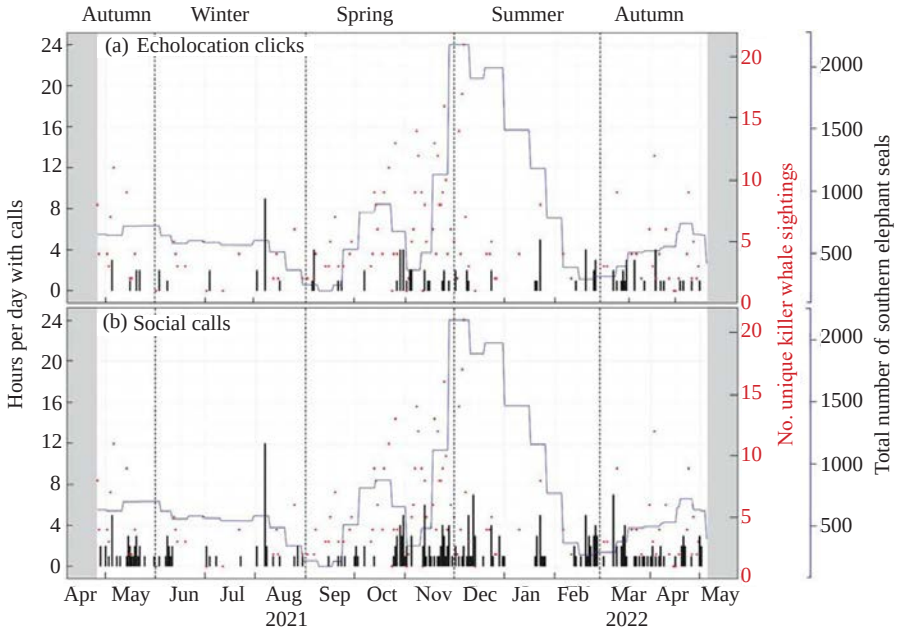

Figure 2. Daily occurrence (bar plots) of killer whale (a) echolocation clicks and (b) social calls around the Prince Edward Islands, together with the number of unique killer whales (dots) and the total number of southern elephant seals (i.e. killer whale prey) sighted (line plots).

35. LISTENING FOR WHALES OFF THE MAUD RISE, ANTARCTICA

Localities around the sea ice edge provide suitable summer feeding environments for marine mammals. These areas are generally understudied as they are remote and dominated by harsh, icy conditions. Passive acoustic monitoring (PAM) instruments are able to sample the marine environment under such challenging conditions without being invasive or lethal to the marine organisms. These instruments record sounds produced by biological organisms, such as marine mammals. They also record non-biological noise (e.g. ship engines). The aim of this work was to determine the acoustic occurrence and behaviour of whales over time at a well-known hotspot for marine mammal occurrence, using PAM. Data were collected using a Rockhopper acoustic recorder that sampled at 250 kHz off the Maud Rise seamount, Antarctica, near the sea ice edge at a water depth of 1,200 m, from January to mid-February 2022 (Fig. 1).

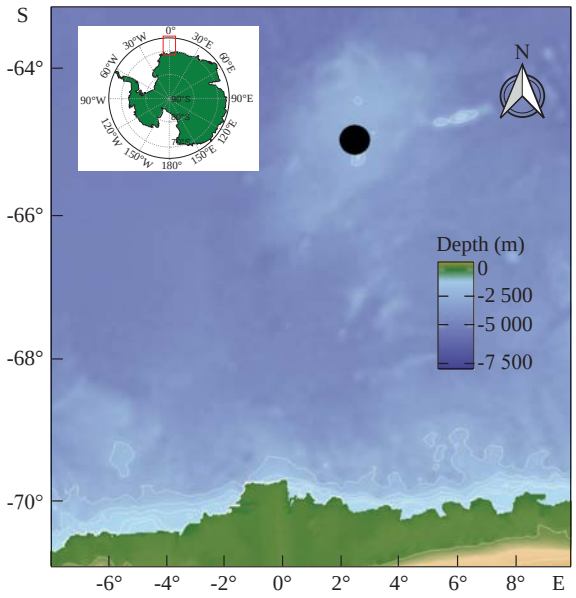

Figure 1. Location of the acoustic recorder (black circle) off the Maud Rise in the eastern Weddell Sea, Antarctica.

Antarctic blue whale Z-calls (most frequently detected), fin whale 20 Hz pulses, blue whale D-calls, Antarctic minke whale bioduck calls, sperm whale clicks (least frequently detected), humpback whale songs, ice cracking sounds, and seismic survey signals were detected from the month-long recordings, likely within 500 km from the recorder location (Fig. 2).

Acoustic presence of these whales at the Maud Rise in summer suggests that these animals could have been foraging around this biologically productive area characterised by high krill abundance. The main highlight was the detection of seismic survey signals and sperm whale clicks that had not previously been detected here. This calls for establishment of long-term monitoring to determine seasonal patterns and long-term trends.

Authors: Shabangu FW (Fisheries R&D); Jacobs LM, van den Berg MA, Louw GS, Lamont T (OC Research); Tessaglia-Hymes CT (Cornell University); Klinck H (Cornell University; Oregon State University)

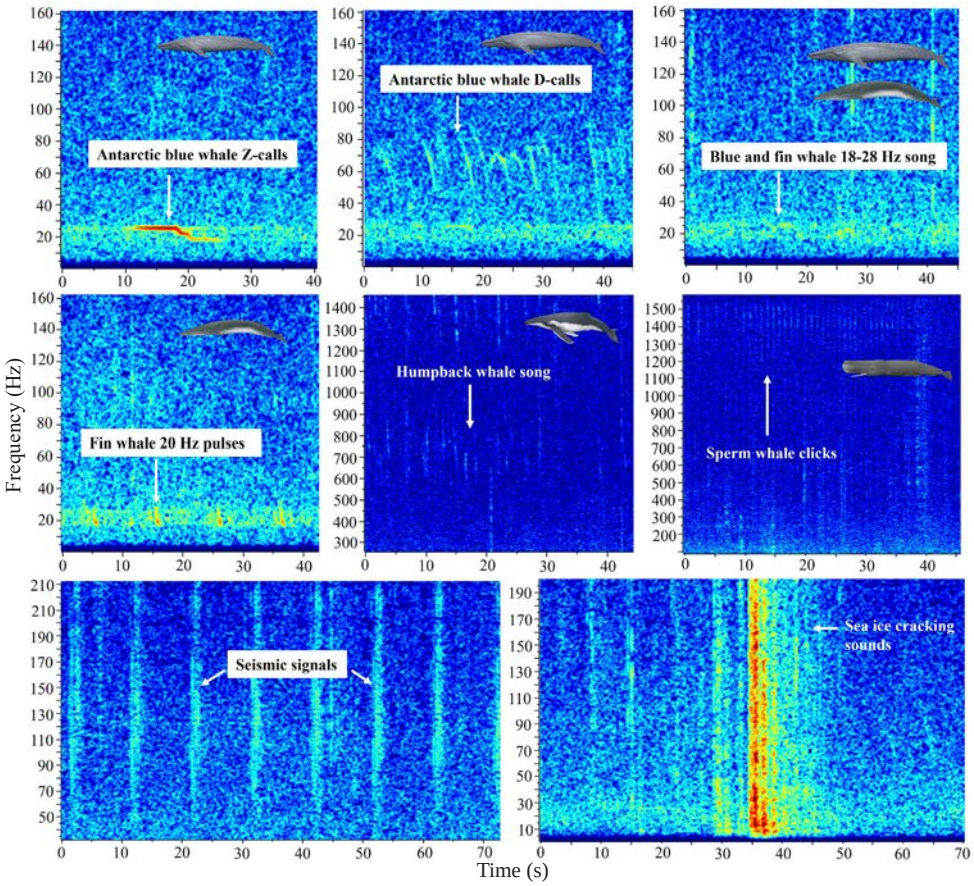

Figure 2. Spectrograms showing different types of sounds recorded off the Maud Rise, Antarctica. Photos of whales producing calls are inserted in the spectrograms.

SCIENCE TO POLICY

36. FISHING CLOSURES AROUND AFRICAN PENGUIN BREEDING COLONIES

The African penguin *Spheniscus demersus* is endemic to southern Africa and currently faces an extremely high risk of going extinct in the wild. Notwithstanding a brief recovery in the late 1990s and early 2000s, their population has declined by ca. 78% over the last 30 years (3 generations) from ca. 44,350 breeding pairs in 1993 to ca. 9,700 pairs in 2023 (Fig. 1). This falls just below the threshold of 80% for a global International Union for Conservation of Nature (IUCN) Red List status of Critically Endangered (CR). Population trajectories indicate a high probability that the decline of the African penguin population will exceed this threshold by 2028.

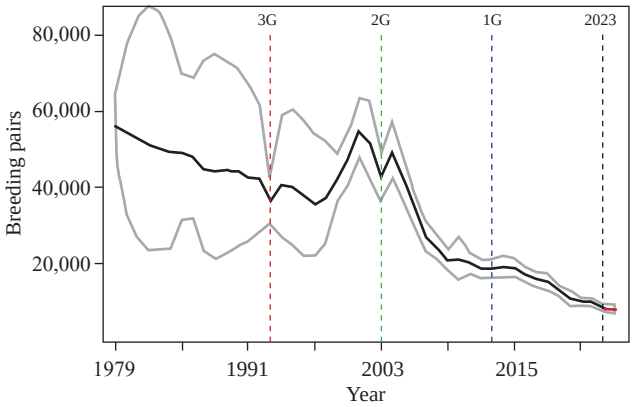

Figure 1. The modelled trajectory (black line) and 95% confidence intervals (grey lines) for South Africa's African penguin breeding population, based on nest counts conducted at 19 colonies between 1979 and 2023. The 10-year generation (G) lengths before 2023 are denoted by a blue dashed line (1G, 2013), a green dashed line (2G, 2003) and a red dashed line (3G, 1993).

Historically, African penguins nested at 39 sites between Hollamsbird Island in central Namibia and Algoa Bay on the southeast coast of South Africa, of which 16 were in Namibia and 23 in South Africa. However, 11 colonies are now extinct. The remaining colonies occur within three regions, namely southern Namibia, south-western South Africa, and Algoa Bay. While the main cause of their recent decline is poor food availability, effects of past guano exploitation on the quality of their breeding habitat, predation, marine noise and oil pollution also adversely affect their reproductive success and survival.

African penguins, like other colony-breeding predators, are range-restricted, central-place foragers when breeding, and thus utilise the available resources around their colonies. Purse-seine fishing is a major competitor for the small epipelagic fish species (sardine and anchovy) that are the staple of the African penguin's diet – for this reason, it is likely that excluding fishing around breeding colonies will improve the availability of prey for the penguins. In early 2006, there was a proposal for precautionary closures of purse-seine fisheries around two south coast penguin colonies (Dyer and St Croix Islands) for a period of six years, but this was not implemented. The proposal followed a large decline in the numbers of African penguins breeding to the north of Cape Town in South Africa. This was attributed to shifts in the distribution of sardine and anchovy from the west coast to the south and east coasts of South Africa, in the late 1990s and early 2000s. Due to the changing distributions and reduced availability of fish off the west coast, the commercial exploitation rate of sardines in this region exceeded 40% of the estimated biomass of the western stock between 2005 and 2007, further reducing foraging opportunities for penguins.

After further decline of its African penguin population (Fig. 1), South Africa finally prohibited purse-seine fishing around six of its largest remaining breeding colonies in 2023 (Fig. 2), for at least 10 years. The six colonies are geographically located to provide refuges for penguins to the north and east of Cape Town in south-western South Africa, as well as in Algoa Bay, thus mitigating some of the effects of the shifts in the distribution of prey species.

The degree of benefit from the fishing closures may depend on the finally agreed areal extent of the delineated closures around each colony. However, it is anticipated that prey densities at all six sites will increase, leading to improved reproductive success and reduced adult mortality. Given the overwhelming evidence that food availability constrains the African penguin in all aspects of its life cycle, it is reasonable to expect that the species' chances of survival should improve with the introduction of fishing closures.

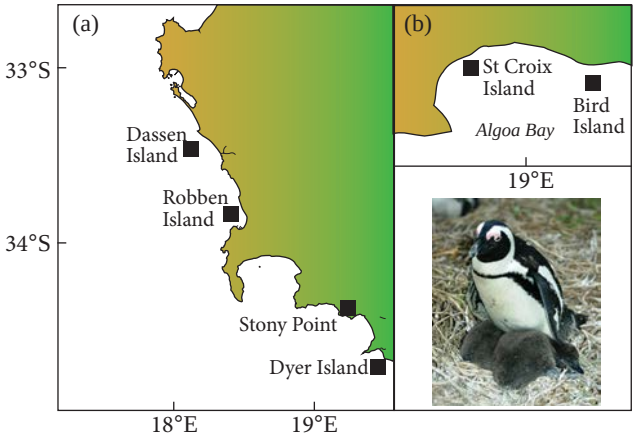

Figure 2. The locations of six major African penguin breeding colonies in South Africa around which fishing was prohibited in 2023, in (a) south-western South Africa and (b) Algoa Bay. The inset shows an African penguin with chicks.

Authors: Makhado AB, Masotla MJ, Upfold L, Crawford R (OC Research)
Contributor: Sherley RB (University of Exeter)

37. MARINE OTHER EFFECTIVE AREA-BASED CONSERVATION MEASURES (OECMS) IN SOUTH AFRICA

South Africa (SA), as a party to the Convention on Biological Diversity (CBD), has committed to the Kunming-Montreal Global Biodiversity Framework (GBF), which was adopted by the CBD in 2022. Target 3 of the GBF, which aims to conserve and effectively manage 30% of inland waters, terrestrial, as well as coastal and marine areas globally by 2030 (30 x 30), has been identified as the apex target informing SA's implementation of the GBF. In addition to protected areas (PAs), Target 3 is inclusive of other effective area-based conservation measures (OECMs). These are defined by the CBD as "a geographically defined area other than a protected area, which is governed and managed in ways that achieve positive and sustained long-term outcomes for the *in situ* conservation of biodiversity, with associated ecosystem functions and services and where applicable, cultural, spiritual, socio-economic, and other locally relevant values".

Currently, about 15% of SA's national waters, including the combined waters of continental SA and the Prince Edward Islands (PEIs), are within marine protected areas (MPAs). However, the bulk of this is attributable to the PEI MPA, with only 5.4% of continental SA's waters under protection. Further MPA expansion is needed to enhance the ecological representativeness of SA's MPA network and the conservation of its marine biodiversity (including coastal and estuarine biodiversity). However, there are challenges to MPA expansion in SA, including (amongst others) competition for ocean space, resistance to MPAs especially in coastal areas (often related to historical legacies of MPAs), as well as funding and resource constraints. There has been cautious optimism that OECMs could make an important contribution in SA to national and global conservation targets (reducing the burden on PA expansion), but the concept is not yet well understood in SA's marine context. To explore this, a national workshop on marine, coastal and estuarine OECMs was conducted in November 2023, led by DFFE and supported by MARISMA and WWF-SA. Its objectives included (i) to trial the evaluation of selected measures against OECM criteria; with consideration of (ii) how to apply criteria in SA's marine context; and ultimately (iii) establish coherence on the OECM concept in SA's marine context. Trial evaluations following presentations by "champions" for each of 12 different measures (Table 1) were the basis for deliberations. The focus of the evaluations was to rapidly explore these measures and assess their potential as OECMs. Measures were considered against six criteria that were adapted and simplified from CBD criteria, to suit local context and the workshop's purpose.

All but one of the potential measures was scored either as "suitable" or "possibly suitable" across all criteria (Table 1). There was general agreement that the single-species focus and small time window of seasonal fisheries closures should preclude them from being considered as OECMs. While most measures showed potential as OECMs, none were found to be consistently and definitively "suitable" across all criteria. This was partly due to the broad scale of the assessment, resulting in nuanced results for measures such as coastal public property, of which there are multiple types with greater or lesser suitability. Ultimately, measures will have to be assessed on a case-by-case basis to determine whether "possibly suitable" scores for certain criteria could be assessed as "suitable" at site level. The workshop highlighted the complexity of OECM evaluation with much work ahead to develop the field of marine OECMs in SA. It also highlighted that marine OECMs present few, if any, "low-hanging fruit" to contribute towards 30 x 30.

Author: Kirkman SP (OC Research)
Contributors: Holness SD (NMU); Kowalski P (Blue Tide Solutions); Adams R, Smith C, (WWF-SA); Goldman T (OC Research)

Table 1. Summary of workshop evaluations for 12 measures (columns) against six OECM criteria (rows). The assessment process used a traffic light system to score measures either as "suitable" (green, 3), "possibly suitable" (yellow, 2) or "not suitable" (red, 1).

Measures → / Criteria ↓	Parts of coastal public property (e.g. admiralty reserves)	Estuary management plans	Penguin island closures	Other fisheries exclusion zones around islands	Seasonal fisheries closures - Kingklip Box	Fishery exclusions in bays	Restricted use lobster sanctuaries	Military zones	Exclusion areas around historical wrecks	Small-scale fishing community areas	Strict conservation zones under MSP	Culturally significant areas
1. Outside of existing MPAs	3	3	3	3	3	3	3	3	3	3	3	3
2. Geographically defined area(s)	2	2	3	3	3	3	2	2	3	3	3	2
3. Supports important biodiversity values	2	2	3	3	3	3	2	2	2	2	3	2
4. Management authority is in place	2	2	2	3	3	3	2	2	2	2	3	2
5. Management achieves *in situ* conservation	2	2	2	3	1	2	2	2	2	2	3	2
6. The conservation is long-term	2	2	2	2	2	3	3	3	3	3	2	2
Overall assessment	2	2	2	2	1	2	2	2	2	2	2	2

38. WORKING TOWARDS SDG 14.1.1.B IN AFRICA, A UNITED NATIONS PROJECT

Durable by design and inexpensive to produce, plastic is an indispensable feature of modern life. In the 150 years since synthetic polymers were invented, and the 70 years since large-scale production began, plastic has transformed the world. Despite its undoubtedly great benefits, many countries are faced with plastic pollution in marine ecosystems. The United Nations' (UN) Sustainable Development Goals (SDGs) include a global indicator (SDG 14.1.1b) specifically to monitor the density of plastic debris. It has become increasingly evident that there is a need for well-trained core groups of dedicated officials that can contribute to this issue at national, regional and global levels.

The UN International Atomic Energy Agency (IAEA) is driving a regional African project to monitor microplastic (<5 mm) pollution. The project is managed by a technical coordinator with 16 participating member states in Africa. The first co-ordination meeting took place in February 2023 at the UN IAEA headquarters in Monaco, and came up with the following findings: (1) no harmonised methodologies for the sampling and analysis of microplastics in the marine environment, which limits the comparison of results and regional evaluations; (2) limited capabilities (equipment and trained personnel) to undertake microplastic sampling (South Africa's capability score was high); (3) disparities in the level of capacities of national laboratories around the region (South Africa's capability score was high); (4) low capacity for analysis of microplastic polymers between 0.3–5.0 mm, preventing reporting on indicator SDG 14.1.1b (South Africa's analytical abilities scored highly; Fig. 1); (5) very low capacity for analysis of microplastics smaller than 300 microns, which limits knowledge on the impact of microplastics (South Africa can analyse microplastics as small as 10 microns); (6) very low capacity for sediment dating, which limits knowledge of microplastic contamination trends (South Africa is lacking in this area); and (7) low linkage with national authorities responsible for reporting on SDG 14 indicators (DFFE, through MIMS, is linked to STATS SA with an established value chain on SDG reporting).

To address these findings the following project objectives were set: (1) harmonise collection and analytical protocols for sampling microplastics in beach sand and water (Fig. 2; step completed); (2) equipment standardisation through UN IAEA contributions (currently in this phase); (3) training in sampling and laboratory methods; (4) using UN IAEA reference laboratories for comparison

Figure 1. South Africa's (DFFE: OC Research) infrastructure to sample and analyse microplastics. (Photo credits: Top row: SA *Agulhas* II - K Findlay).

Figure 2. Second implementation meeting held in Egypt (August 2023) for all participating member states to develop a sampling and laboratory protocol for monitoring microplastics, to be implemented in all 16 African countries. (Photo credit: Egyptian Atomic Energy Authority).

to create endorsed regional laboratories; (5) counterparts to implement national/regional monitoring programmes to fill the data gaps; and (6) ensure linkages between data generation and UN SDG reporting authorities.

The harmonised protocol could be tested in South Africa owing to adequate infrastructure and capacity, although other countries from the regional project are still procuring equipment. Beach and water samples collected locally (Fig. 3) will be used to test the standardised laboratory protocol in 2024.

Figure 3. DFFE (OC Research) microplastics team testing the standardised protocol for beach and water sampling.

Author: Pillay K (OC Research)
Contributors: Worship MM, Setati S, Mooi G, Soeker M (OC Research)

PLATFORMS, TECHNOLOGY AND INNOVATION

39. EVALUATING THE POTENTIAL OF GLORYS AND BRAN OCEAN MODELS FOR MONITORING SOUTH AFRICA'S WEST COAST

The southern Benguela Upwelling System is a highly variable and productive upwelling region. Limited *in situ* ocean observations make it challenging to understand and monitor the temporal variability of physical oceanographic processes and features in this region. Ocean reanalysis products provide an alternative means of examining oceanographic conditions, but their global coverage may limit their regional accuracy. In this study, the performance of Mercator's Ocean Global Reanalysis (GLORYS) and Bluelink ReANalysis (BRAN) products was evaluated by comparing them against *in situ* hydrographic data from four Integrated Ecosystem Programme (IEP) research cruises conducted off South Africa's west coast (Fig. 1).

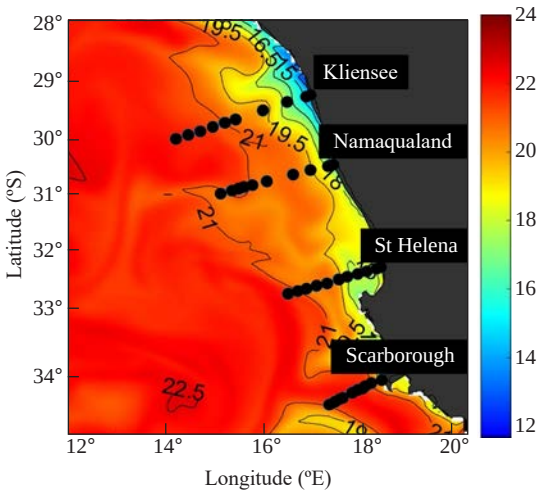

Figure 1. Sea surface temperature (°C) off South Africa's west coast, represented by black contour lines. Black dots indicate CTD stations along the Kleinsee, Namaqualand, St Helena Bay, and Scarborough transects.

During four cruises on the RS *Algoa* in 2019 (1–7 March, 21–26 May, 14–20 August, and 21–27 November), temperature and salinity measurements were obtained from CTD (Conductivity-Temperature-Depth) casts conducted along four transects (Fig. 1). To perform evaluations, model output was co-located with the *in situ* data in time and space. Overall, GLORYS and BRAN reproduced temperature and salinity distributions across all transects reasonably well (Fig. 2). This is indicated by strong positive correlations ($r = 0.80$ to 0.99; $p < 0.001$) between model output and *in situ* data (Fig. 2).

GLORYS generally outperformed BRAN, but underestimated upwelling in summer and overestimated it in winter. During summer, GLORYS was 3–6°C and 0.2–0.4 PSU higher than *in situ* data, but 1–2°C and 0.1–0.3 PSU lower in winter. BRAN consistently underestimated temperature by 2–5°C and salinity by 0.2–0.7 PSU during all cruise periods (Fig. 3). Both models appeared to perform better at deeper depths than at the surface, and simulated temperature better than salinity as can be seen from the distribution of the data points in Figure 3. Model performance also appeared to vary with latitude, with generally stronger correlations along the Scarborough transect in the south compared to the Kleinsee transect in the north, especially for salinity (Fig. 2). The performance of GLORYS and BRAN in simulating the physical oceanographic behaviour on the west coast emphasises the need to refine global models with finer details, sub-grid scale parameters, and more accurate input data for assimilation. This is important for better model characterisation of upwelling, advection, and mixing rates within this dynamic environment.

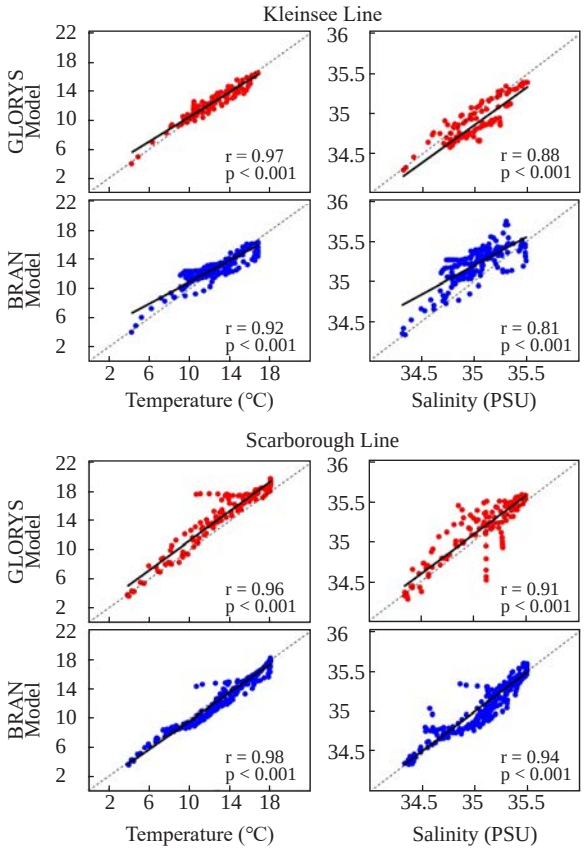

Figure 2. Scatterplots of simulated (model-derived) temperature (°C) and salinity (PSU) against *in situ* temperature and salinity for August 2019 along the Kleinsee and Scarborough transects. The correlation coefficient (r) and its significance level (p) are included. All indicate strong to very strong correlations that are highly significant.

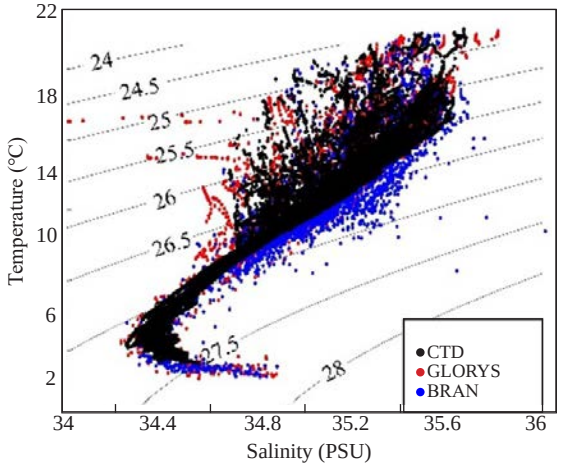

Figure 3. Temperature-salinity relationship for CTD data, and GLORYS and BRAN output for the four cruises in 2019.

Authors: Kupczyk A, Lamont T, Halo I, Russo CS (OC Research)

40. THE GLORYS MODEL SIMULATION OF HYDROGRAPHIC VARIABILITY AT THE PRINCE EDWARD ISLANDS

The Prince Edward Islands (PEIs) support high population densities of marine life. Thus, climate change perturbations to oceanographic variability and ecosystem functioning at the PEIs need to be identified and monitored. However, the remote and hostile PEI oceanic environment makes the collection of *in situ* hydrographic data challenging. Here, we demonstrate the suitability of the GLORYS (Global Ocean Reanalysis and Simulation) model to examine hydrographic variability at the PEIs (Fig. 1).

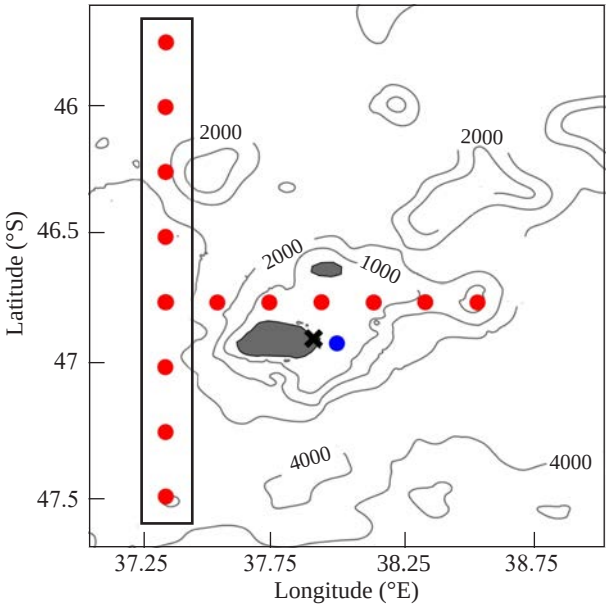

Figure 1. Location of *in situ* SAWS sea surface temperature (SST, °C, black cross) and the GLORYS monthly SST grid point (blue dot). Red dots indicate locations of CTD data used in Figures 3 and 4, with the black box highlighting the transect illustrated in Figure 4.

To assess the GLORYS accuracy at simulating sea surface temperature (SST) variability, we computed the bias between monthly *in situ* SST collected by the South African Weather Services (SAWS) at the Marion Island Base, and the closest GLORYS monthly SST grid point, during 1993–2020 (Fig. 2). Strong, positive, significant correlations ($r > 0.83$, $p < 0.001$) suggested that despite there being a spatial mismatch between data points, GLORYS simulated seasonal SST variability with reasonable accuracy. The bias showed a seasonal pattern, with GLORYS under estimating SST by 0.1–0.2°C in winter and spring, and overestimating SST by 0.01–0.3°C in summer and autumn.

GLORYS output was also compared to *in situ* Conductivity-Temperature-Depth (CTD) profiles collected annually during April/May (Figs. 3 and 4). At the event scale, GLORYS reproduced water masses (Fig. 3) and simulated vertical water column variations reasonably well (Fig. 4). Notably, GLORYS simulated a stronger and more southerly position for the cyclonic eddy observed in 2014 (Fig. 4). In 2016, GLORYS simulated the southern branch of the sub-Antarctic Front to be much further south than that observed in the *in situ* data, evident from the higher proportions of warmer sub-Antarctic surface water (SASW) in GLORYS (Fig. 3b). GLORYS generally performed better at the surface and at depths below 2,500 m. Our findings suggest that, despite some inherent differences between GLORYS output and the *in situ* data, GLORYS is suitable for monitoring and improving our understanding of long-term hydrographic variability at the PEIs.

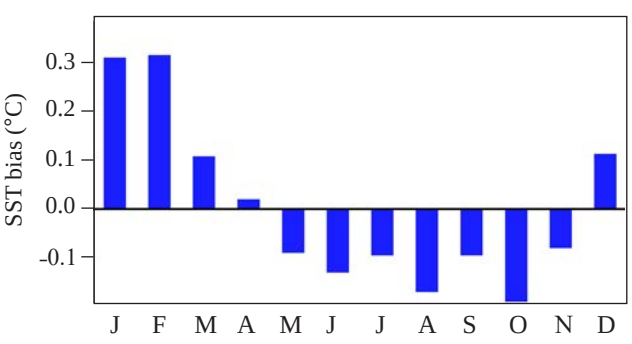

Figure 2. Monthly mean bias (1993 to 2020) between *in situ* SAWS SST (°C) and GLORYS monthly SST.

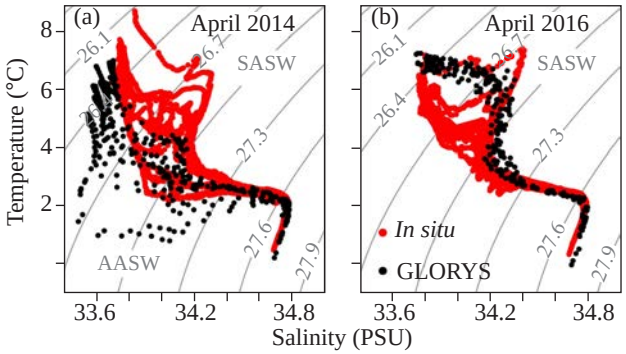

Figure 3. Temperature-salinity relationships for CTD data (red) and GLORYS output (black) for the (a) 2014 and (b) 2016 surveys. Density (kg m^{-3}) contours are indicated in grey. SASW = sub-Antarctic surface water, and AASW = Antarctic surface water.

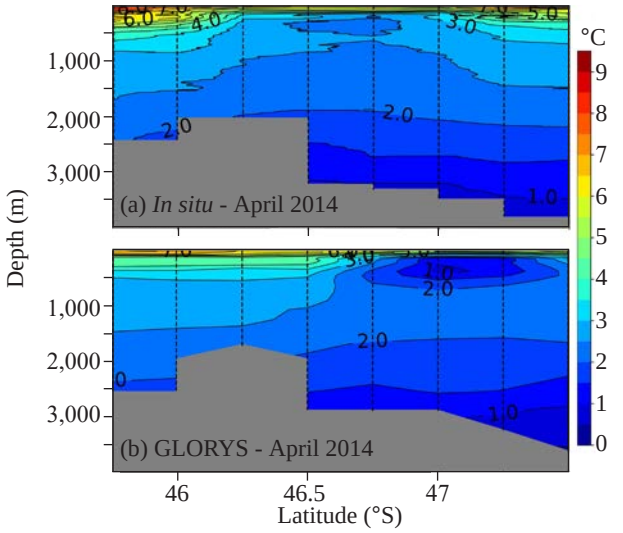

Figure 4. Vertical sections of (a) *in situ* CTD temperature and (b) GLORYS temperature, for April 2014. Dashed black vertical lines indicate CTD station positions along the transect, and grey shading indicates the ocean floor.

Authors: Soares BK (OC Research, UCT); Lamont T, Halo I, Russo CS (OC Research)
Contributors: Tutt GCO, van den Berg MA (OC Research); SAWS

41. OCEAN SOUND MEASUREMENT INSTRUMENTS

Passive Acoustic Monitoring (PAM) is being used by OC Research to conduct research and monitoring on marine soundscapes and impacts of underwater noise on marine biodiversity and ecosystem functioning. This is intended to provide baseline data on marine soundscapes, to inform policy on underwater noise including seismic surveys, and to enhance standards and guidelines, including appropriate mitigation and monitoring measures regarding ocean noise. The application of PAM techniques has become a prevalent approach for gathering time series data on marine soundscapes at various spatial and temporal scales in marine environments. The technique allows sampling in remote regions that are not easily accessible by boat on a day-to-day basis. It also enables 24-hour sampling in conditions of limited visibility, with no harmful impacts on marine life. Due to advances in passive acoustic recording technology, Autonomous Acoustic Recorders (AAAs) that can be deployed at greater ocean depths for longer periods of time than previously possible, are now available.

A total of 16 calibrated long-term acoustic recorders (SoundTrap ST600 HF - Long Term Recorders), manufactured by Ocean Instruments in New Zealand, have been acquired by OC Research. Key features of these recorders include low self-noise, wide 150 kHz bandwidth, and they are rated to 200 m depth, upgradeable to 500 m by installing a pressure valve. The recorders are optimised for long-term deployment and can record for periods longer than a year, allowing year-round automated recording.

The acoustic recorders are being deployed at selected inshore and offshore stations on the west and southeast coasts of South Africa to monitor soundscapes and impacts of underwater noise. They are deployed on sea-floor moorings that consist of an oceanographic buoy, linking lines, acoustic releases, and a seafloor anchor (Fig. 1). In collaboration with Two Oceans Aquarium, Cape Town, the acoustic recorders are tested in fish tanks over a period of 15 days before they are deployed at sea (Fig. 2). This is done to ensure that the instruments are recording according to the selected settings, and this also allows us to gauge battery endurance and memory consumption as per recording settings.

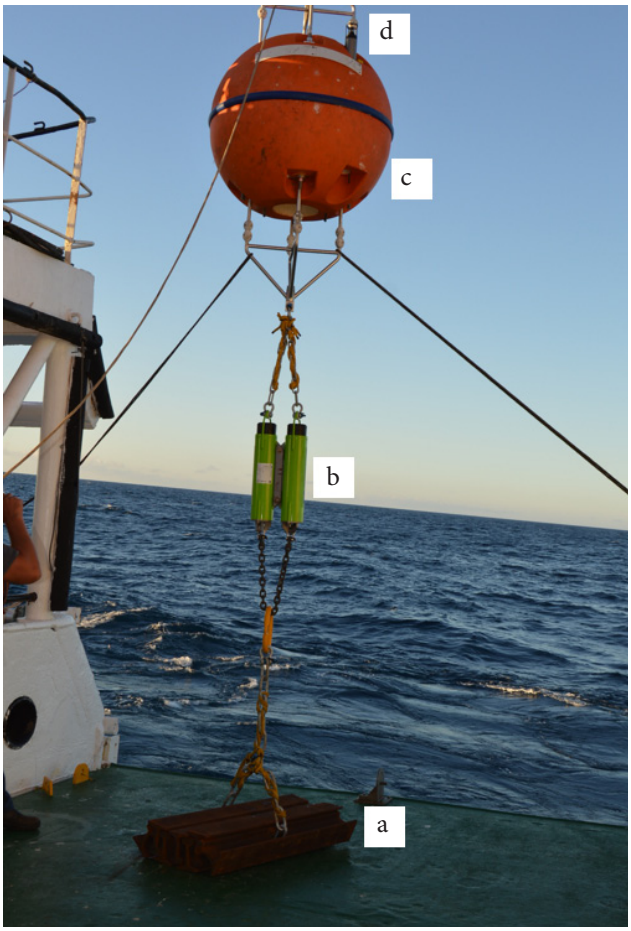

Figure 1. Illustration of an acoustic mooring configuration, showing (a) railway bars, (b) acoustic releases, (c) float and (d) acoustic recorder (Photo credit: Megan Maroen).

To date, four acoustic recorders have been deployed at locations off the west coast of South Africa, namely Child's Bank Marine Protected Area (MPA), Orange Shelf Edge MPA, Namaqua National Park MPA and Hondeklip Bay. The acoustic recorders are programmed to record concurrently with a commercial seismic survey planned offshore of the west coast in early 2024.

The four acoustic recorders are deployed at different distances from the seismic survey block (ca. 30–225 km) and at water depths between 80–1,000 m. At 1,000 m water depth, the acoustic recorder is suspended 500 m from the seafloor, as being deeper would exceed its depth range. At the other locations, which are all shallower than 500 m, the acoustic recorder is moored close to the seafloor (ca. 5 m above). The data obtained from the acoustic recorders will allow us to investigate seismic airgun noise propagation and characteristics at each location. This allows for testing the predictions of noise models that are required in terms of the regulatory framework.

Figure 2. Testing of acoustic recorders in fish tanks at Two Oceans Aquarium.

Author: Hlati K (OC Research)
Contributors: Kirkman SP, Lamont T, van den Berg MA (OC Research); Shabangu FW (Fisheries R&D)

42. THE GLOBAL INTEGRATION OF SOUTH AFRICA'S MARINE INFORMATION MANAGEMENT SYSTEM (MIMS)

South Africa's Marine Information Management System (MIMS) is a component of the Oceans and Coastal Information Management System, a national system built on multiple partnerships. The MIMS is an open data repository (Fig. 1) that archives and publishes collections and subsets of high quality marine-related datasets for the DFFE and its regional partners. It hosts a substantial variety of marine and coastal data, including data products generated from *in situ* data, satellites, and model output.

The development of the MIMS commenced in 2014, with the purpose of providing long-term preservation of marine and coastal data and metadata to advance science imperatives, supporting conservation efforts, and promoting sustainable development. Since its inception, the MIMS has evolved from being a national repository to a multi-faceted international marine data and information system. The MIMS hosts the AfrOBIS which is the sub-Saharan African node for the Ocean Biodiversity Information System – a global open-access data and information system for marine biodiversity. As such, the MIMS coordinates all marine data management activities in the region to promote open-access to data and metadata, while encouraging scientific collaboration. It also serves as a national node for the International Oceanographic Data and Information Exchange (IODE) of the Intergovernmental Oceanographic Commission of UNESCO. This extends its responsibilities to include (1) promotion and mobilisation of marine data and metadata sharing across the region; (2) contributing to the development of the IODE standards and best practices of marine data and metadata management; and (3) serving on the IODE steering committee and relevant task teams to drive the African agenda on international data fora.

The global impact and role of South Africa's MIMS was recently recognised by the IODE, with the MIMS being formally accredited as a national Associate Data Unit on the 17th October 2022 (https://www.iode.org/index.php?). This positions the MIMS (and therefore the DFFE) as a significant role player in the marine data management space at regional and international levels. The IODE accreditation followed the incorporation of the MIMS into the Registry of Research Data Repositories (https://www.re3data.org/) to increase metadata discovery and visibility across international marine data and information platforms. In 2023, this platform became fully integrated into the IODE Ocean Infohub (OIH; https://oceaninfohub.org/), and joined existing and emerging marine systems that interoperate with one another. The integration into the OIH enables and accelerates more effective development and dissemination of digital technology and sharing of ocean data, information, and knowledge.

Data curators are available to assist with data entries of new and existing projects available via the MIMS. Workshops are also hosted by the MIMS team to assist researchers of all disciplines in how to effectively use and enter data into this data repository platform. The global integration of the MIMS has elevated the objective of the system to provide open-access to marine datasets to promote scientific collaboration.

Authors: Rasehlomi T, Rasmeni B (OC Research)

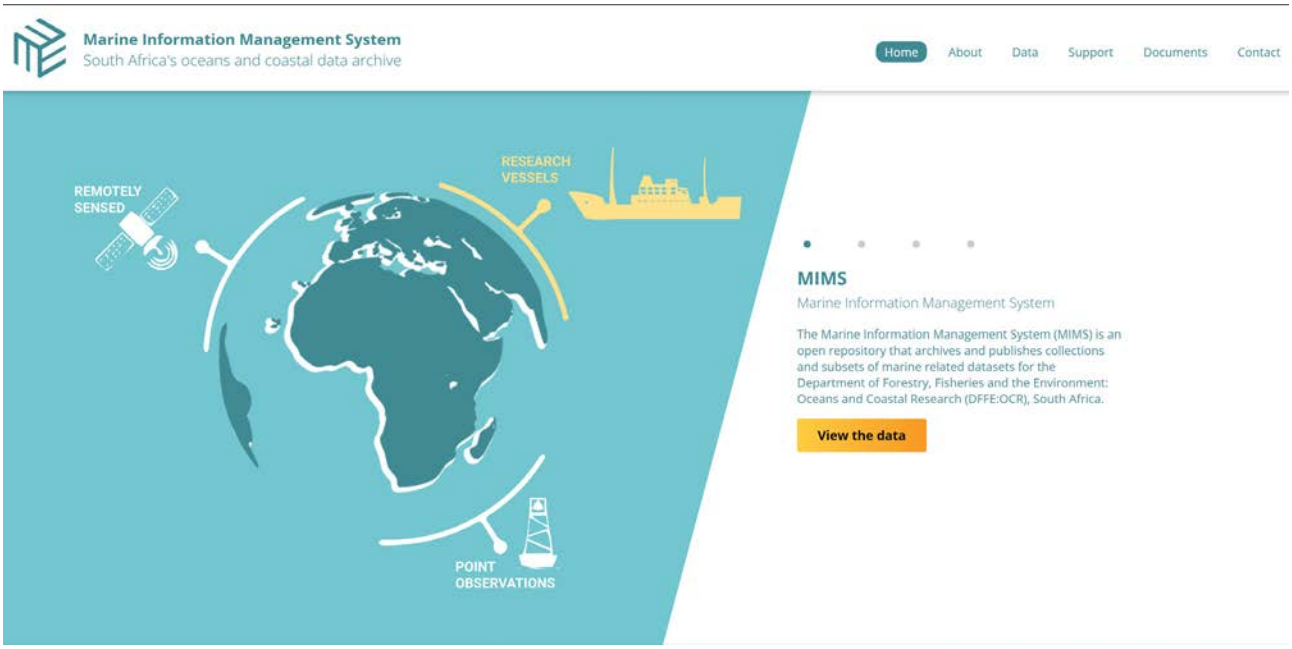

Figure 1. The MIMS web portal available via https://data.ocean.gov.za.

43. MARINE INFORMATION MANAGEMENT SYSTEM: CLIMATE DATA RESCUE INITIATIVE

Access to historical climate data is crucial for an in-depth understanding of Earth's climate system dynamics, including the significant role of the marine environment and how it impacts climate change. These data not only enrich our understanding of climate trends but also support informed decision-making and policy development to tackle climate-related challenges.

Given this backdrop, the endeavour of climate data rescue emerges as a crucial initiative. It involves the process of organising, preserving, and digitising climate data that are at risk of being lost due to deterioration, destruction, neglect, technical obsolescence, or dispersion over time. This effort ensures the maintenance of a continuous and comprehensive record, which is indispensable for grasping past, present, and future climate dynamics.

The Marine Information Management System (MIMS) team has embarked on an initiative to digitise and preserve invaluable paper-based data related to South Africa's coastal and marine environments, including essential weather records from the DFFE. This effort involves transforming many historical records (Fig. 1) into digital formats. The process enhances their accessibility and ensures their longevity, by assigning each dataset with a Digital Object Identifier (DOI) and making it available through the MIMS e-catalogue.

This project plays a vital role in enriching South Africa's historical marine data records, extending the availability of oceanographic data, and facilitating science-based decision-making in crucial areas such as coastal management and marine conservation. It addresses significant data gaps, especially from underrepresented periods and regions, contributing to a more thorough understanding of marine environments.

To date, the MIMS team has successfully digitised a combined total of 23 years of hourly weather recordings from the Cape Columbine and Dias Point lighthouses, organising and labelling the data by month. The records from Cape Columbine date back to 1987, and those from Dias Point to 1970, with the digitisation process ongoing.

In addition to weather records, the team has successfully recovered a Microsoft Access database from the St Helena Bay Monitoring line, originally stored on a compact disk. This database contains a wealth of marine data variables, including temperature, salinity, and oxygen levels, among others. Plans are underway to transfer this database to a modern SQL (Structured Query Language) database system, which will enhance data accessibility and facilitate more sophisticated analysis.

Figure 1. Boxes in the DFFE data storeroom containing hard copies of data that need to be digitised.

Looking ahead, the MIMS aims to ensure that these records are not only accessible but also analysable, by converting the scanned documents into usable data formats such as comma-separated files. Achieving this objective will require significant resources, including Optical Character Recognition software to automate the conversion process, and skilled personnel for data verification and validation. The team is actively seeking support to acquire these critical resources, which are essential for transforming the vast amounts of scanned records into functional data formats.

The MIMS climate data rescue initiative is a cornerstone in preserving South Africa's environmental legacy. By rendering these records easily accessible and usable, the project lays a solid foundation for future scientific research and policymaking, ensuring that invaluable data informs sustainable management practices for the country's marine and coastal ecosystems. This initiative not only protects historical data but will also empower future generations with the knowledge necessary to safeguard and comprehend South Africa's natural heritage.

Authors: Rasmeni B, Lamla S, Mahanjana A, Rasehlomi T (OC Research)

TRAINING AND OUTREACH

44. OVERVIEW AND OUTCOMES OF THE 2023 OCIMS STAKEHOLDER ENGAGEMENT WORKSHOP

During the first developmental phase (2015–2020) of the Oceans and Coastal Information Management System (OCIMS), five annual stakeholder engagements were held. The user input received during these workshops has been invaluable and has significantly informed the OCIMS development strategy. Following the contractual end of phase one in 2020, and a two-year hiatus (2020–2022) during which the OCIMS was maintained but not further developed, the second phase (2022–2027) was implemented. Through this second phase, the Council for Scientific and Industrial Research has remained a key partner while additional new partnerships have been realised with the South African Environmental Observation Network and the South African Weather Services.

The first stakeholder engagement workshop of the 'OCIMS Phase 2' took place at the President Hotel, Cape Town between 22 and 24 May 2023. The workshop objectives were to communicate on the status and progress of the OCIMS project, identify new requirements and needs from stakeholders, and encourage further collaboration and partnerships.

A total of 165 individuals from an estimated 70 organisations were invited to participate. Organisations included government departments (national, provincial, and local), nonprofit organisations, academia, state owned enterprises, and regional environmental organisations, amongst others. Participation over the three days amounted to a total of 102, 97 and 72 participants per day, respectively, with most participating in-person (Fig. 1). Virtual attendance was only made available on a request basis as in-person engagement was the preferred format.

Days one and two were dedicated to presentations highlighting the activities planned for the 'OCIMS Phase 2', and also included new development concepts and presentations from stakeholders demonstrating how they have benefitted from the OCIMS Decision Support Tools. New concepts included the development of data capture applications and the benefits of data standardisation in terms of data analysis and visualisation. The advancements achieved in data management and preservation through the Marine Information Management System (MIMS) and the production of operational ocean forecasts were also presented.

On day three, breakaway sessions focusing on key thematic areas in ocean governance and protection were convened to promote dialogue and feedback from stakeholders. Targeted discussions on the gaps and opportunities to improve maritime domain awareness, marine hazard and coastal protection, ecosystem management, and monitoring took place. The breakaway sessions were also used to seek user participation in the OCIMS Technical advisory Groups (TAGs).

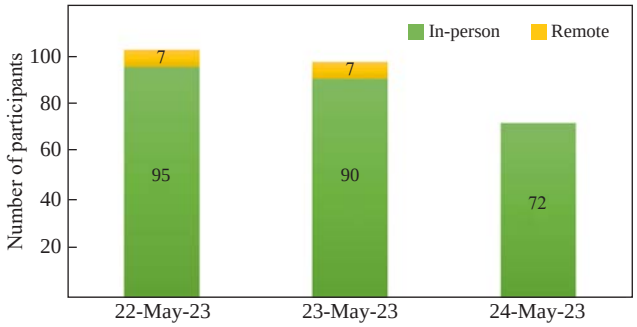

Figure 1. Number of participants per day attending the OCIMS stakeholder workshop 2023.

Following the workshop, attendees were asked to participate in a brief survey to indicate their general sentiments of the OCIMS and willingness to be involved in relevant TAGs. Subsequently, 33 responses were received, with many participants having interest in joining one or more TAG. The highest interest was for participation in the Water Quality (15 responses) and Aquaculture (12 responses) TAGs (Fig. 2).

The OCIMS stakeholder workshop was both well attended and well received, especially the invitation to participate in TAGs and contribute directly to the project. While there were new attendees, most participants were familiar with the OCIMS and had participated in previous workshops. The in-person interaction was welcomed by most stakeholders, but, it was recommended that options for virtual attendance be made available to attract a broader audience. As the OCIMS continues to demonstrate successful co-operative governance, further consideration will be given to mechanisms of reaching a broader audience and fostering new partnerships and collaborations.

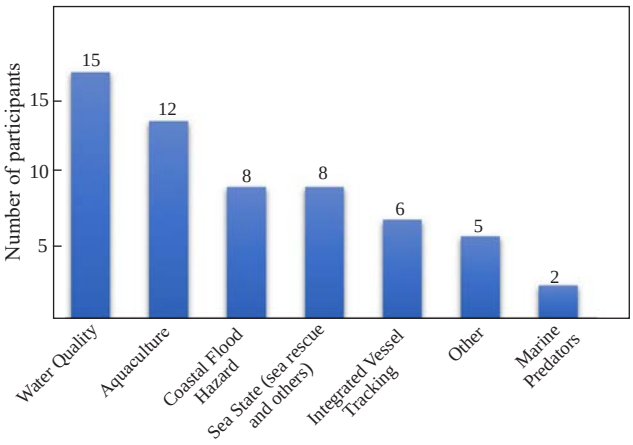

Figure 2. Stakeholder interest in participating in the various Technical Advisory Groups, including Water Quality, Aquaculture, Coastal Flood Hazard, Sea State (sea rescue and others), Integrated Vessel Tracking, Other, and Marine Predators.

Authors: Williams LL, Krug M (OC Research)
Contributor: Pretorius R (CSIR)

45. THE IMPACT OF DFFE COLLABORATIVE INITIATIVES: A STUDENT'S PERSPECTIVE

Imagine being part of a once-in-a-lifetime expedition, delving into the mysteries of marine science, and sailing through the icy Antarctic waters, or traversing halfway between South Africa and Brazil. For us, a group of passionate students and early career scientists, the opportunity to join the yearly summer SANAE-IV Antarctic Expedition on the SA *Agulhas* II to the SANAE research base, and the SAMBA mooring cruises on the RS *Algoa*, among others, has been nothing short of invaluable. This report shares our inspiring journey, highlighting the positive impacts of these experiences and the significance of collaboration between the DFFE and local and international research institutions and universities.

These collaborations have been a catalyst for our growth. Beyond the classroom, working side by side with experienced scientists, these cruises helped us gain hands-on experience at sea. Our professional knowledge and networks have been expanded, providing us with invaluable assets as we navigate our future career paths. The cruises have also equipped us with skills to contribute to understanding the oceans surrounding South Africa, and given us opportunities to unlock our potential for groundbreaking discoveries. As part of the physical oceanography team, we received training on various scientific equipment. These included eXpendable BathyThermographs (XBTs), gliders, drifting buoys, ARGO floats, Conductivity-Temperature-Depth (CTD) sensors with Niskin rosette samplers, continuous plankton recorders (CPRs), Shipboard Acoustic Doppler Current Profilers (S-ADCPs), Current and Pressure Inverted Echo Sounders (CPIES) and MicroCATs (Fig. 1). By operating these instruments ourselves, and troubleshooting on the go, we gained technical skills and a profound appreciation for the dedication, funding, and patience required to obtain ocean-related data. We often assisted in tasks outside our expertise, thus furthering our skills development. Living and working closely with our fellow crew members for extended periods, we quickly learned the importance of teamwork and adaptability. The ship and the SANAE research base became more than just a workplace, they became our home away from home. We faced challenges together, building strong bonds and more effective communication skills. As diverse students, we felt empowered by the DFFE collaborative initiatives with our respective Universities, which appreciate the global lack of diversity in STEM (science, technology, engineering, and mathematics) fields, particularly for people of colour and women. As the only African country represented in the Antarctic treaty, South Africa's Southern Ocean and Antarctic Research projects have become a beacon of inspiration. Similarly, local cruises along the South African coast also provide a welcoming and inclusive environment, encouraging students from all walks of life to embrace the wonders of marine exploration. We find strength in knowing that, regardless of our backgrounds, we belong in the world of marine research. To further advance our scientific endeavors and maximise our impact, it is essential for us to harness the full potential of the remarkable resources at our disposal. These allow us to conduct more comprehensive studies, and collaborate with seasoned scientists from around the globe, further solidifying South Africa's position as a leader in marine science. Our journey as students and early career researchers has been transformative, thanks to the DFFE collaborative initiatives.

Authors: Daniel M, Kajee M (UCT); Kupczyk A (OC Research, CPUT); Fortunato L (Parthenope University of Naples); Ramsarup N (UCT); Soares B (OC Research, UCT)
Contributors: Lamont T, Louw G, Tutt G (OC Research); Ansorge I (UCT); Controneo Y (Parthenope University of Naples)

Figure 1. Collection of images from the expeditions. Top row, left to right: carrying a MicroCAT for deployment, retrieving a mooring, deploying an acoustic transducer, standing outside SANAE base, deploying an XBT; Bottom row, left to right: deploying a CTD, recovered CPIES, readying a glider for deployment, offloading at the Antarctic ice shelf, deploying a drifter.

OUTPUTS FOR 2023

Peer-reviewed publications

Ahusan M, Rico-Seijo N, Amjad F, Gress E, Naeem S, Samaai T, Samimi-Namin K, Woodall LC, Stefanoudis PV. 2023. The Nekton Maldives taxonomic workshop: Exploring the biodiversity of shallow, mesophotic and deep-sea communities in Maldives. *Research Ideas and Outcomes* 9: e114370.

Baker JA, Renshaw R, Jackson LC, Dubois C, Iovino D, Zuo H, Perez RC, Dong S, Kersalé M, Mayer M, Mayer J, Speich S, Lamont T. 2023. South Atlantic overturning and heat transport variations in ocean reanalyses and observation-based estimates. *State of the Planet* 1-osr7: 4. In: von Schuckmann K, Moreira L, Le Traon P-Y, Grégoire M, Marcos M, Staneva J, Brasseur P, Garric G, Lionello P, Karstensen J, and Neukermans G. (Eds.), 7th edition of the Copernicus Ocean State Report (OSR7), Copernicus Publications, *State of the Planet* 1-osr7.

Barlow R, Lamont T, Viljoen J, Airs R, Brewin R, Tilstone G, Aiken J, Woodward E, Harris C. 2023. Latitudinal variability and adaptation of phytoplankton in the Atlantic Ocean. *Journal of Marine Systems* 239: article 103844.

Bode-Dalby M, Würth R, de Oliveira LDF, Lamont T, Verheye HM, Schukat A, Hagen W, Auel H. 2023. Small is beautiful: the important role of small copepods in carbon budgets of the southern Benguela upwelling system. *Journal of Plankton Research* 45: 110–128.

Botha JA, Trueman CN, Kirkman SP, Arnould JPY, Lombard AT, Connan M, Hofmeyr GJG, Seakamela SM, Pistorius PA. 2023. Geographical, temporal, and individual-based differences in the trophic ecology of female Cape fur seals. *Ecology and Evolution* 13: e9790.

Branch GM, Steffani N, Pfaff MC, Baliwe NG, Zeeman Z. 2023. Complex interplays between limpets and alien species in South Africa: multispecies interactions, zonation and size effects. *Frontiers in Marine Science* 10: article 1190456.

Chidichimo MP, Perez RC, Speich S, Kersalé M, Sprintall J, Dong S, Lamont T, Sato OT, Chereskin TK, Hummels R, Schmid C. 2023. Energetic overturning flows, dynamic interocean exchanges, and ocean warming observed in the South Atlantic. *Communications Earth and Environment* 4: article 10.

da Silva C, Samaai T, Kerwath S, Adams LA, Watson KM, Bernard ATF, van der Heever GM, Angel A, Schoombie S, Frainer G. 2023. Leaping into the future: Current application and future direction of computer vision and artificial intelligence in marine sciences in South Africa. *Research Ideas and Outcomes* 9: e112231.

Green DB, Bestley S, Corney SP, Trebilco R, Makhado AB, Lehodey P, Conchon A, Titaud O, Hindell MA. 2023. Modelled prey fields predict marine predator foraging success. *Ecological Indicators* 147: article 109943.

Halo I, Raj RP, Korosov A, Penven P, Johannessen JA, Rouault M†. 2023. Mesoscale variability, critical latitude and eddy mean properties in the Tropical South-East Atlantic Ocean. *Journal of Geophysical Research Oceans* 128: e2022JC019050.

Hancke L, Smeed D, Roberts M, Russo C, Rayner D, Jebri F. 2023. Atmospheric and advective forcing of upwelling on South Africa's central Agulhas Bank. *Deep-Sea Research II* 209: article 105293.

Huggett JA, Noyon M, Carstensen J, Walker DR. 2023. Patterns in the plankton – Spatial distribution and long-term variability of copepods on the Agulhas Bank. *Deep-Sea Research II* 208: article 105265.

Kirkman SP, Kowalski P, Mann BQ, Branch GM, van der Bank MG, Sink KJ, Fielding P, Mann-Lang JB, Pfaff MC, Kotsedi D, Adams R, Dlulisa S, Petersen SL. 2023. The road towards effective governance and management of marine protected areas in South Africa: evolving policies, paradigms and processes. *African Journal of Marine Science* 45: 63–86.

Mubaiwa B, Lerata MS, Sibuyi NRS, Meyer M, Samaai T, Bolton JJ, Antunes EM, Beukes DR. 2023. Green Synthesized sAuNPs as a potential delivery platform for Cytotoxic Alkaloids. *Materials* 16: article 1319.

Mwaala DN, Wilhelm MR, Kirkman SP, Roux J-P. 2023. Geographical and seasonal patterns in the diet of Cape fur seals *Arctocephalus pusillus pusillus* in Namibia, based on extensive scat analyses. *African Journal of Marine Science* 45: 285–294.

Periasamy R, Cárdenas P, Kurian PJ, Ingole B, Samaai T. 2023. Is the North Atlantic *Geodia barretti* (Porifera, Tetractinellida, Geodiidae) present on the Southwest Indian Ridge? *Zootaxa* 5380: 461–474.

Pitcher GC, du Randt A, Seanego KG, Tsanwani M. 2023. Variability and controls of the ocean acidification metrics pH and pCO_2 in a large embayment of an Eastern Boundary Upwelling System (EBUS). *Estuarine, Coastal and Shelf Science* 292: article 108473.

Qwabe W, Samaai T, Harris JM, Palmer RM, Kerwath SE. 2023. First mesophotic *Ecklonia radiata* (Laminariales) records within the iSimangaliso Wetland Park marine-protected area, east coast, South Africa. *Journal of the Marine Biological Association of the United Kingdom* 103: e91.

Ramos EA, Cheeseman T, Marcondes MCC, Olio M, Vogel A, Elwen S, de Melo THM, Facchola C, Cipolotti S, Southerland K, Findlay K, Seyboth E, McCue SA, Kotze PGH, Seakamela SM. 2023. Interchange of Southern Hemisphere humpback whales across the South Atlantic Ocean. *Scientific Reports* 13: article 4621.

Rautenbach G, Hermes J, Halo I, Morris T, Veitch J. 2023. Wind- and eddy-driven upwelling over submarine canyons inshore of the northern Agulhas Current. *African Journal of Marine Science* 45: 1–14.

Roberts LC, Abolnik C, Waller LJ, Shaw K, Ludynia K, Roberts DG, Kock AA, Makhado AB, Snyman A, Abernethy D. 2023. Descriptive epidemiology of and response to the high pathogenicity Avian Influenza (H5N8) epidemic in South African coastal seabirds, 2018. *Transboundary and Emerging Diseases* 2023: article 2708458.

Siddiqui C, Rixen T, Lahajnar N, van der Plas AK, Louw DC, Lamont T, Pillay K. 2023. Regional and global impact of CO_2 uptake in the Benguela Upwelling System through preformed nutrients. *Nature Communications* 14: article 2582..

Singh A, Fietz S, Thomalla SJ, Sanchez N, Ardelan MV, Moreau S, Kauko HM, Fransson A, Chierici M, Samanta S, Mtshali TN, Roychoudhury AN, Ryan-Keogh TJ. 2023. Absence of photophysiological response to iron addition in autumn phytoplankton in the Antarctic sea-ice zone. *Biogeosciences* 20: 3073–3091.

Sink KJ, Adams LA, Franken M-L, Harris LR, Currie J, Karenyi N, Dayaram A, Porter S, Kirkman S, Pfaff M, van Niekerk L, Atkinson LJ, Bernard A, Bessinger M, Cawthra H, de Wet W, Dunga L, Filander Z, Green A, Herbert D, Holness S, Lamberth S, Livingstone T, Lück-Vogel M, Mackay F, Makwela M, Palmer R, Van Zyl W, Skowno A. 2023. Iterative mapping of marine ecosystems for spatial status assessment, prioritization, and decision support. *Frontiers in Ecology and Evolution* 11: article 1108118.

Stefanoudis PV, Talma S, Fassbender N, Swanborn D, Ochieng CN, Mearns K, Komakoma JD, Otwoma LM, Mbije NE, Osuka KE, Samoilys M, Shah N, Samaai T, Trotzuk E, Tuda A, Zivane F, Wagner D, Woodall LC. 2023. Stakeholder-

derived recommendations and actions to support deep-reef conservation in the Western Indian Ocean. *Conservation Letters* 16: e12924.

Sun X, Brewin RJW, Sathyendranath S, Dall'Olmo G, Airs R, Barlow R, Bracher A, Brotas V, Kheireddine M, Lamont T, Marañón E, Morán XAG, Raitsos DE, Shen F, Tilstone GH. 2023. Coupling ecological concepts with an ocean colour model: Phytoplankton size structure. *Remote Sensing of Environment* 285: article 113415.

Williams LL. 2023. A GIS-based technology response to an avian influenza outbreak in South Africa. *Abstracts of the International Cartographic Association* 6, article 276.

Presentations at symposia, conferences and workshops

Baker J, Renshaw R, Jackson L, Dubois C, Lovino D, Zuo H, Perez R, Dong S, Kersalé M, Mayer M, Mayer J, Speich S, Lamont T. 2023. Overturning and heat transport variations in the South Atlantic in an ocean reanalysis ensemble and other estimates. *European Geophysical Union (EGU) General Assembly 2023, Vienna, Austria & Online, 23–28 April 2023*.

Bergman S. 2023. Diagnostics of Vorticity Balance in the Benguela Upwelling System. *DFFE Physical Oceanography Science and Technical Workshop, East Pier, Cape Town, South Africa, 26–27 October 2023*.

Chidichimo MP, Perez R, Speich S, Kersalé M, Sprintall J, Dong S, Lamont T, Sato O, Chereskin TK, Hummels R, Schmid C. 2023. Energetic overturning flows, dynamic interocean exchanges, and ocean warming observed in the South Atlantic. *Workshop on Meeting AMOC Observation Needs in a Changing Climate, University of Hamburg, Hamburg, Germany, 18–20 July 2023*.

Daniels R, Shabangu FW, Jordaan RK, de Bruyn PJN, van den Berg MA, Lamont T. 2023. Killer whale acoustic patterns respond to prey abundance and environmental variability around the Prince Edward Islands, Southern Ocean. *DFFE Physical Oceanography Science and Technical Workshop, East Pier, Cape Town, South Africa, 26–27 October 2023*.

Daniels R, Shabangu FW, Jordaan RK, de Bruyn PJN, van den Berg MA, Lamont T. 2023. Killer whale acoustic patterns respond to prey abundance and environmental variability around the Prince Edward Islands, Southern Ocean. *6th South African National Antarctic Programme (SANAP) Symposium 2023, Houw Hoek, Grabouw, Cape Town, 27 November – 1 December 2023*.

Dong S, Perez R, Kersalé M, Goes M, Goni G, Speich S, Piola A, Lamont T, Campos E, Ansorge I, Chidichimo MP, Sato O, Meinen C, Le Henaff M, Garzoli S. 2023. Multi-decadal records of the South Atlantic Meridional Overturning and Heat transport derived from *in situ* and satellite observations and recent applications. *28th International Union of Geodesy and Geophysics (IUGG) General Assembly, Berlin, Germany, 11–20 July 2023*.

du Preez SA, Lamont T, Huggett JA. 2023. The variability of mesozooplankton around sub-Antarctic Prince Edward Islands and the influence of the environment. *DFFE Physical Oceanography Science and Technical Workshop, East Pier, Cape Town, South Africa, 26–27 October 2023*.

du Preez SA, Lamont T, Huggett JA. 2023. The variability of mesozooplankton around sub-Antarctic Prince Edward Islands and the influence of the environment. *Nansen-Tutu Three Oceans Symposium: marine science and services in the greater Agulhas region, Breakwater Lodge, Victoria & Alfred Waterfront, Cape Town, South Africa, 6–7 November 2023*.

du Preez SA, Lamont T, Huggett JA. 2023. Zooplankton variability around the sub-Antarctic Prince Edward Islands and the influence of the environment. *6th South African National Antarctic Programme (SANAP) Symposium 2023, Houw Hoek, Grabouw, Cape Town, 27 November – 1 December 2023*.

Gebe Z, Pfaff MC, Rocke E, Moloney CL. 2023. Spatio-temporal variability of picophytoplankton groups in the southern Benguela over two seasonal cycles. *5th National Global Change Conference, University of the Free State, Bloemfontein, South Africa, 30 January – 2 February 2023*.

Halo I. 2023. South African East coast canyon oceanography: Challenges for the modelling community. *DFFE Physical Oceanography Science and Technical Workshop, East Pier, Cape Town, South Africa, 26–27 October 2023*.

Halo I, Soares BK, Lamont T, Russo CS, van den Berg MA, Tutt G. 2023. Surface and subsurface hydrographic variability at the Prince Edward Islands: Perspectives from the high-resolution GLORYS model. *Nansen-Tutu Three Oceans Symposium: marine science and services in the greater Agulhas region, Breakwater Lodge, Victoria & Alfred Waterfront, Cape Town, South Africa, 6–7 November 2023*.

Halo I, Soares BK, Lamont T, Russo CS, van den Berg MA, Tutt G. 2023. Surface and subsurface hydrographic variability at the Prince Edward Islands: Perspectives from the high-resolution GLORYS model. *6th South African National Antarctic Programme (SANAP) Symposium 2023, Houw Hoek, Grabouw, Cape Town, 27 November – 1 December 2023*.

Halo I, Penven P, Raj R, Ansorge I, Lamont T, Johannessen J. 2023. Influence of the Madagascar Ridge on the variability of the flow in the Agulhas Current System: a modelling perspective. *International Workshop on Western Boundary Current – Subtropical Continental Shelf Interactions, Savannah, Georgia, USA & Online, 22–24 May 2023*.

Hlati K, Kirkman SP, Huggett J, Lamont T. 2023. Assessing effects of seismic surveys on marine life in South African waters. *The XXVIII International Bioacoustics Congress, Sapporo, Japan, 27 October – 1 November 2023*.

Holliday NP, Ansorge I, Burmeister K, Campos E, Chidichimo MP, DeYoung B, Heymans JJ, Hounpké J, Jackson LC, Lamont T, Lee S-K, Perez RC, Sams C, Snowden J, Zinkann A-C. 2023. Social and economic impacts of changes in the Atlantic Meridional Overturning Circulation. *Workshop on Meeting Atlantic Meridional Overturning Circulation (AMOC) Observation Needs in a Changing Climate, University of Hamburg, Hamburg, Germany, 18–20 July 2023*.

Huggett JA. 2023. South Africa's contribution to the IIOE-2: Summary Report. *6th meeting of the International Steering Committee of the Second International Indian Ocean Expedition 2015-25 (IIOE-2 SC6), Perth, Australia, 6–7 February 2023*.

Huggett JA. 2023. Myelination in copepods – from discovery to functional traits. *3rd Danish–South African ZOOLOGIC Workshop on changes in coastal/shelf systems in response to climate change, Roskilde, Denmark, 3–7 July 2023*.

Huggett JA. 2023. Update on Indian Ocean-related activities. *14th meeting of the Sustained Indian Ocean Biogeochemistry and Ecosystem Research (SIBER) Scientific Committee, Online, 24 July 2023*.

Huggett JA, Carstensen J, Noyon M, Walker D. 2023. Patterns in the plankton: bottom-up or top-down forcing of copepods on the Agulhas Bank? *Nansen-Tutu Three Oceans Sympo-*

sium: marine science and services in the greater Agulhas region, Breakwater Lodge, Victoria & Alfred Waterfront, Cape Town, South Africa, 6–7 November 2023.

Huggett JA, Mdluli N. 2023. Zooplankton sampling in the Indian sector of the Southern Ocean (18–40°E) including the Prince Edward Islands archipelago. *2nd Workshop on Pelagic Ecoregionalisation for the Subantarctic region, Paris, France, 22–26 May 2023*.

Huggett JA, Mdluli NM, du Preez S, Thibault D, Lamont T. 2023. Towards ecoregionalisation of the eastern subantarctic pelagic zone – mapping zooplankton communities at the Prince Edward Islands. *6th South African National Antarctic Programme (SANAP) Symposium 2023, Houw Hoek, Grabouw, Cape Town, 27 November – 1 December 2023*.

Ismail HE, Anders D, Porter SN, van den Berg MA, Lamont T. 2023. Underwater Temperature observations along the south and east coasts of South Africa. *DFFE Physical Oceanography Science and Technical Workshop, East Pier, Cape Town, South Africa, 26–27 October 2023*.

Jacobs L, Huysamen J, van den Berg MA, Lamont T. 2023. Technological development for improved Thermosalinograph (TSG) observations. *DFFE Physical Oceanography Science and Technical Workshop, East Pier, Cape Town, South Africa, 26–27 October 2023*.

Kirkman SP. 2023. Opportunities for action: To 30x30 in South Africa's waters. *Workshop on Sustainably Financing Marine Protected Areas (MPAs) in South Africa – delivering on the 30x30 Ocean Agenda, Two Oceans Aquarium, Cape Town, 2–4 May 2023*.

Kirkman SP. 2023. Other processes: Ocean Economy, Ocean Governance and Marine Spatial Planning. *Workshop on the implementation of the 30x30 Protected Areas target, Boksburg, Gauteng, 6–8 June 2023*.

Kirkman SP. 2023. Example of MSP collaboration at regional level – BCLME (ANGOLA, NAMIBIA, SA). *Marine Regions Forum 2023: Navigating ocean sustainability in the Western Indian Ocean and beyond, Dar es Salaam, Tanzania. 7–9 November 2023*.

Kirkman SP. 2023. Tailoring EBSAs to South Africa's spatial biodiversity management needs. *Convention on Biological Diversity Technical Expert Workshop to Review Modalities for Modifying the Descriptions of Ecologically or Biologically Significant Marine Areas (EBSAs) and Describing New EBSAs, Oslo, Norway, 20–24 November 2023*.

Kirkman SP, Hlati K, Huggett J, Lamont T. 2023. Assessing effects of seismic surveys on marine life in South African waters. *OCEANOISE2023: Towards an Acoustically Sound Ocean, Barcelona, Spain, 22–26 May 2023*.

Kirkman SP, Kowalski P, van der Bank MG, Branch GM, KJ Sink, Mann-Lang JL, Mann BQ, Adams R, Pfaff MC, Fielding P, Dlulisa S, Kotsedi D, Petersen SL. 2023. The road towards effective governance and management of marine protected areas in South Africa: evolving policies, paradigms and processes. *Zoological Society of South Africa (ZSSA) Conference 2023, Champagne Sports Resort, KwaZulu-Natal, South Africa, 25–29 September 2023*.

Kirkman SP, van Niekerk L. Marine and Estuarine protection. *Workshop on the implementation of the 30x30 Protected Areas target, Boksburg, Gauteng, 6–8 June 2023*.

Koubbi P, Makhado AB, Cotté C, Goberville E. 2023. Paris workshop on the pelagic ecoregionalisation in the subantarctic Indian. *2nd Workshop on Pelagic Ecoregionalisation for the Subantarctic region, Paris, France, 22–26 May 2023*.

Krug M. 2023. Improving Ocean Governance with the South African Oceans and Coastal Information System. *International Digital Twins of the Ocean (DITTO) Summit 2023, Xiamen, China, 9–12 November 2023*.

Kupczyk A, Lamont T, Halo I, Russo CS. 2023. GLORYS and BRAN ocean model output evaluation on the west coast of South Africa. *DFFE Physical Oceanography Science and Technical Workshop, East Pier, Cape Town, South Africa, 26–27 October 2023*.

Kupczyk A, Lamont T, Halo I, Russo CS. 2023. An evaluation of GLORYS and BRAN ocean model outputs on the west coast of South Africa. *Nansen-Tutu Three Oceans Symposium: marine science and services in the greater Agulhas region, Breakwater Lodge, Victoria & Alfred Waterfront, Cape Town, South Africa, 6–7 November 2023*.

Kupczyk A, Walker D, Meyer S. 2023. Chlorophyll and phytoplankton distributions along the ASCA transect 2023. *DFFE Physical Oceanography Science and Technical Workshop, East Pier, Cape Town, South Africa, 26–27 October 2023*.

Lahajnar N, Rixen T, Siddiqui C, Meiritz L, Lamont T, van den Berg MA, van der Plas A, Louw D, Libuku V, Morholz V, Koppelmann R, Gaye B, Vorrath E, Fischer G. 2023. The benefit of long-term moorings. *South African–German Workshop on Ocean-Climate-Land Interactions and Feedbacks in southern Africa under climate change, Braunschweig, Germany & Online, 8–10 February 2023*.

Lamont T. 2023. Why research and monitoring matters. *South African–German Workshop on Ocean-Climate-Land Interactions and Feedbacks in southern Africa under climate change, Braunschweig, Germany & Online, 8–10 February 2023*.

Lamont T. 2023. Observing the Agulhas Current – what do we know? *Global Ocean Observing System (GOOS) Boundary Current Workshop and 14th session of the GOOS Observation Coordination Group, Peter Stoker Centre and Waterfront Breakwater Lodge, Cape Town, South Africa & Online, 5–8 June 2023*.

Lamont T. 2023. Status of South African National Ocean Observation Systems. *First Global Ocean Observing System (GOOS) National Focal Points (NFP) Forum, Online, 25 October 2023*.

Lamont T. 2023. Structure and future plans for South African National Ocean Observation Systems: Reflections on National observing system by NFPs. *First Global Ocean Observing System (GOOS) National Focal Points (NFP) Forum, Online, 25 October 2023*.

Lamont T, Halo I, Veitch J. 2023. Overview of DFFE hydrodynamic modelling research and operational activities. *3rd Danish–South African ZOOLOGIC Workshop on changes in coastal/shelf systems in response to climate change, Roskilde, Denmark, 3–7 July 2023*.

Lamont T, Soares BK, Halo I, Russo CS, van den Berg, MA, Tutt G. 2023. Oceanographic variability and the GLORYS model at the Prince Edward Islands. *DFFE Physical Oceanography Science and Technical Workshop, East Pier, Cape Town, South Africa, 26–27 October 2023*.

Lamont T, van den Berg MA. 2023. Mesoscale eddies influencing the sub-Antarctic Prince Edward Islands: Origin, pathways, and characteristics. *6th South African National Antarctic Programme (SANAP) Symposium 2023, Houw Hoek, Grabouw, Cape Town, 27 November – 1 December 2023*.

Maduray S, Huggett JA. 2023. Comparisons between microplankton and mesozooplankton along the Mossel Bay Monitoring Line. *4th Danish-South Africa ZOOLOGIC Workshop on changes in coastal/shelf systems in response to climate change, Hermanus, South Africa, 13–17 November 2023*.

Maduray S, Worship M, Pillay K. 2023. Community structure and diversity of microplankton in the Southern Benguela. *5th National Global Change Conference, University of the Free State, Bloemfontein, South Africa, 30 January – 2 February 2023.*

Makhado A, Koubbi P, Huggett JA, Cotte C, Reisinger R, Swadling K, Azarian C, Barnerias C, d'Ovidio F, Goberville E, Leroy B, Lombard AT, van de Putte A, and workshop participants. 2023. Ecoregionalisation of the pelagic zone in the Subantarctic and subtropical Indian Ocean. *6th South African National Antarctic Programme (SANAP) Symposium 2023, Houw Hoek, Grabouw, Cape Town, 27 November – 1 December 2023.*

Mtshali TN, Ryan-Keogh TJ, Bucciarelli E, van Horsten NR, Nicholson S-A, Thomalla SJ, Sarthou G, Roychoudhury A. 2023. Winter-time distributions and dissolved iron mixed layer budget in the south Atlantic sector of the Southern Ocean. *6th South African National Antarctic Programme (SANAP) Symposium 2023, Houw Hoek, Grabouw, Cape Town, 27 November – 1 December 2023.*

Mtshali TN, van Horsten NR, Thomalla SJ, Ryan-Keogh TJ, Nicholson S-A, Roychoudhury AN, Bucciarelli E, Sarthou G, Tagliabue A, Monteiro P. 2023. Seasonal depletion of the dissolved iron reservoirs in the sub-Antarctic zone of the southern Atlantic Ocean. *5th National Global Change Conference, University of the Free State, Bloemfontein, South Africa, 30 January – 2 February 2023.*

Nhleko J. 2023. Spatio-temporal distribution of benthic macrofauna of a large fluvially dominated Kei Estuary, South Africa, in response to a flood. *Zoological Society of South Africa (ZSSA) Conference 2023, Champagne Sports Resort, KwaZulu-Natal, South Africa, 25–29 September 2023.*

Nhleko J, Kirkman S, Holness S. 2023. Understanding of potential OECMs in marine space and how they should be approached. *Inaugural National Other Effective Area-based Conservation Measures (OECMs) bootcamp: Understanding of OECMs in the South African context, Hatfield, Pretoria, South Africa, 21–22 November 2023.*

Nkadimeng TN, Russo CS, Halo I, Lamont T. 2023. Eddy variability in the Benguela: A comparison of the northern and southern Benguela eddy fields. *DFFE Physical Oceanography Science and Technical Workshop, East Pier, Cape Town, South Africa, 26–27 October 2023.*

Nkadimeng TN, Russo CS, Halo I, Lamont T. 2023. Eddy variability in the Benguela: A comparison of the northern and southern Benguela eddy fields. *Nansen-Tutu Three Oceans Symposium: marine science and services in the greater Agulhas region, Breakwater Lodge, Victoria & Alfred Waterfront, Cape Town, South Africa, 6–7 November 2023.*

Petzer K, Lamont T, Rouault M†. 2023. Marine heatwaves in the Cape Peninsula upwelling cell, Southern Benguela. *5th International Symposium on the Effects of Climate Change on the World's Ocean (ECCWO-5), Bergen, Norway, 17–21 April 2023.*

Petzer K, Lamont T, Rouault M†. 2023. Marine heatwaves in the Cape Peninsula upwelling cell, Southern Benguela. *24th International SST Users Symposium and Group for High Resolution Sea Surface Temperature (GHRSST) Team Meeting, Ahmedabad, India, and online, 16–20 October 2023.*

Petzer K, Lamont T, Rouault M†. 2023. Marine heatwaves in the Cape Peninsula upwelling cell. *DFFE Physical Oceanography Science and Technical Workshop, East Pier, Cape Town, South Africa, 26–27 October 2023.*

Petzer K, Lamont T, Rouault M†. 2023. Marine heatwaves and warm events in the Cape Peninsula upwelling cell. *Nansen-Tutu Three Oceans Symposium: marine science and services in the greater Agulhas region, Breakwater Lodge, Victoria & Alfred Waterfront, Cape Town, South Africa, 6–7 November 2023.*

Pfaff M, Mackensen A, Kirkman S, Govan H, Estradivari, Rakotondrazafy V, Martens C, de Vos D, Tuda A. 2023. Navigating 30x30 – building bridges between conservation and small-scale fisheries. *Invited Keynote. 2023 Western Indian Ocean Science Policy Platform (WIO-SPP): Addressing Global Targets in the WIO in support of a Sustainable Blue Economy, Maputo, Mozambique, 5–7 December 2023.*

Pillay K. 2023. The story of microplastics, where are we at in South Africa. *1st coordination meeting of the International Atomic Energy Agency's (IAEA) project on Reutilizing and Recycling Polymeric Waste through Radiation Modification in the Marine Environment (RAF1010), UN IAEA Headquarters, Monaco, 20–24 February 2023.*

Pillay K. 2023. South African progress on developing a microplastics protocol. *Regional Workshop for the Harmonization of Operational Protocols for the Collection, Identification, and Counting of Microplastics in the Selected Matrices in Africa, Cairo, Egypt, 7–11 August 2023.*

Pillay K. 2023. National OCIMS: Possible database for microplastics data under RAF1010. *Regional Workshop for the Harmonization of Operational Protocols for the Collection, Identification, and Counting of Microplastics in the Selected Matrices in Africa, Cairo, Egypt, 7–11 August 2023.*

Pillay K, Worship MM. 2023. South African microplastics research. *Atlantic Ecosystems Assessment, Forecasting & Sustainability (AtlantECO) General Assembly 2023, Florianopolis, Brazil, 3–10 October 2023.*

Pillay K, Worship MM. 2023. Monitoring microplastics in South Africa: An issue of methodology. *Society of Environmental Toxicology and Chemistry (SETAC) Africa 11th Biennial Conference, Accra, Ghana, 8–11 October 2023.*

Pillay K, Worship MM, Johnson AS. 2023. An ecosystem approach to essential ocean monitoring: The Integrated Ecosystem Programme. *5th National Global Change Conference, University of the Free State, Bloemfontein, South Africa, 30 January – 2 February 2023.*

Pillay K, Worship MM, Johnson AS. 2023. DFFE: Oceans and Coasts assessment of current and ongoing activities related to monitoring microplastics. *1st coordination meeting of the International Atomic Energy Agency's (IAEA) project on Reutilizing and Recycling Polymeric Waste through Radiation Modification in the Marine Environment (RAF1010), UN IAEA Headquarters, Monaco, 20–24 February 2023.*

Pillay K, Worship MM, Johnson AS, van der Poel J, Setati S, Maduray S, Gebe Z Seakamela. 2023. The Integrated Ecosystem Programme: Southern Benguela, a South African multidisciplinary flagship on ocean observations for assessing the marine environment. *5th International Symposium on the Effects of Climate Change on the World's Ocean (ECCWO-5), Bergen, Norway, 17–21 April 2023.*

Russo CS. 2023. Location of the Agulhas Current's Core and Edges – LACCE. *Global Ocean Observing System (GOOS) Boundary Current Workshop and 14th session of the GOOS Observation Coordination Group, Peter Stoker Centre and Waterfront Breakwater Lodge, Cape Town, South Africa & Online, 5-8 June 2023.*

Russo CS, Lamont T. 2023. Monitoring variability in the Agulhas Current. *DFFE Physical Oceanography Science and Technical Workshop, East Pier, Cape Town, South Africa, 26–27 October 2023.*

Russo CS, Lamont T. 2023. Monitoring variability in the Agulhas Current. *Nansen-Tutu Three Oceans Symposium: marine science and services in the greater Agulhas region, Breakwater Lodge, Victoria & Alfred Waterfront, Cape Town, South Africa, 6–7 November 2023*.

Russo CS, Louw GS, van den Berg MA, Lamont T. 2023. SAMOC, SAMBA and C/PIES. *DFFE Physical Oceanography Science and Technical Workshop, East Pier, Cape Town, South Africa, 26–27 October 2023*.

Savidge W, Brandini F, Hofmann E, Krug M, Lamont T, Roughan M, Savidge D, Silveira I, Suthers I, Yang D. 2023. Western Boundary Current – Subtropical Continental Shelf Interactions May 22nd-24th 2023, Savannah GA. *Coastal Ocean Dynamics Gordon Research Conference: Coastal Ocean Physics and its Connections to Marine Ecosystems, Bryant University, Smithfield, Rhode Island, USA, 18–23 June 2023*.

Schäfer I, Shabangu FW, Lamont T. 2023. Acoustic occurrence and behavior of Baleen Whales during winter around Prince Edward Islands. *6th South African National Antarctic Programme (SANAP) Symposium 2023, Houw Hoek, Grabouw, Cape Town, 27 November – 1 December 2023*.

Shabangu FW, Tessaglia-Hymes CT, Jacobs L, van den Berg MA, Louw G, Lamont T. 2023. Life near the sea ice edge: Listening for whales off the Maud Rise, Antarctica. *6th South African National Antarctic Programme (SANAP) Symposium 2023, Houw Hoek, Grabouw, Cape Town, 27 November – 1 December 2023*.

Sneddon A, Lamont T, Reason CJC, Russo CS. 2023. Marine Heatwave characteristics in the South Atlantic and South Indian Oceans. *DFFE Physical Oceanography Science and Technical Workshop, East Pier, Cape Town, South Africa, 26–27 October 2023*.

Sneddon A, Lamont T, Reason CJC, Russo CS. 2023. Marine Heatwave characteristics in the South Atlantic and South Indian Oceans. *Nansen-Tutu Three Oceans Symposium: marine science and services in the greater Agulhas region, Breakwater Lodge, Victoria & Alfred Waterfront, Cape Town, South Africa, 6–7 November 2023*.

Sneddon A, Lamont T, Reason CJC, Russo CS. 2023. Marine Heatwave characteristics in the South Atlantic and South Indian Oceans. *6th South African National Antarctic Programme (SANAP) Symposium 2023, Houw Hoek, Grabouw, Cape Town, 27 November – 1 December 2023*.

Sololo P, Halo I, Russo CS, Lamont T. 2023. Change in sea surface temperature gradient and the effects it has on distribution of Cape anchovy spawners on the Agulhas Bank. *DFFE Physical Oceanography Science and Technical Workshop, East Pier, Cape Town, South Africa, 26–27 October 2023*.

Taukoor S, Penven P, Ansorge I, Mashifane T, Lamont T. 2023. Port Alfred upwelling: A numerical modelling approach. *Nansen-Tutu Three Oceans Symposium: marine science and services in the greater Agulhas region, Breakwater Lodge, Victoria & Alfred Waterfront, Cape Town, South Africa, 6–7 November 2023*.

Toolsee T, Lamont T. 2023. The interannual/decadal scale and long-term trends of surface hydrography around the sub-Antarctic Prince Edward Islands. *6th South African National Antarctic Programme (SANAP) Symposium 2023, Houw Hoek, Grabouw, Cape Town, 27 November – 1 December 2023*.

Toolsee T, Lamont T, Rouault M†. 2023. Interannual variability and long-term trends of surface hydrography around the Prince Edward Islands Archipelago, Southern Ocean. *Nansen-Tutu Three Oceans Symposium: marine science and services in the greater Agulhas region, Breakwater Lodge, Victoria & Alfred Waterfront, Cape Town, South Africa, 6–7 November 2023*.

van den Berg MA, Lamont T, Ansorge IJ. 2023. Influence of eddies and fronts on the shelf seas of the sub-Antarctic Prince Edward Islands. *6th South African National Antarctic Programme (SANAP) Symposium 2023, Houw Hoek, Grabouw, Cape Town, 27 November – 1 December 2023*.

Williams LL. 2023. A GIS-based technology response to an avian influenza outbreak in South Africa. *International Cartographic Conference 2023, Cape Town, South Africa, 13–18 August 2023*.

Worship M, Pillay K, van der Poel J, Setati S. 2023. Picture Perfect: Creating a mesozooplankton digital archive. *International Marine Technician's Workshop (INMARTECH), Barcelona, Spain, 20–22 June 2023*.

Yemane D, Samaai T, Kirkman S. 2023. Changes in species distribution and biodiversity patterns in response to projected climate change off South Africa. *5th International Symposium on the Effects of Climate Change on the World's Ocean (ECCWO-5), Bergen, Norway, 17–21 April 2023*.

Published datasets

Anders D, Frantz F, Jacobs L, van den Berg MA, Lamont T. 2023. Processed underway Thermosalinograph (TSG) observations from the Integrated Ecosystem Programme: Southern Benguela (IEP:SB) on the Algoa Voyage 274, August 2021. DFFE. doi: 10.15493/DEA.MIMS.09962023.

Anders D, Frantz F, Jacobs L, van den Berg MA, Lamont T. 2023. Raw underway Thermosalinograph (TSG) observations from the Integrated Ecosystem Programme: Southern Benguela (IEP:SB) on the Algoa Voyage 274, August 2021. DFFE. doi: 10.15493/DEA.MIMS.09972023.

Anders D, Frantz F, Jacobs L, van den Berg MA, Lamont T. 2023. Processed underway Thermosalinograph (TSG) observations from the South Atlantic Meridional Overturning Circulation Basin-wide Array (SAMBA) Monitoring Line cruise on the Algoa Voyage 253, October 2018. DFFE. doi: 10.15493/DEA.MIMS.10522023.

Anders D, Frantz F, Jacobs L, van den Berg MA, Lamont T. 2023. Raw underway Thermosalinograph (TSG) observations from the South Atlantic Meridional Overturning Circulation Basin-wide Array (SAMBA) Monitoring Line cruise on the Algoa Voyage 253, October 2018. DFFE. doi: 10.15493/DEA.MIMS.10532023.

Anders D, Frantz F, Jacobs L, van den Berg MA, Lamont T. 2023. Processed underway Thermosalinograph (TSG) observations from the Integrated Ecosystem Programme: Southern Benguela (IEP: SB) on the Algoa Voyage 277, November 2021. DFFE. doi: 10.15493/DEA.MIMS.10562023.

Anders D, Frantz F, Jacobs L, van den Berg MA, Lamont T. 2023. Raw underway Thermosalinograph (TSG) observations from the Integrated Ecosystem Programme: Southern Benguela (IEP: SB) on the Algoa Voyage 277, November 2021. DFFE. doi: 10.15493/DEA.MIMS.10572023.

Anders D, Jacobs L, van den Berg MA, Lamont T. 2023. Processed underway Thermosalinograph (TSG) observations from the Algoa Voyage 257, January 2019. DFFE. doi: 10.15493/DEA.MIMS.09882023.

Anders D, Jacobs L, van den Berg MA, Lamont T. 2023. Raw underway Thermosalinograph (TSG) observations from the Algoa Voyage 257, January 2019. DFFE. doi: 10.15493/DEA.MIMS.09892023.

Anders D, Jacobs L, van den Berg MA, Lamont T. 2023. Processed underway Thermosalinograph (TSG) observations from the Integrated Ecosystem Programme: Southern Ben-

guela (IEP:SB) on the Algoa Voyage 258, February 2019. DFFE. doi: 10.15493/DEA.MIMS.09902023.

Anders D, Jacobs L, van den Berg MA, Lamont T. 2023. Raw underway Thermosalinograph (TSG) observations from the Integrated Ecosystem Programme: Southern Benguela (IEP:SB) on the Algoa Voyage 258, February 2019. DFFE. doi: 10.15493/DEA.MIMS.09912023.

Anders D, Jacobs L, van den Berg MA, Lamont T. 2023. Processed underway Thermosalinograph (TSG) observations from the Integrated Ecosystem Programme: Southern Benguela (IEP:SB) on the Algoa Voyage 259, May 2019. DFFE. doi: 10.15493/DEA.MIMS.09922023.

Anders D, Jacobs L, van den Berg MA, Lamont T. 2023. Raw underway Thermosalinograph (TSG) observations from the Integrated Ecosystem Programme: Southern Benguela (IEP:SB) on the Algoa Voyage 259, May 2019. DFFE. doi: 10.15493/DEA.MIMS.09932023.

Anders D, Jacobs L, van den Berg MA, Lamont T. 2023. Processed underway Thermosalinograph (TSG) observations from the Integrated Ecosystem Programme: Southern Benguela (IEP: SB) on the Algoa Voyage 255, November 2018. DFFE. doi: 10.15493/DEA.MIMS.10542023.

Anders D, Jacobs L, van den Berg MA, Lamont T. 2023. Raw underway Thermosalinograph (TSG) observations from the Integrated Ecosystem Programme: Southern Benguela (IEP: SB) on the Algoa Voyage 255, November 2018. DFFE. doi: 10.15493/DEA.MIMS.10552023.

Anders D, Jacobs L, van den Berg MA, Lamont T. 2023. Processed underway Thermosalinograph (TSG) observations from the Integrated Ecosystem Programme: Southern Benguela (IEP: SB) on the Algoa Voyage 287, November 2022. DFFE. doi: 10.15493/DEA.MIMS.10582023.

Anders D, Jacobs L, van den Berg MA, Lamont T. 2023. Raw underway Thermosalinograph (TSG) observations from the Integrated Ecosystem Programme: Southern Benguela (IEP: SB) on the Algoa Voyage 287, November 2022. DFFE. doi: 10.15493/DEA.MIMS.10592023.

Filander Z, Lamont T. 2023. Averaged bottom temperature and dissolved oxygen in and around the Cape Canyon. DFFE. doi: 10.15493/DEA.MIMS.05332023.

Frantz F, Anders D, Jacobs L, van den Berg MA, Lamont T. 2023. Processed underway Thermosalinograph (TSG) observations from the Integrated Ecosystem Programme: Southern Benguela (IEP:SB) on the Algoa Voyage 262, August 2019. DFFE. doi: 10.15493/DEA.MIMS.09942023.

Frantz F, Anders D, Jacobs L, van den Berg MA, Lamont T. 2023. Raw underway Thermosalinograph (TSG) observations from the Integrated Ecosystem Programme: Southern Benguela (IEP:SB) on the Algoa Voyage 262, August 2019. DFFE. doi: 10.15493/DEA.MIMS.09952023.

Frantz F, Anders D, Jacobs L, van den Berg MA, Lamont T. 2023. Processed underway Thermosalinograph (TSG) observations from the Southern Ocean Seasonal Experiment 2022 on the SA Agulhas II Voyage 053, July 2022. DFFE. doi: 10.15493/DEA.MIMS.09982023.

Frantz F, Anders D, Jacobs L, van den Berg MA, Lamont T. 2023. Raw underway Thermosalinograph (TSG) observations from the Southern Ocean Seasonal Experiment 2022 on the SA Agulhas II Voyage 053, July 2022. DFFE. doi: 10.15493/DEA.MIMS.09992023.

Huggett J, Noyon, M, Carstensen J, Walker D. 2023. Dataset for: 'Patterns in the Plankton – Spatial distribution and long-term variability of copepods on the Agulhas Bank'. Zenodo. doi: 10.5281/zenodo.7569712.

Ismail H, van den Berg MA, Lamont T. 2023. Raw temperature data for long-term observations of bottom temperatures at Elands Bay (October 1990 - December 1990). DFFE. doi: 10.15493/DEA.MIMS.01952023.

Ismail H, van den Berg MA, Lamont T. 2023. Raw temperature data for long-term observations of bottom temperatures at Elands Bay (December 1990 - February 1991). DFFE. doi: 10.15493/DEA.MIMS.01962023.

Ismail H, van den Berg MA, Lamont T. 2023. Raw temperature data for long-term observations of bottom temperatures at Elands Bay (February 1991 - May 1991). DFFE. doi: 10.15493/DEA.MIMS.01972023.

Ismail H, van den Berg MA, Lamont T. 2023. Raw temperature data for long-term observations of bottom temperatures at Elands Bay (May 1991 - October 1991). DFFE. doi: 10.15493/DEA.MIMS.01982023.

Ismail H, van den Berg MA, Lamont T. 2023. Raw temperature data for long-term observations of bottom temperatures at Elands Bay (October 1991 - February 1992). DFFE. doi: 10.15493/DEA.MIMS.01992023.

Ismail H, van den Berg MA, Lamont T. 2023. Raw temperature data for long-term observations of bottom temperatures at Elands Bay (February 1992 - May 1992). DFFE. doi: 10.15493/DEA.MIMS.02002023.

Ismail H, van den Berg MA, Lamont T. 2023. Raw temperature data for long-term observations of bottom temperatures at Elands Bay (May 1992 - August 1992). DFFE. doi: 10.15493/DEA.MIMS.02012023.

Ismail H, van den Berg MA, Lamont T. 2023. Raw temperature data for long-term observations of bottom temperatures at Elands Bay (August 1992 - September 1992). DFFE. doi: 10.15493/DEA.MIMS.02022023.

Ismail H, van den Berg MA, Lamont T. 2023. Raw temperature data for long-term observations of bottom temperatures at Elands Bay (September 1992 - October 1992). DFFE. doi: 10.15493/DEA.MIMS.02032023.

Ismail H, van den Berg MA, Lamont T. 2023. Raw temperature data for long-term observations of bottom temperatures at Elands Bay (December 1992 - January 1993). DFFE. doi: 10.15493/DEA.MIMS.02042023.

Ismail H, van den Berg MA, Lamont T. 2023. Raw temperature data for long-term observations of bottom temperatures at Elands Bay (January 1993 - February 1993). DFFE. doi: 10.15493/DEA.MIMS.02052023.

Ismail H, van den Berg MA, Lamont T. 2023. Raw temperature data for long-term observations of bottom temperatures at Elands Bay (February 1993 - March 1993). DFFE. doi: 10.15493/DEA.MIMS.02062023.

Ismail H, van den Berg MA, Lamont T. 2023. Raw temperature data for long-term observations of bottom temperatures at Elands Bay (March 1993 - April 1993). DFFE. doi: 10.15493/DEA.MIMS.02072023.

Ismail H, van den Berg MA, Lamont T. 2023. Raw temperature data for long-term observations of bottom temperatures at Elands Bay (July 1993 - August 1993). DFFE. doi: 10.15493/DEA.MIMS.02082023.

Ismail H, van den Berg MA, Lamont T. 2023. Raw temperature data for long-term observations of bottom temperatures at Elands Bay (February 1994 - July 1994). DFFE. doi: 10.15493/DEA.MIMS.02092023.

Ismail H, van den Berg MA, Lamont T. 2023. Raw temperature data for long-term observations of bottom temperatures at Elands Bay (July 1994 - November 1994). DFFE. doi: 10.15493/DEA.MIMS.02102023.

Ismail H, van den Berg MA, Lamont T. 2023. Raw temperature data for long-term observations of bottom temperatures at Elands Bay (November 1994 - February 1995). DFFE. doi: 10.15493/DEA.MIMS.02112023.

Ismail H, van den Berg MA, Lamont T. 2023. Raw temperature data for long-term observations of bottom temperatures at Elands Bay (February 1995 - July 1995). DFFE. doi: 10.15493/DEA.MIMS.02122023.

Ismail H, van den Berg MA, Lamont T. 2023. Raw temperature data for long-term observations of bottom temperatures at Elands Bay (August 1995 - February 1996). DFFE. doi: 10.15493/DEA.MIMS.02132023.

Ismail H, van den Berg MA, Lamont T. 2023. Raw temperature data for long-term observations of bottom temperatures at Elands Bay (March 1996 - April 1996). DFFE. doi: 10.15493/DEA.MIMS.02142023.

Ismail H, van den Berg MA, Lamont T. 2023. Raw temperature data for long-term observations of bottom temperatures at Elands Bay (April 1996 - May 1996). DFFE. doi: 10.15493/DEA.MIMS.02152023.

Ismail H, van den Berg MA, Lamont T. 2023. Long-term observations of hourly bottom temperatures at Elands Bay (October 1990 - December 1990). Department of Forestry, Fisheries and the Environment. doi: 10.15493/DEA.MIMS.02162023.

Ismail H, van den Berg MA, Lamont T. 2023. Long-term observations of hourly bottom temperatures at Elands Bay (December 1990 - February 1991). DFFE. doi: 10.15493/DEA.MIMS.02172023.

Ismail H, van den Berg MA, Lamont T. 2023. Long-term observations of hourly bottom temperatures at Elands Bay (February 1991 - May 1991). DFFE. doi: 10.15493/DEA.MIMS.02182023.

Ismail H, van den Berg MA, Lamont T. 2023. Long-term observations of hourly bottom temperatures at Elands Bay (May 1991 - October 1991). DFFE. doi: 10.15493/DEA.MIMS.02192023.

Ismail H, van den Berg MA, Lamont T. 2023. Long-term observations of hourly bottom temperatures at Elands Bay (October 1991 - February 1992). DFFE. doi: 10.15493/DEA.MIMS.02202023.

Ismail H, van den Berg MA, Lamont T. 2023. Long-term observations of hourly bottom temperatures at Elands Bay (February 1992 - May 1992). DFFE. doi: 10.15493/DEA.MIMS.02212023.

Ismail H, van den Berg MA, Lamont T. 2023. Long-term observations of hourly bottom temperatures at Elands Bay (May 1992 - August 1992). DFFE. doi: 10.15493/DEA.MIMS.02222023.

Ismail H, van den Berg MA, Lamont T. 2023. Long-term observations of hourly bottom temperatures at Elands Bay (August 1992 - September 1992). DFFE. doi: 10.15493/DEA.MIMS.02232023.

Ismail H, van den Berg MA, Lamont T. 2023. Long-term observations of hourly bottom temperatures at Elands Bay (September 1992 - October 1992). DFFE. doi: 10.15493/DEA.MIMS.02242023.

Ismail H, van den Berg MA, Lamont T. 2023. Long-term observations of hourly bottom temperatures at Elands Bay (December 1992 - January 1993). DFFE. doi: 10.15493/DEA.MIMS.02252023.

Ismail H, van den Berg MA, Lamont T. 2023. Long-term observations of hourly bottom temperatures at Elands Bay (January 1993 - February 1993). DFFE. doi: 10.15493/DEA.MIMS.02262023.

Ismail H, van den Berg MA, Lamont T. 2023. Long-term observations of hourly bottom temperatures at Elands Bay (February 1993 - March 1993). DFFE. doi: 10.15493/DEA.MIMS.02272023.

Ismail H, van den Berg MA, Lamont T. 2023. Long-term observations of hourly bottom temperatures at Elands Bay (March 1993 - April 1993). DFFE. doi: 10.15493/DEA.MIMS.02282023.

Ismail H, van den Berg MA, Lamont T. 2023. Long-term observations of hourly bottom temperatures at Elands Bay (July 1993 - August 1993). DFFE. doi: 10.15493/DEA.MIMS.02292023.

Ismail H, van den Berg MA, Lamont T. 2023. Long-term observations of hourly bottom temperatures at Elands Bay (February 1994 - July 1994). DFFE. doi: 10.15493/DEA.MIMS.02302023.

Ismail H, van den Berg MA, Lamont T. 2023. Long-term observations of hourly bottom temperatures at Elands Bay (July 1994 - November 1994). DFFE. doi: 10.15493/DEA.MIMS.02312023.

Ismail H, van den Berg MA, Lamont T. 2023. Long-term observations of hourly bottom temperatures at Elands Bay (November 1994 - February 1995). DFFE. doi: 10.15493/DEA.MIMS.02322023.

Ismail H, van den Berg MA, Lamont T. 2023. Long-term observations of hourly bottom temperatures at Elands Bay (February 1995 - July 1995). DFFE. doi: 10.15493/DEA.MIMS.02332023.

Ismail H, van den Berg MA, Lamont T. 2023. Long-term observations of hourly bottom temperatures at Elands Bay (August 1995 - February 1996). DFFE. doi: 10.15493/DEA.MIMS.02342023.

Ismail H, van den Berg MA, Lamont T. 2023. Long-term observations of hourly bottom temperatures at Elands Bay (March 1996 - April 1996). DFFE. doi: 10.15493/DEA.MIMS.02352023.

Ismail H, van den Berg MA, Lamont T. 2023. Long-term observations of hourly bottom temperatures at Elands Bay (April 1996 - May 1996). DFFE. doi: 10.15493/DEA.MIMS.02362023.

Ismail H, van den Berg MA, Lamont T. 2023. Raw temperature data for long-term observations of bottom temperatures at Paternoster (January 1990 - March 1990). DFFE. doi: 10.15493/DEA.MIMS.03642023.

Ismail H, van den Berg MA, Lamont T. 2023. Raw temperature data for long-term observations of bottom temperatures at Paternoster (March 1990 - May 1990). DFFE. doi: 10.15493/DEA.MIMS.03652023.

Ismail H, van den Berg MA, Lamont T. 2023. Raw temperature data for long-term observations of bottom temperatures at Paternoster (May 1990 - June 1990). DFFE. doi: 10.15493/DEA.MIMS.03662023.

Ismail H, van den Berg MA, Lamont T. 2023. Raw temperature data for long-term observations of bottom temperatures at Paternoster (June 1990 - August 1990). DFFE. doi: 10.15493/DEA.MIMS.03672023.

Ismail H, van den Berg MA, Lamont T. 2023. Raw temperature data for long-term observations of bottom temperatures at Paternoster (August 1990 - November 1990). DFFE. doi: 10.15493/DEA.MIMS.03682023.

Ismail H, van den Berg MA, Lamont T. 2023. Raw temperature data for long-term observations of bottom temperatures at Paternoster (November 1990 - February 1991). DFFE. doi: 10.15493/DEA.MIMS.03692023.

Ismail H, van den Berg MA, Lamont T. 2023. Raw temperature data for long-term observations of bottom temperatures

at Paternoster (February 1991 - April 1991). DFFE. doi: 10.15493/DEA.MIMS.03702023.

Ismail H, van den Berg MA, Lamont T. 2023. Raw temperature data for long-term observations of bottom temperatures at Paternoster (February 1992 - May 1992). DFFE. doi: 10.15493/DEA.MIMS.03712023.

Ismail H, van den Berg MA, Lamont T. 2023. Raw temperature data for long-term observations of bottom temperatures at Paternoster (May 1992 - September 1992). DFFE. doi: 10.15493/DEA.MIMS.03722023.

Ismail H, van den Berg MA, Lamont T. 2023. Raw temperature data for long-term observations of bottom temperatures at Paternoster (September 1992 - January 1993). DFFE. doi: 10.15493/DEA.MIMS.03732023.

Ismail H, van den Berg MA, Lamont T. 2023. Raw temperature data for long-term observations of bottom temperatures at Paternoster (January 1993 - August 1993). DFFE. doi: 10.15493/DEA.MIMS.03742023.

Ismail H, van den Berg MA, Lamont T. 2023. Raw temperature data for long-term observations of bottom temperatures at Paternoster (August 1993 - February 1994). DFFE. doi: 10.15493/DEA.MIMS.03752023.

Ismail H, van den Berg MA, Lamont T. 2023. Raw temperature data for long-term observations of bottom temperatures at Paternoster (February 1994 - March 1994). DFFE. doi: 10.15493/DEA.MIMS.03762023.

Ismail H, van den Berg MA, Lamont T. 2023. Raw temperature data for long-term observations of bottom temperatures at Paternoster (March 1994 - August 1994). DFFE. doi: 10.15493/DEA.MIMS.03772023.

Ismail H, van den Berg MA, Lamont T. 2023. Raw temperature data for long-term observations of bottom temperatures at Paternoster (August 1994 - February 1995). DFFE. doi: 10.15493/DEA.MIMS.03782023.

Ismail H, van den Berg MA, Lamont T. 2023. Raw temperature data for long-term observations of bottom temperatures at Paternoster (February 1995 - August 1995). DFFE. doi: 10.15493/DEA.MIMS.03792023.

Ismail H, van den Berg MA, Lamont T. 2023. Raw temperature data for long-term observations of bottom temperatures at Paternoster (August 1995 - February 1996). DFFE. doi: 10.15493/DEA.MIMS.03802023.

Ismail H, van den Berg MA, Lamont T. 2023. Raw temperature data for long-term observations of bottom temperatures at Paternoster (February 1996 - September 1996). DFFE. doi: 10.15493/DEA.MIMS.03812023.

Ismail H, van den Berg MA, Lamont T. 2023. Raw temperature data for long-term observations of bottom temperatures at Paternoster (September 1996 - April 1997). DFFE. doi: 10.15493/DEA.MIMS.03822023

Ismail H, van den Berg MA, Lamont T. 2023. Raw temperature data for long-term observations of bottom temperatures at Paternoster (April 1997 - October 1997). DFFE. doi: 10.15493/DEA.MIMS.03832023.

Ismail H, van den Berg MA, Lamont T. 2023. Raw temperature data for long-term observations of bottom temperatures at Paternoster (October 1997 - March 1998). DFFE. doi: 10.15493/DEA.MIMS.03842023.

Ismail H, van den Berg MA, Lamont T. 2023. Raw temperature data for long-term observations of bottom temperatures at Paternoster (March 1998 - September 1998). DFFE. doi: 10.15493/DEA.MIMS.03852023.

Ismail H., van den Berg MA, Lamont T. 2023. Raw temperature data for long-term observations of bottom temperatures at Paternoster (September 1998 - March 1999). DFFE. doi: 10.15493/DEA.MIMS.03862023,

Ismail H, van den Berg MA, Lamont T. 2023. Raw temperature data for long-term observations of bottom temperatures at Paternoster (March 1999 - August 1999). DFFE. doi: 10.15493/DEA.MIMS.03872023.

Ismail H, van den Berg MA, Lamont T. 2023. Raw temperature data for long-term observations of bottom temperatures at Paternoster (August 1999 - February 2000). DFFE. doi: 10.15493/DEA.MIMS.03882023.

Ismail H, van den Berg MA, Lamont T. 2023. Raw temperature data for long-term observations of bottom temperatures at Paternoster (February 2000 - March 2002). DFFE. doi: 10.15493/DEA.MIMS.03892023.

Ismail H, van den Berg MA, Lamont T. 2023. Raw temperature data for long-term observations of bottom temperatures at Paternoster (September 2003 - April 2004). DFFE. doi: 10.15493/DEA.MIMS.03902023.

Ismail H, van den Berg MA, Lamont T. 2023. Raw temperature data for long-term observations of bottom temperatures at Paternoster (April 2004 - May 2009). DFFE. doi: 10.15493/DEA.MIMS.03912023.

Ismail H, van den Berg MA, Lamont T. 2023. Long-term observations of hourly bottom temperatures at Paternoster (January 1990 - March 1990). DFFE. doi: 10.15493/DEA.MIMS.03922023.

Ismail H, van den Berg MA, Lamont T. 2023. Long-term observations of hourly bottom temperatures at Paternoster (March 1990 - May 1990). DFFE. doi: 10.15493/DEA.MIMS.03932023.

Ismail H, van den Berg MA, Lamont T. 2023. Long-term observations of hourly bottom temperatures at Paternoster (May 1990 - June 1990). DFFE. doi: 10.15493/DEA.MIMS.03942023.

Ismail H, van den Berg MA, Lamont T. 2023. Long-term observations of hourly bottom temperatures at Paternoster (June 1990 - August 1990). DFFE. doi: 10.15493/DEA.MIMS.03952023.

Ismail H, van den Berg MA, Lamont T. 2023. Long-term observations of hourly bottom temperatures at Paternoster (August 1990 - November 1990). DFFE. doi: 10.15493/DEA.MIMS.03962023.

Ismail H, van den Berg MA, Lamont T. 2023. Long-term observations of hourly bottom temperatures at Paternoster (November 1990 - February 1991). DFFE. doi: 10.15493/DEA.MIMS.03972023.

Ismail H, van den Berg MA, Lamont T. 2023. Long-term observations of hourly bottom temperatures at Paternoster (February 1991 - April 1991). DFFE. doi: 10.15493/DEA.MIMS.03982023.

Ismail H, van den Berg MA, Lamont T. 2023. Long-term observations of hourly bottom temperatures at Paternoster (February 1992 - May 1992). DFFE. doi: 10.15493/DEA.MIMS.03992023.

Ismail H, van den Berg MA, Lamont T. 2023. Long-term observations of hourly bottom temperatures at Paternoster (May 1992 - September 1992). DFFE. doi: 10.15493/DEA.MIMS.04002023.

Ismail H, van den Berg MA, Lamont T. 2023. Long-term observations of hourly bottom temperatures at Paternoster (September 1992 - January 1993). DFFE. doi: 10.15493/DEA.MIMS.04012023.

Ismail H, van den Berg MA, Lamont T. 2023. Long-term observations of hourly bottom temperatures at Paternoster (January 1993 - August 1993). DFFE. doi: 10.15493/DEA.MIMS.04022023.

Ismail H, van den Berg MA, Lamont T. 2023. Long-term observations of hourly bottom temperatures at Paternoster (Au-

gust 1993 - February 1994). DFFE. doi: 10.15493/DEA.MIMS.04032023.

Ismail H, van den Berg MA, Lamont T. 2023. Long-term observations of hourly bottom temperatures at Paternoster (February 1994 - March 1994). DFFE. doi: 10.15493/DEA.MIMS.04042023.

Ismail H, van den Berg MA, Lamont T. 2023. Long-term observations of hourly bottom temperatures at Paternoster (March 1994 - August 1994). DFFE. doi: 10.15493/DEA.MIMS.04052023.

Ismail H, van den Berg MA, Lamont T. 2023. Long-term observations of hourly bottom temperatures at Paternoster (August 1994 - February 1995). DFFE. doi: 10.15493/DEA.MIMS.04062023.

Ismail H, van den Berg MA, Lamont T. 2023. Long-term observations of hourly bottom temperatures at Paternoster (February 1995 - August 1995). DFFE. doi: 10.15493/DEA.MIMS.04072023.

Ismail H, van den Berg MA, Lamont T. 2023. Long-term observations of hourly bottom temperatures at Paternoster (August 1995 - February 1996). DFFE. doi: 10.15493/DEA.MIMS.04082023.

Ismail H, van den Berg MA, Lamont T. 2023. Long-term observations of hourly bottom temperatures at Paternoster (February 1996 - September 1996). DFFE. doi: 10.15493/DEA.MIMS.04092023.

Ismail H., van den Berg MA, Lamont T. 2023. Long-term observations of hourly bottom temperatures at Paternoster (September 1996 - April 1997). DFFE. doi: 10.15493/DEA.MIMS.04102023.

Ismail H, van den Berg MA, Lamont T. 2023. Long-term observations of hourly bottom temperatures at Paternoster (April 1997 - October 1997). DFFE. doi: 10.15493/DEA.MIMS.04112023.

Ismail H, van den Berg MA, Lamont T. 2023. Long-term observations of hourly bottom temperatures at Paternoster (October 1997 - March 1998). DFFE. doi: 10.15493/DEA.MIMS.04122023.

Ismail H, van den Berg MA, Lamont T. 2023. Long-term observations of hourly bottom temperatures at Paternoster (March 1998 - September 1998). DFFE. doi: 10.15493/DEA.MIMS.04132023.

Ismail H, van den Berg MA, Lamont T. 2023. Long-term observations of hourly bottom temperatures at Paternoster (September 1998 - March 1999). DFFE. doi: 10.15493/DEA.MIMS.04142023.

Ismail H, van den Berg MA, Lamont T. 2023. Long-term observations of hourly bottom temperatures at Paternoster (March 1999 - August 1999). DFFE. doi: 10.15493/DEA.MIMS.04152023.

Ismail H, van den Berg MA, Lamont T. 2023. Long-term observations of hourly bottom temperatures at Paternoster (August 1999 - February 2000). DFFE. doi: 10.15493/DEA.MIMS.04162023.

Ismail H, van den Berg MA, Lamont T. 2023. Long-term observations of hourly bottom temperatures at Paternoster (February 2000 - March 2002). DFFE. doi: 10.15493/DEA.MIMS.04172023.

Ismail H., van den Berg MA, Lamont T. 2023. Long-term observations of hourly bottom temperatures at Paternoster (September 2003 - April 2004). DFFE. doi: 10.15493/DEA.MIMS.04182023.

Ismail H, van den Berg MA, Lamont T. 2023. Long-term observations of hourly bottom temperatures at Paternoster (April 2004 - May 2009). DFFE. doi: 10.15493/DEA.MIMS.04192023.

Ismail H, van den Berg MA, Lamont T. 2023. Raw temperature data for long-term observations of bottom temperatures at Hout Bay (March 1991 - September 1991). DFFE. doi: 10.15493/DEA.MIMS.02572023.

Ismail H, van den Berg MA, Lamont T. 2023. Raw temperature data for long-term observations of bottom temperatures at Hout Bay (February 1992 - June 1992). DFFE. doi: 10.15493/DEA.MIMS.02582023.

Ismail H, van den Berg MA, Lamont T. 2023. Raw temperature data for long-term observations of bottom temperatures at Hout Bay (June 1992 - November 1992). DFFE. doi: 10.15493/DEA.MIMS.02592023.

Ismail H, van den Berg MA, Lamont T. 2023. Raw temperature data for long-term observations of bottom temperatures at Hout Bay (November 1992 - August 1993). DFFE. doi: 10.15493/DEA.MIMS.02602023.

Ismail H, van den Berg MA, Lamont T. 2023. Raw temperature data for long-term observations of bottom temperatures at Hout Bay (August 1993 - January 1994). DFFE. doi: 10.15493/DEA.MIMS.02612023.

Ismail H, van den Berg MA, Lamont T. 2023. Raw temperature data for long-term observations of bottom temperatures at Hout Bay (January 1994 - August 1994). DFFE. doi: 10.15493/DEA.MIMS.02622023.

Ismail H, van den Berg MA, Lamont T. 2023. Raw temperature data for long-term observations of bottom temperatures at Hout Bay (August 1994 - April 1995). DFFE. doi: 10.15493/DEA.MIMS.02632023.

Ismail H, van den Berg MA, Lamont T. 2023. Raw temperature data for long-term observations of bottom temperatures at Hout Bay (April 1995 - September 1995). DFFE. doi: 10.15493/DEA.MIMS.02642023.

Ismail H, van den Berg MA, Lamont T. 2023. Raw temperature data for long-term observations of bottom temperatures at Hout Bay (September 1995 - July 1996). DFFE. doi: 10.15493/DEA.MIMS.02652023.

Ismail H, van den Berg MA, Lamont T. 2023. Raw temperature data for long-term observations of bottom temperatures at Hout Bay (July 1996 - December 1996). DFFE. doi: 10.15493/DEA.MIMS.02662023.

Ismail H, van den Berg MA, Lamont T. 2023. Raw temperature data for long-term observations of bottom temperatures at Hout Bay (December 1996 - September 1997). DFFE. doi: 10.15493/DEA.MIMS.02672023.

Ismail H, van den Berg MA, Lamont T. 2023. Raw temperature data for long-term observations of bottom temperatures at Hout Bay (September 1997 - February 1998). DFFE. doi: 10.15493/DEA.MIMS.02682023.

Ismail H, van den Berg MA, Lamont T. 2023. Raw temperature data for long-term observations of bottom temperatures at Hout Bay (February 1998 - November 1998). DFFE. doi: 10.15493/DEA.MIMS.02692023.

Ismail H, van den Berg MA, Lamont T. 2023. Raw temperature data for long-term observations of bottom temperatures at Hout Bay (November 1998 - October 1999). DFFE. doi: 10.15493/DEA.MIMS.02702023.

Ismail H, van den Berg MA, Lamont T. 2023. Raw temperature data for long-term observations of bottom temperatures at Hout Bay (October 1999 - May 2000). DFFE. doi: 10.15493/DEA.MIMS.02712023.

Ismail H, van den Berg MA, Lamont T. 2023. Raw temperature data for long-term observations of bottom temperatures at Hout Bay (May 2000 - February 2001). DFFE. doi: 10.15493/DEA.MIMS.02722023.

Ismail H, van den Berg MA, Lamont T. 2023. Raw temperature data for long-term observations of bottom temperatures at

Hout Bay (February 2001 - December 2001). DFFE. doi: 10.15493/DEA.MIMS.02732023.
Ismail H, van den Berg MA, Lamont T. 2023. Raw temperature data for long-term observations of bottom temperatures at Hout Bay (December 2001 - October 2003). DFFE. doi: 10.15493/DEA.MIMS.02742023.
Ismail H, van den Berg MA, Lamont T. 2023. Raw temperature data for long-term observations of bottom temperatures at Hout Bay (October 2003 - October 2004). DFFE. doi: 10.15493/DEA.MIMS.02752023.
Ismail H, van den Berg MA, Lamont T. 2023. Raw temperature data for long-term observations of bottom temperatures at Hout Bay (October 2004 - April 2008). DFFE. doi: 10.15493/DEA.MIMS.02762023.
Ismail H, van den Berg MA, Lamont T. 2023. Long-term observations of hourly bottom temperatures at Hout Bay (March 1991 - September 1991). DFFE. doi: 10.15493/DEA.MIMS.02372023.
Ismail H, van den Berg MA, Lamont T. 2023. Long-term observations of hourly bottom temperatures at Hout Bay (February 1992 - June 1992). DFFE. doi: 10.15493/DEA.MIMS.02382023.
Ismail H, van den Berg MA, Lamont T. 2023. Long-term observations of hourly bottom temperatures at Hout Bay (June 1992 - November 1992). DFFE. doi: 10.15493/DEA.MIMS.02392023.
Ismail H, van den Berg MA, Lamont T. 2023. Long-term observations of hourly bottom temperatures at Hout Bay (November 1992 - August 1993). DFFE. doi: 10.15493/DEA.MIMS.02402023.
Ismail H, van den Berg MA, Lamont T. 2023. Long-term observations of hourly bottom temperatures at Hout Bay (August 1993 - January 1994). DFFE. doi: 10.15493/DEA.MIMS.02412023.
Ismail H, van den Berg MA, Lamont T. 2023. Long-term observations of hourly bottom temperatures at Hout Bay (January 1994 - August 1994). DFFE. doi: 10.15493/DEA.MIMS.02422023.
Ismail H, van den Berg MA, Lamont T. 2023. Long-term observations of hourly bottom temperatures at Hout Bay (August 1994 - April 1995). DFFE. doi: 10.15493/DEA.MIMS.02432023.
Ismail H., van den Berg MA, Lamont T. 2023. Long-term observations of hourly bottom temperatures at Hout Bay (April 1995 - September 1995). DFFE. doi: 10.15493/DEA.MIMS.02442023.
Ismail H, van den Berg MA, Lamont T. 2023. Long-term observations of hourly bottom temperatures at Hout Bay (September 1995 - July 1996). DFFE. doi: 10.15493/DEA.MIMS.02452023.
Ismail H, van den Berg MA, Lamont T. 2023. Long-term observations of hourly bottom temperatures at Hout Bay (July 1996 - December 1996). DFFE. doi: 10.15493/DEA.MIMS.02462023.
Ismail H, van den Berg MA, Lamont T. 2023. Long-term observations of hourly bottom temperatures at Hout Bay (December 1996 - September 1997). DFFE. doi: 10.15493/DEA.MIMS.02472023.
Ismail H, van den Berg MA, Lamont T. 2023. Long-term observations of hourly bottom temperatures at Hout Bay (September 1997 - February 1998). DFFE. doi: 10.15493/DEA.MIMS.02482023.
Ismail H, van den Berg MA, Lamont T. 2023. Long-term observations of hourly bottom temperatures at Hout Bay (February 1998 - November 1998). DFFE. doi: 10.15493/DEA.MIMS.02492023.
Ismail H, van den Berg MA, Lamont T. 2023. Long-term observations of hourly bottom temperatures at Hout Bay (November 1998 - October 1999). DFFE. doi: 10.15493/DEA.MIMS.02502023.
Ismail H, van den Berg MA, Lamont T. 2023. Long-term observations of hourly bottom temperatures at Hout Bay (October 1999 - May 2000). DFFE. doi: 10.15493/DEA.MIMS.02512023.
Ismail H, van den Berg MA, Lamont T. 2023. Long-term observations of hourly bottom temperatures at Hout Bay (May 2000 - February 2001). DFFE. doi: 10.15493/DEA.MIMS.02522023.
Ismail H, van den Berg MA, Lamont T. 2023. Long-term observations of hourly bottom temperatures at Hout Bay (February 2001 - December 2001). DFFE. doi: 10.15493/DEA.MIMS.02532023.
Ismail H, van den Berg MA, Lamont T. 2023. Long-term observations of hourly bottom temperatures at Hout Bay (December 2001 - October 2003). DFFE. doi: 10.15493/DEA.MIMS.02542023.
Ismail H, van den Berg MA, Lamont T. 2023. Long-term observations of hourly bottom temperatures at Hout Bay (October 2003 - October 2004). DFFE. doi: 10.15493/DEA.MIMS.02552023.
Ismail H, van den Berg MA, Lamont T. 2023. Long-term observations of hourly bottom temperatures at Hout Bay (October 2004 - April 2008). DFFE. doi: 10.15493/DEA.MIMS.02562023.
Ismail H, van den Berg MA, Lamont T. 2023. Raw temperature data for long-term observations of bottom temperatures at Ystervarkpunt (October 1995 - May 1996). DFFE. doi: 10.15493/DEA.MIMS.04712023.
Ismail H, van den Berg MA, Lamont T. 2023. Raw temperature data for long-term observations of bottom temperatures at Ystervarkpunt (May 1996 - August 1996). DFFE. doi: 10.15493/DEA.MIMS.04722023.
Ismail H, van den Berg MA, Lamont T. 2023. Raw temperature data for long-term observations of bottom temperatures at Ystervarkpunt (August 1996 - November 1996). DFFE. doi: 10.15493/DEA.MIMS.04732023.
Ismail H, van den Berg MA, Lamont T. 2023. Raw temperature data for long-term observations of bottom temperatures at Ystervarkpunt (November 1996 - March 1997). DFFE. doi: 10.15493/DEA.MIMS.04742023.
Ismail H, van den Berg MA, Lamont T. 2023. Raw temperature data for long-term observations of bottom temperatures at Ystervarkpunt (March 1997 - January 1998). DFFE. doi: 10.15493/DEA.MIMS.04752023.
Ismail H, van den Berg MA, Lamont T. 2023. Raw temperature data for long-term observations of bottom temperatures at Ystervarkpunt (January 1998 - July 1998). DFFE. doi: 10.15493/DEA.MIMS.04762023.
Ismail H, van den Berg MA, Lamont T. 2023. Raw temperature data for long-term observations of bottom temperatures at Ystervarkpunt (July 1998 - November 1998). DFFE. doi: 10.15493/DEA.MIMS.04772023.
Ismail H, van den Berg MA, Lamont T. 2023. Raw temperature data for long-term observations of bottom temperatures at Ystervarkpunt (November 1998 - March 1999). DFFE. doi: 10.15493/DEA.MIMS.04782023.
Ismail H, van den Berg MA, Lamont T. 2023. Raw temperature data for long-term observations of bottom temperatures at Ystervarkpunt (March 1999 - July 1999). DFFE. doi: 10.15493/DEA.MIMS.04792023.
Ismail H, van den Berg MA, Lamont T. 2023. Raw temperature data for long-term observations of bottom temperatures at

Ystervarkpunt (July 1999 - November 1999). DFFE. doi: 10.15493/DEA.MIMS.04802023.

Ismail H, van den Berg MA, Lamont T. 2023. Raw temperature data for long-term observations of bottom temperatures at Ystervarkpunt (November 1999 - April 2000). DFFE. doi: 10.15493/DEA.MIMS.04812023.

Ismail H, van den Berg MA, Lamont T. 2023. Raw temperature data for long-term observations of bottom temperatures at Ystervarkpunt (April 2000 - December 2000). DFFE. doi: 10.15493/DEA.MIMS.04822023.

Ismail H, van den Berg MA, Lamont T. 2023. Raw temperature data for long-term observations of bottom temperatures at Ystervarkpunt (December 2000 - August 2001). DFFE. doi: 10.15493/DEA.MIMS.04832023.

Ismail H, van den Berg MA, Lamont T. 2023. Raw temperature data for long-term observations of bottom temperatures at Ystervarkpunt (August 2001 - November 2001). DFFE. doi: 10.15493/DEA.MIMS.04842023.

Ismail H, van den Berg MA, Lamont T. 2023. Raw temperature data for long-term observations of bottom temperatures at Ystervarkpunt (November 2001 - June 2002). DFFE. doi: 10.15493/DEA.MIMS.04852023.

Ismail H, van den Berg MA, Lamont T. 2023. Raw temperature data for long-term observations of bottom temperatures at Ystervarkpunt (June 2002 - November 2002). DFFE. doi: 10.15493/DEA.MIMS.04862023.

Ismail H, van den Berg MA, Lamont T. 2023. Raw temperature data for long-term observations of bottom temperatures at Ystervarkpunt (November 2002 - November 2003). DFFE. doi: 10.15493/DEA.MIMS.04872023.

Ismail H, van den Berg MA, Lamont T. 2023. Raw temperature data for long-term observations of bottom temperatures at Ystervarkpunt (November 2003 - August 2005). DFFE. doi: 10.15493/DEA.MIMS.04882023.

Ismail H, van den Berg MA, Lamont T. 2023. Raw temperature data for long-term observations of bottom temperatures at Ystervarkpunt (August 2005 - June 2006). DFFE. doi: 10.15493/DEA.MIMS.04892023.

Ismail H, van den Berg MA, Lamont T. 2023. Raw temperature data for long-term observations of bottom temperatures at Ystervarkpunt (June 2006 - June 2007). DFFE. doi: 10.15493/DEA.MIMS.04902023.

Ismail H, van den Berg MA, Lamont T. 2023. Raw temperature data for long-term observations of bottom temperatures at Ystervarkpunt (June 2007 - November 2010). DFFE. doi: 10.15493/DEA.MIMS.04912023.

Ismail H, van den Berg MA, Lamont T. 2023. Raw temperature data for long-term observations of bottom temperatures at Ystervarkpunt (November 2010 - October 2011). DFFE. doi: 10.15493/DEA.MIMS.04922023.

Ismail H, van den Berg MA, Lamont T. 2023. Raw temperature data for long-term observations of bottom temperatures at Ystervarkpunt (October 2011 - November 2019). DFFE. doi: 10.15493/DEA.MIMS.04932023.

Ismail H, van den Berg MA, Lamont T. 2023. Raw temperature data for long-term observations of bottom temperatures at Ystervarkpunt (November 2019 – August 2022). DFFE. doi: 10.15493/DEA.MIMS.11912023.

Ismail H, van den Berg MA, Lamont T. 2023. Long-term observations of hourly bottom temperatures at Ystervarkpunt (October 1995 - May 1996). DFFE. doi: 10.15493/DEA.MIMS.04482023.

Ismail H, van den Berg MA, Lamont T. 2023. Long-term observations of hourly bottom temperatures at Ystervarkpunt (May 1996 - August 1996). DFFE. doi: 10.15493/DEA.MIMS.04492023.

Ismail H, van den Berg MA, Lamont T. 2023. Long-term observations of hourly bottom temperatures at Ystervarkpunt (August 1996 - November 1996). DFFE. doi: 10.15493/DEA.MIMS.04502023.

Ismail H, van den Berg MA, Lamont T. 2023. Long-term observations of hourly bottom temperatures at Ystervarkpunt (November 1996 - March 1997). DFFE. doi: 10.15493/DEA.MIMS.04512023.

Ismail H, van den Berg MA, Lamont T. 2023. Long-term observations of hourly bottom temperatures at Ystervarkpunt (March 1997 - January 1998). DFFE. doi: 10.15493/DEA.MIMS.04522023.

Ismail H, van den Berg MA, Lamont T. 2023. Long-term observations of hourly bottom temperatures at Ystervarkpunt (January 1998 - July 1998). DFFE. doi: 10.15493/DEA.MIMS.04532023.

Ismail H, van den Berg MA, Lamont T. 2023. Long-term observations of hourly bottom temperatures at Ystervarkpunt (July 1998 - November 1998). DFFE. doi: 10.15493/DEA.MIMS.04542023.

Ismail H, van den Berg MA, Lamont T. 2023. Long-term observations of hourly bottom temperatures at Ystervarkpunt (November 1998 - March 1999). DFFE. doi: 10.15493/DEA.MIMS.04552023.

Ismail H, van den Berg MA, Lamont T. 2023. Long-term observations of hourly bottom temperatures at Ystervarkpunt (March 1999 - July 1999). DFFE. doi: 10.15493/DEA.MIMS.04562023.

Ismail H, van den Berg MA, Lamont T. 2023. Long-term observations of hourly bottom temperatures at Ystervarkpunt (July 1999 - November 1999). DFFE. doi: 10.15493/DEA.MIMS.04572023.

Ismail H, van den Berg MA, Lamont T. 2023. Long-term observations of hourly bottom temperatures at Ystervarkpunt (November 1999 - April 2000). DFFE. doi: 10.15493/DEA.MIMS.04582023.

Ismail H, van den Berg MA, Lamont T. 2023. Long-term observations of hourly bottom temperatures at Ystervarkpunt (April 2000 - December 2000). DFFE. doi: 10.15493/DEA.MIMS.04592023.

Ismail H, van den Berg MA, Lamont T. 2023. Long-term observations of hourly bottom temperatures at Ystervarkpunt (December 2000 - August 2001). DFFE. doi: 10.15493/DEA.MIMS.04602023.

Ismail H, van den Berg MA, Lamont T. 2023. Long-term observations of hourly bottom temperatures at Ystervarkpunt (August 2001 - November 2001). DFFE. doi: 10.15493/DEA.MIMS.04612023.

Ismail H, van den Berg MA, Lamont T. 2023. Long-term observations of hourly bottom temperatures at Ystervarkpunt (November 2001 - June 2002). DFFE. doi: 10.15493/DEA.MIMS.04622023.

Ismail H, van den Berg MA, Lamont T. 2023. Long-term observations of hourly bottom temperatures at Ystervarkpunt (June 2002 - November 2002). DFFE. doi: 10.15493/DEA.MIMS.04632023.

Ismail H, van den Berg MA, Lamont T. 2023. Long-term observations of hourly bottom temperatures at Ystervarkpunt (November 2002 - November 2003). DFFE. doi: 10.15493/DEA.MIMS.04642023.

Ismail H, van den Berg MA, Lamont T. 2023. Long-term observations of hourly bottom temperatures at Ystervarkpunt (November 2003 - August 2005). DFFE. doi: 10.15493/DEA.MIMS.04652023.

Ismail H, van den Berg MA, Lamont T. 2023. Long-term observations of hourly bottom temperatures at Ystervarkpunt

(August 2005 - June 2006). DFFE. doi: 10.15493/DEA.MIMS.04662023.

Ismail H, van den Berg MA, Lamont T. 2023. Long-term observations of hourly bottom temperatures at Ystervarkpunt (June 2006 - June 2007). DFFE. doi: 10.15493/DEA.MIMS.04672023.

Ismail H, van den Berg MA, Lamont T. 2023. Long-term observations of hourly bottom temperatures at Ystervarkpunt (June 2007 - November 2010). DFFE. doi: 10.15493/DEA.MIMS.04682023.

Ismail H, van den Berg MA, Lamont T. 2023. Long-term observations of hourly bottom temperatures at Ystervarkpunt (November 2010 - October 2011). DFFE. doi: 10.15493/DEA.MIMS.04692023.

Ismail H, van den Berg MA, Lamont T. 2023. Long-term observations of hourly bottom temperatures at Ystervarkpunt (October 2011 - November 2019). DFFE. doi: 10.15493/DEA.MIMS.04702023.

Ismail H, van den Berg MA, Lamont T. 2023. Long-term observations of hourly bottom temperatures at Ystervarkpunt (November 2019 - August 2022). DFFE. doi: 10.15493/DEA.MIMS.11902023.

Ismail H, van den Berg MA, Lamont T. 2023. Raw temperature data for long-term observations of bottom temperatures at Mossel Bay (June 1991 - October 1991). DFFE. doi: 10.15493/DEA.MIMS.03132023.

Ismail H, van den Berg MA, Lamont T. 2023. Raw temperature data for long-term observations of bottom temperatures at Mossel Bay (October 1991 - January 1992). DFFE. doi: 10.15493/DEA.MIMS.03142023.

Ismail H, van den Berg MA, Lamont T. 2023. Raw temperature data for long-term observations of bottom temperatures at Mossel Bay (January 1992 - May 1992). DFFE. doi: 10.15493/DEA.MIMS.03152023.

Ismail H, van den Berg MA, Lamont T. 2023. Raw temperature data for long-term observations of bottom temperatures at Mossel Bay (August 1992 - November 1992). DFFE. doi: 10.15493/DEA.MIMS.03162023.

Ismail H, van den Berg MA, Lamont T. 2023. Raw temperature data for long-term observations of bottom temperatures at Mossel Bay (November 1992 - January 1993). DFFE. doi: 10.15493/DEA.MIMS.03172023.

Ismail H, van den Berg MA, Lamont T. 2023. Raw temperature data for long-term observations of bottom temperatures at Mossel Bay (January 1993 - May 1993). DFFE. doi: 10.15493/DEA.MIMS.03182023.

Ismail H, van den Berg MA, Lamont T. 2023. Raw temperature data for long-term observations of bottom temperatures at Mossel Bay (May 1993 - November 1993). DFFE. doi: 10.15493/DEA.MIMS.03192023.

Ismail H, van den Berg MA, Lamont T. 2023. Raw temperature data for long-term observations of bottom temperatures at Mossel Bay (November 1993 - February 1994). DFFE. doi:10.15493/DEA.MIMS.03202023.

Ismail H, van den Berg MA, Lamont T. 2023. Raw temperature data for long-term observations of bottom temperatures at Mossel Bay (February 1994 - August 1994). DFFE. doi: 10.15493/DEA.MIMS.03212023.

Ismail H, van den Berg MA, Lamont T. 2023. Raw temperature data for long-term observations of bottom temperatures at Mossel Bay (August 1994 - October 1994). DFFE. doi: 10.15493/DEA.MIMS.03222023.

Ismail H, van den Berg MA, Lamont T. 2023. Raw temperature data for long-term observations of bottom temperatures at Mossel Bay (October 1994 - March 1995). DFFE. doi: 10.15493/DEA.MIMS.03232023.

Ismail H, van den Berg MA, Lamont T. 2023. Raw temperature data for long-term observations of bottom temperatures at Mossel Bay (March 1995 - July 1995). DFFE. doi: 10.15493/DEA.MIMS.03242023.

Ismail H, van den Berg MA, Lamont T. 2023. Raw temperature data for long-term observations of bottom temperatures at Mossel Bay (July 1995 - October 1995). DFFE. doi: 10.15493/DEA.MIMS.03252023.

Ismail H, van den Berg MA, Lamont T. 2023. Raw temperature data for long-term observations of bottom temperatures at Mossel Bay (October 1995 - May 1996). DFFE. doi: 10.15493/DEA.MIMS.03262023.

Ismail H, van den Berg MA, Lamont T. 2023. Raw temperature data for long-term observations of bottom temperatures at Mossel Bay (May 1996 - August 1996). DFFE. doi: 10.15493/DEA.MIMS.03272023.

Ismail H, van den Berg MA, Lamont T. 2023. Raw temperature data for long-term observations of bottom temperatures at Mossel Bay (August 1996 - November 1996). DFFE. doi: 10.15493/DEA.MIMS.03282023.

Ismail H, van den Berg MA, Lamont T. 2023. Raw temperature data for long-term observations of bottom temperatures at Mossel Bay (November 1996 - March 1997). DFFE. doi: 10.15493/DEA.MIMS.03292023.

Ismail H, van den Berg MA, Lamont T. 2023. Raw temperature data for long-term observations of bottom temperatures at Mossel Bay (March 1997 - January 1998). DFFE. doi: 10.15493/DEA.MIMS.03302023.

Ismail H, van den Berg MA, Lamont T. 2023. Raw temperature data for long-term observations of bottom temperatures at Mossel Bay (January 1998 - July 1998). DFFE. doi: 10.15493/DEA.MIMS.03312023.

Ismail H, van den Berg MA, Lamont T. 2023. Raw temperature data for long-term observations of bottom temperatures at Mossel Bay (July 1998 - November 1998). DFFE. doi: 10.15493/DEA.MIMS.03322023.

Ismail H, van den Berg MA, Lamont T. 2023. Raw temperature data for long-term observations of bottom temperatures at Mossel Bay (November 1998 - March 1999). DFFE. doi: 10.15493/DEA.MIMS.03332023.

Ismail H, van den Berg MA, Lamont T. 2023. Raw temperature data for long-term observations of bottom temperatures at Mossel Bay (March 1999 - December 1999). DFFE. doi: 10.15493/DEA.MIMS.03342023.

Ismail H, van den Berg MA, Lamont T. 2023. Raw temperature data for long-term observations of bottom temperatures at Mossel Bay (December 1999 - April 2000). DFFE. doi: 10.15493/DEA.MIMS.03352023.

Ismail H, van den Berg MA, Lamont T. 2023. Raw temperature data for long-term observations of bottom temperatures at Mossel Bay (April 2000 - November 2000). DFFE. doi: 10.15493/DEA.MIMS.03362023.

Ismail H, van den Berg MA, Lamont T. 2023. Raw temperature data for long-term observations of bottom temperatures at Mossel Bay (November 2000 - August 2001). DFFE. doi: 10.15493/DEA.MIMS.03372023.

Ismail H, van den Berg MA, Lamont T. 2023. Raw temperature data for long-term observations of bottom temperatures at Mossel Bay (August 2001 - November 2001). DFFE. doi: 10.15493/DEA.MIMS.03382023.

Ismail H, van den Berg MA, Lamont T. 2023. Raw temperature data for long-term observations of bottom temperatures at Mossel Bay (November 2001 - June 2002). DFFE. doi: 10.15493/DEA.MIMS.03392023.

Ismail H, van den Berg MA, Lamont T. 2023. Raw temperature data for long-term observations of bottom temperatures

at Mossel Bay (June 2002 - November 2002). DFFE. doi: 10.15493/DEA.MIMS.03402023.

Ismail H, van den Berg MA, Lamont T. 2023. Raw temperature data for long-term observations of bottom temperatures at Mossel Bay (November 2002 - November 2003). DFFE. doi: 10.15493/DEA.MIMS.03412023.

Ismail H, van den Berg MA, Lamont T. 2023. Raw temperature data for long-term observations of bottom temperatures at Mossel Bay (November 2003 - June 2005). DFFE. doi: 10.15493/DEA.MIMS.03422023.

Ismail H, van den Berg MA, Lamont T. 2023. Raw temperature data for long-term observations of bottom temperatures at Mossel Bay (June 2005 - June 2006). DFFE. doi: 10.15493/DEA.MIMS.03432023.

Ismail H, van den Berg MA, Lamont T. 2023. Raw temperature data for long-term observations of bottom temperatures at Mossel Bay (June 2006 - June 2007). DFFE. doi: 10.15493/DEA.MIMS.03442023.

Ismail H, van den Berg MA, Lamont T. 2023. Raw temperature data for long-term observations of bottom temperatures at Mossel Bay (June 2007 - November 2010). DFFE. doi: 10.15493/DEA.MIMS.03452023.

Ismail H, van den Berg MA, Lamont T. 2023. Raw temperature data for long-term observations of bottom temperatures at Mossel Bay (November 2010 - October 2011). DFFE. doi: 10.15493/DEA.MIMS.03462023.

Ismail H, van den Berg MA, Lamont T. 2023. Raw temperature data for long-term observations of bottom temperatures at Mossel Bay (October 2011 - September 2019). DFFE. doi: 10.15493/DEA.MIMS.03472023.

Ismail H, van den Berg MA, Lamont T. 2023. Raw temperature data for long-term observations of bottom temperatures at Mossel Bay (September 2019 - August 2022). DFFE. doi: 10.15493/DEA.MIMS.03482023.

Ismail H, van den Berg MA, Lamont T. 2023. Long-term observations of hourly bottom temperatures at Mossel Bay (June 1991 - October 1991). DFFE. doi: 10.15493/DEA.MIMS.02772023.

Ismail H, van den Berg MA, Lamont T. 2023. Long-term observations of hourly bottom temperatures at Mossel Bay (October 1991 - January 1992). DFFE. doi: 10.15493/DEA.MIMS.02782023.

Ismail H, van den Berg MA, Lamont T. 2023. Long-term observations of hourly bottom temperatures at Mossel Bay (January 1992 - May 1992). DFFE. doi: 10.15493/DEA.MIMS.02792023.

Ismail H, van den Berg MA, Lamont T. 2023. Long-term observations of hourly bottom temperatures at Mossel Bay (August 1992 - November 1992). DFFE. doi: 10.15493/DEA.MIMS.02802023.

Ismail H, van den Berg MA, Lamont T. 2023. Long-term observations of hourly bottom temperatures at Mossel Bay (November 1992 - January 1993). DFFE. doi: 10.15493/DEA.MIMS.02812023.

Ismail H, van den Berg MA, Lamont T. 2023. Long-term observations of hourly bottom temperatures at Mossel Bay (January 1993 - May 1993). DFFE. doi: 10.15493/DEA.MIMS.02822023.

Ismail H, van den Berg MA, Lamont T. 2023. Long-term observations of hourly bottom temperatures at Mossel Bay (May 1993 - November 1993). DFFE. doi: 10.15493/DEA.MIMS.02832023.

Ismail H, van den Berg MA, Lamont T. 2023. Long-term observations of hourly bottom temperatures at Mossel Bay (November 1993 - February 1994). DFFE. doi: 10.15493/DEA.MIMS.02842023.

Ismail H, van den Berg MA, Lamont T. 2023. Long-term observations of hourly bottom temperatures at Mossel Bay (February 1994 - August 1994). DFFE. doi: 10.15493/DEA.MIMS.02852023.

Ismail H, van den Berg MA, Lamont T. 2023. Long-term observations of hourly bottom temperatures at Mossel Bay (August 1994 - October 1994). DFFE. doi: 10.15493/DEA.MIMS.02862023.

Ismail H, van den Berg MA, Lamont T. 2023. Long-term observations of hourly bottom temperatures at Mossel Bay (October 1994 - March 1995). DFFE. doi: 10.15493/DEA.MIMS.02872023.

Ismail H, van den Berg MA, Lamont T. 2023. Long-term observations of hourly bottom temperatures at Mossel Bay (March 1995 - July 1995). DFFE. doi: 10.15493/DEA.MIMS.02882023.

Ismail H, van den Berg MA, Lamont T. 2023. Long-term observations of hourly bottom temperatures at Mossel Bay (July 1995 - October 1995). DFFE. doi: 10.15493/DEA.MIMS.02892023.

Ismail H, van den Berg MA, Lamont T. 2023. Long-term observations of hourly bottom temperatures at Mossel Bay (October 1995 - May 1996). DFFE. doi: 10.15493/DEA.MIMS.02902023.

Ismail H, van den Berg MA, Lamont T. 2023. Long-term observations of hourly bottom temperatures at Mossel Bay (May 1996 - August 1996). DFFE. doi: 10.15493/DEA.MIMS.02912023.

Ismail H, van den Berg MA, Lamont T. 2023. Long-term observations of hourly bottom temperatures at Mossel Bay (August 1996 - November 1996). DFFE. doi: 10.15493/DEA.MIMS.02922023.

Ismail H, van den Berg MA, Lamont T. 2023. Long-term observations of hourly bottom temperatures at Mossel Bay (November 1996 - March 1997). DFFE. doi: 10.15493/DEA.MIMS.02932023.

Ismail H, van den Berg MA, Lamont T. 2023. Long-term observations of hourly bottom temperatures at Mossel Bay (March 1997 - January 1998). DFFE. doi: 10.15493/DEA.MIMS.02942023.

Ismail H, van den Berg MA, Lamont T. 2023. Long-term observations of hourly bottom temperatures at Mossel Bay (January 1998 - July 1998). DFFE. doi: 10.15493/DEA.MIMS.02952023.

Ismail H, van den Berg MA, Lamont T. 2023. Long-term observations of hourly bottom temperatures at Mossel Bay (July 1998 - November 1998). DFFE. doi: 10.15493/DEA.MIMS.02962023.

Ismail H, van den Berg MA, Lamont T. 2023. Long-term observations of hourly bottom temperatures at Mossel Bay (November 1998 - March 1999). DFFE. doi: 10.15493/DEA.MIMS.02972023.

Ismail H, van den Berg MA, Lamont T. 2023. Long-term observations of hourly bottom temperatures at Mossel Bay (March 1999 - December 1999). DFFE. doi: 10.15493/DEA.MIMS.02982023.

Ismail H, van den Berg MA, Lamont T. 2023. Long-term observations of hourly bottom temperatures at Mossel Bay (December 1999 - April 2000). DFFE. doi: 10.15493/DEA.MIMS.02992023.

Ismail H, van den Berg MA, Lamont T. 2023. Long-term observations of hourly bottom temperatures at Mossel Bay (April 2000 - November 2000). DFFE. doi: 10.15493/DEA.MIMS.03002023.

Ismail H, van den Berg MA, Lamont T. 2023. Long-term observations of hourly bottom temperatures at Mossel Bay (No-

vember 2000 - August 2001). DFFE. doi: 10.15493/DEA.MIMS.03012023.
Ismail H, van den Berg MA, Lamont T. 2023. Long-term observations of hourly bottom temperatures at Mossel Bay (August 2001 - November 2001). DFFE. doi: 10.15493/DEA.MIMS.03022023.
Ismail H, van den Berg MA, Lamont T. 2023. Long-term observations of hourly bottom temperatures at Mossel Bay (November 2001 - June 2002). DFFE. doi: 10.15493/DEA.MIMS.03032023.
Ismail H, van den Berg MA, Lamont T. 2023. Long-term observations of hourly bottom temperatures at Mossel Bay (June 2002 - November 2002). DFFE. doi: 10.15493/DEA.MIMS.03042023.
Ismail H, van den Berg MA, Lamont T. 2023. Long-term observations of hourly bottom temperatures at Mossel Bay (November 2002 - November 2003). DFFE. doi: 10.15493/DEA.MIMS.03052023.
Ismail H, van den Berg MA, Lamont T. 2023. Long-term observations of hourly bottom temperatures at Mossel Bay (November 2003 - June 2005). DFFE. doi: 10.15493/DEA.MIMS.03062023.
Ismail H, van den Berg MA, Lamont T. 2023. Long-term observations of hourly bottom temperatures at Mossel Bay (June 2005 - June 2006). DFFE. doi: 10.15493/DEA.MIMS.03072023.
Ismail H, van den Berg MA, Lamont T. 2023. Long-term observations of hourly bottom temperatures at Mossel Bay (June 2006 - June 2007). DFFE. doi: 10.15493/DEA.MIMS.03082023.
Ismail H, van den Berg MA, Lamont T. 2023. Long-term observations of hourly bottom temperatures at Mossel Bay (June 2007 - November 2010). DFFE. doi: 10.15493/DEA.MIMS.03092023.
Ismail H, van den Berg MA, Lamont T. 2023. Long-term observations of hourly bottom temperatures at Mossel Bay (November 2010 - October 2011). DFFE. doi: 10.15493/DEA.MIMS.03102023.
Ismail H, van den Berg MA, Lamont T. 2023. Long-term observations of hourly bottom temperatures at Mossel Bay (October 2011 - September 2019). DFFE. doi: 10.15493/DEA.MIMS.03112023.
Ismail H, van den Berg MA, Lamont T. 2023. Long-term observations of hourly bottom temperatures at Mossel Bay (September 2019 - August 2022). DFFE. doi: 10.15493/DEA.MIMS.03122023.
Ismail H, van den Berg MA, Lamont T. 2023. Raw temperature data for long-term observations of bottom temperatures at Tsitsikamma (June 1991 - October 1991). DFFE. doi: 10.15493/DEA.MIMS.05592023.
Ismail H, van den Berg MA, Lamont T. 2023. Raw temperature data for long-term observations of bottom temperatures at Tsitsikamma (October 1991 - January 1992). DFFE. doi: 10.15493/DEA.MIMS.05602023.
Ismail H, van den Berg MA, Lamont T. 2023. Raw temperature data for long-term observations of bottom temperatures at Tsitsikamma (January 1992 - May 1992). DFFE. doi: 10.15493/DEA.MIMS.05612023.
Ismail H, van den Berg MA, Lamont T. 2023. Raw temperature data for long-term observations of bottom temperatures at Tsitsikamma (May 1992 - August 1992). DFFE. doi: 10.15493/DEA.MIMS.05622023.
Ismail H, van den Berg MA, Lamont T. 2023. Raw temperature data for long-term observations of bottom temperatures at Tsitsikamma (August 1992 - November 1992). DFFE. doi: 10.15493/DEA.MIMS.05632023.
Ismail H, van den Berg MA, Lamont T. 2023. Raw temperature data for long-term observations of bottom temperatures at Tsitsikamma (November 1992 - January 1993). DFFE. doi: 10.15493/DEA.MIMS.05642023.
Ismail H, van den Berg MA, Lamont T. 2023. Raw temperature data for long-term observations of bottom temperatures at Tsitsikamma (January 1993 - June 1993). DFFE. doi: 10.15493/DEA.MIMS.05652023.
Ismail H, van den Berg MA, Lamont T. 2023. Raw temperature data for long-term observations of bottom temperatures at Tsitsikamma (June 1993 - November 1993). DFFE. doi: 10.15493/DEA.MIMS.05662023.
Ismail H, van den Berg MA, Lamont T. 2023. Raw temperature data for long-term observations of bottom temperatures at Tsitsikamma (November 1993 - March 1994). DFFE. doi: 10.15493/DEA.MIMS.05672023.
Ismail H, van den Berg MA, Lamont T. 2023. Raw temperature data for long-term observations of bottom temperatures at Tsitsikamma (March 1994 - August 1994). DFFE. doi: 10.15493/DEA.MIMS.05682023
Ismail H, van den Berg MA, Lamont T. 2023. Raw temperature data for long-term observations of bottom temperatures at Tsitsikamma (August 1994 - October 1994). DFFE. doi: 10.15493/DEA.MIMS.05692023.
Ismail H, van den Berg MA, Lamont T. 2023. Raw temperature data for long-term observations of bottom temperatures at Tsitsikamma (October 1994 - May 1995). DFFE. doi: 10.15493/DEA.MIMS.05702023.
Ismail H, van den Berg MA, Lamont T. 2023. Raw temperature data for long-term observations of bottom temperatures at Tsitsikamma (May 1995 - August 1995). DFFE. doi: 10.15493/DEA.MIMS.05712023.
Ismail H, van den Berg MA, Lamont T. 2023. Raw temperature data for long-term observations of bottom temperatures at Tsitsikamma (August 1995 - November 1995). DFFE. doi: 10.15493/DEA.MIMS.05722023.
Ismail H, van den Berg MA, Lamont T. 2023. Raw temperature data for long-term observations of bottom temperatures at Tsitsikamma (November 1995 - May 1996). DFFE. doi: 10.15493/DEA.MIMS.05742023.
Ismail H, van den Berg MA, Lamont T. 2023. Raw temperature data for long-term observations of bottom temperatures at Tsitsikamma (May 1996 - August 1996). DFFE. doi: 10.15493/DEA.MIMS.05752023.
Ismail H, van den Berg MA, Lamont T. 2023. Raw temperature data for long-term observations of bottom temperatures at Tsitsikamma (August 1996 - January 1997). DFFE. doi: 10.15493/DEA.MIMS.05762023
Ismail H, van den Berg MA, Lamont T. 2023. Raw temperature data for long-term observations of bottom temperatures at Tsitsikamma (January 1997 - April 1997). DFFE. doi: 10.15493/DEA.MIMS.05772023.
Ismail H, van den Berg MA, Lamont T. 2023. Raw temperature data for long-term observations of bottom temperatures at Tsitsikamma (April 1997 - June 1997). DFFE. doi: 10.15493/DEA.MIMS.05782023.
Ismail H, van den Berg MA, Lamont T. 2023. Raw temperature data for long-term observations of bottom temperatures at Tsitsikamma (June 1997 - January 1998). DFFE. doi: 10.15493/DEA.MIMS.05792023.
Ismail H, van den Berg MA, Lamont T. 2023. Raw temperature data for long-term observations of bottom temperatures at Tsitsikamma (January 1998 - July 1998). DFFE. doi: 10.15493/DEA.MIMS.05802023.
Ismail H, van den Berg MA, Lamont T. 2023. Raw temperature data for long-term observations of bottom temperatures at

Tsitsikamma (July 1998 - November 1998). DFFE. doi: 10.15493/DEA.MIMS.05822023.

Ismail H, van den Berg MA, Lamont T. 2023. Raw temperature data for long-term observations of bottom temperatures at Tsitsikamma (November 1998 - March 1999). DFFE. doi: 10.15493/DEA.MIMS.05832023.

Ismail H, van den Berg MA, Lamont T. 2023. Raw temperature data for long-term observations of bottom temperatures at Tsitsikamma (March 1999 - July 1999). DFFE. doi: 10.15493/DEA.MIMS.05842023.

Ismail H, van den Berg MA, Lamont T. 2023. Raw temperature data for long-term observations of bottom temperatures at Tsitsikamma (April 2000 - August 2000). DFFE. doi: 10.15493/DEA.MIMS.05852023.

Ismail H, van den Berg MA, Lamont T. 2023. Raw temperature data for long-term observations of bottom temperatures at Tsitsikamma (August 2000 - November 2000). DFFE. doi: 10.15493/DEA.MIMS.05862023.

Ismail H, van den Berg MA, Lamont T. 2023. Raw temperature data for long-term observations of bottom temperatures at Tsitsikamma (November 2000 - March 2001). DFFE. doi: 10.15493/DEA.MIMS.05872023.

Ismail H, van den Berg MA, Lamont T. 2023. Raw temperature data for long-term observations of bottom temperatures at Tsitsikamma (March 2001 - July 2001). DFFE. doi: 10.15493/DEA.MIMS.05882023.

Ismail H, van den Berg MA, Lamont T. 2023. Raw temperature data for long-term observations of bottom temperatures at Tsitsikamma (July 2001 - November 2001). DFFE. doi: 10.15493/DEA.MIMS.05892023.

Ismail H, van den Berg MA, Lamont T. 2023. Raw temperature data for long-term observations of bottom temperatures at Tsitsikamma (November 2001 - November 2002). DFFE. doi: 10.15493/DEA.MIMS.05902023.

Ismail H, van den Berg MA, Lamont T. 2023. Raw temperature data for long-term observations of bottom temperatures at Tsitsikamma (November 2002 - June 2003). DFFE. doi: 10.15493/DEA.MIMS.05912023.

Ismail H, van den Berg MA, Lamont T. 2023. Raw temperature data for long-term observations of bottom temperatures at Tsitsikamma (June 2003 - March 2004). DFFE. doi: 10.15493/DEA.MIMS.05922023.

Ismail H, van den Berg MA, Lamont T. 2023. Raw temperature data for long-term observations of bottom temperatures at Tsitsikamma (March 2004 - June 2004). DFFE. doi: 10.15493/DEA.MIMS.05932023.

Ismail H, van den Berg MA, Lamont T. 2023. Raw temperature data for long-term observations of bottom temperatures at Tsitsikamma (June 2004 - February 2005). DFFE. doi: 10.15493/DEA.MIMS.05942023.

Ismail H, van den Berg MA, Lamont T. 2023. Raw temperature data for long-term observations of bottom temperatures at Tsitsikamma (February 2005 - November 2005). DFFE. doi: 10.15493/DEA.MIMS.05952023.

Ismail H, van den Berg MA, Lamont T. 2023. Raw temperature data for long-term observations of bottom temperatures at Tsitsikamma (November 2005 - June 2006). DFFE. doi: 10.15493/DEA.MIMS.05962023.

Ismail H, van den Berg MA, Lamont T. 2023. Raw temperature data for long-term observations of bottom temperatures at Tsitsikamma (June 2006 - November 2006). DFFE. doi: 10.15493/DEA.MIMS.05982023.

Ismail H, van den Berg MA, Lamont T. 2023. Raw temperature data for long-term observations of bottom temperatures at Tsitsikamma (November 2006 - June 2007). DFFE. doi: 10.15493/DEA.MIMS.05992023.

Ismail H, van den Berg MA, Lamont T. 2023. Raw temperature data for long-term observations of bottom temperatures at Tsitsikamma (June 2007 - March 2008). DFFE. doi: 10.15493/DEA.MIMS.06002023.

Ismail H, van den Berg MA, Lamont T. 2023. Raw temperature data for long-term observations of bottom temperatures at Tsitsikamma (March 2008 - July 2008). DFFE. doi: 10.15493/DEA.MIMS.06022023.

Ismail H, van den Berg MA, Lamont T. 2023. Raw temperature data for long-term observations of bottom temperatures at Tsitsikamma (July 2008 - June 2009). DFFE. doi: 10.15493/DEA.MIMS.06042023.

Ismail H, van den Berg MA, Lamont T. 2023. Raw temperature data for long-term observations of bottom temperatures at Tsitsikamma (June 2009 - November 2009). DFFE. doi: 10.15493/DEA.MIMS.06052023.

Ismail H, van den Berg MA, Lamont T. 2023. Raw temperature data for long-term observations of bottom temperatures at Tsitsikamma (November 2009 - November 2010). DFFE. doi: 10.15493/DEA.MIMS.06072023.

Ismail H, van den Berg MA, Lamont T. 2023. Raw temperature data for long-term observations of bottom temperatures at Tsitsikamma (November 2010 - November 2011). DFFE. doi: 10.15493/DEA.MIMS.06092023.

Ismail H, van den Berg MA, Lamont T. 2023. Raw temperature data for long-term observations of bottom temperatures at Tsitsikamma (November 2011 - March 2013). DFFE. doi: 10.15493/DEA.MIMS.06102023.

Ismail H, van den Berg MA, Lamont T. 2023. Raw temperature data for long-term observations of bottom temperatures at Tsitsikamma (March 2013 - November 2013). DFFE. doi: 10.15493/DEA.MIMS.06122023.

Ismail H, van den Berg MA, Lamont T. 2023. Raw temperature data for long-term observations of bottom temperatures at Tsitsikamma (November 2013 - November 2015). DFFE. doi: 10.15493/DEA.MIMS.06132023.

Ismail H, van den Berg MA, Lamont T. 2023. Raw temperature data for long-term observations of bottom temperatures at Tsitsikamma (November 2015 - September 2019). DFFE. doi: 10.15493/DEA.MIMS.06152023.

Ismail H, van den Berg MA, Lamont T. 2023. Raw temperature data for long-term observations of bottom temperatures at Tsitsikamma (September 2019 - June 2022). DFFE. doi: 10.15493/DEA.MIMS.06172023.

Ismail H, van den Berg MA, Lamont T. 2023. Long-term observations of hourly bottom temperatures at Tsitsikamma (June 1991 - October 1991). DFFE. doi: 10.15493/DEA.MIMS.06192023.

Ismail H, van den Berg MA, Lamont T. 2023. Long-term observations of hourly bottom temperatures at Tsitsikamma (October 1991 - January 1992). DFFE. doi: 10.15493/DEA.MIMS.06202023.

Ismail H, van den Berg MA, Lamont T. 2023. Long-term observations of hourly bottom temperatures at Tsitsikamma (January 1992 - May 1992). DFFE. doi: 10.15493/DEA.MIMS.06212023.

Ismail H, van den Berg MA, Lamont T. 2023. Long-term observations of hourly bottom temperatures at Tsitsikamma (May 1992 - August 1992). DFFE. doi: 10.15493/DEA.MIMS.06222023.

Ismail H, van den Berg MA, Lamont T. 2023. Long-term observations of hourly bottom temperatures at Tsitsikamma (August 1992 - November 1992). DFFE. doi: 10.15493/DEA.MIMS.06232023.

Ismail H, van den Berg MA, Lamont T. 2023. Long-term observations of hourly bottom temperatures at Tsitsikamma (No-

vember 1992 - January 1993). DFFE. doi: 10.15493/DEA.MIMS.06242023.

Ismail H, van den Berg MA, Lamont T. 2023. Long-term observations of hourly bottom temperatures at Tsitsikamma (January 1993 - June 1993). DFFE. doi: 10.15493/DEA.MIMS.06252023.

Ismail H, van den Berg MA, Lamont T. 2023. Long-term observations of hourly bottom temperatures at Tsitsikamma (June 1993 - November 1993). DFFE. doi: 10.15493/DEA.MIMS.06262023.

Ismail H, van den Berg MA, Lamont T. 2023. Long-term observations of hourly bottom temperatures at Tsitsikamma (November 1993 - March 1994). DFFE. doi: 10.15493/DEA.MIMS.06272023

Ismail H, van den Berg MA, Lamont T. 2023. Long-term observations of hourly bottom temperatures at Tsitsikamma (March 1994 - August 1994). DFFE. doi: 10.15493/DEA.MIMS.06282023.

Ismail H, van den Berg MA, Lamont T. 2023. Long-term observations of hourly bottom temperatures at Tsitsikamma (August 1994 - October 1994). DFFE. doi: 10.15493/DEA.MIMS.06292023.

Ismail H, van den Berg MA, Lamont T. 2023. Long-term observations of hourly bottom temperatures at Tsitsikamma (October 1994 - May 1995). DFFE. doi: 10.15493/DEA.MIMS.06302023.

Ismail H, van den Berg MA, Lamont T. 2023. Long-term observations of hourly bottom temperatures at Tsitsikamma (May 1995 - August 1995). DFFE. doi: 10.15493/DEA.MIMS.06312023.

Ismail H, van den Berg MA, Lamont T. 2023. Long-term observations of hourly bottom temperatures at Tsitsikamma (August 1995 - November 1995). DFFE. doi: 10.15493/DEA.MIMS.06322023.

Ismail H, van den Berg MA, Lamont T. 2023. Long-term observations of hourly bottom temperatures at Tsitsikamma (November 1995 - May 1996). DFFE. doi: 10.15493/DEA.MIMS.06332023.

Ismail H, van den Berg MA, Lamont T. 2023. Long-term observations of hourly bottom temperatures at Tsitsikamma (May 1996 - August 1996). DFFE. doi: 10.15493/DEA.MIMS.06342023.

Ismail H, van den Berg MA, Lamont T. 2023. Long-term observations of hourly bottom temperatures at Tsitsikamma (August 1996 - January 1997). DFFE. doi: 10.15493/DEA.MIMS.06352023.

Ismail H, van den Berg MA, Lamont T. 2023. Long-term observations of hourly bottom temperatures at Tsitsikamma (January 1997 - April 1997). DFFE. doi: 10.15493/DEA.MIMS.06362023.

Ismail H, van den Berg MA, Lamont T. 2023. Long-term observations of hourly bottom temperatures at Tsitsikamma (April 1997 - June 1997). DFFE. doi: 10.15493/DEA.MIMS.06372023.

Ismail H, van den Berg MA, Lamont T. 2023. Long-term observations of hourly bottom temperatures at Tsitsikamma (June 1997 - January 1998). DFFE. doi: 10.15493/DEA.MIMS.06382023.

Ismail H, van den Berg MA, Lamont T. 2023. Long-term observations of hourly bottom temperatures at Tsitsikamma (January 1998 - July 1998). DFFE. doi: 10.15493/DEA.MIMS.06392023.

Ismail H, van den Berg MA, Lamont T. 2023. Long-term observations of hourly bottom temperatures at Tsitsikamma (July 1998 - November 1998). DFFE. doi: 10.15493/DEA.MIMS.06402023.

Ismail H, van den Berg MA, Lamont T. 2023. Long-term observations of hourly bottom temperatures at Tsitsikamma (November 1998 - March 1999). DFFE. doi: 10.15493/DEA.MIMS.06412023

Ismail H, van den Berg MA, Lamont T. 2023. Long-term observations of hourly bottom temperatures at Tsitsikamma (March 1999 - July 1999). DFFE. doi: 10.15493/DEA.MIMS.06432023.

Ismail H, van den Berg MA, Lamont T. 2023. Long-term observations of hourly bottom temperatures at Tsitsikamma (April 2000 - August 2000). DFFE. doi: 10.15493/DEA.MIMS.06422023.

Ismail H, van den Berg MA, Lamont T. 2023. Long-term observations of hourly bottom temperatures at Tsitsikamma (August 2000 - November 2000). DFFE. doi: 10.15493/DEA.MIMS.06442023.

Ismail H, van den Berg MA, Lamont T. 2023. Long-term observations of hourly bottom temperatures at Tsitsikamma (November 2000 - March 2001). DFFE. doi: 10.15493/DEA.MIMS.06452023.

Ismail H, van den Berg MA, Lamont T. 2023. Long-term observations of hourly bottom temperatures at Tsitsikamma (March 2001 - July 2001). DFFE. doi: 10.15493/DEA.MIMS.06462023.

Ismail H, van den Berg MA, Lamont T. 2023. Long-term observations of hourly bottom temperatures at Tsitsikamma (July 2001 - November 2001). DFFE. doi: 10.15493/DEA.MIMS.06472023.

Ismail H, van den Berg MA, Lamont T. 2023. Long-term observations of hourly bottom temperatures at Tsitsikamma (November 2001 - November 2002). DFFE. doi: 10.15493/DEA.MIMS.06482023.

Ismail H, van den Berg MA, Lamont T. 2023. Long-term observations of hourly bottom temperatures at Tsitsikamma (November 2002 - June 2003). DFFE. doi: 10.15493/DEA.MIMS.06492023.

Ismail H, van den Berg MA, Lamont T. 2023. Long-term observations of hourly bottom temperatures at Tsitsikamma (June 2003 - March 2004). DFFE. doi: 10.15493/DEA.MIMS.06502023.

Ismail H, van den Berg MA, Lamont T. 2023. Long-term observations of hourly bottom temperatures at Tsitsikamma (March 2004 - June 2004). DFFE. doi: 10.15493/DEA.MIMS.06512023.

Ismail H, van den Berg MA, Lamont T. 2023. Long-term observations of hourly bottom temperatures at Tsitsikamma (June 2004 - February 2005). DFFE. doi: 10.15493/DEA.MIMS.06522023.

Ismail H, van den Berg MA, Lamont T. 2023. Long-term observations of hourly bottom temperatures at Tsitsikamma (February 2005 - November 2005). DFFE. doi: 10.15493/DEA.MIMS.06532023.

Ismail H, van den Berg MA, Lamont T. 2023. Long-term observations of hourly bottom temperatures at Tsitsikamma (November 2005 - June 2006). DFFE. doi: 10.15493/DEA.MIMS.06542023.

Ismail H, van den Berg MA, Lamont T. 2023. Long-term observations of hourly bottom temperatures at Tsitsikamma (June 2006 - November 2006). DFFE. doi: 10.15493/DEA.MIMS.06552023

Ismail H, van den Berg MA, Lamont T. 2023. Long-term observations of hourly bottom temperatures at Tsitsikamma (November 2006 - June 2007). DFFE. doi: 10.15493/DEA.MIMS.06562023.

Ismail H, van den Berg MA, Lamont T. 2023. Long-term observations of hourly bottom temperatures at Tsitsikamma

(June 2007 - March 2008). DFFE. doi: 10.15493/DEA.MIMS.06572023

Ismail H, van den Berg MA, Lamont T. 2023. Long-term observations of hourly bottom temperatures at Tsitsikamma (March 2008 - July 2008). DFFE. doi: 10.15493/DEA.MIMS.06582023

Ismail H, van den Berg MA, Lamont T. 2023. Long-term observations of hourly bottom temperatures at Tsitsikamma (July 2008 - June 2009). DFFE. doi: 10.15493/DEA.MIMS.06592023

Ismail H, van den Berg MA, Lamont T. 2023. Long-term observations of hourly bottom temperatures at Tsitsikamma (June 2009 - November 2009). DFFE. doi: 10.15493/DEA.MIMS.06602023

Ismail H, van den Berg MA, Lamont T. 2023. Long-term observations of hourly bottom temperatures at Tsitsikamma (November 2009 - November 2010). DFFE. doi: 10.15493/DEA.MIMS.06612023.

Ismail H, van den Berg MA, Lamont T. 2023. Long-term observations of hourly bottom temperatures at Tsitsikamma (November 2010 - November 2011). DFFE. doi: 10.15493/DEA.MIMS.06622023.

Ismail H, van den Berg MA, Lamont T. 2023. Long-term observations of hourly bottom temperatures at Tsitsikamma (November 2011 - March 2013). DFFE. doi: 10.15493/DEA.MIMS.06632023.

Ismail H, van den Berg MA, Lamont T. 2023. Long-term observations of hourly bottom temperatures at Tsitsikamma (March 2013 - November 2013). DFFE. doi: 10.15493/DEA.MIMS.06642023.

Ismail H, van den Berg MA, Lamont T. 2023. Long-term observations of hourly bottom temperatures at Tsitsikamma (November 2013 - November 2015). DFFE. doi: 10.15493/DEA.MIMS.06652023.

Ismail H, van den Berg MA, Lamont T. 2023. Long-term observations of hourly bottom temperatures at Tsitsikamma (November 2015 - September 2019). DFFE. doi: 10.15493/DEA.MIMS.06662023.

Ismail H, van den Berg MA, Lamont T. 2023. Long-term observations of hourly bottom temperatures at Tsitsikamma (September 2019 - June 2022). DFFE. doi: 10.15493/DEA.MIMS.06672023.

Ismail H, van den Berg MA, Lamont T. 2023. Raw temperature data for long-term observations of bottom temperatures at Aliwal Shoal (October 2001 - February 2002). DFFE. doi: 10.15493/DEA.MIMS.10622023.

Ismail H, van den Berg MA, Lamont T. 2023. Raw temperature data for long-term observations of bottom temperatures at Aliwal Shoal (February 2002 - June 2002). DFFE. doi: 10.15493/DEA.MIMS.10632023.

Ismail H, van den Berg MA, Lamont T. 2023. Raw temperature data for long-term observations of bottom temperatures at Aliwal Shoal (June 2002 - October 2002). DFFE. doi: 10.15493/DEA.MIMS.10642023.

Ismail H, van den Berg MA, Lamont T. 2023. Raw temperature data for long-term observations of bottom temperatures at Aliwal Shoal (October 2002 - February 2003). DFFE. doi: 10.15493/DEA.MIMS.10652023.

Ismail H, van den Berg MA, Lamont T. 2023. Raw temperature data for long-term observations of bottom temperatures at Aliwal Shoal (February 2003 - February 2004). DFFE. doi: 10.15493/DEA.MIMS.10662023.

Ismail H, van den Berg MA, Lamont T. 2023. Raw temperature data for long-term observations of bottom temperatures at Aliwal Shoal (February 2004 - November 2004). DFFE. doi: 10.15493/DEA.MIMS.10672023.

Ismail H, van den Berg MA, Lamont T. 2023. Raw temperature data for long-term observations of bottom temperatures at Aliwal Shoal (November 2004 - May 2005). DFFE. doi: 10.15493/DEA.MIMS.10682023.

Ismail H, van den Berg MA, Lamont T. 2023. Raw temperature data for long-term observations of bottom temperatures at Aliwal Shoal (May 2005 - December 2005). DFFE. doi: 10.15493/DEA.MIMS.10692023.

Ismail H, van den Berg MA, Lamont T. 2023. Raw temperature data for long-term observations of bottom temperatures at Aliwal Shoal (December 2005 - July 2006). DFFE. doi: 10.15493/DEA.MIMS.10702023.

Ismail H, van den Berg MA, Lamont T. 2023. Raw temperature data for long-term observations of bottom temperatures at Aliwal Shoal (July 2006 - February 2007). DFFE. doi: 10.15493/DEA.MIMS.10712023.

Ismail H, van den Berg MA, Lamont T. 2023. Raw temperature data for long-term observations of bottom temperatures at Aliwal Shoal (February 2007 - July 2007). DFFE. doi: 10.15493/DEA.MIMS.10722023.

Ismail H, van den Berg MA, Lamont T. 2023. Raw temperature data for long-term observations of bottom temperatures at Aliwal Shoal (July 2007 - April 2008). DFFE. doi: 10.15493/DEA.MIMS.10732023.

Ismail H, van den Berg MA, Lamont T. 2023. Raw temperature data for long-term observations of bottom temperatures at Aliwal Shoal (April 2008 - August 2008). DFFE. doi: 10.15493/DEA.MIMS.10742023.

Ismail H, van den Berg MA, Lamont T. 2023. Raw temperature data for long-term observations of bottom temperatures at Aliwal Shoal (August 2008 - January 2010). DFFE. doi: 10.15493/DEA.MIMS.10752023.

Ismail H, van den Berg MA, Lamont T. 2023. Raw temperature data for long-term observations of bottom temperatures at Aliwal Shoal (January 2010 - December 2010). DFFE. doi: 10.15493/DEA.MIMS.10762023.

Ismail H, van den Berg MA, Lamont T. 2023. Raw temperature data for long-term observations of bottom temperatures at Aliwal Shoal (December 2010 - August 2011). DFFE. doi: 10.15493/DEA.MIMS.10772023.

Ismail H, van den Berg MA, Lamont T. 2023. Raw temperature data for long-term observations of bottom temperatures at Aliwal Shoal (August 2011 - October 2012). DFFE. doi: 10.15493/DEA.MIMS.10782023.

Ismail H, van den Berg MA, Lamont T. 2023. Raw temperature data for long-term observations of bottom temperatures at Aliwal Shoal (October 2012 - February 2013). DFFE. doi: 10.15493/DEA.MIMS.10792023.

Ismail H, van den Berg MA, Lamont T. 2023. Raw temperature data for long-term observations of bottom temperatures at Aliwal Shoal (February 2013 - May 2014). DFFE. doi: 10.15493/DEA.MIMS.10802023.

Ismail H, van den Berg MA, Lamont T. 2023. Raw temperature data for long-term observations of bottom temperatures at Aliwal Shoal (May 2014 - February 2016). DFFE. doi: 10.15493/DEA.MIMS.10812023.

Ismail H, van den Berg MA, Lamont T. 2023. Long-term observations of hourly bottom temperatures at Aliwal Shoal (October 2001 - February 2002). DFFE. doi: 10.15493/DEA.MIMS.10822023.

Ismail H, van den Berg MA, Lamont T. 2023. Long-term observations of hourly bottom temperatures at Aliwal Shoal (February 2002 - June 2002). DFFE. doi: 10.15493/DEA.MIMS.10832023.

Ismail H, van den Berg MA, Lamont T. 2023. Long-term observations of hourly bottom temperatures at Aliwal Shoal

(June 2002 - October 2002). DFFE. doi: 10.15493/DEA.MIMS.10842023.

Ismail H, van den Berg MA, Lamont T. 2023. Long-term observations of hourly bottom temperatures at Aliwal Shoal (October 2002 - February 2003). DFFE. doi: 10.15493/DEA.MIMS.10852023.

Ismail H, van den Berg MA, Lamont T. 2023. Long-term observations of hourly bottom temperatures at Aliwal Shoal (February 2003 - February 2004). DFFE. doi: 10.15493/DEA.MIMS.10862023.

Ismail H, van den Berg MA, Lamont T. 2023. Long-term observations of hourly bottom temperatures at Aliwal Shoal (February 2004 - November 2004). DFFE. doi: 10.15493/DEA.MIMS.10872023.

Ismail H, van den Berg MA, Lamont T. 2023. Long-term observations of hourly bottom temperatures at Aliwal Shoal (November 2004 - May 2005). DFFE. doi: 10.15493/DEA.MIMS.10882023.

Ismail H, van den Berg MA, Lamont T. 2023. Long-term observations of hourly bottom temperatures at Aliwal Shoal (May 2005 - December 2005). DFFE. doi: 10.15493/DEA.MIMS.10892023.

Ismail H, van den Berg MA, Lamont T. 2023. Long-term observations of hourly bottom temperatures at Aliwal Shoal (December 2005 - July 2006). DFFE. doi: 10.15493/DEA.MIMS.10902023.

Ismail H, van den Berg MA, Lamont T. 2023. Long-term observations of hourly bottom temperatures at Aliwal Shoal (July 2006 - February 2007). DFFE. doi: 10.15493/DEA.MIMS.10912023.

Ismail H, van den Berg MA, Lamont T. 2023. Long-term observations of hourly bottom temperatures at Aliwal Shoal (February 2007 - July 2007). DFFE. doi: 10.15493/DEA.MIMS.10922023

Ismail H, van den Berg MA, Lamont T. 2023. Long-term observations of hourly bottom temperatures at Aliwal Shoal (July 2007 - April 2008). DFFE. doi: 10.15493/DEA.MIMS.10932023.

Ismail H, van den Berg MA, Lamont T. 2023. Long-term observations of hourly bottom temperatures at Aliwal Shoal (April 2008 - August 2008). DFFE. doi: 10.15493/DEA.MIMS.10942023.

Ismail H, van den Berg MA, Lamont T. 2023. Long-term observations of hourly bottom temperatures at Aliwal Shoal (August 2008 - January 2010). DFFE. doi: 10.15493/DEA.MIMS.10952023.

Ismail H, van den Berg MA, Lamont T. 2023. Long-term observations of hourly bottom temperatures at Aliwal Shoal (January 2010 - December 2010). DFFE. doi: 10.15493/DEA.MIMS.10962023.

Ismail H, van den Berg MA, Lamont T. 2023. Long-term observations of hourly bottom temperatures at Aliwal Shoal (December 2010 - August 2011). DFFE. doi: 10.15493/DEA.MIMS.10972023.

Ismail H, van den Berg MA, Lamont T. 2023. Long-term observations of hourly bottom temperatures at Aliwal Shoal (August 2011 - October 2012). DFFE. doi: 10.15493/DEA.MIMS.10982023.

Ismail H, van den Berg MA, Lamont T. 2023. Long-term observations of hourly bottom temperatures at Aliwal Shoal (October 2012 - February 2013). DFFE. doi: 10.15493/DEA.MIMS.10992023.

Ismail H, van den Berg MA, Lamont T. 2023. Long-term observations of hourly bottom temperatures at Aliwal Shoal (February 2013 - May 2014). DFFE. doi: 10.15493/DEA.MIMS.11002023.

Ismail H, van den Berg MA, Lamont T. 2023. Long-term observations of hourly bottom temperatures at Aliwal Shoal (May 2014 - February 2016). DFFE. doi: 10.15493/DEA.MIMS.11012023.

Ismail H, van den Berg MA, Lamont T. 2023. Raw temperature data for long-term observations of bottom temperatures at Sodwana Bay (March 1994 - July 1994). DFFE. doi: 10.15493/DEA.MIMS.08182023.

Ismail H, van den Berg MA, Lamont T. 2023. Raw temperature data for long-term observations of bottom temperatures at Sodwana Bay (July 1994 - November 1994). DFFE. doi: 10.15493/DEA.MIMS.08192023.

Ismail H, van den Berg MA, Lamont T. 2023. Raw temperature data for long-term observations of bottom temperatures at Sodwana Bay (November 1994 - February 1995). DFFE. doi: 10.15493/DEA.MIMS.08202023.

Ismail H, van den Berg MA, Lamont T. 2023. Raw temperature data for long-term observations of bottom temperatures at Sodwana Bay (February 1995 - June 1995). DFFE. doi: 10.15493/DEA.MIMS.08212023.

Ismail H, van den Berg MA, Lamont T. 2023. Raw temperature data for long-term observations of bottom temperatures at Sodwana Bay (June 1995 - November 1995). DFFE. doi: 10.15493/DEA.MIMS.08222023.

Ismail H, van den Berg MA, Lamont T. 2023. Raw temperature data for long-term observations of bottom temperatures at Sodwana Bay (November 1995 - March 1996). DFFE. doi: 10.15493/DEA.MIMS.08232023.

Ismail H, van den Berg MA, Lamont T. 2023. Raw temperature data for long-term observations of bottom temperatures at Sodwana Bay (March 1996 - July 1996). DFFE. doi: 10.15493/DEA.MIMS.08242023.

Ismail H, van den Berg MA, Lamont T. 2023. Raw temperature data for long-term observations of bottom temperatures at Sodwana Bay (July 1996 - November 1996). DFFE. doi: 10.15493/DEA.MIMS.08252023.

Ismail H, van den Berg MA, Lamont T. 2023. Raw temperature data for long-term observations of bottom temperatures at Sodwana Bay (November 1996 - March 1997). DFFE. doi: 10.15493/DEA.MIMS.08262023.

Ismail H, van den Berg MA, Lamont T. 2023. Raw temperature data for long-term observations of bottom temperatures at Sodwana Bay (March 1997 - June 1997). DFFE. doi: 10.15493/DEA.MIMS.08272023.

Ismail H, van den Berg MA, Lamont T. 2023. Raw temperature data for long-term observations of bottom temperatures at Sodwana Bay (June 1997 - November 1997). DFFE. doi: 10.15493/DEA.MIMS.08282023.

Ismail H, van den Berg MA, Lamont T. 2023. Raw temperature data for long-term observations of bottom temperatures at Sodwana Bay (November 1997 - March 1998). DFFE. doi: 10.15493/DEA.MIMS.08292023.

Ismail H, van den Berg MA, Lamont T. 2023. Raw temperature data for long-term observations of bottom temperatures at Sodwana Bay (March 1998 - August 1998). DFFE. doi: 10.15493/DEA.MIMS.08302023.

Ismail H, van den Berg MA, Lamont T. 2023. Raw temperature data for long-term observations of bottom temperatures at Sodwana Bay (August 1998 - January 1999). DFFE. doi: 10.15493/DEA.MIMS.08312023.

Ismail H, van den Berg MA, Lamont T. 2023. Raw temperature data for long-term observations of bottom temperatures at Sodwana Bay (January 1999 - June 1999). DFFE. doi: 10.15493/DEA.MIMS.08322023.

Ismail H, van den Berg MA, Lamont T. 2023. Raw temperature data for long-term observations of bottom temperatures

at Sodwana Bay (June 1999 - January 2000). DFFE. doi: 10.15493/DEA.MIMS.08332023.

Ismail H, van den Berg MA, Lamont T. 2023. Raw temperature data for long-term observations of bottom temperatures at Sodwana Bay (January 2000 - May 2000). DFFE. doi: 10.15493/DEA.MIMS.08342023.

Ismail H, van den Berg MA, Lamont T. 2023. Raw temperature data for long-term observations of bottom temperatures at Sodwana Bay (May 2000 - August 2000). DFFE. doi: 10.15493/DEA.MIMS.08352023.

Ismail H, van den Berg MA, Lamont T. 2023. Raw temperature data for long-term observations of bottom temperatures at Sodwana Bay (August 2000 - November 2000). DFFE. doi: 10.15493/DEA.MIMS.08362023.

Ismail H, van den Berg MA, Lamont T. 2023. Raw temperature data for long-term observations of bottom temperatures at Sodwana Bay (November 2000 - March 2001). DFFE. doi: 10.15493/DEA.MIMS.08372023.

Ismail H, van den Berg MA, Lamont T. 2023. Raw temperature data for long-term observations of bottom temperatures at Sodwana Bay (March 2001 - October 2001). DFFE. doi: 10.15493/DEA.MIMS.08382023.

Ismail H, van den Berg MA, Lamont T. 2023. Raw temperature data for long-term observations of bottom temperatures at Sodwana Bay (October 2001 - February 2002). DFFE. doi: 10.15493/DEA.MIMS.08392023.

Ismail H, van den Berg MA, Lamont T. 2023. Raw temperature data for long-term observations of bottom temperatures at Sodwana Bay (February 2002 - May 2002). DFFE. doi: 10.15493/DEA.MIMS.08402023.

Ismail H, van den Berg MA, Lamont T. 2023. Raw temperature data for long-term observations of bottom temperatures at Sodwana Bay (May 2002 - October 2002). DFFE. doi: 10.15493/DEA.MIMS.08412023.

Ismail H, van den Berg MA, Lamont T. 2023. Raw temperature data for long-term observations of bottom temperatures at Sodwana Bay (February 2003 - April 2003). DFFE. doi: 10.15493/DEA.MIMS.08422023.

Ismail H, van den Berg MA, Lamont T. 2023. Raw temperature data for long-term observations of bottom temperatures at Sodwana Bay (April 2003 - August 2003). DFFE. doi: 10.15493/DEA.MIMS.08432023.

Ismail H, van den Berg MA, Lamont T. 2023. Raw temperature data for long-term observations of bottom temperatures at Sodwana Bay (August 2003 - September 2004). DFFE. doi: 10.15493/DEA.MIMS.08442023.

Ismail H, van den Berg MA, Lamont T. 2023. Raw temperature data for long-term observations of bottom temperatures at Sodwana Bay (September 2004 - April 2005). DFFE. doi: 10.15493/DEA.MIMS.08452023.

Ismail H, van den Berg MA, Lamont T. 2023. Raw temperature data for long-term observations of bottom temperatures at Sodwana Bay (April 2005 - April 2006). DFFE. doi: 10.15493/DEA.MIMS.08462023.

Ismail H, van den Berg MA, Lamont T. 2023. Raw temperature data for long-term observations of bottom temperatures at Sodwana Bay (April 2006 - September 2006). DFFE. doi: 10.15493/DEA.MIMS.08472023.

Ismail H, van den Berg MA, Lamont T. 2023. Raw temperature data for long-term observations of bottom temperatures at Sodwana Bay (September 2006 - March 2007). DFFE. doi: 10.15493/DEA.MIMS.08482023.

Ismail H, van den Berg MA, Lamont T. 2023. Raw temperature data for long-term observations of bottom temperatures at Sodwana Bay (March 2007 - September 2007). DFFE. doi: 10.15493/DEA.MIMS.08492023.

Ismail H, van den Berg MA, Lamont T. 2023. Raw temperature data for long-term observations of bottom temperatures at Sodwana Bay (September 2007 - February 2008). DFFE. doi: 10.15493/DEA.MIMS.08502023.

Ismail H, van den Berg MA, Lamont T. 2023. Raw temperature data for long-term observations of bottom temperatures at Sodwana Bay (February 2008 - July 2008). DFFE. doi: 10.15493/DEA.MIMS.08512023.

Ismail H, van den Berg MA, Lamont T. 2023. Raw temperature data for long-term observations of bottom temperatures at Sodwana Bay (July 2008 - February 2009). DFFE. doi: 10.15493/DEA.MIMS.08522023.

Ismail H, van den Berg MA, Lamont T. 2023. Raw temperature data for long-term observations of bottom temperatures at Sodwana Bay (February 2009 - September 2009). DFFE. doi: 10.15493/DEA.MIMS.08532023.

Ismail H, van den Berg MA, Lamont T. 2023. Raw temperature data for long-term observations of bottom temperatures at Sodwana Bay (September 2009 - January 2010). DFFE. doi: 10.15493/DEA.MIMS.08542023.

Ismail H, van den Berg MA, Lamont T. 2023. Raw temperature data for long-term observations of bottom temperatures at Sodwana Bay (January 2010 - September 2010). DFFE. doi: 10.15493/DEA.MIMS.08552023.

Ismail H, van den Berg MA, Lamont T. 2023. Raw temperature data for long-term observations of bottom temperatures at Sodwana Bay (September 2010 - February 2011). DFFE. doi: 10.15493/DEA.MIMS.08562023.

Ismail H, van den Berg MA, Lamont T. 2023. Raw temperature data for long-term observations of bottom temperatures at Sodwana Bay (February 2011 - October 2011). DFFE. doi: 10.15493/DEA.MIMS.08572023.

Ismail H, van den Berg MA, Lamont T. 2023. Raw temperature data for long-term observations of bottom temperatures at Sodwana Bay (October 2011 - February 2012). DFFE. doi: 10.15493/DEA.MIMS.08582023.

Ismail H, van den Berg MA, Lamont T. 2023. Raw temperature data for long-term observations of bottom temperatures at Sodwana Bay (February 2012 - August 2012). DFFE. doi: 10.15493/DEA.MIMS.08592023.

Ismail H, van den Berg MA, Lamont T. 2023. Raw temperature data for long-term observations of bottom temperatures at Sodwana Bay (August 2012 - March 2013). DFFE. doi: 10.15493/DEA.MIMS.08602023.

Ismail H, van den Berg MA, Lamont T. 2023. Raw temperature data for long-term observations of bottom temperatures at Sodwana Bay (March 2013 - June 2013). DFFE. doi: 10.15493/DEA.MIMS.08612023.

Ismail H, van den Berg MA, Lamont T. 2023. Raw temperature data for long-term observations of bottom temperatures at Sodwana Bay (June 2013 - February 2014). DFFE. doi: 10.15493/DEA.MIMS.08622023.

Ismail H, van den Berg MA, Lamont T. 2023. Raw temperature data for long-term observations of bottom temperatures at Sodwana Bay (February 2014 - October 2014). DFFE. doi: 10.15493/DEA.MIMS.08632023.

Ismail H, van den Berg MA, Lamont T. 2023. Raw temperature data for long-term observations of bottom temperatures at Sodwana Bay (October 2014 - March 2015). DFFE. doi: 10.15493/DEA.MIMS.08642023.

Ismail H, van den Berg MA, Lamont T. 2023. Raw temperature data for long-term observations of bottom temperatures at Sodwana Bay (March 2015 - September 2015). DFFE. doi: 10.15493/DEA.MIMS.08652023.

Ismail H, van den Berg MA, Lamont T. 2023. Raw temperature data for long-term observations of bottom temperatures at

Sodwana Bay (September 2015 - February 2016). DFFE. doi: 10.15493/DEA.MIMS.08662023.

Ismail H, van den Berg MA, Lamont T. 2023. Raw temperature data for long-term observations of bottom temperatures at Sodwana Bay (February 2016 - September 2016). DFFE. doi: 10.15493/DEA.MIMS.08672023.

Ismail H, van den Berg MA, Lamont T. 2023. Raw temperature data for long-term observations of bottom temperatures at Sodwana Bay (September 2016 - February 2017). DFFE. doi: 10.15493/DEA.MIMS.08682023.

Ismail H, van den Berg MA, Lamont T. 2023. Raw temperature data for long-term observations of bottom temperatures at Sodwana Bay (February 2017 - September 2017). DFFE. doi: 10.15493/DEA.MIMS.08692023.

Ismail H, van den Berg MA, Lamont T. 2023. Raw temperature data for long-term observations of bottom temperatures at Sodwana Bay (September 2017 - January 2018). DFFE. doi: 10.15493/DEA.MIMS.08702023.

Ismail H, van den Berg MA, Lamont T. 2023. Raw temperature data for long-term observations of bottom temperatures at Sodwana Bay (January 2018 - September 2018). DFFE. doi: 10.15493/DEA.MIMS.08712023.

Ismail H, van den Berg MA, Lamont T. 2023. Raw temperature data for long-term observations of bottom temperatures at Sodwana Bay (September 2018 - February 2019). DFFE. doi: 10.15493/DEA.MIMS.08722023.

Ismail H, van den Berg MA, Lamont T. 2023. Raw temperature data for long-term observations of bottom temperatures at Sodwana Bay (February 2019 - November 2019). DFFE. doi: 10.15493/DEA.MIMS.08732023.

Ismail H, van den Berg MA, Lamont T. 2023. Raw temperature data for long-term observations of bottom temperatures at Sodwana Bay (November 2019 - April 2021). DFFE. doi: 10.15493/DEA.MIMS.08742023.

Ismail H, van den Berg MA, Lamont T. 2023. Raw temperature data for long-term observations of bottom temperatures at Sodwana Bay (April 2021 - February 2022). DFFE. doi: 10.15493/DEA.MIMS.08752023.

Ismail H, van den Berg MA, Lamont T. 2023. Raw temperature data for long-term observations of bottom temperatures at Sodwana Bay (February 2022 - August 2022). DFFE. doi: 10.15493/DEA.MIMS.08762023.

Ismail H, van den Berg MA, Lamont T. 2023. Long-term observations of hourly bottom temperatures at Sodwana Bay (March 1994 - July 1994). DFFE. doi: 10.15493/DEA.MIMS.08772023

Ismail H, van den Berg MA, Lamont T. 2023. Long-term observations of hourly bottom temperatures at Sodwana Bay (July 1994 - November 1994). DFFE. doi: 10.15493/DEA.MIMS.08782023.

Ismail H, van den Berg MA, Lamont T. 2023. Long-term observations of hourly bottom temperatures at Sodwana Bay (November 1994 - February 1995). DFFE. doi: 10.15493/DEA.MIMS.08792023.

Ismail H, van den Berg MA, Lamont T. 2023. Long-term observations of hourly bottom temperatures at Sodwana Bay (February 1995 - June 1995). DFFE. doi: 10.15493/DEA.MIMS.08802023.

Ismail H, van den Berg MA, Lamont T. 2023. Long-term observations of hourly bottom temperatures at Sodwana Bay (June 1995 - November 1995). DFFE. doi: 10.15493/DEA.MIMS.08812023.

Ismail H, van den Berg MA, Lamont T. 2023. Long-term observations of hourly bottom temperatures at Sodwana Bay (November 1995 - March 1996). DFFE. doi: 10.15493/DEA.MIMS.08822023.

Ismail H, van den Berg MA, Lamont T. 2023. Long-term observations of hourly bottom temperatures at Sodwana Bay (March 1996 - July 1996). DFFE. doi: 10.15493/DEA.MIMS.08832023.

Ismail H, van den Berg MA, Lamont T. 2023. Long-term observations of hourly bottom temperatures at Sodwana Bay (July 1996 - November 1996). DFFE. doi: 10.15493/DEA.MIMS.08842023.

Ismail H, van den Berg MA, Lamont T. 2023. Long-term observations of hourly bottom temperatures at Sodwana Bay (November 1996 - March 1997). DFFE. doi: 10.15493/DEA.MIMS.08852023.

Ismail H, van den Berg MA, Lamont T. 2023. Long-term observations of hourly bottom temperatures at Sodwana Bay (March 1997 - June 1997). DFFE. doi: 10.15493/DEA.MIMS.08862023.

Ismail H, van den Berg MA, Lamont T. 2023. Long-term observations of hourly bottom temperatures at Sodwana Bay (June 1997 - November 1997). DFFE. doi: 10.15493/DEA.MIMS.08872023.

Ismail H, van den Berg MA, Lamont T. 2023. Long-term observations of hourly bottom temperatures at Sodwana Bay (November 1997 - March 1998). DFFE. doi: 10.15493/DEA.MIMS.08882023.

Ismail H, van den Berg MA, Lamont T. 2023. Long-term observations of hourly bottom temperatures at Sodwana Bay (March 1998 - August 1998). DFFE. doi: 10.15493/DEA.MIMS.08892023.

Ismail H, van den Berg MA, Lamont T. 2023. Long-term observations of hourly bottom temperatures at Sodwana Bay (August 1998 - January 1999). DFFE. doi: 10.15493/DEA.MIMS.08902023.

Ismail H, van den Berg MA, Lamont T. 2023. Long-term observations of hourly bottom temperatures at Sodwana Bay (January 1999 - June 1999). DFFE. doi: 10.15493/DEA.MIMS.08912023.

Ismail H, van den Berg MA, Lamont T. 2023. Long-term observations of hourly bottom temperatures at Sodwana Bay (June 1999 - January 2000). DFFE. doi: 10.15493/DEA.MIMS.08922023.

Ismail H, van den Berg MA, Lamont T. 2023. Long-term observations of hourly bottom temperatures at Sodwana Bay (January 2000 - May 2000). DFFE. doi: 10.15493/DEA.MIMS.08932023.

Ismail H, van den Berg MA, Lamont T. 2023. Long-term observations of hourly bottom temperatures at Sodwana Bay (May 2000 - August 2000). DFFE. doi: 10.15493/DEA.MIMS.08942023.

Ismail H, van den Berg MA, Lamont T. 2023. Long-term observations of hourly bottom temperatures at Sodwana Bay (August 2000 - November 2000). DFFE. doi: 10.15493/DEA.MIMS.08952023.

Ismail H, van den Berg MA, Lamont T. 2023. Long-term observations of hourly bottom temperatures at Sodwana Bay (November 2000 - March 2001). DFFE. doi: 10.15493/DEA.MIMS.08962023.

Ismail H, van den Berg MA, Lamont T. 2023. Long-term observations of hourly bottom temperatures at Sodwana Bay (March 2001 - October 2001). DFFE. doi: 10.15493/DEA.MIMS.08972023.

Ismail H, van den Berg MA, Lamont T. 2023. Long-term observations of hourly bottom temperatures at Sodwana Bay (October 2001 - February 2002). DFFE. doi: 10.15493/DEA.MIMS.08982023.

Ismail H, van den Berg MA, Lamont T. 2023. Long-term observations of hourly bottom temperatures at Sodwana Bay

(February 2002 - May 2002). DFFE. doi: 10.15493/DEA.MIMS.08992023.

Ismail H, van den Berg MA, Lamont T. 2023. Long-term observations of hourly bottom temperatures at Sodwana Bay (May 2002 - October 2002). DFFE. doi: 10.15493/DEA.MIMS.09002023.

Ismail H, van den Berg MA, Lamont T. 2023. Long-term observations of hourly bottom temperatures at Sodwana Bay (February 2003 - April 2003). DFFE. doi: 10.15493/DEA.MIMS.09012023.

Ismail H, van den Berg MA, Lamont T. 2023. Long-term observations of hourly bottom temperatures at Sodwana Bay (April 2003 - August 2003). DFFE. doi: 10.15493/DEA.MIMS.09022023.

Ismail H, van den Berg MA, Lamont T. 2023. Long-term observations of hourly bottom temperatures at Sodwana Bay (August 2003 - September 2004). DFFE. doi: 10.15493/DEA.MIMS.09032023.

Ismail H, van den Berg MA, Lamont T. 2023. Long-term observations of hourly bottom temperatures at Sodwana Bay (September 2004 - April 2005). DFFE. doi: 10.15493/DEA.MIMS.09042023.

Ismail H, van den Berg MA, Lamont T. 2023. Long-term observations of hourly bottom temperatures at Sodwana Bay (April 2005 - April 2006). DFFE. doi: 10.15493/DEA.MIMS.09052023.

Ismail H, van den Berg MA, Lamont T. 2023. Long-term observations of hourly bottom temperatures at Sodwana Bay (April 2006 - September 2006). DFFE. doi: 10.15493/DEA.MIMS.09062023.

Ismail H, van den Berg MA, Lamont T. 2023. Long-term observations of hourly bottom temperatures at Sodwana Bay (September 2006 - March 2007). DFFE. doi: 10.15493/DEA.MIMS.09072023.

Ismail H, van den Berg MA, Lamont T. 2023. Long-term observations of hourly bottom temperatures at Sodwana Bay (March 2007 - September 2007). DFFE. doi: 10.15493/DEA.MIMS.09082023.

Ismail H, van den Berg MA, Lamont T. 2023. Long-term observations of hourly bottom temperatures at Sodwana Bay (September 2007 - February 2008). DFFE. doi: 10.15493/DEA.MIMS.09092023.

Ismail H, van den Berg MA, Lamont T. 2023. Long-term observations of hourly bottom temperatures at Sodwana Bay (February 2008 - July 2008). DFFE. doi: 10.15493/DEA.MIMS.09102023.

Ismail H, van den Berg MA, Lamont T. 2023. Long-term observations of hourly bottom temperatures at Sodwana Bay (July 2008 - February 2009). DFFE. doi: 10.15493/DEA.MIMS.09112023.

Ismail H, van den Berg MA, Lamont T. 2023. Long-term observations of hourly bottom temperatures at Sodwana Bay (February 2009 - September 2009). DFFE. doi: 10.15493/DEA.MIMS.09122023.

Ismail H, van den Berg MA, Lamont T. 2023. Long-term observations of hourly bottom temperatures at Sodwana Bay (September 2009 - January 2010). DFFE. doi: 10.15493/DEA.MIMS.09132023.

Ismail H, van den Berg MA, Lamont T. 2023. Long-term observations of hourly bottom temperatures at Sodwana Bay (January 2010 - September 2010). DFFE. doi: 10.15493/DEA.MIMS.09142023.

Ismail H, van den Berg MA, Lamont T. 2023. Long-term observations of hourly bottom temperatures at Sodwana Bay (September 2010 - February 2011). DFFE. doi: 10.15493/DEA.MIMS.09152023.

Ismail H, van den Berg MA, Lamont T. 2023. Long-term observations of hourly bottom temperatures at Sodwana Bay (February 2011 - October 2011). DFFE. doi: 10.15493/DEA.MIMS.09162023.

Ismail H, van den Berg MA, Lamont T. 2023. Long-term observations of hourly bottom temperatures at Sodwana Bay (October 2011 - February 2012). DFFE. doi: 10.15493/DEA.MIMS.09172023.

Ismail H, van den Berg MA, Lamont T. 2023. Long-term observations of hourly bottom temperatures at Sodwana Bay (February 2012 - August 2012). DFFE. doi: 10.15493/DEA.MIMS.09182023.

Ismail H, van den Berg MA, Lamont T. 2023. Long-term observations of hourly bottom temperatures at Sodwana Bay (August 2012 - March 2013). DFFE. doi: 10.15493/DEA.MIMS.09192023.

Ismail H, van den Berg MA, Lamont T. 2023. Long-term observations of hourly bottom temperatures at Sodwana Bay (March 2013 - June 2013). DFFE. doi: 10.15493/DEA.MIMS.09202023.

Ismail H, van den Berg MA, Lamont T. 2023. Long-term observations of hourly bottom temperatures at Sodwana Bay (June 2013 - February 2014). DFFE. doi: 10.15493/DEA.MIMS.09212023.

Ismail H, van den Berg MA, Lamont T. 2023. Long-term observations of hourly bottom temperatures at Sodwana Bay (February 2014 - October 2014). DFFE. doi: 10.15493/DEA.MIMS.09222023.

Ismail H, van den Berg MA, Lamont T. 2023. Long-term observations of hourly bottom temperatures at Sodwana Bay (October 2014 - March 2015). DFFE. doi: 10.15493/DEA.MIMS.09232023.

Ismail H, van den Berg MA, Lamont T. 2023. Long-term observations of hourly bottom temperatures at Sodwana Bay (March 2015 - September 2015). DFFE. doi: 10.15493/DEA.MIMS.09242023.

Ismail H, van den Berg MA, Lamont T. 2023. Long-term observations of hourly bottom temperatures at Sodwana Bay (September 2015 - February 2016). DFFE. doi: 10.15493/DEA.MIMS.09252023.

Ismail H, van den Berg MA, Lamont T. 2023. Long-term observations of hourly bottom temperatures at Sodwana Bay (February 2016 - September 2016). DFFE. doi: 10.15493/DEA.MIMS.09262023.

Ismail H, van den Berg MA, Lamont T. 2023. Long-term observations of hourly bottom temperatures at Sodwana Bay (September 2016 - February 2017). DFFE. doi: 10.15493/DEA.MIMS.09272023.

Ismail H, van den Berg MA, Lamont T. 2023. Long-term observations of hourly bottom temperatures at Sodwana Bay (February 2017 - September 2017). DFFE. doi: 10.15493/DEA.MIMS.09282023.

Ismail H, van den Berg MA, Lamont T. 2023. Long-term observations of hourly bottom temperatures at Sodwana Bay (September 2017 - January 2018). DFFE. doi: 10.15493/DEA.MIMS.09292023.

Ismail H, van den Berg MA, Lamont T. 2023. Long-term observations of hourly bottom temperatures at Sodwana Bay (January 2018 - September 2018). DFFE. doi: 10.15493/DEA.MIMS.09302023.

Ismail H, van den Berg MA, Lamont T. 2023. Long-term observations of hourly bottom temperatures at Sodwana Bay (September 2018 - February 2019). DFFE. doi: 10.15493/DEA.MIMS.09312023.

Ismail H, van den Berg MA, Lamont T. 2023. Long-term observations of hourly bottom temperatures at Sodwana Bay

(February 2019 - November 2019). DFFE. doi: 10.15493/DEA.MIMS.09322023.

Ismail H, van den Berg MA, Lamont T. 2023. Long-term observations of hourly bottom temperatures at Sodwana Bay (November 2019 - April 2021). DFFE. doi: 10.15493/DEA.MIMS.09332023.

Ismail H, van den Berg MA, Lamont T. 2023. Long-term observations of hourly bottom temperatures at Sodwana Bay (April 2021 - February 2022). DFFE. doi: 10.15493/DEA.MIMS.09342023.

Ismail H, van den Berg MA, Lamont T. 2023. Long-term observations of hourly bottom temperatures at Sodwana Bay (February 2022 - August 2022). DFFE. doi: 10.15493/DEA.MIMS.09352023.

Ismail H, van den Berg MA, Lamont T. 2023. Raw temperature data for long-term observations of bottom temperatures at Xai-Xai, Mozambique (April 2006 - July 2007). DFFE. doi: 10.15493/DEA.MIMS.04452023.

Ismail H, van den Berg MA, Lamont T. 2023. Raw temperature data for long-term observations of bottom temperatures at Xai-Xai, Mozambique (July 2007 - March 2013). DFFE. doi: 10.15493/DEA.MIMS.04472023.

Ismail H, van den Berg MA, Lamont T. 2023. Long-term observations of hourly bottom temperatures at Xai-Xai, Mozambique (April 2006 - July 2007). DFFE. doi: 10.15493/DEA.MIMS.04432023.

Ismail H, van den Berg MA, Lamont T. 2023. Long-term observations of hourly bottom temperatures at Xai-Xai, Mozambique (July 2007 - March 2013). DFFE. doi:10.15493/DEA.MIMS.04442023.

Ismail H, van den Berg MA, Lamont T. 2023. Raw temperature data for long-term observations of bottom temperatures at Arcadia Reef, Mozambique (March 2012 - April 2015). DFFE. doi: 10.15493/DEA.MIMS.01842023.

Ismail H, van den Berg MA, Lamont T. 2023. Raw temperature data for long-term observations of bottom temperatures at Arcadia Reef, Mozambique (April 2015 - June 2017). DFFE. doi: 10.15493/DEA.MIMS.01862023.

Ismail H, van den Berg MA, Lamont T. 2023. Raw temperature data for long-term observations of bottom temperatures at Arcadia Reef, Mozambique (June 2017 - September 2018). DFFE. doi: 10.15493/DEA.MIMS.01882023.

Ismail H, van den Berg MA, Lamont T. 2023. Raw temperature data for long-term observations of bottom temperatures at Arcadia Reef, Mozambique (September 2018 - August 2019). DFFE. doi: 10.15493/DEA.MIMS.01892023.

Ismail H, van den Berg MA, Lamont T. 2023. Raw temperature data for long-term observations of bottom temperatures at Arcadia Reef, Mozambique (August 2019 - November 2020). DFFE. doi: 10.15493/DEA.MIMS.01912023.

Ismail H, van den Berg MA, Lamont T. 2023. Raw temperature data for long-term observations of bottom temperatures at Arcadia Reef, Mozambique (November 2020 - April 2021). DFFE. doi: 10.15493/DEA.MIMS.01932023.

Ismail H, van den Berg MA, Lamont T. 2023. Long-term observations of hourly bottom temperatures at Arcadia Reef, Mozambique (March 2012 - April 2015). DFFE. doi: 10.15493/DEA.MIMS.01782023.

Ismail H, van den Berg MA, Lamont T. 2023. Long-term observations of hourly bottom temperatures at Arcadia Reef, Mozambique (April 2015 - June 2017). DFFE. doi: 10.15493/DEA.MIMS.01792023.

Ismail H, van den Berg MA, Lamont T. 2023. Long-term observations of hourly bottom temperatures at Arcadia Reef, Mozambique (June 2017 - September 2018). DFFE. doi: 10.15493/DEA.MIMS.01802023.

Ismail H, van den Berg MA, Lamont T. 2023. Long-term observations of hourly bottom temperatures at Arcadia Reef, Mozambique (September 2018 - August 2019). DFFE. doi: 10.15493/DEA.MIMS.01812023.

Ismail H, van den Berg MA, Lamont T. 2023. Long-term observations of hourly bottom temperatures at Arcadia Reef, Mozambique (August 2019 - November 2020). DFFE. doi: 10.15493/DEA.MIMS.01822023.

Ismail H, van den Berg MA, Lamont T. 2023. Long-term observations of hourly bottom temperatures at Arcadia Reef, Mozambique (November 2020 - April 2021). DFFE. doi: 10.15493/DEA.MIMS.01832023.

Ismail H, van den Berg MA, Lamont T. 2023. Raw temperature data for long-term observations of bottom temperatures at Ponta Zavora, Mozambique (April 2006 - July 2007). DFFE. doi: 10.15493/DEA.MIMS.04282023.

Ismail H, van den Berg MA, Lamont T. 2023. Raw temperature data for long-term observations of bottom temperatures at Ponta Zavora, Mozambique (July 2007 - February 2010). DFFE. doi: 10.15493/DEA.MIMS.04302023.

Ismail H, van den Berg MA, Lamont T. 2023. Raw temperature data for long-term observations of bottom temperatures at Ponta Zavora, Mozambique (February 2010 - May 2011). DFFE. doi: 10.15493/DEA.MIMS.04322023.

Ismail H, van den Berg MA, Lamont T. 2023. Raw temperature data for long-term observations of bottom temperatures at Ponta Zavora, Mozambique (May 2011 - April 2015). DFFE. doi: 10.15493/DEA.MIMS.04342023.

Ismail H, van den Berg MA, Lamont T. 2023. Raw temperature data for long-term observations of bottom temperatures at Ponta Zavora, Mozambique (April 2015 - June 2017). DFFE. doi: 10.15493/DEA.MIMS.04362023.

Ismail H, van den Berg MA, Lamont T. 2023. Raw temperature data for long-term observations of bottom temperatures at Ponta Zavora, Mozambique (June 2017 - September 2018). DFFE. doi: 10.15493/DEA.MIMS.04382023.

Ismail H, van den Berg MA, Lamont T. 2023. Raw temperature data for long-term observations of bottom temperatures at Ponta Zavora, Mozambique (September 2018 - July 2019). DFFE. doi: 10.15493/DEA.MIMS.04392023.

Ismail H, van den Berg MA, Lamont T. 2023. Raw temperature data for long-term observations of bottom temperatures at Ponta Zavora, Mozambique (July 2019 - November 2020). DFFE. doi: 10.15493/DEA.MIMS.04412023.

Ismail H, van den Berg MA, Lamont T. 2023.Long-term observations of hourly bottom temperatures at Ponta Zavora, Mozambique (April 2006 - July 2007). DFFE. doi: 10.15493/DEA.MIMS.04202023.

Ismail H, van den Berg MA, Lamont T. 2023. Long-term observations of hourly bottom temperatures at Ponta Zavora, Mozambique (July 2007 - February 2010). DFFE. doi: 10.15493/DEA.MIMS.04212023.

Ismail H, van den Berg MA, Lamont T. 2023. Long-term observations of hourly bottom temperatures at Ponta Zavora, Mozambique (February 2010 - May 2011). DFFE. doi: 10.15493/DEA.MIMS.04222023.

Ismail H, van den Berg MA, Lamont T. 2023. Long-term observations of hourly bottom temperatures at Ponta Zavora, Mozambique (May 2011 - April 2015). DFFE. doi: 10.15493/DEA.MIMS.04232023.

Ismail H, van den Berg MA, Lamont T. 2023. Long-term observations of hourly bottom temperatures at Ponta Zavora, Mozambique (April 2015 - June 2017). DFFE. doi: 10.15493/DEA.MIMS.04242023.

Ismail H, van den Berg MA, Lamont T. 2023. Long-term observations of hourly bottom temperatures at Ponta Zavora,

Mozambique (June 2017 - September 2018). DFFE. doi: 10.15493/DEA.MIMS.04252023.

Ismail H, van den Berg MA, Lamont T. 2023. Long-term observations of hourly bottom temperatures at Ponta Zavora, Mozambique (September 2018 - July 2019). DFFE. doi: 10.15493/DEA.MIMS.04262023.

Ismail H., van den Berg MA, Lamont T. 2023. Long-term observations of hourly bottom temperatures at Ponta Zavora, Mozambique (July 2019 - November 2020). DFFE. doi: 10.15493/DEA.MIMS.04272023.

Ismail H, van den Berg MA, Lamont T. 2023. Raw temperature data for long-term observations of bottom temperatures at Zambia Reef, Mozambique (August 2002 - July 2003). DFFE. doi: 10.15493/DEA.MIMS.05022023.

Ismail H, van den Berg MA, Lamont T. 2023. Raw temperature data for long-term observations of bottom temperatures at Zambia Reef, Mozambique (July 2003 - August 2004). DFFE. doi: 10.15493/DEA.MIMS.05042023.

Ismail H, van den Berg MA, Lamont T. 2023. Raw temperature data for long-term observations of bottom temperatures at Zambia Reef, Mozambique (August 2004 - April 2005). DFFE. doi: 10.15493/DEA.MIMS.05062023.

Ismail H, van den Berg MA, Lamont T. 2023. Raw temperature data for long-term observations of bottom temperatures at Zambia Reef, Mozambique (April 2005 - April 2006). DFFE. doi: 10.15493/DEA.MIMS.05082023.

Ismail H, van den Berg MA, Lamont T. 2023. Raw temperature data for long-term observations of bottom temperatures at Zambia Reef, Mozambique (April 2006 - September 2007). DFFE. doi: 10.15493/DEA.MIMS.05102023.

Ismail H, van den Berg MA, Lamont T. 2023. Raw temperature data for long-term observations of bottom temperatures at Zambia Reef, Mozambique (September 2007 - May 2011). DFFE. doi: 10.15493/DEA.MIMS.05122023.

Ismail H, van den Berg MA, Lamont T. 2023. Raw temperature data for long-term observations of bottom temperatures at Zambia Reef, Mozambique (May 2011 - February 2012). DFFE. doi: 10.15493/DEA.MIMS.05142023.

Ismail H, van den Berg MA, Lamont T. 2023. Raw temperature data for long-term observations of bottom temperatures at Zambia Reef, Mozambique (February 2012 - April 2021). DFFE. doi: 10.15493/DEA.MIMS.05162023.

Ismail H, van den Berg MA, Lamont T. 2023. Long-term observations of hourly bottom temperatures at Zambia Reef, Mozambique (August 2002 - July 2003). DFFE. doi: 10.15493/DEA.MIMS.04942023.

Ismail H, van den Berg MA, Lamont T. 2023. Long-term observations of hourly bottom temperatures at Zambia Reef, Mozambique (July 2003 - August 2004). DFFE. doi: 10.15493/DEA.MIMS.04952023.

Ismail H, van den Berg MA, Lamont T. 2023. Long-term observations of hourly bottom temperatures at Zambia Reef, Mozambique (August 2004 - April 2005). DFFE. doi: 10.15493/DEA.MIMS.04962023.

Ismail H, van den Berg MA, Lamont T. 2023. Long-term observations of hourly bottom temperatures at Zambia Reef, Mozambique (April 2005 - April 2006). DFFE. doi: 10.15493/DEA.MIMS.04972023.

Ismail H, van den Berg MA, Lamont T. 2023. Long-term observations of hourly bottom temperatures at Zambia Reef, Mozambique (April 2006 - September 2007). DFFE. doi: 10.15493/DEA.MIMS.04982023.

Ismail H, van den Berg MA, Lamont T. 2023. Long-term observations of hourly bottom temperatures at Zambia Reef, Mozambique (September 2007 - May 2011). DFFE. doi: 10.15493/DEA.MIMS.04992023.

Ismail H, van den Berg MA, Lamont T. 2023. Long-term observations of hourly bottom temperatures at Zambia Reef, Mozambique (May 2011 - February 2012). DFFE. doi: 10.15493/DEA.MIMS.05002023.

Ismail H, van den Berg MA, Lamont T. 2023. Long-term observations of hourly bottom temperatures at Zambia Reef, Mozambique (February 2012 - April 2021). DFFE. doi: 10.15493/DEA.MIMS.05012023.

Ismail H, van den Berg MA, Lamont T. 2023. Raw temperature data for long-term observations of bottom temperatures at Mozambique Island, Mozambique (August 2002 - July 2003). DFFE. doi: 10.15493/DEA.MIMS.03542023.

Ismail H, van den Berg MA, Lamont T. 2023. Raw temperature data for long-term observations of bottom temperatures at Mozambique Island, Mozambique (July 2003 - September 2004). DFFE. doi: 10.15493/DEA.MIMS.03562023.

Ismail H, van den Berg MA, Lamont T. 2023. Raw temperature data for long-term observations of bottom temperatures at Mozambique Island, Mozambique (September 2004 - October 2007). DFFE. doi: 10.15493/DEA.MIMS.03582023.

Ismail H, van den Berg MA, Lamont T. 2023. Raw temperature data for long-term observations of bottom temperatures at Mozambique Island, Mozambique (October 2007 - February 2012). DFFE. doi: 10.15493/DEA.MIMS.03602023.

Ismail H, van den Berg MA, Lamont T. 2023. Raw temperature data for long-term observations of bottom temperatures at Mozambique Island, Mozambique (February 2012 - May 2021). DFFE. doi: 10.15493/DEA.MIMS.03622023.

Ismail H, van den Berg MA, Lamont T. 2023. Long-term observations of hourly bottom temperatures at Mozambique Island, Mozambique (August 2002 - July 2003). DFFE. doi: 10.15493/DEA.MIMS.03492023.

Ismail H, van den Berg MA, Lamont T. 2023. Long-term observations of hourly bottom temperatures at Mozambique Island, Mozambique (July 2003 - September 2004). DFFE. doi: 10.15493/DEA.MIMS.03502023.

Ismail H, van den Berg MA, Lamont T. 2023. Long-term observations of hourly bottom temperatures at Mozambique Island, Mozambique (September 2004 - October 2007). DFFE. doi: 10.15493/DEA.MIMS.03512023.

Ismail H, van den Berg MA, Lamont T. 2023. Long-term observations of hourly bottom temperatures at Mozambique Island, Mozambique (October 2007 - February 2012). DFFE. doi: 10.15493/DEA.MIMS.03522023.

Ismail H, van den Berg MA, Lamont T. 2023. Long-term observations of hourly bottom temperatures at Mozambique Island, Mozambique (February 2012 - May 2021). DFFE. doi: 10.15493/DEA.MIMS.03532023.

Ismail H, van den Berg MA, Lamont T. 2023. Raw temperature data for long-term observations of Bottom Temperatures at Songa Mnara, Tanzania (August 2004 - October 2007). DFFE. doi: 10.15493/DEA.MIMS.11252023.

Ismail H, van den Berg MA, Lamont T. 2023. Long-term observations of hourly bottom temperatures at Songa Mnara, Tanzania (August 2004 - October 2007). DFFE. doi: 10.15493/DEA.MIMS.11242023.

Ismail H, van den Berg MA, Lamont T. 2023. Raw temperature data for long-term observations of Bottom Temperatures at Zanzibar, Tanzania (July 2003 - August 2004). DFFE. doi: 10.15493/DEA.MIMS.11272023.

Ismail H, van den Berg MA, Lamont T. 2023. Raw temperature data for long-term observations of Bottom Temperatures at Zanzibar, Tanzania (August 2004 - October 2007). DFFE. doi: 10.15493/DEA.MIMS.11292023.

Ismail H, van den Berg MA, Lamont T. 2023. Raw temperature data for long-term observations of Bottom Temperatures

at Zanzibar, Tanzania (October 2007 - September 2010). DFFE. doi: 10.15493/DEA.MIMS.11312023.

Ismail H, van den Berg MA, Lamont T. 2023. Raw temperature data for long-term observations of Bottom Temperatures at Zanzibar, Tanzania (September 2010 - February 2013). DFFE. doi: 10.15493/DEA.MIMS.11332023.

Ismail H, van den Berg MA, Lamont T. 2023. Long-term observations of hourly bottom temperatures at Zanzibar, Tanzania (July 2003 - August 2004). DFFE. doi: 10.15493/DEA.MIMS.11262023.

Ismail H, van den Berg MA, Lamont T. 2023. Long-term observations of hourly bottom temperatures at Zanzibar, Tanzania (August 2004 - October 2007). DFFE. doi: 10.15493/DEA.MIMS.11282023.

Ismail H, van den Berg MA, Lamont T. 2023. Long-term observations of hourly bottom temperatures at Zanzibar, Tanzania (October 2007 - September 2010). DFFE. doi: 10.15493/DEA.MIMS.11302023.

Ismail H, van den Berg MA, Lamont T. 2023. Long-term observations of hourly bottom temperatures at Zanzibar, Tanzania (September 2010 - February 2013). DFFE. doi: 10.15493/DEA.MIMS.11322023.

Ismail H, van den Berg MA, Lamont T. 2023. Raw temperature data for long-term observations of Bottom Temperatures at Mnemba Atoll, Zanzibar, Tanzania (September 2010 - February 2013). DFFE. doi: 10.15493/DEA.MIMS.11352023.

Ismail H, van den Berg MA, Lamont T. 2023. Raw temperature data for long-term observations of Bottom Temperatures at Mnemba Atoll, Zanzibar, Tanzania (February 2013 - March 2017). DFFE. doi: 10.15493/DEA.MIMS.11372023.

Ismail H, van den Berg MA, Lamont T. 2023. Long-term observations of hourly bottom temperatures at Mnemba Atoll, Zanzibar, Tanzania (September 2010 - February 2013). DFFE. doi: 10.15493/DEA.MIMS.11342023.

Ismail H, van den Berg MA, Lamont T. 2023. Long-term observations of hourly bottom temperatures at Mnemba Atoll, Zanzibar, Tanzania (February 2013 - March 2017). DFFE. doi: 10.15493/DEA.MIMS.11362023.

Ismail H, van den Berg MA, Lamont T. 2023. Raw temperature data for long-term observations of Bottom Temperatures at Grande Comore, Comoros (August 2003 - August 2004). DFFE. doi: 10.15493/DEA.MIMS.11392023.

Ismail H, van den Berg MA, Lamont T. 2023. Raw temperature data for long-term observations of Bottom Temperatures at Grande Comore, Comoros (August 2004 - October 2007). DFFE. doi: 10.15493/DEA.MIMS.11412023.

Ismail H, van den Berg MA, Lamont T. 2023. Long-term observations of hourly bottom temperatures at Grande Comore, Comoros (August 2003 - August 2004). DFFE. doi: 10.15493/DEA.MIMS.11382023.

Ismail H, van den Berg MA, Lamont T. 2023. Long-term observations of hourly bottom temperatures at Grande Comore, Comoros (August 2004 - October 2007). DFFE. doi: 10.15493/DEA.MIMS.11402023.

Jacobs L. 2023. South African National Antarctic Expedition (SANAE) on the SA Agulhas II Voyage 049, November 2021. DFFE. doi: 10.15493/DEA.MIMS.05312023.

Jacobs L, Anders D, van den Berg MA, Lamont T. 2023. Processed underway Thermosalinograph (TSG) observations from the Integrated Ecosystem Programme: Southern Benguela (IEP:SB) on the Algoa Voyage 282, May 2022. DFFE. doi: 10.15493/DEA.MIMS.01252023.

Jacobs L, Anders D, van den Berg MA, Lamont T. 2023. Raw underway Thermosalinograph (TSG) observations from the Integrated Ecosystem Programme: Southern Benguela (IEP:SB) on the Algoa Voyage 282, May 2022. DFFE. doi: 10.15493/DEA.MIMS.01262023.

Jacobs L, Frantz F, van den Berg MA, Lamont T. 2023. Processed underway Thermosalinograph (TSG) observations from the Transkei Shelf Oceanography Cruise on the Algoa Voyage 241, July 2017. DFFE. doi: 10.15493/DEA.MIMS.09862023.

Jacobs L, Frantz F, van den Berg MA, Lamont T. 2023. Raw underway Thermosalinograph (TSG) observations from the Transkei Shelf Oceanography Cruise on the Algoa Voyage 241, July 2017. DFFE. doi: 10.15493/DEA.MIMS.09872023.

Jacobs L, van den Berg MA, Lamont T. 2023. Processed underway Thermosalinograph (TSG) observations from the Algoa Voyage 254, November 2018. DFFE. doi: 10.15493/DEA.MIMS.07512023.

Jacobs L, van den Berg MA, Lamont T. 2023. Raw underway Thermosalinograph (TSG) observations from the Algoa Voyage 254, November 2018. DFFE. doi: 10.15493/DEA.MIMS.07522023.

Jacobs L, van den Berg MA, Lamont T. 2023. Processed underway Thermosalinograph (TSG) observations from the Algoa Voyage 271, March 2021. DFFE. doi: 10.15493/DEA.MIMS.07532023.

Jacobs L, van den Berg MA, Lamont T. 2023. Raw underway Thermosalinograph (TSG) observations from Algoa Voyage 271, March 2021. DFFE. doi: 10.15493/DEA.MIMS.07542023.

Jacobs L, van den Berg MA, Lamont T. 2023. Processed underway Thermosalinograph (TSG) observations from the Integrated Ecosystem Programme: Southern Benguela (IEP:SB) cruise on the Algoa Voyage 272, May 2021. DFFE. doi: 10.15493/DEA.MIMS.01172023.

Jacobs L, van den Berg MA, Lamont T. 2023. Raw underway Thermosalinograph (TSG) observations from the Integrated Ecosystem Programme: Southern Benguela (IEP:SB) cruise on the Algoa Voyage 272, May 2021. DFFE. doi: 10.15493/DEA.MIMS.01182023.

Jacobs L, van den Berg MA, Lamont T. 2023. Processed underway Thermosalinograph (TSG) observations from the SAMBA Monitoring Line cruise on the Algoa Voyage 275, September 2021. DFFE. doi: 10.15493/DEA.MIMS.01192023.

Jacobs L, van den Berg MA, Lamont T. 2023. Raw underway Thermosalinograph (TSG) observations from the SAMBA Monitoring Line cruise on the Algoa Voyage 275, September 2021. DFFE. doi: 10.15493/DEA.MIMS.01202023.

Jacobs L, van den Berg MA, Lamont T. 2023. Processed underway Thermosalinograph (TSG) observations from the Benguela Air-Sea CO2 and Heat Flux Experiment on the Algoa Voyage 278, December 2021. DFFE. doi: 10.15493/DEA.MIMS.01212023.

Jacobs L, van den Berg MA, Lamont T. 2023. Raw underway Thermosalinograph (TSG) observations from the Benguela Air-Sea CO2 and Heat Flux Experiment on the Algoa Voyage 278, December 2021. DFFE. doi: 10.15493/DEA.MIMS.01222023.

Jacobs L, van den Berg MA, Lamont T. 2023. Processed underway Thermosalinograph (TSG) observations from the Integrated Ecosystem Programme: Southern Benguela (IEP:SB) on the Algoa Voyage 279, February 2022. DFFE. doi: 10.15493/DEA.MIMS.01232023.

Jacobs L, van den Berg MA, Lamont T. 2023. Raw underway Thermosalinograph (TSG) observations from the Integrated Ecosystem Programme: Southern Benguela (IEP:SB) on the

Algoa Voyage 279, February 2022. DFFE. doi: 10.15493/DEA.MIMS.01242023.

Jacobs L, van den Berg MA, Lamont T. 2023. Processed underway Thermosalinograph (TSG) observations from Algoa Voyage 281, March 2022. DFFE. doi: 10.15493/DEA.MIMS.07552023.

Jacobs L, van den Berg MA, Lamont T. 2023. Raw underway Thermosalinograph (TSG) observations from Algoa Voyage 281, March 2022. DFFE. doi: 10.15493/DEA.MIMS.07562023.

Jacobs L, van den Berg MA, Lamont T. 2023. Processed underway Thermosalinograph (TSG) observations from the Integrated Ecosystem Programme: Southern Benguela (IEP:SB) on the Algoa Voyage 283, August 2022. DFFE. doi: 10.15493/DEA.MIMS.01272023.

Jacobs L, van den Berg MA, Lamont T. 2023. Raw underway Thermosalinograph (TSG) observations from the Integrated Ecosystem Programme: Southern Benguela (IEP:SB) on the Algoa Voyage 283, August 2022. DFFE. doi: 10.15493/DEA.MIMS.01282023.

Jacobs L, van den Berg MA, Lamont T. 2023. Processed underway Thermosalinograph (TSG) observations from the SAMBA Monitoring Line cruise on the Algoa Voyage 285, September 2022. DFFE. doi: 10.15493/DEA.MIMS.01332023.

Jacobs L, van den Berg MA, Lamont T. 2023. Raw underway Thermosalinograph (TSG) observations from the SAMBA Monitoring Line cruise on the Algoa Voyage 285, September 2022. DFFE. doi: 10.15493/DEA.MIMS.01342023.

Jacobs L, van den Berg MA, Lamont T. 2023. Processed underway Thermosalinograph (TSG) observations from the South Atlantic Meridional Overturning Circulation Basin-wide Array (SAMBA) Monitoring Line cruise on the Algoa Voyage 291, March 2023. DFFE. doi: 10.15493/DEA.MIMS.10602023.

Jacobs L, van den Berg MA, Lamont T. 2023. Raw underway Thermosalinograph (TSG) observations from the South Atlantic Meridional Overturning Circulation Basin-wide Array (SAMBA) Monitoring Line cruise on the Algoa Voyage 291, March 2023. DFFE. doi: 10.15493/DEA.MIMS.10612023.

Jacobs L, van den Berg MA, Lamont T. 2023 Processed near-surface underway temperature and salinity (TSG) observations from the South African National Antarctic Expedition (SANAE) on the SA Agulhas II Voyage 005, December 2012. DFFE. doi: 10.15493/DEA.MIMS.01292023.

Jacobs L, van den Berg MA, Lamont T. 2023. Processed near-surface underway Thermosalinograph (TSG) observations from the Marion Island Relief Voyage on the SA Agulhas II Voyage 045, May 2021. DFFE. doi: 10.15493/DEA.MIMS.01372023.

Jacobs L, van den Berg MA, Lamont T. 2023. Raw near-surface underway Thermosalinograph (TSG) observations from the Marion Island Relief Voyage on the SA Agulhas II Voyage 045, May 2021. DFFE. doi: 10.15493/DEA.MIMS.01382023.

Jacobs L, van den Berg MA, Lamont T. 2023. Processed near-surface underway temperature and salinity (TSG) observations from SA Agulhas II Voyage 049 during December 2021 to January 2022. DFFE. doi: 10.15493/DEA.MIMS.01352023.

Jacobs L, van den Berg MA, Lamont T. 2023. Raw near-surface underway temperature and salinity (TSG) observations from SA Agulhas II Voyage 049 during December 2021 to January 2022. DFFE. doi: 10.15493/DEA.MIMS.01362023.

Jacobs L, van den Berg MA, Lamont T. 2023. Processed near-surface underway temperature and salinity (TSG) observations from the Marion Island Relief Voyage on the SA Agulhas II Voyage 051, March 2022. DFFE. doi: 10.15493/DEA.MIMS.01312023

Jacobs L, van den Berg MA, Lamont T. 2023. Raw near-surface underway temperature and salinity (TSG) observations from the Marion Island Relief Voyage on the SA Agulhas II Voyage 051, March 2022. DFFE. doi: 10.15493/DEA.MIMS.01322023.

Jacobs L, van den Berg MA, Lamont T. 2023. Processed near-surface underway temperature and salinity (TSG) observations from the SEAmester and ASCA Scientific Cruise on the SA Agulhas II Voyage 052, June 2022. DFFE. doi: 10.15493/DEA.MIMS.01402023.

Jacobs L, van den Berg MA, Lamont T. 2023. Raw near-surface underway temperature and salinity (TSG) observations from the SEAmester and ASCA Scientific Cruise on the SA Agulhas II Voyage 052, June 2022. DFFE. doi: 10.15493/DEA.MIMS.01412023.

Lamont T, van den Berg MA. 2023. Long-term observations of daily currents on the Prince Edward Island shelf at Mooring 1 (April 2020 - April 2021). DFFE. doi: 10.15493/DEA.MIMS.01442023.

Lamont T, van den Berg MA. 2023. Long-term observations of hourly currents on the Prince Edward Island shelf at Mooring 1 (April 2020 - April 2021). DFFE. doi: 10.15493/DEA.MIMS.01452023.

Lamont T, van den Berg MA. 2023. Long-term observations of daily currents on the Prince Edward Island shelf at Mooring 2 (April 2020 - April 2021). DFFE. doi: 10.15493/DEA.MIMS.01462023.

Lamont T, van den Berg MA. 2023. Long-term observations of hourly currents on the Prince Edward Island shelf at Mooring 2 (April 2020 - April 2021). DFFE. doi: 10.15493/DEA.MIMS.01472023.

Lamont T, van den Berg MA. 2023. Long-term observations of daily currents on the Prince Edward Island shelf at Mooring 1 (April 2021 - May 2022). DFFE. doi: 10.15493/DEA.MIMS.11042023.

Lamont T, van den Berg MA. 2023. Long-term observations of hourly currents on the Prince Edward Island shelf at Mooring 1 (April 2021 - May 2022). DFFE. doi: 10.15493/DEA.MIMS.11052023.

Lamont T, van den Berg MA. 2023. Long-term observations of daily currents on the Prince Edward Island shelf at Mooring 2 (April 2021 - May 2022). DFFE. doi: 10.15493/DEA.MIMS.11062023.

Lamont T, van den Berg MA. 2023. Long-term observations of hourly currents on the Prince Edward Island shelf at Mooring 2 (April 2021 - May 2022). DFFE. doi: 10.15493/DEA.MIMS.11072023.

Lamont T, van den Berg MA. 2023. Long-term observations of daily currents on the Prince Edward Island shelf at Mooring 1 (May 2022 - April 2023). DFFE. doi: 10.15493/DEA.MIMS.11142023.

Lamont T, van den Berg MA. 2023. Long-term observations of hourly currents on the Prince Edward Island shelf at Mooring 1 (May 2022 - April 2023). DFFE. doi: 10.15493/DEA.MIMS.11152023.

Lamont T, van den Berg MA. 2023. Long-term observations of daily currents on the Prince Edward Island shelf at Mooring 2 (May 2022 - April 2023). DFFE. doi: 10.15493/DEA.MIMS.11162023.

Lamont T, van den Berg MA. 2023. Long-term observations of hourly currents on the Prince Edward Island shelf at Mooring 2 (May 2022 - April 2023). DFFE. doi: 10.15493/DEA.MIMS.11172023.

Lamont T, van den Berg MA. 2023. Long-term observations of daily bottom temperatures on the Prince Edward Island shelf at Mooring 1 (April 2020 - April 2021). DFFE. doi: 10.15493/DEA.MIMS.01502023.

Lamont T, van den Berg MA. 2023. Long-term observations of hourly bottom temperatures on the Prince Edward Island shelf at Mooring 1 (April 2020 - April 2021). DFFE. doi: 10.15493/DEA.MIMS.01512023.

Lamont T, van den Berg MA. 2023. Long-term observations of daily bottom temperatures on the Prince Edward Island shelf at Mooring 2 (April 2020 - April 2021). DFFE. doi: 10.15493/DEA.MIMS.01522023.

Lamont T, van den Berg MA. 2023. Long-term observations of hourly bottom temperatures on the Prince Edward Island shelf at Mooring 2 (April 2020 - April 2021). DFFE. doi: 10.15493/DEA.MIMS.01532023.

Lamont T, van den Berg MA. 2023. Long-term observations of daily bottom temperatures on the Prince Edward Island shelf at Mooring 1 (April 2021 - May 2022). DFFE. doi: 10.15493/DEA.MIMS.11082023.

Lamont T, van den Berg MA. 2023. Long-term observations of hourly bottom temperatures on the Prince Edward Island shelf at Mooring 1 (April 2021 - May 2022). DFFE. doi: 10.15493/DEA.MIMS.11092023.

Lamont T, van den Berg MA. 2023. Long-term observations of daily bottom temperatures on the Prince Edward Island shelf at Mooring 2 (April 2021 - May 2022). DFFE. doi: 10.15493/DEA.MIMS.11102023.

Lamont T, van den Berg MA. 2023. Long-term observations of hourly bottom temperatures on the Prince Edward Island shelf at Mooring 2 (April 2021 - May 2022). DFFE. doi: 10.15493/DEA.MIMS.11112023.

Lamont T, van den Berg MA. 2023. Long-term observations of daily bottom temperatures on the Prince Edward Island shelf at Mooring 1 (May 2022 - April 2023). DFFE. doi: 10.15493/DEA.MIMS.11182023.

Lamont T, van den Berg MA. 2023. Long-term observations of hourly bottom temperatures on the Prince Edward Island shelf at Mooring 1 (May 2022 - April 2023). DFFE doi: 10.15493/DEA.MIMS.11192023.

Lamont T, van den Berg MA. 2023. Long-term observations of daily bottom temperatures on the Prince Edward Island shelf at Mooring 2 (May 2022 - April 2023). DFFE. doi: 10.15493/DEA.MIMS.11202023.

Lamont T, van den Berg MA. 2023. Long-term observations of hourly bottom temperatures on the Prince Edward Island shelf at Mooring 2 (May 2022 - April 2023). DFFE. doi: 10.15493/DEA.MIMS.11212023.

Lamont T, van den Berg MA. 2023. Raw Acoustic Doppler Current Profiler (ADCP) data for long-term observations of currents on the Prince Edward Island shelf at Mooring 2 (April 2020 - April 2021). DFFE. doi: 10.15493/DEA.MIMS.01482023.

Lamont T, van den Berg MA. 2023. Raw Acoustic Doppler Current Profiler (ADCP) data for long-term observations of currents on the Prince Edward Island shelf at Mooring 1 (April 2020 - April 2021). DFFE. doi: 10.15493/DEA.MIMS.01492023.

Lamont T, van den Berg MA. 2023. Raw ADCP Data for long-term observations of currents on the Prince Edward Island shelf at Mooring 1 (April 2021 - May 2022). DFFE. doi: 10.15493/DEA.MIMS.11022023.

Lamont T, van den Berg MA. 2023. Raw ADCP Data for long-term observations of currents on the Prince Edward Island shelf at Mooring 2 (April 2021 - May 2022). DFFE. doi: 10.15493/DEA.MIMS.11032023.

Lamont T, van den Berg MA. 2023. Raw ADCP Data for long-term observations of currents on the Prince Edward Island shelf at Mooring 1 (May 2022 - April 2023). DFFE. doi: 10.15493/DEA.MIMS.11122023.

Lamont T, van den Berg MA. 2023. Raw ADCP Data for long-term observations of currents on the Prince Edward Island shelf at Mooring 2 (May 2022 - April 2023). DFFE. doi: 10.15493/DEA.MIMS.11132023.

Lamont T, van den Berg MA. 2023. Long-term observations of daily currents at SAMBA Mooring 4 (October 2018 - September 2020). DFFE. doi: 10.15493/DEA.MIMS.01582023.

Lamont T, van den Berg MA. 2023. Long-term observations of hourly currents at SAMBA Mooring 4 (October 2018 - September 2020). DFFE. doi: 10.15493/DEA.MIMS.01592023.

Lamont T, van den Berg MA. 2023. Long-term observations of daily currents along at SAMBA Mooring 8 (October 2018 - October 2020). DFFE. doi: 10.15493/DEA.MIMS.01602023.

Lamont T, van den Berg MA. 2023. Long-term observations of daily currents measured by DVS at SAMBA Mooring 8 (October 2018 - October 2020). DFFE. doi: 10.15493/DEA.MIMS.01612023.

Lamont T, van den Berg MA. 2023. Long-term observations of hourly currents at SAMBA Mooring 8 (October 2018 - October 2020). DFFE. doi: 10.15493/DEA.MIMS.01622023.

Lamont T, van den Berg MA. 2023. Long-term observations of hourly currents measured by DVS at SAMBA Mooring 8 (October 2018 - October 2020). DFFE. doi: 10.15493/DEA.MIMS.01632023.

Lamont T, van den Berg MA. 2023. Long-term observations of daily currents at SAMBA Mooring 9 (October 2018 - October 2020). DFFE. doi: 10.15493/DEA.MIMS.01642023.

Lamont T, van den Berg MA. 2023. Long-term observations of daily currents measured by DVS at SAMBA Mooring 9 (October 2018 - October 2020). DFFE. doi: 10.15493/DEA.MIMS.01652023.

Lamont T, van den Berg MA. 2023. Long-term observations of hourly currents at SAMBA Mooring 9 (October 2018 - October 2020). DFFE. doi: 10.15493/DEA.MIMS.01662023.

Lamont T, van den Berg MA. 2023. Long-term observations of hourly currents measured by DVS at SAMBA Mooring 9 (October 2018 - October 2020). DFFE. doi: 10.15493/DEA.MIMS.01672023.

Lamont T, van den Berg MA. 2023. Long-term observations of daily currents at SAMBA Mooring 10 (October 2018 - October 2020). DFFE. doi: 10.15493/DEA.MIMS.01682023.

Lamont T, van den Berg MA. 2023. Long-term observations of hourly currents at SAMBA Mooring 10 (October 2018 - October 2020). DFFE. doi: 10.15493/DEA.MIMS.01692023.

Lamont T, van den Berg MA. 2023. Long-term observations of daily bottom temperatures at location Mooring 4 (October 2018 - September 2020). DFFE. doi: 10.15493/DEA.MIMS.01702023.

Lamont T, van den Berg MA. 2023. Long-term observations of hourly bottom temperatures at location Mooring 4 (October 2018 - September 2020). DFFE. doi: 10.15493/DEA.MIMS.01712023.

Lamont T, van den Berg MA. 2023. Long-term observations of daily subsurface temperatures at location Mooring 8 (October 2018 - October 2020). DFFE. doi: 10.15493/DEA.MIMS.01722023.

Lamont T, van den Berg MA. 2023. Long-term observations of hourly subsurface temperatures at location Mooring 8 (Oc-

tober 2018 - October 2020). DFFE. doi: 10.15493/DEA.MIMS.01732023.

Lamont T, van den Berg MA. 2023. Long-term observations of daily subsurface temperatures at location Mooring 9 (October 2018 - October 2020). DFFE. doi: 10.15493/DEA.MIMS.01742023.

Lamont T, van den Berg MA. 2023. Long-term observations of hourly subsurface temperatures at location Mooring 9 (October 2018 - October 2020). DFFE. doi: 10.15493/DEA.MIMS.01752023.

Lamont T, van den Berg MA. 2023. Long-term observations of daily subsurface temperatures at location Mooring 10 (October 2018 - October 2020). DFFE. doi: 10.15493/DEA.MIMS.01762023.

Lamont T, van den Berg MA. 2023. Long-term observations of hourly subsurface temperatures at location Mooring 10 (October 2018 - October 2020). DFFE. doi: 10.15493/DEA.MIMS.01772023.

Lamont T, van den Berg MA. 2023. Raw Acoustic Doppler Current Profiler (ADCP) data for long-term observations of currents at SAMBA Mooring 4 (October 2018 - September 2020). DFFE. doi: 10.15493/DEA.MIMS.01542023.

Lamont T, van den Berg MA. 2023. Raw Acoustic Doppler Current Profiler (ADCP) data from long-term observations of currents at SAMBA Mooring 8 (October 2018 - October 2020). DFFE. doi: 10.15493/DEA.MIMS.01552023.

Lamont T, van den Berg MA. 2023. Raw Acoustic Doppler Current Profiler (ADCP) data from long-term observations of currents at SAMBA Mooring 9 (October 2018 - October 2020). DFFE. doi: 10.15493/DEA.MIMS.01562023.

Lamont T, van den Berg MA. 2023. Raw Acoustic Doppler Current Profiler (ADCP) data from long-term observations of currents at SAMBA Mooring 10 (October 2018 - October 2020). DFFE. doi: 10.15493/DEA.MIMS.01572023.

Makhetha M, Tutt G, Lamont T. 2023. Processed CTD discrete observations from the Anchovy Recruitment on the Africana Voyage 047, August 1986. DFFE. doi: 10.15493/DEA.MIMS.03632023.

Makhetha M, Tutt G, Lamont T. 2023. Processed CTD discrete observations from the South Coast Hake Biomass Survey on the Africana Voyage 048, September 1986. DFFE. doi: 10.15493/DEA.MIMS.04352023.

Makhetha M, Tutt G, Lamont T. 2023. Processed CTD discrete observations from the West Coast Hake Biomass Survey on the Africana Voyage 050, January 1987. DFFE. doi: 10.15493/DEA.MIMS.04462023.

Makhetha M, Tutt G, Lamont T. 2023. Processed CTD discrete observations from the West Coast Hake Biomass Survey on the Africana Voyage 054, June 1987. DFFE. doi: 10.15493/DEA.MIMS.05092023.

Makhetha M, Tutt G, Lamont T. 2023. Processed CTD discrete observations from the South Coast Hake Biomass Survey on the Africana Voyage 056, September 1987. DFFE. doi: 10.15493/DEA.MIMS.05172023.

Makhetha M, Tutt G, Lamont T. 2023. Processed CTD discrete observations from the Anchovy and Pilchard Spawning Stock Survey on the Africana Voyage 057, November 1987. DFFE. doi: 10.15493/DEA.MIMS.05212023.

Makhetha M, Tutt G, Lamont T. 2023. Processed CTD discrete observations from the South Coast Hake Biomass Survey on the Africana Voyage 063, May 1988. DFFE. doi: 10.15493/DEA.MIMS.05292023.

Makhetha M, Tutt G, Lamont T. 2023. Processed CTD discrete observations from the Physical-Chemical Oceanography Cruise on the Africana Voyage 067, September 1988. DFFE. doi: 10.15493/DEA.MIMS.11502023.

Makhetha M, Tutt G, Lamont T. 2023. Processed CTD discrete observations from the West Coast Hake Biomass Survey on the Africana Voyage 069, January 1989. DFFE. doi: 10.15493/DEA.MIMS.11532023.

Makhetha M, Tutt G, Lamont T. 2023. Processed CTD discrete observations from the Physical-Chemical Oceanography Cruise on the Africana Voyage 070, March 1989. DFFE. doi: 10.15493/DEA.MIMS.11562023.

Makhetha M, Tutt G, Lamont T. 2023. Processed CTD discrete observations from the South-east Atlantic Expedition on the Africana Voyage 071, April 1989. DFFE. doi: 10.15493/DEA.MIMS.11592023.

Makhetha M, Tutt G, Lamont T. 2023. Processed CTD discrete observations from the West Coast Hake Biomass Survey on the Africana Voyage 075, July 1989. DFFE. doi: 10.15493/DEA.MIMS.11692023.

Makhetha M, Tutt G, Lamont T. 2023. Processed CTD discrete observations from the Physical-Chemical Oceanography Cruise on the Africana Voyage 077, September 1989. DFFE. doi: 10.15493/DEA.MIMS.11722023.

Makhetha M, Tutt G, Lamont T. 2023. Processed CTD discrete observations from the Pelagic Fish Biomass Survey on the Africana Voyage 078, November 1989. DFFE. doi: 10.15493/DEA.MIMS.11752023.

Sabelani Z, Ismail H, van den Berg MA, Lamont T. 2023. Raw temperature data for long-term observations of bottom temperatures at Plettenberg Bay, South Africa (April 1991 - June 1991). DFFE. doi: 10.15493/DEA.MIMS.05342023.

Sabelani Z, Ismail H, van den Berg MA, Lamont T. 2023. Raw temperature data for long-term observations of bottom temperatures at Plettenberg Bay, South Africa (June 1991 - January 1992). DFFE. doi: 10.15493/DEA.MIMS.05352023.

Sabelani Z, Ismail H, van den Berg MA, Lamont T. 2023. Raw temperature data for long-term observations of bottom temperatures at Plettenberg Bay, South Africa (January 1992 - August 1992). DFFE. doi: 10.15493/DEA.MIMS.05372023.

Sabelani Z, Ismail H, van den Berg MA, Lamont T. 2023. Raw temperature data for long-term observations of bottom temperatures at Plettenberg Bay, South Africa (August 1992 - November 1992). DFFE. doi: 10.15493/DEA.MIMS.05382023.

Sabelani Z, Ismail H, van den Berg MA, Lamont T. 2023. Raw temperature data for long-term observations of bottom temperatures at Plettenberg Bay, South Africa (November 1992 - January 1993). DFFE. doi: 10.15493/DEA.MIMS.05392023.

Sabelani Z, Ismail H, van den Berg MA, Lamont T. 2023. Raw temperature data for long-term observations of bottom temperatures at Plettenberg Bay, South Africa (January 1993 - August 1993). DFFE. doi: 10.15493/DEA.MIMS.05402023.

Sabelani Z, Ismail H, van den Berg MA, Lamont T. 2023. Raw temperature data for long-term observations of bottom temperatures at Plettenberg Bay, South Africa (August 1993 - November 1993). DFFE. doi: 10.15493/DEA.MIMS.05412023.

Sabelani Z, Ismail H, van den Berg MA, Lamont T. 2023. Raw temperature data for long-term observations of bottom temperatures at Plettenberg Bay, South Africa (November 1993 - March 1994). DFFE. doi: 10.15493/DEA.MIMS.05422023.

Sabelani Z, Ismail H, van den Berg MA, Lamont T. 2023. Raw temperature data for long-term observations of bottom tem-

peratures at Plettenberg Bay, South Africa (March 1994 - August 1994). DFFE. doi: 10.15493/DEA.MIMS.05432023.

Sabelani Z, Ismail H, van den Berg MA, Lamont T. 2023. Raw temperature data for long-term observations of bottom temperatures at Plettenberg Bay, South Africa (August 1994 - October 1994). DFFE. doi: 10.15493/DEA.MIMS.05442023.

Sabelani Z, Ismail H, van den Berg MA, Lamont T. 2023. Raw temperature data for long-term observations of bottom temperatures at Plettenberg Bay, South Africa (October 1994 - March 1995). DFFE. doi: 10.15493/DEA.MIMS.05452023.

Sabelani Z, Ismail H, van den Berg MA, Lamont T. 2023. Raw temperature data for long-term observations of bottom temperatures at Plettenberg Bay, South Africa (March 1995 - July 1995). DFFE. doi: 10.15493/DEA.MIMS.05462023.

Sabelani Z, Ismail H, van den Berg MA, Lamont T. 2023. Long-term observations of hourly bottom temperatures at Plettenberg Bay, South Africa (April 1991 - June 1991). DFFE. doi: 10.15493/DEA.MIMS.05472023.

Sabelani Z, Ismail H, van den Berg MA, Lamont T. 2023. Long-term observations of hourly bottom temperatures at Plettenberg Bay, South Africa (June 1991 - January 1992). DFFE. doi: 10.15493/DEA.MIMS.05482023.

Sabelani Z, Ismail H, van den Berg MA, Lamont T. 2023. Long-term observations of hourly bottom temperatures at Plettenberg Bay, South Africa (January 1992 - August 1992). DFFE. doi: 10.15493/DEA.MIMS.05492023.

Sabelani Z, Ismail H, van den Berg MA, Lamont T. 2023. Long-term observations of hourly bottom temperatures at Plettenberg Bay, South Africa (August 1992 - November 1992). DFFE. doi: 10.15493/DEA.MIMS.05502023.

Sabelani Z, Ismail H, van den Berg MA, Lamont T. 2023. Long-term observations of hourly bottom temperatures at Plettenberg Bay, South Africa (November 1992 - January 1993). DFFE. doi: 10.15493/DEA.MIMS.05512023.

Sabelani Z, Ismail H, van den Berg MA, Lamont T. 2023. Long-term observations of hourly bottom temperatures at Plettenberg Bay, South Africa (January 1993 - August 1993). DFFE. doi: 10.15493/DEA.MIMS.05522023.

Sabelani Z, Ismail H, van den Berg MA, Lamont T. 2023. Long-term observations of hourly bottom temperatures at Plettenberg Bay, South Africa (August 1993 - November 1993). DFFE. doi: 10.15493/DEA.MIMS.05532023.

Sabelani Z, Ismail H, van den Berg MA, Lamont T. 2023. Long-term observations of hourly bottom temperatures at Plettenberg Bay, South Africa (November 1993 - March 1994). DFFE. doi: 10.15493/DEA.MIMS.05542023.

Sabelani Z, Ismail H, van den Berg MA, Lamont T. 2023. Long-term observations of hourly bottom temperatures at Plettenberg Bay, South Africa (March 1994 - August 1994). DFFE. doi: 10.15493/DEA.MIMS.05552023.

Sabelani Z, Ismail H, van den Berg MA, Lamont T. 2023. Long-term observations of hourly bottom temperatures at Plettenberg Bay, South Africa (August 1994 - October 1994). DFFE. doi: 10.15493/DEA.MIMS.05562023.

Sabelani Z, Ismail H, van den Berg MA, Lamont T. 2023. Long-term observations of hourly bottom temperatures at Plettenberg Bay, South Africa (October 1994 - March 1995). DFFE. doi: 10.15493/DEA.MIMS.05572023.

Sabelani Z, Ismail H, van den Berg MA, Lamont T. 2023. Long-term observations of hourly bottom temperatures at Plettenberg Bay, South Africa (March 1995 - July 1995). DFFE. doi: 10.15493/DEA.MIMS.05582023.

Sabelani Z, Ismail H, van den Berg MA, Lamont T. 2023. Raw temperature data for long-term observations of bottom temperatures at Mangolds Pool, South Africa (January 1992 - May 1992). DFFE. doi: 10.15493/DEA.MIMS.09362023.

Sabelani Z, Ismail H, van den Berg MA, Lamont T. 2023. Raw temperature data for long-term observations of bottom temperatures at Mangolds Pool, South Africa (May 1992 - August 1992). DFFE. doi: 10.15493/DEA.MIMS.09372023.

Sabelani Z, Ismail H, van den Berg MA, Lamont T. 2023. Raw temperature data for long-term observations of bottom temperatures at Mangolds Pool, South Africa (August 1992 - November 1992). DFFE. doi: 10.15493/DEA.MIMS.09382023.

Sabelani Z, Ismail H, van den Berg MA, Lamont T. 2023. Raw temperature data for long-term observations of bottom temperatures at Mangolds Pool, South Africa (November 1992 - January 1993). DFFE. doi: 10.15493/DEA.MIMS.09392023.

Sabelani Z, Ismail H, van den Berg MA, Lamont T. 2023. Raw temperature data for long-term observations of bottom temperatures at Mangolds Pool, South Africa (January 1993 - June 1993). DFFE. doi: 10.15493/DEA.MIMS.09402023.

Sabelani Z, Ismail H, van den Berg MA, Lamont T. 2023. Raw temperature data for long-term observations of bottom temperatures at Mangolds Pool, South Africa (June 1993 - November 1993). DFFE. doi: 10.15493/DEA.MIMS.09412023.

Sabelani Z, Ismail H, van den Berg MA, Lamont T. 2023. Raw temperature data for long-term observations of bottom temperatures at Mangolds Pool, South Africa (November 1993 - March 1994). DFFE. doi: 10.15493/DEA.MIMS.09422023.

Sabelani Z, Ismail H, van den Berg MA, Lamont T. 2023. Raw temperature data for long-term observations of bottom temperatures at Mangolds Pool, South Africa (March 1994 - August 1994). DFFE. doi: 10.15493/DEA.MIMS.09432023.

Sabelani Z, Ismail H, van den Berg MA, Lamont T. 2023. Raw temperature data for long-term observations of bottom temperatures at Mangolds Pool, South Africa (August 1994 - October 1994). DFFE. doi: 10.15493/DEA.MIMS.09442023.

Sabelani Z, Ismail H, van den Berg MA, Lamont T. 2023. Raw temperature data for long-term observations of bottom temperatures at Mangolds Pool, South Africa (October 1994 - April 1995). DFFE. doi: 10.15493/DEA.MIMS.09452023.

Sabelani Z, Ismail H, van den Berg MA, Lamont T. 2023. Raw temperature data for long-term observations of bottom temperatures at Mangolds Pool, South Africa (April 1995 - July 1995). DFFE. doi: 10.15493/DEA.MIMS.09462023.

Sabelani Z, Ismail H, van den Berg MA, Lamont T. 2023. Raw temperature data for long-term observations of bottom temperatures at Mangolds Pool, South Africa (July 1995 - November 1995). DFFE. doi: 10.15493/DEA.MIMS.09472023.

Sabelani Z, Ismail H, van den Berg MA, Lamont T. 2023. Raw temperature data for long-term observations of bottom temperatures at Mangolds Pool, South Africa (November 1995 - April 1996). DFFE. doi: 10.15493/DEA.MIMS.09482023.

Sabelani Z, Ismail H, van den Berg MA, Lamont T. 2023. Raw temperature data for long-term observations of bottom temperatures at Mangolds Pool, South Africa (April 1996 - October 1996). DFFE. doi: 10.15493/DEA.MIMS.09492023.

Sabelani Z, Ismail H, van den Berg MA, Lamont T. 2023. Raw temperature data for long-term observations of bottom temperatures at Mangolds Pool, South Africa (October 1996 - May 1997). DFFE. doi: 10.15493/DEA.MIMS.09502023.

Sabelani Z, Ismail H, van den Berg MA, Lamont T. 2023. Raw temperature data for long-term observations of bottom temperatures at Mangolds Pool, South Africa (March 2000 - Au-

gust 2000). DFFE. doi: 10.15493/DEA.MIMS.09512023.
Sabelani Z, Ismail H, van den Berg MA, Lamont T. 2023. Raw temperature data for long-term observations of bottom temperatures at Mangolds Pool, South Africa (August 2000 - March 2001). DFFE. doi: 10.15493/DEA.MIMS.09522023.
Sabelani Z, Ismail H, van den Berg MA, Lamont T. 2023. Raw temperature data for long-term observations of bottom temperatures at Mangolds Pool, South Africa (March 2001 - July 2001). DFFE. doi: 10.15493/DEA.MIMS.09532023.
Sabelani Z, Ismail H, van den Berg MA, Lamont T. 2023. Raw temperature data for long-term observations of bottom temperatures at Mangolds Pool, South Africa (July 2001 - November 2001). DFFE. doi: 10.15493/DEA.MIMS.09542023.
Sabelani Z, Ismail H, van den Berg MA, Lamont T. 2023. Raw temperature data for long-term observations of bottom temperatures at Mangolds Pool, South Africa (November 2001 - November 2002). DFFE. doi: 10.15493/DEA.MIMS.09552023.
Sabelani Z, Ismail H, van den Berg MA, Lamont T. 2023. Raw temperature data for long-term observations of bottom temperatures at Mangolds Pool, South Africa (November 2002 - June 2003). DFFE. doi: 10.15493/DEA.MIMS.09562023.
Sabelani Z, Ismail H, van den Berg MA, Lamont T. 2023. Raw temperature data for long-term observations of bottom temperatures at Mangolds Pool, South Africa (November 2003 - June 2004). DFFE. doi: 10.15493/DEA.MIMS.09572023.
Sabelani Z, Ismail H, van den Berg MA, Lamont T. 2023. Raw temperature data for long-term observations of bottom temperatures at Mangolds Pool, South Africa (June 2004 - November 2004). DFFE. doi: 10.15493/DEA.MIMS.09582023.
Sabelani Z, Ismail H, van den Berg MA, Lamont T. 2023. Raw temperature data for long-term observations of bottom temperatures at Mangolds Pool, South Africa (November 2004 - November 2005). DFFE. doi: 10.15493/DEA.MIMS.09592023.
Sabelani Z, Ismail H, van den Berg MA, Lamont T. 2023. Long-term observations of hourly bottom temperatures at Mangolds Pool, South Africa (January 1992 - May 1992). DFFE. doi: 10.15493/DEA.MIMS.09602023.
Sabelani Z, Ismail H, van den Berg MA, Lamont T. 2023. Long-term observations of hourly bottom temperatures at Mangolds Pool, South Africa (May 1992 - August 1992). DFFE. doi: 10.15493/DEA.MIMS.09612023.
Sabelani Z, Ismail H, van den Berg MA, Lamont T. 2023. Long-term observations of hourly bottom temperatures at Mangolds Pool, South Africa (August 1992 - November 1992). DFFE. doi: 10.15493/DEA.MIMS.09622023.
Sabelani Z, Ismail H, van den Berg MA, Lamont T. 2023. Long-term observations of hourly bottom temperatures at Mangolds Pool, South Africa (November 1992 - January 1993). DFFE. doi: 10.15493/DEA.MIMS.09632023.
Sabelani Z, Ismail H, van den Berg MA, Lamont T. 2023. Long-term observations of hourly bottom temperatures at Mangolds Pool, South Africa (January 1993 - June 1993). DFFE. doi: 10.15493/DEA.MIMS.09642023.
Sabelani Z, Ismail H, van den Berg MA, Lamont T. 2023. Long-term observations of hourly bottom temperatures at Mangolds Pool, South Africa (June 1993 - November 1993). DFFE. doi: 10.15493/DEA.MIMS.09652023.
Sabelani Z, Ismail H, van den Berg MA, Lamont T. 2023. Long-term observations of hourly bottom temperatures at Mangolds Pool, South Africa (November 1993 - March 1994). DFFE. doi: 10.15493/DEA.MIMS.09662023.
Sabelani Z, Ismail H, van den Berg MA, Lamont T. 2023. Long-term observations of hourly bottom temperatures at Mangolds Pool, South Africa (March 1994 - August 1994). DFFE. doi: 10.15493/DEA.MIMS.09672023.
Sabelani Z, Ismail H, van den Berg MA, Lamont T. 2023. Long-term observations of hourly bottom temperatures at Mangolds Pool, South Africa (August 1994 - October 1994). DFFE. doi: 10.15493/DEA.MIMS.09682023.
Sabelani Z, Ismail H, van den Berg MA, Lamont T. 2023. Long-term observations of hourly bottom temperatures at Mangolds Pool, South Africa (October 1994 - April 1995). DFFE. doi: 10.15493/DEA.MIMS.09692023.
Sabelani Z, Ismail H, van den Berg MA, Lamont T. 2023. Long-term observations of hourly bottom temperatures at Mangolds Pool, South Africa (April 1995 - July 1995). DFFE. doi: 10.15493/DEA.MIMS.09702023.
Sabelani Z, Ismail H, van den Berg MA, Lamont T. 2023. Long-term observations of hourly bottom temperatures at Mangolds Pool, South Africa (July 1995 - November 1995). DFFE. doi: 10.15493/DEA.MIMS.09712023
Sabelani Z, Ismail H, van den Berg MA, Lamont T. 2023. Long-term observations of hourly bottom temperatures at Mangolds Pool, South Africa (November 1995 - April 1996). DFFE. doi: 10.15493/DEA.MIMS.09722023.
Sabelani Z, Ismail H, van den Berg MA, Lamont T. 2023. Long-term observations of hourly bottom temperatures at Mangolds Pool, South Africa (April 1996 - October 1996). DFFE. doi: 10.15493/DEA.MIMS.09732023.
Sabelani Z, Ismail H, van den Berg MA, Lamont T. 2023. Long-term observations of hourly bottom temperatures at Mangolds Pool, South Africa (October 1996 - May 1997). DFFE. doi: 10.15493/DEA.MIMS.09742023.
Sabelani Z, Ismail H, van den Berg MA, Lamont T. 2023. Long-term observations of hourly bottom temperatures at Mangolds Pool, South Africa (March 2000 - August 2000). DFFE. doi: 10.15493/DEA.MIMS.09752023.
Sabelani Z, Ismail H, van den Berg MA, Lamont T. 2023. Long-term observations of hourly bottom temperatures at Mangolds Pool, South Africa (August 2000 - March 2001). DFFE. doi: 10.15493/DEA.MIMS.09762023.
Sabelani Z, Ismail H, van den Berg MA, Lamont T. 2023. Long-term observations of hourly bottom temperatures at Mangolds Pool, South Africa (March 2001 - July 2001). DFFE. doi: 10.15493/DEA.MIMS.09772023.
Sabelani Z, Ismail H, van den Berg MA, Lamont T. 2023. Long-term observations of hourly bottom temperatures at Mangolds Pool, South Africa (July 2001 - November 2001). DFFE. doi: 10.15493/DEA.MIMS.09782023.
Sabelani Z, Ismail H, van den Berg MA, Lamont T. 2023. Long-term observations of hourly bottom temperatures at Mangolds Pool, South Africa (November 2001 - November 2002). DFFE. doi: 10.15493/DEA.MIMS.09792023.
Sabelani Z, Ismail H, van den Berg MA, Lamont T. 2023. Long-term observations of hourly bottom temperatures at Mangolds Pool, South Africa (November 2002 - June 2003). DFFE. doi: 10.15493/DEA.MIMS.09802023.
Sabelani Z, Ismail H, van den Berg MA, Lamont T. 2023. Long-term observations of hourly bottom temperatures at Mangolds Pool, South Africa (November 2003 - June 2004). DFFE. doi: 10.15493/DEA.MIMS.09812023.
Sabelani Z, Ismail H, van den Berg MA, Lamont T. 2023. Long-term observations of hourly bottom temperatures at Mangolds Pool, South Africa (June 2004 - November 2004). DFFE. doi: 10.15493/DEA.MIMS.09822023.

Sabelani Z, Ismail H, van den Berg MA, Lamont T. 2023. Long-term observations of hourly bottom temperatures at Mangolds Pool, South Africa (November 2004 - November 2005). DFFE. doi: 10.15493/DEA.MIMS.09832023.

Sabelani Z, Ismail H, van den Berg MA, Lamont T. 2023. Raw temperature data for long-term observations of Bottom Temperatures at Kasa Reef Mombasa, Kenya (October 2011 - April 2012). DFFE. doi: 10.15493/DEA.MIMS.11452023.

Sabelani Z, Ismail H, van den Berg MA, Lamont T. 2023. Long-term observations of hourly bottom temperatures at Kasa Reef Mombasa, Kenya (October 2011 - April 2012). DFFE. doi: 10.15493/DEA.MIMS.11442023.

Sabelani Z, Ismail H, van den Berg MA, Lamont T. 2023. Raw temperature data for long-term observations of Bottom Temperatures at Nosy Iranja, Madagascar (August 2003 - October 2007). DFFE. doi: 10.15493/DEA.MIMS.11432023.

Sabelani Z, Ismail H, van den Berg MA, Lamont T. 2023. Long-term observations of hourly bottom temperatures at Nosy Iranja, Madagascar (August 2003 - October 2007). DFFE. doi: 10.15493/DEA.MIMS.11422023.

Speich S, Lamont T, Louw GS, van den Berg MA, Meinen CS, Garcia R, Perez RC, Dong S. 2023. Long-term observations of daily bottom currents along the SAMBA transect at PIES Mooring P1 (September 2013 – August 2015). DFFE. doi: 10.15493/DEA.MIMS.08012023.

Speich S, Lamont T, Louw GS, van den Berg MA, Meinen CS, Garcia R, Perez RC, Dong S. 2023. Long-term observations of daily bottom currents along the SAMBA transect at PIES Mooring P1 (August 2015 – July 2017). DFFE. doi: 10.15493/DEA.MIMS.08082023.

Speich S, Lamont T, Louw GS, van den Berg MA, Meinen CS, Garcia R, Perez RC, Dong S. 2023. Long-term observations of daily bottom currents along the SAMBA transect at PIES Mooring P1 (July 2017 – September 2019). DFFE. doi: 10.15493/DEA.MIMS.08142023.

Speich S, Lamont T, Louw GS, van den Berg MA, Meinen CS, Garcia R, Perez RC, Dong S. 2023. Long-term observations of daily bottom currents along the SAMBA transect at PIES Mooring P1 (October 2019 – October 2021). DFFE. doi: 10.15493/DEA.MIMS.08152023.

Speich S, Lamont T, Louw GS, van den Berg MA, Meinen CS, Garcia R, Perez RC, Dong S. 2023. Long-term observations of daily bottom currents along the SAMBA transect at PIES Mooring P2 (September 2013 – July 2015). DFFE. doi: 10.15493/DEA.MIMS.08022023.

Speich S, Lamont T, Louw GS, van den Berg MA, Meinen CS, Garcia R, Perez RC, Dong S. 2023. Long-term observations of daily bottom currents along the SAMBA transect at PIES Mooring P2 (August 2015 – July 2017). DFFE. doi: 10.15493/DEA.MIMS.08092023.

Speich S, Lamont T, Louw GS, van den Berg MA, Meinen CS, Garcia R, Perez RC, Dong S. 2023. Long-term observations of daily bottom currents along the SAMBA transect at PIES Mooring P3 (August 2015 – July 2017). DFFE. doi: 10.15493/DEA.MIMS.08102023.

Speich S, Lamont T, Louw GS, van den Berg MA, Meinen CS, Garcia R, Perez RC, Dong S. 2023. Long-term observations of daily bottom currents along the SAMBA transect at PIES Mooring P3 (October 2019 – October 2021). DFFE. doi: 10.15493/DEA.MIMS.08162023.

Speich S, Lamont T, Louw GS, van den Berg MA, Meinen CS, Garcia R, Perez RC, Dong S. 2023. Long-term observations of daily bottom currents along the SAMBA transect at PIES Mooring P4 (September 2013 – August 2015). DFFE. doi: 10.15493/DEA.MIMS.08032023.

Speich S, Lamont T, Louw GS, van den Berg MA, Meinen CS, Garcia R, Perez RC, Dong S. 2023. Long-term observations of daily bottom currents along the SAMBA transect at PIES Mooring P4 (October 2019 – October 2021). DFFE. doi: 10.15493/DEA.MIMS.08172023.

Speich S, Lamont T, Louw GS, van den Berg MA, Meinen CS, Garcia R, Perez RC, Dong S. 2023. Long-term observations of daily bottom currents along the SAMBA transect at PIES Mooring P5 (September 2013 – August 2015). DFFE. doi: 10.15493/DEA.MIMS.08042023.

Speich S, Lamont T, Louw GS, van den Berg MA, Meinen CS, Garcia R, Perez RC, Dong S. 2023. Long-term observations of daily bottom currents along the SAMBA transect at PIES Mooring P5 (August 2015 – July 2017). DFFE. doi: 10.15493/DEA.MIMS.08112023.

Speich S, Lamont T, Louw GS, van den Berg MA, Meinen CS, Garcia R, Perez RC, Dong S. 2023. Long-term observations of daily bottom currents along the SAMBA transect at PIES Mooring P6 (September 2013 – August 2015). DFFE. doi: 10.15493/DEA.MIMS.08052023.

Speich S, Lamont T, Louw GS, van den Berg MA, Meinen CS, Garcia R, Perez RC, Dong S. 2023. Long-term observations of daily bottom currents along the SAMBA transect at PIES Mooring P6 (August 2015 – July 2017). DFFE. doi: 10.15493/DEA.MIMS.08122023.

Speich S, Lamont T, Louw GS, van den Berg MA, Meinen CS, Garcia R, Perez RC, Dong S. 2023. Long-term observations of daily bottom currents along the SAMBA transect at PIES Mooring P7 (September 2013 – August 2015). DFFE. doi: 10.15493/DEA.MIMS.08062023.

Speich S, Lamont T, Louw GS, van den Berg MA, Meinen CS, Garcia R, Perez RC, Dong S. 2023. Long-term observations of daily bottom currents along the SAMBA transect at PIES Mooring P8 (September 2013 – August 2015). DFFE. doi: 10.15493/DEA.MIMS.08072023.

Speich S, Lamont T, Louw GS, van den Berg MA, Meinen CS, Garcia R, Perez RC, Dong S. 2023. Long-term observations of daily bottom currents along the SAMBA transect at PIES Mooring P8 (August 2015 – July 2017). DFFE. doi: 10.15493/DEA.MIMS.08132023.

Speich S, Lamont T, Louw GS, van den Berg MA, Meinen CS, Garcia R, Perez RC, Dong S. 2023. Long-term observations of daily acoustic travel time along the SAMBA transect at PIES Mooring P1 (September 2013 – August 2015). DFFE. doi: 10.15493/DEA.MIMS.07772023.

Speich S, Lamont T, Louw GS, van den Berg MA, Meinen CS, Garcia R, Perez RC, Dong S. 2023. Long-term observations of daily acoustic travel time along the SAMBA transect at PIES Mooring P1 (August 2015 – July 2017). DFFE. doi: 10.15493/DEA.MIMS.07842023.

Speich S, Lamont T, Louw GS, van den Berg MA, Meinen CS, Garcia R, Perez RC, Dong S. 2023. Long-term observations of daily acoustic travel time along the SAMBA transect at PIES Mooring P1 (July 2017 – September 2019). DFFE. doi: 10.15493/DEA.MIMS.07912023.

Speich S, Lamont T, Louw GS, van den Berg MA, Meinen CS, Garcia R, Perez RC, Dong S. 2023. Long-term observations of daily acoustic travel time along the SAMBA transect at PIES Mooring P1 (October 2019 – October 2021). DFFE. doi: 10.15493/DEA.MIMS.07962023.

Speich S, Lamont T, Louw GS, van den Berg MA, Meinen CS, Garcia R, Perez RC, Dong S. 2023. Long-term observations of daily acoustic travel time along the SAMBA transect at PIES Mooring P2 (September 2013 – July 2015). DFFE. doi: 10.15493/DEA.MIMS.07782023.

Speich S, Lamont T, Louw GS, van den Berg MA, Meinen CS, Garcia R, Perez RC, Dong S. 2023. Long-term observations of daily acoustic travel time along the SAMBA transect at PIES Mooring P2 (August 2015 – July 2017). DFFE. doi: 10.15493/DEA.MIMS.07852023.

Speich S, Lamont T, Louw GS, van den Berg MA, Meinen CS, Garcia R, Perez RC, Dong S. 2023. Long-term observations of daily acoustic travel time along the SAMBA transect at PIES Mooring P2 (July 2017 – September 2019). DFFE. doi: 10.15493/DEA.MIMS.07922023.

Speich S, Lamont T, Louw GS, van den Berg MA, Meinen CS, Garcia R, Perez RC, Dong S. 2023. Long-term observations of daily acoustic travel time along the SAMBA transect at PIES Mooring P2 (October 2019 – October 2021). DFFE. doi: 10.15493/DEA.MIMS.07972023.

Speich S, Lamont T, Louw GS, van den Berg MA, Meinen CS, Garcia R, Perez RC, Dong S. 2023. Long-term observations of daily acoustic travel time along the SAMBA transect at PIES Mooring P3 (August 2015 – July 2017). DFFE. doi: 10.15493/DEA.MIMS.07862023.

Speich S, Lamont T, Louw GS, van den Berg MA, Meinen CS, Garcia R, Perez RC, Dong S. 2023. Long-term observations of daily acoustic travel time along the SAMBA transect at PIES Mooring P3 (July 2017 – September 2019). DFFE. doi: 10.15493/DEA.MIMS.07932023.

Speich S, Lamont T, Louw GS, van den Berg MA, Meinen CS, Garcia R, Perez RC, Dong S. 2023. Long-term observations of daily acoustic travel time along the SAMBA transect at PIES Mooring P3 (October 2019 – October 2021). DFFE. doi: 10.15493/DEA.MIMS.07982023.

Speich S, Lamont T, Louw GS, van den Berg MA, Meinen CS, Garcia R, Perez RC, Dong S. 2023. Long-term observations of daily acoustic travel time along the SAMBA transect at PIES Mooring P4 (September 2013 – August 2015). DFFE. doi: 10.15493/DEA.MIMS.07792023.

Speich S, Lamont T, Louw GS, van den Berg MA, Meinen CS, Garcia R, Perez RC, Dong S. 2023. Long-term observations of daily acoustic travel time along the SAMBA transect at PIES Mooring P4 (August 2015 – July 2017). DFFE. doi: 10.15493/DEA.MIMS.07872023.

Speich S, Lamont T, Louw GS, van den Berg MA, Meinen CS, Garcia R, Perez RC, Dong S. 2023. Long-term observations of daily acoustic travel time along the SAMBA transect at PIES Mooring P4 (July 2017 – January 2019). DFFE. doi: 10.15493/DEA.MIMS.07942023.

Speich S, Lamont T, Louw GS, van den Berg MA, Meinen CS, Garcia R, Perez RC, Dong S. 2023. Long-term observations of daily acoustic travel time along the SAMBA transect at PIES Mooring P4 (October 2019 – October 2021). DFFE. doi: 10.15493/DEA.MIMS.07992023.

Speich S, Lamont T, Louw GS, van den Berg MA, Meinen CS, Garcia R, Perez RC, Dong S. 2023. Long-term observations of daily acoustic travel time along the SAMBA transect at PIES Mooring P5 (September 2013 – August 2015). DFFE. doi: 10.15493/DEA.MIMS.07802023.

Speich S, Lamont T, Louw GS, van den Berg MA, Meinen CS, Garcia R, Perez RC, Dong S. 2023. Long-term observations of daily acoustic travel time along the SAMBA transect at PIES Mooring P5 (August 2015 – July 2017). DFFE. doi: 10.15493/DEA.MIMS.07882023.

Speich S, Lamont T, Louw GS, van den Berg MA, Meinen CS, Garcia R, Perez RC, Dong S. 2023. Long-term observations of daily acoustic travel time along the SAMBA transect at PIES Mooring P6 (September 2013 – August 2015). DFFE. doi: 10.15493/DEA.MIMS.07812023.

Speich S, Lamont T, Louw GS, van den Berg MA, Meinen CS, Garcia R, Perez RC, Dong S. 2023. Long-term observations of daily acoustic travel time along the SAMBA transect at PIES Mooring P6 (August 2015 – July 2017). DFFE. doi: 10.15493/DEA.MIMS.07892023.

Speich S, Lamont T, Louw GS, van den Berg MA, Meinen CS, Garcia R, Perez RC, Dong S. 2023. Long-term observations of daily acoustic travel time along the SAMBA transect at PIES Mooring P7 (September 2013 – August 2015). DFFE. doi: 10.15493/DEA.MIMS.07822023.

Speich S, Lamont T, Louw GS, van den Berg MA, Meinen CS, Garcia R, Perez RC, Dong S. 2023. Long-term observations of daily acoustic travel time along the SAMBA transect at PIES Mooring P8 (September 2013 – August 2015). DFFE. doi: 10.15493/DEA.MIMS.07832023.

Speich S, Lamont T, Louw GS, van den Berg MA, Meinen CS, Garcia R, Perez RC, Dong S. 2023. Long-term observations of daily acoustic travel time along the SAMBA transect at PIES Mooring P8 (August 2015 – July 2017). DFFE. doi: 10.15493/DEA.MIMS.07902023.

Speich S, Lamont T, Louw GS, van den Berg MA, Meinen CS, Garcia R, Perez RC, Dong S. 2023. Long-term observations of daily acoustic travel time along the SAMBA transect at PIES Mooring P8 (July 2017 – March 2018). DFFE. doi: 10.15493/DEA.MIMS.07952023.

Speich S, Lamont T, Louw GS, van den Berg MA, Meinen CS, Garcia R, Perez RC, Dong S. 2023. Long-term observations of daily acoustic travel time along the SAMBA transect at PIES Mooring P8 (October 2019 – September 2021). DFFE. doi: 10.15493/DEA.MIMS.08002023.

Speich S, Lamont T, van den Berg MA, Louw GS, Meinen CS, Garcia R, Perez RC, Dong S. 2023. Raw PIES and current data for long-term observations of acoustic travel time (tau); bottom pressure and currents along the SAMBA transect at PIES P1 (October 2019 - October 2021). DFFE. doi: 10.15493/DEA.MIMS.07722023.

Speich S, Lamont T, van den Berg MA, Louw GS, Meinen CS, Garcia R, Perez RC, Dong S. 2023. Raw PIES data for long-term observations of acoustic travel time (tau) and bottom pressure along the SAMBA transect at PIES P2 (October 2019 - October 2021). DFFE. doi: 10.15493/DEA.MIMS.07732023.

Speich S, Lamont T, van den Berg MA, Louw GS, Meinen CS, Garcia R, Perez RC, Dong S. 2023. Raw PIES and current data for long-term observations of acoustic travel time (tau); bottom pressure and currents along the SAMBA transect at PIES P3 (October 2019 - October 2021). DFFE. doi: 10.15493/DEA.MIMS.07742023.

Speich S, Lamont T, van den Berg MA, Louw GS, Meinen CS, Garcia R, Perez RC, Dong S. 2023. Raw PIES and current data for long-term observations of acoustic travel time (tau); bottom pressure and currents along the SAMBA transect at PIES P4 (October 2019 - October 2021). DFFE. doi: 10.15493/DEA.MIMS.07752023.

Speich S, Lamont T, van den Berg MA, Louw GS, Meinen CS, Garcia R, Perez RC, Dong S. 2023. Raw PIES data for long-term observations of acoustic travel time (tau) and bottom pressure along the SAMBA transect at PIES P8 (October 2019 - September 2021). DFFE. doi: 10.15493/DEA.MIMS.07762023.

Tutt G, Lamont T. 2023. Processed CTD continuous observations from the Anchovy Recruitment on the Africana Voyage 047, August 1986. DFFE. doi: 10.15493/DEA.MIMS.03612023.

Tutt G, Lamont T. 2023. Raw CTD continuous observations from the Anchovy Recruitment on the Africana Voyage 047, August 1986. DFFE. doi: 10.15493/DEA.MIMS.04292023.

Tutt G, Lamont T. 2023. Processed CTD continuous observations from the South Coast Hake Biomass Survey on the Africana

Voyage 048, September 1986. DFFE. doi: 10.15493/DEA.MIMS.04332023.

Tutt G, Lamont T. 2023. Raw CTD continuous observations from the South Coast Hake Biomass Survey on the Africana Voyage 048, September 1986. DFFE. doi: 10.15493/DEA.MIMS.04372023.

Tutt G, Lamont T. 2023. Processed CTD continuous observations from the West Coast Hake Biomass Survey on the Africana Voyage 050, January 1987. DFFE. doi: 10.15493/DEA.MIMS.04422023.

Tutt G, Lamont T. 2023. Raw CTD continuous observations from the West Coast Hake Biomass Survey on the Africana Voyage 050, January 1987. DFFE. doi: 10.15493/DEA.MIMS.05032023.

Tutt G, Lamont T. 2023. Raw CTD discrete observations from the West Coast Hake Biomass Survey on the Africana Voyage 050, January 1987. DFFE. doi: 10.15493/DEA.MIMS.05052023.

Tutt G, Lamont T. 2023. Processed CTD continuous observations from the West Coast Hake Biomass Survey on the Africana Voyage 054, June 1987. DFFE. doi: 10.15493/DEA.MIMS.05072023.

Tutt G, Lamont T. 2023. Raw CTD continuous observations from the West Coast Hake Biomass Survey on the Africana Voyage 054, June 1987. DFFE. doi: 10.15493/DEA.MIMS.05112023.

Tutt G, Lamont T. 2023. Raw CTD discrete observations from the West Coast Hake Biomass Survey on the Africana Voyage 054, June 1987. DFFE. doi: 10.15493/DEA.MIMS.05132023.

Tutt G, Lamont T. 2023. Processed CTD continuous observations from the South Coast Hake Biomass Survey on the Africana Voyage 056, September 1987. DFFE. doi: 10.15493/DEA.MIMS.05152023.

Tutt G, Lamont T. 2023. Raw CTD continuous observations from the South Coast Hake Biomass Survey on the Africana Voyage 056, September 1987. DFFE. doi: 10.15493/DEA.MIMS.05182023.

Tutt G, Lamont T. 2023. Processed CTD continuous observations from the Anchovy and Pilchard Spawning Stock Survey on the Africana Voyage 057, November 1987. DFFE. doi: 10.15493/DEA.MIMS.05202023.

Tutt G, Lamont T. 2023. Raw CTD continuous observations from the Anchovy and Pilchard Spawning Stock Survey on the Africana Voyage 057, November 1987. DFFE. doi: 10.15493/DEA.MIMS.05222023.

Tutt G, Lamont T. 2023. Processed CTD continuous observations from the West Coast Hake Biomass Survey on the Africana Voyage 059, February 1988. DFFE. doi: 10.15493/DEA.MIMS.05242023.

Tutt G, Lamont T. 2023. Processed CTD discrete observations from the West Coast Hake Biomass Survey on the Africana Voyage 059, February 1988. DFFE. doi: 10.15493/DEA.MIMS.05252023.

Tutt G, Lamont T. 2023. Raw CTD continuous observations from the West Coast Hake Biomass Survey on the Africana Voyage 059, February 1988. DFFE. doi: 10.15493/DEA.MIMS.05262023.

Tutt G, Lamont T. 2023. Raw CTD discrete observations from the West Coast Hake Biomass Survey on the Africana Voyage 059, February 1988. DFFE. doi: 10.15493/DEA.MIMS.05272023.

Tutt G, Lamont T. 2023. Processed CTD continuous observations from the South Coast Hake Biomass Survey on the Africana Voyage 063, May 1988. DFFE. doi: 10.15493/DEA.MIMS.05282023.

Tutt G, Lamont T. 2023. Raw CTD continuous observations from the South Coast Hake Biomass Survey on the Africana Voyage 063, May 1988. DFFE. doi: 10.15493/DEA.MIMS.05302023.

Tutt G, Lamont T. 2023. Processed CTD continuous observations from the Physical-Chemical Oceanography Cruise on the Africana Voyage 067, September 1988. DFFE. doi: 10.15493/DEA.MIMS.11492023.

Tutt G, Lamont T. 2023. Raw CTD continuous observations from the Physical-Chemical Oceanography Cruise on the Africana Voyage 067, September 1988. DFFE. doi: 10.15493/DEA.MIMS.11512023

Tutt G, Lamont T. 2023. Processed CTD continuous observations from the West Coast Hake Biomass Survey on the Africana Voyage 069, January 1989. DFFE. doi: 10.15493/DEA.MIMS.11522023.

Tutt G, Lamont T. 2023. Raw CTD continuous observations from the West Coast Hake Biomass Survey on the Africana Voyage 069, January 1989. DFFE. doi: 10.15493/DEA.MIMS.11542023.

Tutt G, Lamont T. 2023. Processed CTD continuous observations from the Physical-Chemical Oceanography Cruise on the Africana Voyage 070, March 1989. DFFE. doi: 10.15493/DEA.MIMS.11552023.

Tutt G, Lamont T. 2023. Raw CTD continuous observations from the Physical-Chemical Oceanography Cruise on the Africana Voyage 070, March 1989. DFFE. doi: 10.15493/DEA.MIMS.11572023.

Tutt G, Lamont T. 2023. Processed CTD continuous observations from the South-east Atlantic Expedition on the Africana Voyage 071, April 1989. DFFE. doi: 10.15493/DEA.MIMS.11582023.

Tutt G, Lamont T. 2023. Raw CTD continuous observations from the South-east Atlantic Expedition on the Africana Voyage 071, April 1989. DFFE. doi: 10.15493/DEA.MIMS.11602023.

Tutt G, Lamont T. 2023. Processed CTD continuous observations from the Anchovy Recruitment Survey on the Africana Voyage 073, June 1989. DFFE. doi: 10.15493/DEA.MIMS.11612023.

Tutt G, Lamont T. 2023. Processed CTD discrete observations from the Anchovy Recruitment Survey on the Africana Voyage 073, June 1989. DFFE. doi: 10.15493/DEA.MIMS.11622023.

Tutt G, Lamont T. 2023. Raw CTD continuous observations from the Anchovy Recruitment Survey on the Africana Voyage 073, June 1989. DFFE. doi: 10.15493/DEA.MIMS.11632023.

Tutt G, Lamont T. 2023. Raw CTD discrete observations from the Anchovy Recruitment Survey on the Africana Voyage 073, June 1989. DFFE. doi: 10.15493/DEA.MIMS.11642023.

Tutt G, Lamont T. 2023. Processed CTD continuous observations from the South West African Pilchard and Anchovy Biomass Survey on the Africana Voyage 074, June 1989. DFFE. doi: 10.15493/DEA.MIMS.11652023.

Tutt G, Lamont T. 2023. Processed CTD discrete observations from the South West African Pilchard and Anchovy Biomass Survey on the Africana Voyage 074, June 1989. DFFE. doi: 10.15493/DEA.MIMS.11662023.

Tutt G, Lamont T. 2023. Raw CTD continuous observations from the South West African Pilchard and Anchovy Biomass

Survey on the Africana Voyage 074, June 1989. DFFE. doi: 10.15493/DEA.MIMS.11672023.

Tutt G, Lamont T. 2023. Processed CTD continuous observations from the West Coast Hake Biomass Survey on the Africana Voyage 075, July 1989. DFFE. doi: 10.15493/DEA.MIMS.11682023.

Tutt G, Lamont T. 2023. Raw CTD continuous observations from the West Coast Hake Biomass Survey on the Africana Voyage 075, July 1989. DFFE. doi: 10.15493/DEA.MIMS.11702023.

Tutt G, Lamont T. 2023. Processed CTD continuous observations from the Physical-Chemical Oceanography Cruise on the Africana Voyage 077, September 1989. DFFE. doi: 10.15493/DEA.MIMS.11712023.

Tutt G, Lamont T. 2023. Raw CTD continuous observations from the Physical-Chemical Oceanography Cruise on the Africana Voyage 077, September 1989. DFFE. doi: 10.15493/DEA.MIMS.11732023.

Tutt G, Lamont T. 2023. Processed CTD continuous observations from the Pelagic Fish Biomass Survey on the Africana Voyage 078, November 1989. DFFE. doi: 10.15493/DEA.MIMS.11742023.

Tutt G, Lamont T. 2023. Raw CTD continuous observations from the Pelagic Fish Biomass Survey on the Africana Voyage 078, November 1989. DFFE. doi: 10.15493/DEA.MIMS.11762023.

van den Berg MA. 2023. South Atlantic Meridional Overturning Circulation Basin-wide Array (SAMBA) Monitoring Line cruise on the Algoa Voyage 275, September 2021. DFFE. doi: 10.15493/DEA.MIMS.01112023.

van den Berg MA. 2023. South Atlantic Meridional Overturning Circulation Basin-wide Array (SAMBA) Monitoring Line cruise on the Algoa Voyage 285, September 2022. DFFE. doi: 10.15493/DEA.MIMS.01132023.

van den Berg MA. 2023. South Atlantic Meridional Overturning Circulation Basin-wide Array (SAMBA) Monitoring Line cruise on the Algoa Voyage 253, October 2018. DFFE. doi: 10.15493/DEA.MIMS.11472023.

van den Berg MA. 2023. South Atlantic Meridional Overturning Circulation Basin-wide Array (SAMBA) Monitoring Line on the Algoa Voyage 291, March 2023. DFFE. doi: 10.15493/DEA.MIMS.11482023.

van den Berg MA. 2023. Marion Island Relief Voyage on the SA Agulhas II Voyage 045, May 2021. DFFE. doi: 10.15493/DEA.MIMS.01102023.

van den Berg MA. 2023. Marion Island Relief Voyage on the SA Agulhas II Voyage 051, March 2022. DFFE. doi: 10.15493/DEA.MIMS.01122023.

van den Berg MA. 2023. Marion Island Relief Voyage on the SA Agulhas II Voyage 057, May 2023. DFFE. doi: 10.15493/DEA.MIMS.11232023.

van den Berg MA. 2023. Raw Expendable Bathythermograph (XBT) casts collected during the Marion Island Relief Voyage on the SA Agulhas II Voyage 045, May 2021. DFFE. doi:10.15493/DEA.MIMS.01152023.

van den Berg MA. 2023. Processed Expendable Bathythermograph (XBT) casts collected during the Marion Island Relief Voyage on the SA Agulhas II Voyage 045, May 2021. DFFE. doi: 10.15493/DEA.MIMS.01162023.

van den Berg MA. 2023. Raw Expendable Bathythermograph (XBT) casts collected during the 2022 Marion Relief Voyage on the SA Agulhas II Voyage 051. DFFE. doi: 10.15493/DEA.MIMS.01422023.

van den Berg MA. 2023. Processed Expendable Bathythermograph (XBT) casts collected during the 2022 Marion Relief Voyage on the SA Agulhas II Voyage 051. DFFE. doi: 10.15493/DEA.MIMS.01432023.

van den Berg MA. 2023. Raw Expendable Bathythermograph (XBT) casts collected during the Marion Island Relief Voyage on the SA Agulhas II Voyage 057, May 2023. DFFE. doi: 10.15493/DEA.MIMS.11222023.

van den Berg MA. 2023. Processed Expendable Bathythermograph (XBT) casts collected during the Marion Island Relief Voyage on the SA Agulhas II Voyage 057, May 2023. DFFE. doi: 10.15493/DEA.MIMS.11462023.

Published reports

Huggett JA, Lamont T, Haupt T, Halo I, Kirkman SP. 2023. Oceans and Coasts Annual Science Report 2022. *Oceans and Coasts, DFFE, Report 22, May 2023, ISBN: 978-0-621-51000-3, 42 pp*.

Published educational material

Filander Z. 2023. Where the weird things are: An ocean twilight zone adventure. EarthAware Kids, San Rafael, United States of America. ISBN: 978–1–64722–588–9.

Theses

Daniels R. 2023. Acoustic ecology and occurrence of Killer Whales at sub-Antarctic Marion Island. BSc Honours Thesis (Oceanography), University of Cape Town, Cape Town, 76 pp.

Edward JJN. 2023. Larval fish assemblages off the south east coast of South Africa. MSc thesis (Biodiversity and Conservation Biology), University of the Western Cape, Bellville, 70 pp.

Filander ZNP. 2023. The taxonomy, phylogeny and biogeographic patterns of the South African azooxanthellate scleractinian coral (Cnidaria: Hexacorallia) fauna: with implications for marine spatial planning. PhD Thesis (Zoology), Nelson Mandela University, Gqeberha, 422 pp.

Forsberg STW. 2023. Disentangling entanglement in Cape fur seals for better management of plastic pollution impacts. MSc Dissertation (Conservation Biology), University of Cape Town, Cape Town, 44 pp.

Gumede NC. 2023. Variability in the diet of Cape fur seals and their interaction with fisheries off the South African coast, 2010-2019. MSc thesis (Biological Sciences), University of Cape Town, South Africa.

Mdluli NM. 2023. Zooplankton assemblages associated with submarine canyons off the east coast of South Africa. MSc Thesis (Biological Sciences), University of KwaZulu-Natal, Durban, 94 pp.

Petzer K. 2023. Marine heatwaves and warm events in the Cape Peninsula Upwelling Cell, Southern Benguela. MSc Thesis (Oceanography), University of Cape Town, Cape Town, 79 pp.

Rasmeni B. 2023. Warming trends in the Agulhas Current system from 1980 to 2019. MSc Thesis (Marine Sciences), Cape Peninsula University of Technology, Cape Town, 55 pp.

Soares B. 2023. Surface and sub-surface hydrographic variability at the Prince Edward Islands: Perspectives from the high-resolution GLORYS model. MSc Thesis (Oceanography), University of Cape Town, Cape Town, 148 pp.

Torr M. 2023. Distribution shifts in the relative abundance of *Engraulis encrasicolus* (anchovy), *Sardinops sagax* (sardine), and *Etrumeus whiteheadi* (redeye) as a response to changing sea surface temperatures in the Southern Benguela region, BSc Honours Thesis (Oceanography), University of Cape Town, Cape Town, 47 pp.

Unpublished reports

Dakwa FE, Shabangu F, Izard L, Makhado AB. 2023. Large scale pelagic acoustic ecoregionalisation in the eastern part of the sub-Antarctic region. *Commission for the Conservation of Antarctic Marine Living Resources (CCAMLR) WG-EMM-2023/51, 19 June 2023, 11 pp.*

Huggett J, Mdluli N, Thibault D. 2023. Zooplankton communities near the Prince Edward Islands – recent progress from image analysis. *Commission for the Conservation of Antarctic Marine Living Resources (CCAMLR) WG-EMM-2023/38, 19 June 2023, 13 pp.*

Makhado AB, Huggett J, Dakwa F, Mdluli N, Shabangu F, Koubbi P, Cotté C, d'Ovidio F, Djian V, Goberville E, Izard L, Kristiansen A, Leroy B, Merland C, Ly Rintz C, Thellier M, Thibault D, Delord K, Bost C, Tavernier E, Azarian C, Swadling K, Melvin J, Kitchener J, Brokensha L, Lea M-A, Walters A. 2023. Baseline spatial data prior to the ecoregionalisation of the eastern sub-Antarctic region. *Commission for the Conservation of Antarctic Marine Living Resources (CCAMLR) WG-EMM-2023/31, 17 June 2023, 5 pp*.

Makhado A, Huggett J, Dakwa F, Mdluli N, Shabangu F, Koubbi P, Cotté C, Djian V, Goberville E, Izard L, Leroy B, Merland C, Rintz CL, Thellier M, Swadling K, Melvin J, Kitchener J, Brokensha L, Reisinger R. 2023. Baseline spatial data prior to the Ecoregionalisation of the Eastern Sub-Antarctic Region. *Antarctic and Southern Ocean Coalition (ASOC) Final Project Report, 172 pp.*

Makhado A, Koubbi P, Huggett JA, Cotté C, Reisinger R, Swadling KA, Azarian C, Barnerias C, d'Ovidio F, Gauthier L, Goberville E, Leroy B, Lombard AT, Muller L, van de Putte A, and workshop participants. 2023. Ecoregionalisation of the pelagic zone in the Subantarctic and Subtropical Indian Ocean. *Commission for the Conservation of Antarctic Marine Living Resources (CCAMLR) SC-CAMLR-42/08, 30 August 2023, 32 pp*.

Makhado AB, Reisinger R, Ryan P, Masotla MJ, Dyer B, Seakamela SM, Shabangu F, Somhlaba S, Dakwa F. 2023. Seabirds assemblages, abundance and distribution in the African sector of the Southern Indian Ocean. *Commission for the Conservation of Antarctic Marine Living Resources (CCAMLR) WG-EMM-2023/37, 19 June 2023, 19pp.*

Reisinger R, Makhado AB, Delord K, Bost C, Lea M-A, Pistorius PA. 2023. Towards higher predator ecoregionalisation of the pelagic zone in the subantarctic and subtropical Indian Ocean. *Commission for the Conservation of Antarctic Marine Living Resources (CCAMLR) WG-EMM-2023/32, 17 June 2023, 14pp*.

Swadling K, Huggett J, Brokensha L, Goberville E, Melvin J, Kitchener J, Koubbi P. 2023. Using CPR surveys to map distributions of trophically important subantarctic prey species. *Commission for the Conservation of Antarctic Marine Living Resources (CCAMLR) WG-EMM-2023/58, 29 June 2023, 18 pp*.

NOTES